A New Approach To Estimate Congestion Impacts For Highway Evaluation
-Effects On Fuel Consumption And Vehicle Emissions

Ian Douglas Greenwood

Supervised by
Associate Professor Roger C.M. Dunn
and
Associate Professor Robert R. Raine

A thesis submitted in partial fulfilment of the requirements for the degree of Doctor of Philosophy in Engineering, The University of Auckland, 2003.

ABSTRACT

The evaluation of highway projects where traffic congestion is a significant problem requires careful analysis to accurately identify the true costs, and therefore potential benefits, of operational changes. Models have previously been derived that employ either simplistic speed-flow approaches or highly detailed micro-simulation techniques. Another approach, and the goal for this research, is to develop a mid-range modelling framework whereby the predictive capability could be enhanced in comparison to the simple speed-flow models but without the onerous data issues of micro-simulation, for use in highway evaluation projects.

The approach adopted was based on modelling of acceleration noise defined as the standard deviation of the accelerations. During periods of high traffic congestion there is a greater variability in speed resulting in higher acceleration noise levels. Once the acceleration noise level is estimated, the impact on fuel consumption and vehicle emissions can then be determined.

The framework consists of a series of discrete sub-models that firstly estimate the base (steady-speed) fuel consumption and then the acceleration noise level value. From these data, the additional fuel consumption from congestion is calculated and vehicle emissions are finally estimated. In this way, the model can be made more flexible for application to future research because it allows replacement of any portion of the model sub-routines without the need for a complete restructuring of the model framework.

Data collection and analysis of the regimes for modelling were undertaken on highways in Auckland (New Zealand), Kuala Lumpur (Malaysia) and Bangkok (Thailand). The new modelling approach and the results of the work have been integrated into with the International Study of Highway Development and Management Tools (ISOHDM) in order to provide a model for inclusion into the Highway Development and Management Model version 4 (HDM-4).

Fuel consumption predictions were tested both with and without the impact of a simulated acceleration noise level. For the latter of the two (i.e. a given drive cycle) the predictions were within 0.25 per cent. When including the impacts of a generated drive cycle from a known level of acceleration noise, the results show a consistent under-prediction of some 25 percent when compared with on-road test results. It is believed that this under-prediction is largely due to the assumption of the acceleration noise data conforming to a Normal Distribution.

The research results of the new modelling approach for emissions have been tested against an existing data set of seven vehicles sourced from independent research on Auckland's motorways. Vehicle emissions of carbon dioxide and hydrocarbons were under-predicted by some 50 per cent in relation to the average tested vehicle, but were still well within the range of the seven observed results. Carbon monoxide and oxides of nitrogen were grossly under-predicted and were below the minimum observed values.

The new modelling approach, even with the above limitations, still has wide application in improving the prediction of vehicles operating on highways in congested conditions. The patterns of fuel consumption and emissions are showing the appropriate changes in relation to traffic congestion, and therefore further calibration is required. Furthermore, the model framework readily lends itself to enhancement via adoption of some new sub-models.

DEDICATION

This thesis is dedicated to Michelle, Hamish and to all those who asked along the journey *"how is that thesis coming along Ian?"*.

ACKNOWLEDGEMENTS

This research project is the result of several years of study, into which numerous organisations and individuals have provided a combination of technical and financial assistance. Accordingly, the author would like to acknowledge this assistance and in particular the assistance of those mentioned below.

Firstly, the author wishes to thank his employers, Opus International Consultants, for approving his involvement in both the ISOHDM study and subsequent work towards the completion of this thesis. In particular he wishes to thank those who supported him in the early stages of arranging his secondment to the ISOHDM study team.

The input of his supervisors, Associate Professors Roger Dunn and Dr Robert Raine, who have provided guidance on this research, is most valued. Roger and Robert's advice throughout this research project was most appreciated.

The author also wishes to thank Dr Christopher Bennett for his assistance in arranging the project from the outset, providing invaluable assistance, supplying technical equipment and arranging financing for the early portion of this work.

To his fellow researchers at IKRAM in Malaysia, the University of Birmingham in England, and at Dessau-Soprin in Thailand, the author expresses thanks for both their contributions to his work and to his general enjoyment of his time in these overseas locations. Acknowledgement also goes to Transit New Zealand for approval to utilise their data within this research project.

The author wishes to thank his wife Michelle, who during the course of this work provided support and encouragement from the outset, along with several proof reads, editorial comments and assisted with data collection tasks. And to our son Hamish, you can now have your room to yourself, without the piles of research documentation to play in.

TABLE OF CONTENTS

LIST OF FIGURES

LIST OF TABLES

1 INTRODUCTION

1.1 Background

As motor vehicle volumes increase around the globe, further pressure is placed on limited financial budgets to fund projects that address traffic congestion on the road networks. In order for an appropriate distribution of funds to be obtained, accurate predictions of the various alternative projects are required. This thesis presents a methodology for the evaluation of traffic congestion within the highway evaluation context, wherein the trade-off between accuracy of prediction and simplicity of application of methods needs to be made.

The analysis of congestion has traditionally been confined to either the simplistic concept of increased flows resulting in decreased speeds and increased travel times or the highly complex use of traffic assignment and micro-simulation models. The simple models are often disregarded as being too unsophisticated to warrant use in heavily congested conditions, while the full-scale simulations require so much data to calibrate, that they are unwarranted for many day-to-day projects.

This thesis sets out to fill the middle ground between these two approaches - namely a method of analysing congestion that produces an enhancement on the old "speed-flow" approach, yet does not have the data requirements of the full scale simulation models.

The basic assumption behind the majority of congestion work to date is that of steady state speed conditions. This means that regardless of a vehicle's mean speed, it maintains this speed constantly along the road section, namely, a vehicle travels at a steady 100 km/h or a steady 30 km/h. This assumption greatly simplifies the analysis of operational effects – however, more importantly, it introduces a bias away from undertaking congestion-related work as it under-estimates the costs of congestion.

In particular, most vehicles have an optimum fuel consumption rate at a speed in the range of 40 to 60 km/h, thus reducing speeds from 100 km/h to this level is deemed to be of benefit (offset to some degree by increased travel times). However, if the reason those vehicles having slowed is due to congestion, then it is most likely that those vehicles are no longer travelling at a constant speed and that the additional fuel consumed by the speed fluctuations more than accounts for the benefits identified from steady state principles.

Greenwood and Bennett (1996) indicate that under high congestion levels, fuel consumption for passenger cars can be as much as 30 per cent above the steady speed levels. Earlier work by Greenwood and Bennett (1995b) indicates that for heavy commercial vehicles, this increase may be up to 200 per cent.

This thesis presents the findings of research into the secondary effects of congestion, in particular the effect of non-steady state speed on fuel consumption and vehicular emissions. In particular, the model development was based around the need to introduce reliable congestion modelling into pavement management systems, an area in which the author has spent many years of practice.

To enable the results of the work to be transferable to different locations, mechanistic models have been utilised wherever possible. Mechanistic models predict the effects

of congestion using basic force equations and therefore enable minor variations in vehicle attributes to be modelled.

1.2 Research Goal and Objectives

The intended use of the results of the research is for the evaluation of highway projects. Consequently, the new modelling framework is not intended to be either a highly sophisticated traffic micro-simulation model or a simple steady speed model. Nor is it intended to develop an engine performance model that could be used in vehicle design by the automotive industry. Rather it is the middle ground between these two detailed requirements and the traditionally simple steady speed approach that this research is targeting.

The goal of the research is to develop fuel consumption and vehicle emission models for use in highway evaluation projects, which can estimate the impacts of traffic congestion and the marginal benefits of operational changes.

The objective is to have a new modelling framework that significantly improves the predictive capability in comparison with traditional steady speed models, yet does not require the significant and detailed modelling associated with micro-simulation models.

The focus is to accurately model mid-block congestion that occurs in uninterrupted conditions, and results in a series of 'unsteady waves'. Interrupted flow, such as occurs at traffic signals or at other times, where drivers make deliberate speed changes, are not the focus of this work.

1.3 Tasks

In order to fulfil the objectives of the research various tasks required completion. As is illustrated in Figure 1.1, the work contained in this thesis can be summarised into a number of steps:

1. Determination of factors that influence driving patterns or styles
2. Estimation of the driving profile based on the information in step 1
3. Estimation of the costs associated with the driving profile in step 2
4. Comparison of the costs estimated in step 3, with the equivalent steady-speed costs

As summarised in Figure 1.1 this thesis does not intend to cover all the impacts of traffic congestion, with the particular exclusion of accidents and parts consumption. What is intended, is that this research will yield models suitable to first predict the combined driver-vehicle behaviour under a given range of conditions, and that second the impact of this behaviour on fuel consumption and vehicle emissions will be possible.

The modelling approach is based to a large extent on being able to separate out the deterministic (or steady speed) component from the probabilistic (or variable) component. The former is taken into account through the use of speed-flow curves which yield average speeds for a given traffic flow level, while the latter component is the focus of this research project.

The results presented in this thesis are the outcome of data collection and analysis in the following locations:

- Kuala Lumpur, Malaysia
- Bangkok, Thailand
- Auckland, New Zealand

The study has used a total of some seven vehicles and six drivers, with the primary emphasis being on the passenger car, which dominates the traffic stream during periods of high congestion.

A comparison study of the results of this thesis against independently collected data has also been made to establish the credibility of the results.

To date the results from this research have been incorporated into the HDM-4 project for the international road funding agencies, the New Zealand Project Evaluation Manual (PEM, 1997) (via the NZ Vehicle Operating Cost Model) and is in use around the world in the evaluation of road improvement projects (Opus, 2003).

1.4 Outline of Thesis

The structure of this thesis is contained in Table 1.1. Further information on section makeup within each chapter is included in the Table of Contents.

Table 1.1: Structure of Thesis

Chapter	Contents
2	Background material and literature review in fuel consumption and vehicle emission modelling
3	Measures to describe non-steady speed driving styles
4	Data collection equipment, calibration and use
5	Measuring acceleration noise in Malaysia, Thailand and New Zealand
6	Fuel consumption modelling and testing of the predictions
7	Vehicle emission modelling framework
8	A comparison study of the predicted impact of traffic congestion with independently sourced information
9	Summary of main findings of the research and outline of the overall process and uncertainty
10	Major conclusions of the study and areas recommended for further research
11	Appendices
12	References
13	Glossary

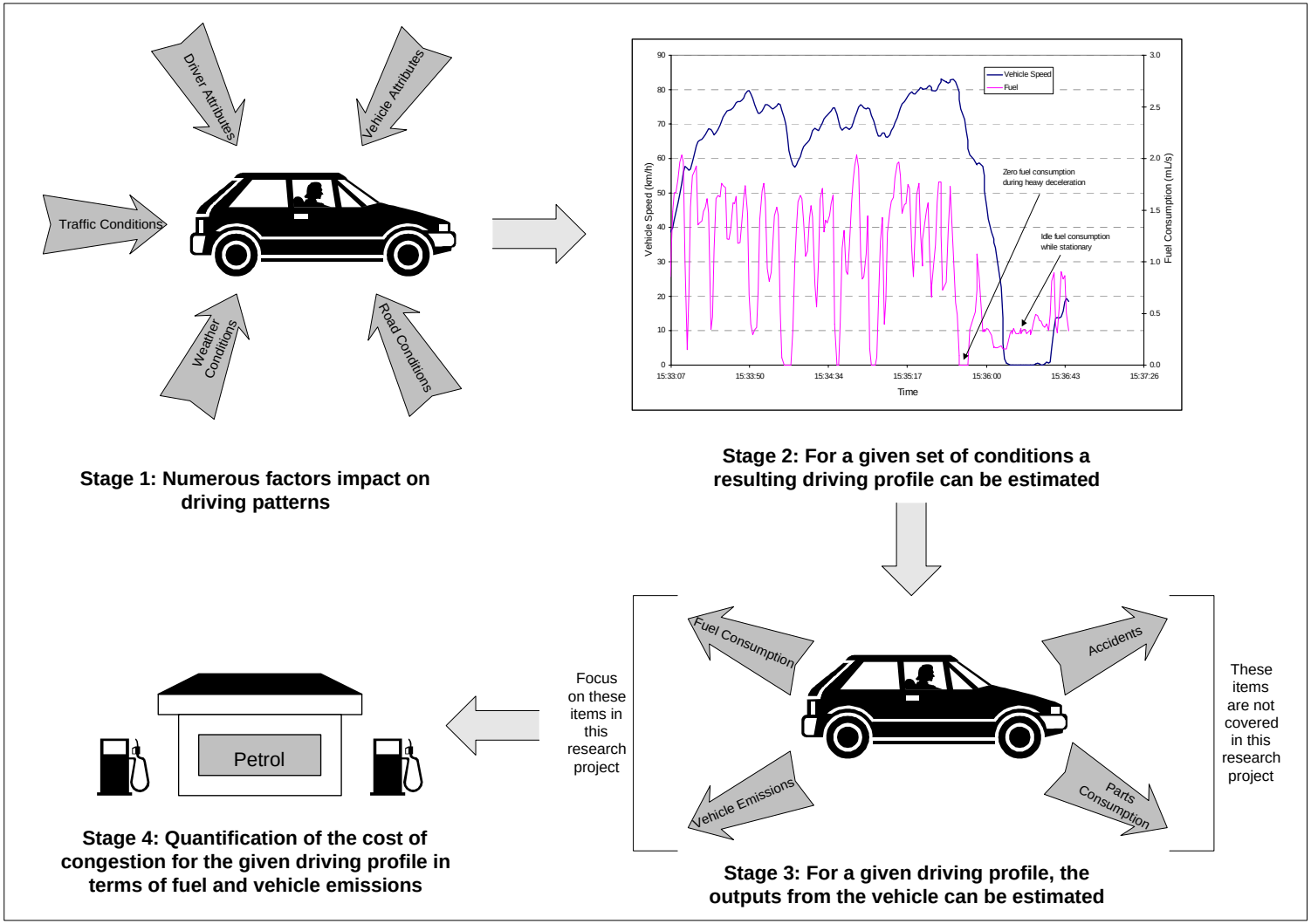

Figure 1.1: Overall Concept of Research Project

2 BACKGROUND AND LITERATURE REVIEW

2.1 Introduction

There are many forms of speed-flow models available to predict the impact of increasing flow on mean vehicle speeds. Models such as the HDM-Q 3-zone model (Hoban et al, 1994) and those in the Highway Capacity Manual (TRB, 2000) are two of the more common generic models in use today. A further discussion on these is contained later in this section, but for now it can simply be concluded that these models are the simplest form of analysis of the effects of congestion on road users.

At the other end of the range of congestion modelling are highly complex simulation packages such as PARAMICS and AIMSUN2, wherein each vehicle is simulated individually, with driver characteristics and network coding requiring many days (if not weeks) of calibration. In between the aforementioned speed-flow models, and these full-scale simulation models lies the area of interest for this research.

Figure 2.1 below describes in broad terms the three levels of detail that are considered to be appropriate for the modelling of traffic congestion. As is discussed in the remainder of this chapter, while plenty of work has been undertaken at the macroscopic and microscopic levels, the mesoscopic alternative has been largely devoid of any significant research.

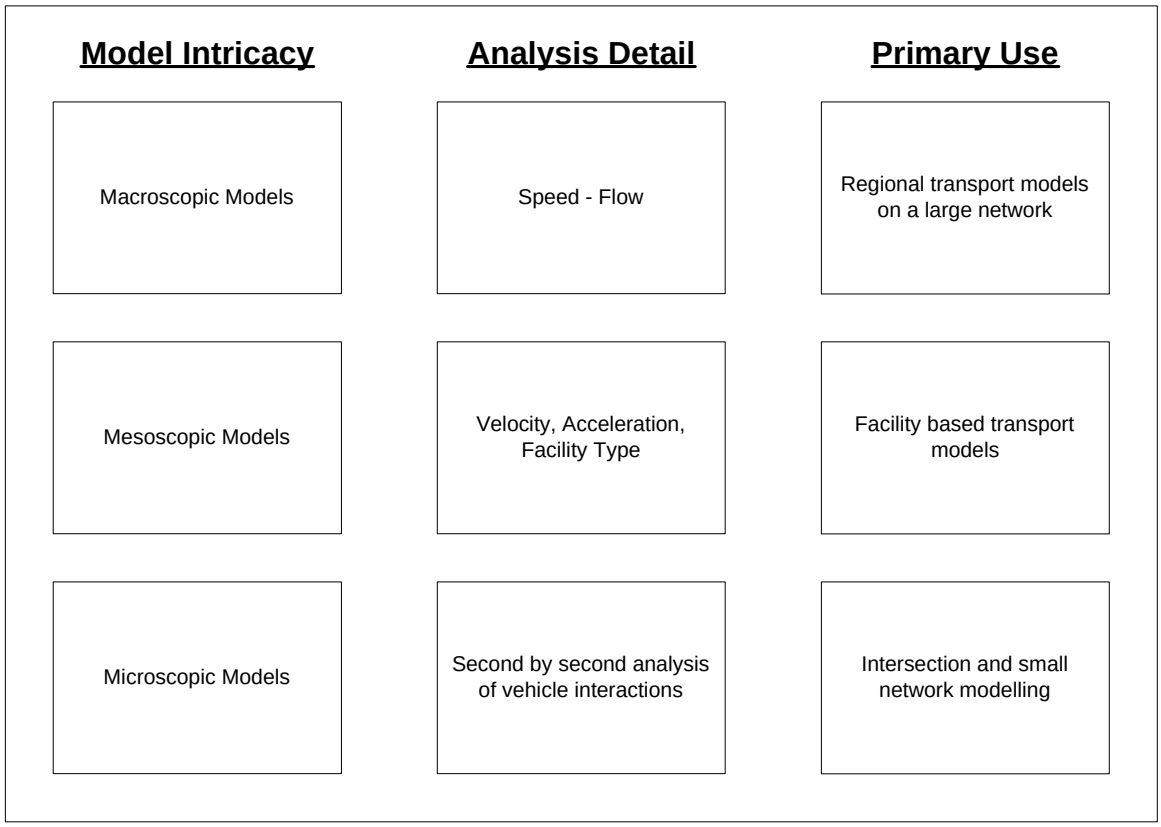

Figure 2.1: Levels of Congestion Analysis

It is anticipated that through research at the mesoscopic level, that much of the benefits of a full scale simulation can be attained, without the cost overheads associated with a microscopic model.

As was illustrated in Figure 1.1, the research in this thesis can broadly be split into two areas:

- the impact of congestion on driver-vehicle combinations
- the impact of the above on fuel consumption and vehicle emissions.

Primary research in this thesis is concentrated on the former, wherein extensive data collection and analysis has taken place. For the latter, fuel consumption has been collected and utilised to calibrate/refine existing models, while the vehicle emissions work has utilised previously published research. The remainder of this chapter presents the results of a literature review on the various topics relevant to the research. The sections approximately follow the main chapters of this thesis.

Additionally, this chapter presents an overview of various technical measurements that are used, but not discussed elsewhere in this thesis.

2.2 Speed-Flow Models

As noted by Greenwood and Bennett (1995b), one of the traditional means of analysing congestion effects is through the use of speed-flow models. These models provide a method of estimating an average vehicle speed for a given flow rate (often used in terms of a volume to capacity ratio) and are termed as macroscopic models.

Many forms of speed-flow models are described in documents, from the smooth curves of the Highway Capacity Manual (TRB, 2000), to models containing various distinct sections such as the three-zone model proposed by Hoban et al (1994). The Hoban et al (1994) model is that adopted for the HDM-4 pavement management model (NDLI, 1995 and Bennett and Greenwood, 2001).

It is noted that with all these various models, there is in general a large variation in speeds for any given mean speed. Bennett (1994), recommended that the coefficient of variation[1] of vehicle speeds based on New Zealand data is in the range of 0.14 to 0.16, although some sites had values as high as 0.25 for certain vehicle classes. A value of 0.15 indicates that for a mean speed of 100 km/h, actual speeds in the range of 70 to 130 km/h would be expected (allowing for two standard deviations from the mean).

Although it is possibly a better technical solution to use continuous smooth functions as presented in the Highway Capacity Manual, the simplifications enabled by adopting the three-zone model as presented by Hoban et al (1994) have resulted in this model being used for the remainder of this thesis. The actual form of the model and recommended parameter values from the HDM-4 report (NDLI, 1995) are presented in Figure 2.2 and Table 2.1.

[1] The coefficient of variation is defined as the standard deviation divided by the mean. For vehicle speeds, this parameter has been found to be very stable both within a region and internationally (Bennett, 1994).

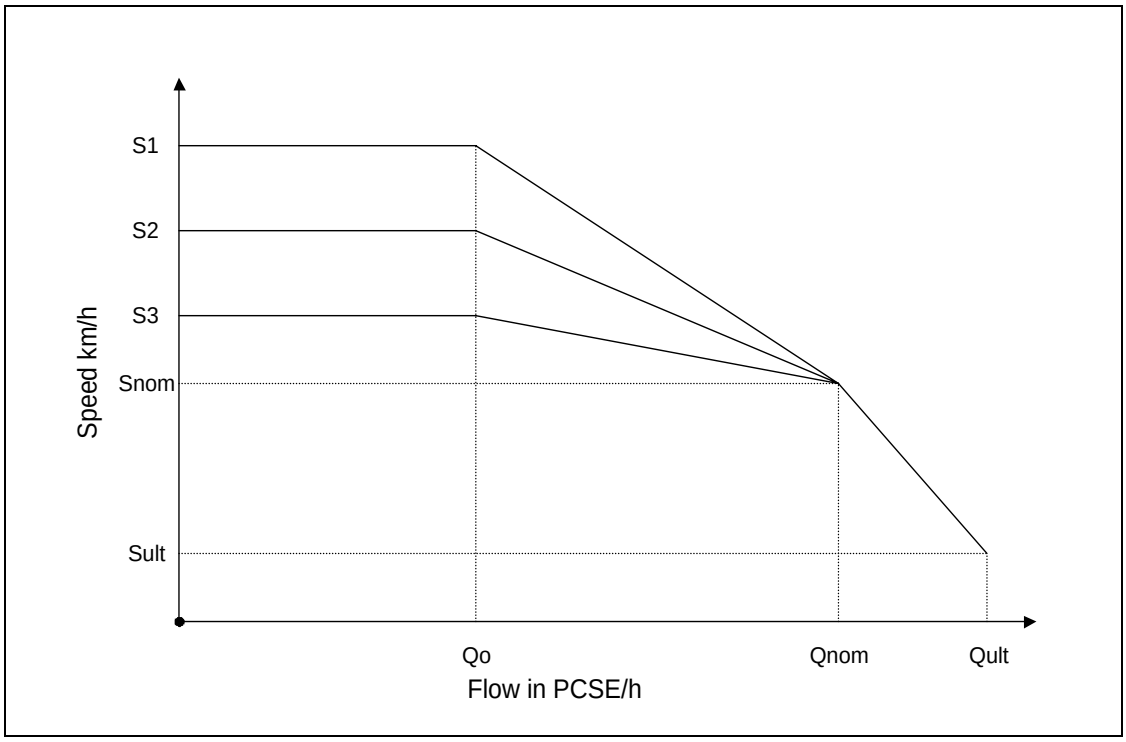

Source: NDLI (1995)

Figure 2.2: Standard Notation of Three-Zone Speed-Flow Model

In Figure 2.2, the notation is as follows:

Qo	flow level below which traffic interactions are negligible in PCSE/h
Qnom	the nominal capacity of the road in PCSE/h
Qult	the ultimate capacity of the road in PCSE/h
Snom	the speed at the nominal capacity in km/h
Sult	the speed at the ultimate capacity in km/h
S1 to S3	free flow speeds of different vehicle types in km/h
PCSE	are passenger car space equivalents (see below)

The use of the passenger car space equivalent value, as opposed to using vehicles or passenger car units, enables the model to separately deal with the speed impact of differing vehicles and differing flow levels.

Table 2.1: Parameter Values for the Three-Zone Speed-Flow Model

Road Type	Width (m)	Qo (PCSE/h)	Qnom (PCSE/h)	Qult (PCSE/h)	Sult (km/h)
Single Lane Road	< 4	0	420	600	10
Intermediate Road	4 to 5.5	0	420	1800	20
Two Lane Road	5.5 to 9	280	2520	2800	25
Wide Two Lane Road	9 to 12	640	2880	3200	30
Four Lane Road	>12	3200	7600	8000	40

Source: Adapted from Hoban, et. al. (1994)

Bennett (1999), in calibrating the HDM-4 speed-flow model for use in Thailand found that the above default parameter values were suitable for all road types except the four lane road where much higher capacities were recorded.

2.3 Speed-Flow-Density Relationship

One of the primary laws of traffic is that which relates speed to flow and density. It is often conceptually easier to understand when flow is expressed as the product of speed (being the speed of a single vehicle) and density (being the number of vehicles per given distance). It is calculated at a point in space over a period of time, which as noted later when considering measures such as headway (the inverse of density), can have significant impacts on the resulting value.

The primary relationship is therefore presented as Equation 2.1 below.

$$\text{Speed} = \text{Flow} / \text{Density} \qquad (2.1)$$

where Speed is the mean vehicle speed in km/h
Flow is the vehicle flow in veh/h
Density is the vehicle density in veh/km

Of interest is that these three factors are measured over a combination of time and space. For instance to measure speed requires both a change in distance and time, to measure flow requires a change in time, while to measure density requires a change in distance.

The above relationship is therefore reliant on average values, which remain constant over time and space, in order to yield correct answers. It is not possible to calibrate the above relationship either at an instant in time, or at a specific location on the road. This is discussed further in the following section on vehicle headways.

2.4 Vehicle Headways

Vehicle headways is a term that is normally applied to a vehicle stream. Gaps between vehicles are often approximated with vehicle headway data and is commonly utilised in intersection analyses. For an analysis of this type, many of the idiosyncrasies of the actual definition and measurement can be ignored, as their impact on the overall distribution of headways is minimal. However, when considering the interaction between a single pair of vehicles, the impact of the definition and measurement of headway becomes more important and is therefore discussed below.

The definition of vehicle headways is the time difference from when one vehicle crosses a point on the road, to when the following vehicle crosses that same point. The definition is sufficiently loose so as to not directly dictate whether the measurement should be from the front of one vehicle to the front of the next, or from the rear of the lead to the rear of the next, or to some other combination. With the use of traffic counters often used to collect data on vehicle headways, the primary in-use definition of headways is the time from the front axle on the lead vehicle to the time the front axle of the following vehicle cross the same count station.

In theory it is not possible to measure vehicle headways without making an assumption of continued uniform travel speed by both the leading and following vehicles, as the definition is essentially one of measuring a time at a point. As this research project is based around the fact that vehicles do not maintain a constant speed, the above assumption is also invalid, hence the accurate measurement of headway is also not possible. This concept is discussed more below.

Consider two vehicles in the configuration shown in Figure 2.3 below. As is demonstrated in the calculations, even with a moderately small speed difference of 5 km/h between the two vehicles, by the time the headway can be measured, it has already changed by approximately 10 per cent.

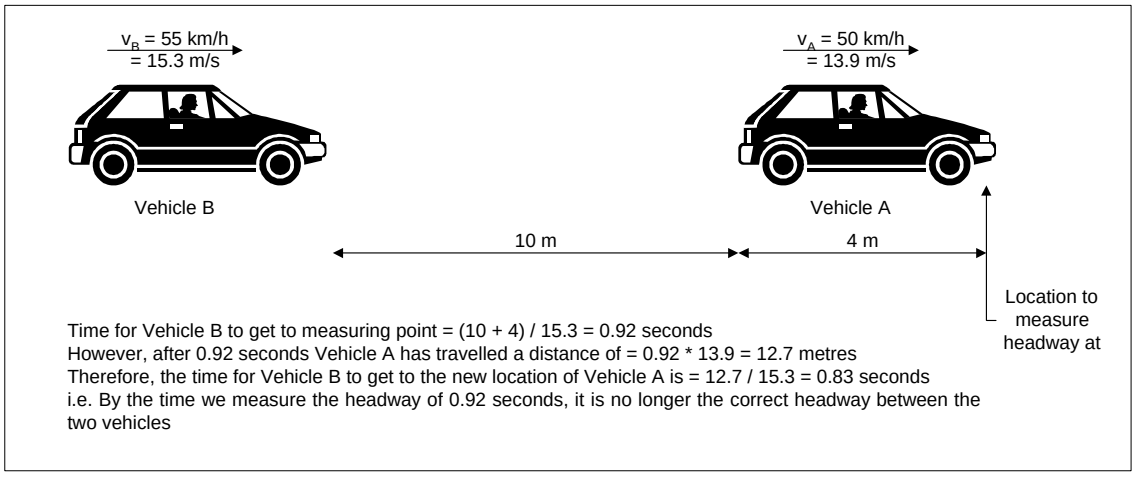

Figure 2.3: Calculation of Vehicle Headways

Another issue with the use of headways is that of vehicles with varying lengths. As noted previously in this section, the headway is measured from a point on one vehicle to the matching point on the next. Typically this is front bumper to front bumper, or front axle to front axle, although measuring rear bumper to rear bumper is equally valid within the definition of headways.

Consider the case of a large bus being followed by a car as illustrated in Figure 2.4. Dependent on which two locations are chosen, two different answers are arrived at for the headway between these two vehicles. These two values have a variation of some 25 per cent, indicating the significant impact of measurement definition.

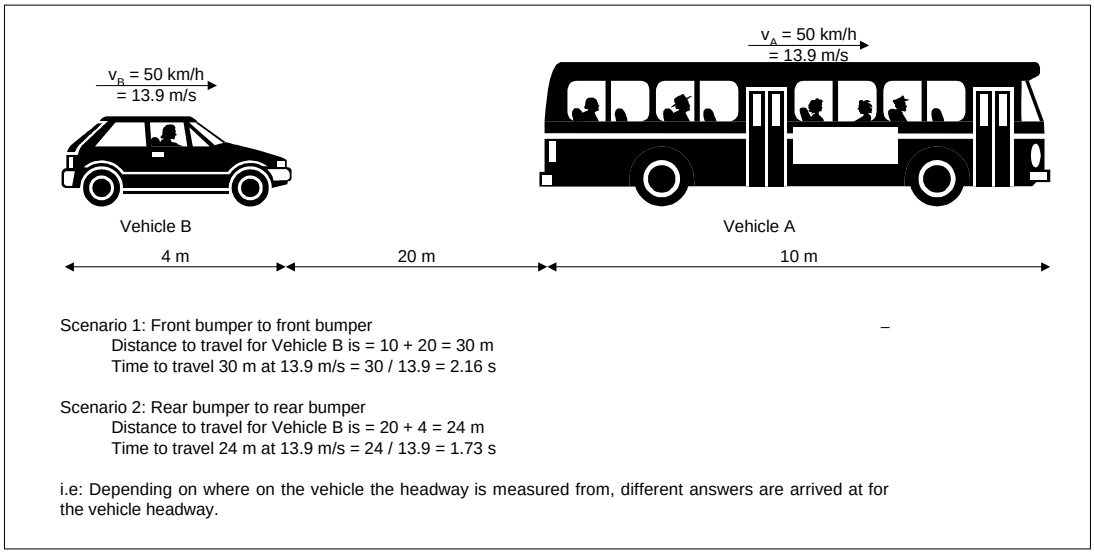

Figure 2.4: Effect of Vehicle Length on Headways

The situation outlined in Figure 2.4 above is generally not a problem when dealing with a long period of time, where only average headways, or headway distributions are required. If one considers three vehicles in a platoon, then the measuring point may alter the actual headways reported between the two pairs of vehicles. However, differing locations will result in an increase in one headway and a decrease in the other, therefore yielding an overall result for a large number of vehicle combinations that is somewhat independent of measuring location.

In summary then, the following conditions need to be met in order to state the headway between two vehicles:

- both vehicles have the same speed
- this speed is maintained until both vehicles have passed the measuring location
- both vehicles have the same length

Any variations on the above will result in some level of ambiguity in the resultant headway measurement between two consecutive vehicles.

Having discussed the theoretical problems with the measurement of headways, this measure is still both commonly used and of practical use when dealing with a stream of vehicles. Bennett (1994) discussed the various forms of the headway model including the history of development from simple model forms through to complex models.

The irony of the headway measurement is that it is primarily of interest in congested networks, where its accuracy is lowest owing to non-adherence to the above conditions. Given the above issues arising from the use of headways, it is decided that this unit of measurement is inappropriate for inclusion as a key parameter in this research.

2.5 Vehicle Spacing

Vehicle spacing is defined as the distance in metres between a point on one vehicle and the matching location on the next, measured at a point in time. Vehicle spacing has fewer conditions to meet than that of headways discussed prior, although the issue surrounding the vehicle length that is presented in Figure 2.4 still remains.

Owing to the difficulty in measuring vehicle spacing[2] this measure tends to be calculated or inferred from other measures, but not directly used. When averaged over a number of vehicles, this measure forms the reciprocal of vehicle density.

2.6 Gap Between Vehicles

Of interest in the modelling work of this thesis is the impact of the physical gap existing between two vehicles. This distance excludes the length of the vehicle and is measured at a point in time.

Measurement of the gap between vehicles can either be made from an aerial photograph to yield an average gap value, or by an instrument such as a laser device that can provide continuous distance readings.

It was noted in Greenwood, et al. (1998) that:

> *"The distance to the vehicle in front is expected to play an important role in determining driver characteristics, especially acceleration habits".*

It is anticipated that the effect of the gap size and the type of vehicles involved in the combination (i.e. type of vehicle being followed and type doing the following) would be a significant component in the modelling of vehicle accelerations.

2.7 Fuel consumption models

2.7.1 Introduction

As was noted in Greenwood and Bennett (1995a), research into the fuel consumption of motor vehicles has been undertaken almost since they were first invented. Greenwood and Bennett (1995a) go on to state that initially researchers used coarse empirical data (e.g. de Weille, 1966) to produce fuel consumption models, these were then superseded by experimental studies that related the fuel consumption to operating conditions (i.e. gradient, roughness, speed, etc.).

The models developed from these studies are often termed *empirical models*. The recent approach has been to utilise *mechanistic models*, wherein the fuel consumed is related to the efficiency of the engine in converting fuel to energy and the forces opposing motion.

Greenwood and Bennett (1995a) stated that mechanistic models are considered to be markedly superior to empirical models in that they directly account for the individual vehicle characteristics and the forces acting on the vehicle. As a result of this work, it was concluded that only mechanistic models would be considered for this research project.

[2] Realistically the only means of measuring vehicle spacing is through the use of an aerial photograph or similar view from a still frame of a high mounted video camera etc.

Suzuki (1997) states that in an attempt to regain market share in 1979, GM Corporation invested US$2.7 billion to develop a car that had significantly lower fuel consumption. The factors that they chose to address in reaching this goal are shown in Figure 2.5. As a result of this development, GM developed a front-engine front-wheel drive vehicle known as the "X Car". Suzuki (1997) indicates that owing to reliability problems, the development of the X Car was not a great success in regaining market share, although a substantial reduction in weight of around 24 per cent was realised.

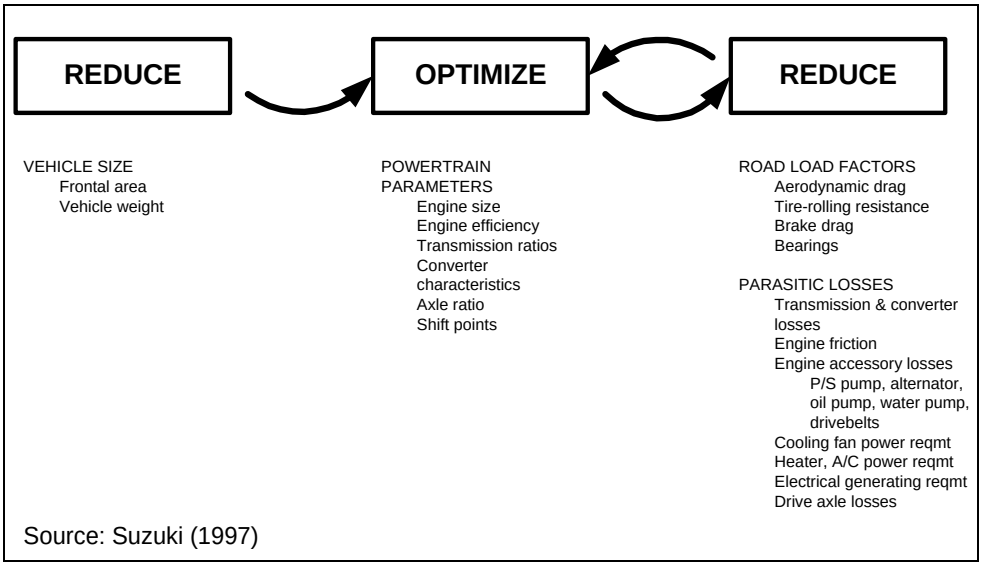

Figure 2.5: GM's Technical Measures for Reducing Fuel Consumption

The National Research Council (NRC, 1992) states that fuel economy of the average car in the USA improved from 15.8 mpg to 27.8 mpg (6.7 km/L to 11.8 km/L) over the period 1975 to 1991. This is an improvement of around 76 per cent and the NRC (1992) state that the following factors accounted for this improvement:

- a reduction in vehicle weight
- changing from rear wheel to front wheel drive
- decrease in exterior dimensions of vehicles (interior size remained relatively unchanged)
- using lightweight aluminium and plastic materials
- improvements in engine efficiency
- better aerodynamic design
- increased drivetrain efficiency
- reductions in rolling resistance and other frictional losses.

Of these changes, the majority are modelled through changes to the physical attributes of the vehicle, which directly influence the tractive power required from the engine (refer to Chapter 6.3). The rest of this section presents a brief review of some of the major fuel consumption models in use internationally. The models have been grouped into empirical and mechanistic based models.

2.7.2 Empirical Models

The early empirical models related fuel consumption principally to vehicle speed (Greenwood and Bennett, 1995a). A number of studies found that the relationship between fuel consumption (per unit distance) and vehicle speed is U-shaped. There are relatively high fuel consumption rates at both low and high speeds with the minimum fuel consumption arising at an "optimum" speed, generally around 40 to 60 km/h.

The common empirical formulation for fuel consumption is given by Equation 2.2 (Chesher & Harrison, 1987 and IRC, 1993) :

$$FC = a0 + \frac{a1}{S} + a2\ S^2 + a3\ RISE + a4\ FALL + a5\ IRI \qquad (2.2)$$

where FC is the fuel consumption in L/1000 km
S is the vehicle speed in km/h
IRI is the international roughness index in m/km (or mm/m)
RISE is the rise of the road in m/km
FALL is the fall of the road in m/km
a0 to a5 are constants

The coefficients established for the above model from studies in the Caribbean, India and Kenya for different vehicles are given in Table 2.2. Figure 2.6 is an example of the effect of speed on the predictions for passenger cars using these coefficients. It shows that there are marked differences in the speed effects for the different vehicle types, not only between countries but also for different vehicles in the same country. As will be shown in the section describing mechanistic modelling, this is a reflection of the physical properties of the different vehicles.

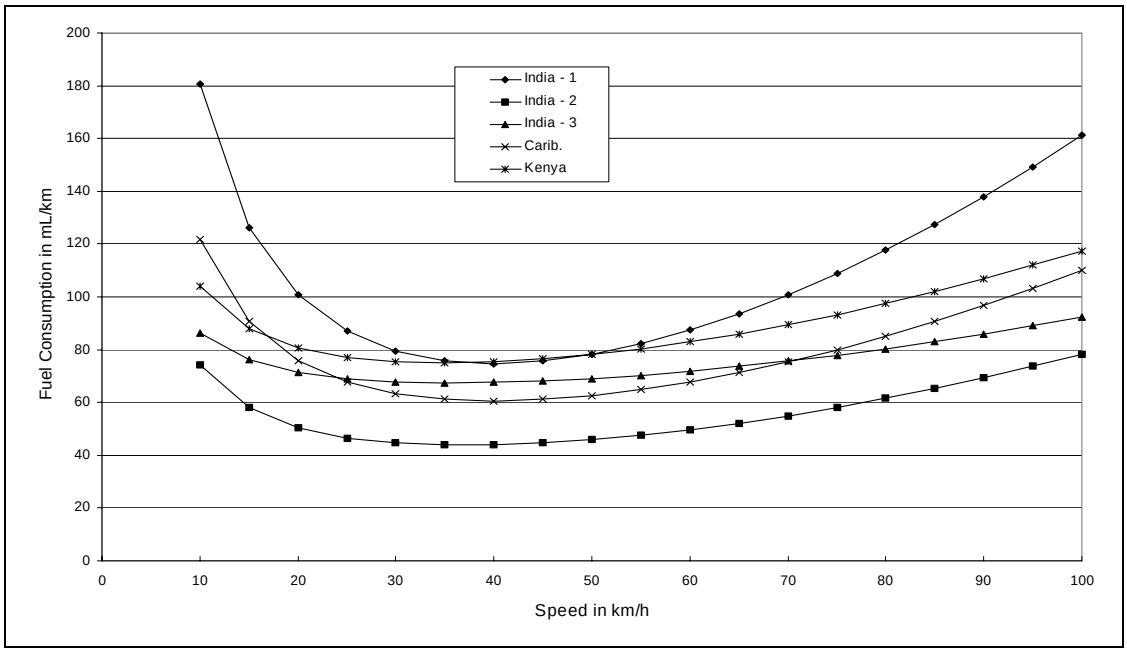

Figure 2.6: Effect of Speed on Passenger Car Fuel Consumption

Table 2.2: Coefficients Estimated for Empirical Fuel Consumption Model

Vehicle	Country	a0	a1	a2	a3	a4	a5	Other Variables	Source
Passenger Cars	India	10.3	1676	0.0133	1.39	-1.03	0.43		Chesher & Harrison (1987)
	India	21.85	504	0.0050	1.07	-0.37	0.47		IRC (1993)
	India	49.8	319	0.0035	0.94	-0.68	1.39		Chesher & Harrison (1987)
	Caribbean	24.3	969	0.0076	1.33	-0.63		+ 0.00286 $FALL^2$	Chesher & Harrison (1987)
	Kenya	53.4	499	0.0059	1.59	-0.85			Chesher & Harrison (1987)
Light Commercials	India	30.8	2258	0.0242	1.28	-0.56	0.86		Chesher & Harrison (1987)
	India	21.3	1615	0.0245	5.38	-0.83	1.09		IRC (1993)
	Caribbean	72.2	949	0.0048	2.34	-1.18		+ 0.0057 $FALL^2$ + 1.12 (GVW - 2.11) RISE	Chesher & Harrison (1987)
	Kenya	74.7	1151	0.0131	2.91	-1.28			Chesher & Harrison (1987)
Heavy Bus	India	33.0	3905	0.0207	3.33	-1.78	0.86		IRC (1993)
	India	-12.4	3940	0.0581	0.79		2.00	+ 0.0061 CKM	Chesher & Harrison (1987)
Truck	India	44.1	3905	0.0207	3.33	-1.78	0.86		IRC (1993)
	India	141.0	2696	0.0517	17.75	-5.40	2.50		IRC (1993)
	India	85.1	3905	0.0207	3.33	-1.78	0.86	- 6.24 PW	Chesher & Harrison (1987)
	India	266.5	2517	0.0362	4.27	-2.74	4.72	-6.26 PW	Chesher & Harrison (1987)
	India	71.70	5670	0.0787	1.43			- 9.20 PW - 3.98 WIDTH	Chesher & Harrison (1987)
	Caribbean	29.2	2219	0.0203	5.93	-2.60		+ 0.85 (GVW - 7.0) RISE + 0.013 $FALL^2$	Chesher & Harrison (1987)
	Kenya	105.4	903	0.0143	4.36	-1.83		-3.22 PW	Chesher & Harrison (1987)

2.7.3 Mechanistic Models

Mechanistic models predict that the fuel consumption of a vehicle is proportional to the forces acting on the vehicle. Thus, by quantifying the magnitude of the forces opposing motion one can establish the fuel consumption. Mechanistic models are an improvement over empirical models since they can allow for changes in the vehicle characteristics and are inherently more flexible when trying to apply the models to different conditions.

Because of their numerous advantages over empirical models, mechanistic models were preferred for use in this research project and in HDM-4 (Bennett and Greenwood, 2001).

One of the more comprehensive mechanistic fuel consumption models available is the ARFCOM model (Biggs, 1988), and its approach is summarised in Figure 2.7. This shows how the total power requirements are based on the tractive forces, the power required to run accessories, and internal engine friction. The fuel consumption is then taken as proportional to the total power requirements.

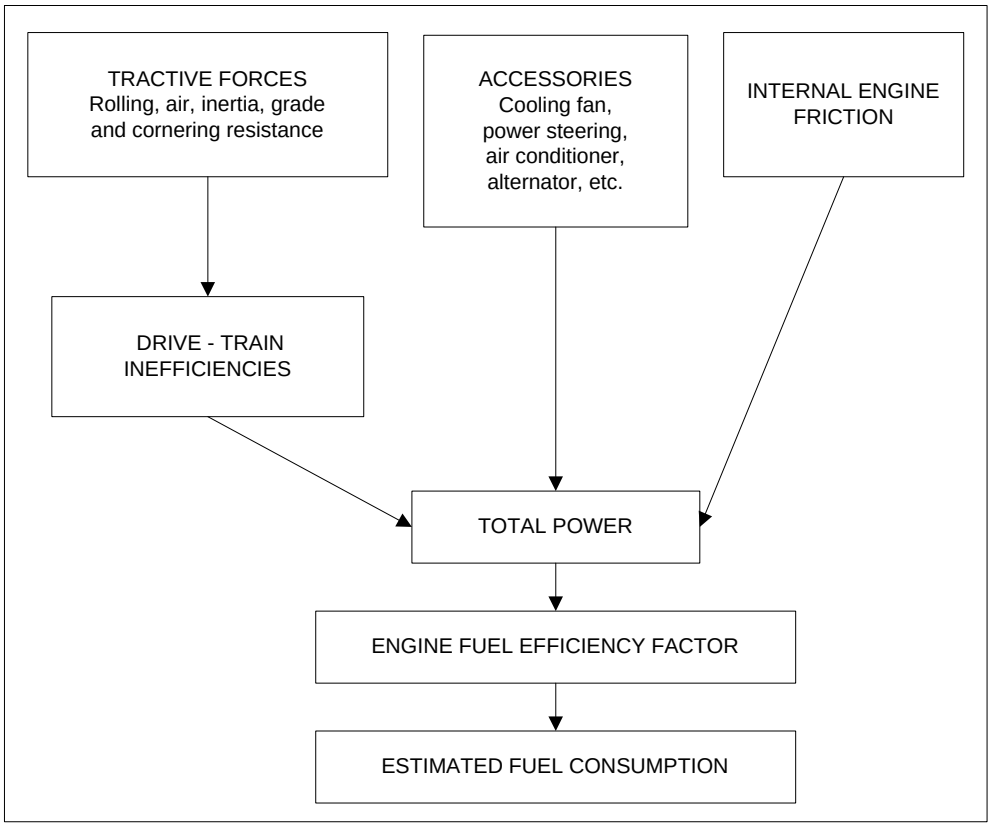

Figure 2.7: ARFCOM Approach to Modelling Fuel Consumption

Greenwood and Bennett (1995a) noted that there have been three major studies that developed mechanistic models: the HDM-III study (Watanatada, et al. 1987a), research in South Africa (Bester, 1981), and research in Australia (Biggs, 1987 and 1988). As described by Greenwood and Bennett (1995a), all have similarities in that they use the magnitude of the forces opposing motion as the basis for the predictions.

With the South African and Australian models, fuel experiments or other data were used to calculate an efficiency factor ξ. The efficiency factor is utilised to convert the total power requirements to fuel consumption and has been found to be dependent upon fuel type, engine size and power output. The fuel consumption is the product of the total power requirements and this factor. The ARFCOM model offers improved predictions over the South African model through explicitly considering the fuel required to maintain engine operation.

The HDM-III model in many respects is a hybrid mechanistic model. Although it uses the forces opposing motion as the basis for its calculations, it resorts to the use of a series of regression parameters to convert the forces to the fuel consumption. Unlike the South African model, it explicitly considers engine speed.

It is the ARFCOM model that NDLI (1995) recommended for inclusion into the HDM-4 system. Greenwood, et al. (1998) highlighted several deficiencies in the model proposed for HDM-4 brought about by recent vehicle technologies. In particular the ability of modern vehicles to run at zero fuel consumption for short periods of time is not currently included in the HDM-4 fuel consumption model (NDLI, 1988 and Odoki and Kerali, 1999).

This particular issue can occur when in heavy periods of deceleration (such as observed in congested conditions) or on steep downgrades, where the engine essentially acts as a brake. It is therefore necessary to ensure the fuel consumption model can accurately predict under congested conditions.

2.7.4 Summary

Based on the review, it was decided to utilise mechanistic modelling wherever possible. After reviewing the three groups of mechanistic models, their appropriateness for modelling various tasks was questioned. These tasks and questions were:

1. **Forces opposing motion:** can the model predict the fuel consumption using different equations for predicting the magnitude of the forces opposing motion?
2. **Internal vehicle forces:** does the model explicitly consider the fuel required overcoming the internal vehicle forces such as engine drag?
3. **Engine speed**: does the model explicitly consider engine speed effects?
4. **Appropriate for acceleration fuel consumption:** can the model be used to predict the fuel consumption during acceleration and deceleration?
5. **Transferable to different vehicles**: how suitable is the model for being applied to different vehicle technology?

The results of this assessment are given in Table 2.3. It can be seen that the model that offered the greatest potential for meeting the varied requirements of this research was ARFCOM. Accordingly, ARFCOM was selected as the basis for the fuel consumption model. The sections that follow discuss the implementation of ARFCOM into this research project.

Table 2.3: Assessment of Mechanistic Models

Fuel Model	Forces Opposing Motion	Internal Vehicle Forces	Engine Speed Effects	Appropriate for Acceleration Fuel	Transferable to Different Vehicles
HDM-III	•		•		
South African	•			•	•
ARFCOM	•	•	•	•	•

Source: Greenwood and Bennett (1995a)

2.8 Measures of Unsteadiness

A key focus of this research project is that under congested conditions, drivers do not maintain constant speed. In order to quantify the level of unsteadiness present in a traffic stream, it is necessary to utilise a parameter that reflects this facet of the traffic stream.

Parameters available for measuring the level of non-steady driving can relate to either primary aspects, such as vehicle speed and acceleration, or to some secondary measure such as vehicle power requirements or fuel consumption. To enable a mechanistic model to be developed, wherein the result is transportable between vehicle technologies and geographic locations, it is necessary to utilise the former of these approaches.

With regard to vehicle speed and accelerations, a range of variables exist that could potentially yield some quantification as to the level of unsteadiness present in the traffic stream - in particular, the following values would all yield a measure considered to quantify the unsteady component:

- maximum difference in speeds
- maximum absolute acceleration (either +ve or –ve)
- maximum variation in accelerations
- sum of positive accelerations (positive kinetic energy)
- standard deviation of speeds
- standard deviation of accelerations (acceleration noise)

It is important to remember that the method is to be used only in measuring the level of variability in speeds about some average speed, and is not to be used in situations where deliberate changes in average speed occur.

The above “maximum” options are considered inappropriate, in that they cannot distinguish between a one-off significant change in speed followed by constant speed, and a similar one-off event followed by more significant variations. These measures were, therefore, discarded from further consideration.

The use of the positive kinetic energy (PKE) approach has had wide spread use by many researchers (eg Watson, 1995; Haworth et al, 2001, Milkins and Watson, 1983). This approach, while of use in many circumstances, cannot discern between a number of small accelerations (as occur under non-congested conditions) and a

one off large acceleration. The use of PKE, as the name suggests, focuses on the positive acceleration portion of the drive cycle and consequently is unable to determine what period of the time the decelerations are significantly large to enable the vehicle to run at zero fuel consumption (refer to Section 6.4.6), a situation that can occur under heavily congested conditions.

The follow-on issue associated with the inability to distinguish between a number of small accelerations or one large acceleration, is that it is not possible to confidently recreate the driving profile within a simulation programme. As a consequence of the above issues, it is considered that the use of PKE is not appropriate as a basis for the development of this modelling approach.

The decision on whether to use the distribution of speeds or accelerations is best determined by consideration of the overall modelling framework (refer to Figure 1.1). Under this framework, the prediction of fuel consumption is a two-step process. Firstly the steady speed fuel consumption is predicted and secondly the incremental increase from non-steady (congested) driving is added. Based on this, it is considered that the use of the distributions of accelerations is more appropriate, as it better aligns to the overall modelling framework.

The use of acceleration noise also readily lends itself to inclusion into simulation packages, wherein drive cycles can be generated to model the impact of congestion. It also aligns well with the adopted fuel consumption model (refer Section 2.7)

2.9 Vehicle Emissions

2.9.1 Introduction

Vehicles emit various chemical compounds as a direct result of the combustion process. The type and quantity of these emissions depends on a variety of factors including the tuning of the engine, fuel type and driving conditions. When dealing with vehicle emissions, researchers focus primarily on the following substances; hydrocarbons (HC), carbon monoxide (CO), carbon dioxide (CO_2), oxides of nitrogen (NOx), sulphur dioxide (SO_2), lead (Pb) and particulate matter (PM). These compounds are considered to not only form the majority of the emissions, but also form the most damaging to the natural environment and human health.

Heywood (1997) states that in the United States, vehicles are estimated to produce about 40 to 50 per cent of the HC, 50 per cent of the NOx and 80 to 90 per cent of the CO emissions in urban areas. The effect of these emissions both locally and globally is of growing concern, and thus it is imperative that in the evaluation of road options, the effect on vehicle emissions can be accurately modelled.

Although not a primary concern of this research, the above emissions are reported to create or add to a range of environment problems as set out in Table 2.4 (EPA, 1997). Patel (1996) estimates that around 40,000 deaths per year in India's major cities are caused by air pollution.

Table 2.4: Emissions and their associated Problems

Emission	Problems Caused by Pollutant
Hydrocarbons	Urban ozone (smog) and air toxics
Carbon monoxide	Poisonous gas
Oxides of nitrogen	Urban ozone (smog) and acid rain
Carbon dioxide	Global warming
Particulate matter	Carcinogenic, lung damage

Source: EPA (1997)

Paterson and Henein (1972) quoted Dr John Middleton as stating in 1968:

> *"The day may soon come – if it's not already here – in which the individual automobile can no longer be tolerated as a convenient form of transportation, simply because of its adverse effects on the health of people, not just the aesthetic of the atmosphere."*

In response to this issue, which is just as strong today, many countries have signed agreements to reduce their total emission levels, with particular focus on those emissions coming from motor vehicles. Since the 1960s when the above quote was taken, the desire to improve the emission output of vehicles has resulted in substantial reductions. Heywood (1997) shows that the average production of vehicle emissions in modern vehicles is around 2 to 10 per cent of the levels recorded in the 1960s prior to emission controls. This reduction is in response to ever-stricter standards placed on vehicle manufacturers, which have responded with technology such as catalytic converters and cleaner burning fuels.

Heywood (1997) states that *"it sounds too simple to say half the total fleets' CO and HC emissions come from the worst 10 percent of the vehicles on the road, but it is indeed true!"* For this to be the case, there is clearly a significant variation in the quantity of emissions coming out of seemingly similar vehicles. Any predictive models will therefore need to either recognise this distribution, or clearly be used to predict average conditions only.

For estimating regional or national emissions the use of average emission rates is quite acceptable, and, owing to their generally simplified mathematical form, even preferable for such tasks. The USA Environmental Protection Agency (EPA) gives the following average emission values for a passenger car and a light truck (EPA, 1997). The data in Table 2.5 is based on an annual usage of 17,700 km (11,000 miles) and 22,500 km (14,000 miles) for the passenger car and light truck respectively.

Table 2.5: Annual Emissions and Fuel Consumption for a Passenger Car and a Light Truck.

Vehicle	Pollutant	Average Amount[1] g/km	Average/year[1] kg/year
Passenger Car	Hydrocarbons	1.9	34.0
	Carbon monoxide	14.3	262.7
	Oxides of nitrogen	1.0	17.7
	Carbon dioxide	225.5	3992.0
	Gasoline	88	1561.3
Light Truck	Hydrocarbons	2.5	57.2
	Carbon monoxide	19.9	447.7
	Oxides of nitrogen	1.2	28.1
	Carbon dioxide	338.3	7620.5
	Gasoline	123.5	2782.0

Source: EPA (1997)
Notes: 1. Values converted from g/mile and lbs/year.
2. Conversion rates of 1 gallon = 3.785 litres and a specific gravity of 0.75 for gasoline were used

Unlike many commodities, such as computers, where life is measured in months, motor vehicles are durable with lives often greater than 20 years. This long life has a marked impact on the overall effectiveness of new technologies. Typically less than 10 per cent (LTSA, 2000 and BTCE, 1996) of all cars are newly registered each year. As noted in BTCE (1996), any innovation in vehicle technology that improves the fuel or emission performance of new vehicles will therefore take several years to affect a sizeable proportion of the total fleet.

Assuming that a sudden improvement in efficiency of 50 per cent was achieved for new vehicles, then after one year the overall impact on the total fleet would be less 5 per cent. The up side of this long gestation period, is that a greater level of stability in fleet characteristics can be assumed by the modeller.

It is noted that some characteristics that differentiate between old and new technology, such as fuel efficiency and tyre rolling resistance, can already be addressed within the current modelling framework through the appropriate selection of parameter values.

2.9.2 Levels of Analysis Detail

Bennett and Greenwood (2001) presented the recommended vehicle emission model framework for the pavement management system HDM-4. Bennett and Greenwood (2001) noted that as with most items that are modelled, a range of levels of sophistication is available for the modelling of vehicle emissions. An, *et al. (*1997) present the following diagram that relates the type of emission model to various levels of transportation models. This is similar to that presented in Figure 2.1, with the HDM-4 model best equated to the mesoscopic/macroscopic level, compared to the microscopic simulation modelling within the HDM-4 Tools ACCFUEL[3] program.

[3] ACCFUEL is one of the HDM Tools suite of software programs written by the author. It is used to simulate vehicle accelerations for estimating the effects of speed cycles on fuel and tyre consumption. Further details are given in Section 5.6.

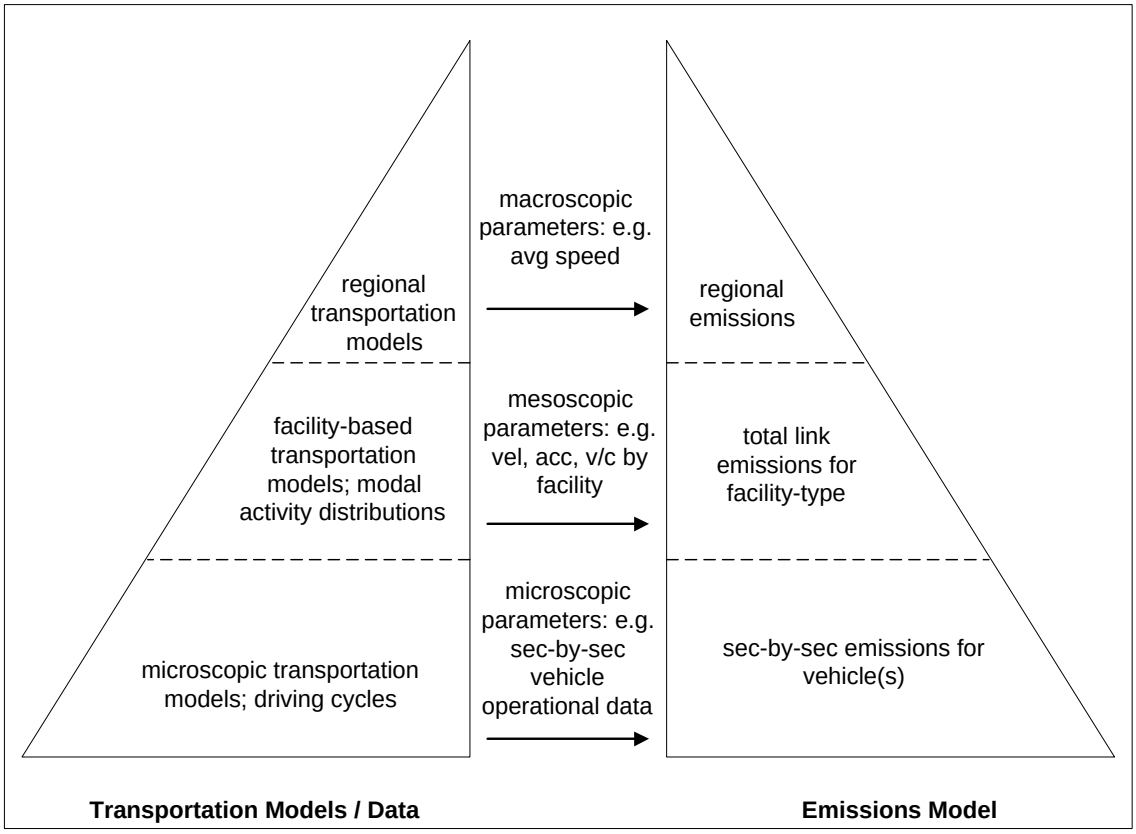

Source: An, et al. (1997)

Figure 2.8: Transportation/Emission Model Interface

By considering the required level of sophistication desired in the output, one can set about collecting the appropriate input parameters. For instance, when evaluating two broad investment regimes, the collection and calibration of second by second data will generally be unwarranted, in which case the use of emission rates based on road link parameters will be sufficient. However, when evaluating various widening scenarios for capacity improvement projects, the use of second by second data should be considered.

2.9.3 Factors Influencing Emissions

Petrol versus Diesel Engines

There is a significant variation in the quantity of the various emissions produced between petrol and diesel engines. These variations arise as a consequence of the differences in both the raw fuel and the means by which it is combusted.

Petrol engines operate at significantly different temperatures and pressures to diesel engines, which in turn influences the production of a number of vehicle emissions. In addition to this variation caused by the differing combustion methods, the chemical makeup of petrol and diesel are also different.

The models presented in the remainder of this chapter have been generated to enable the same basic model form to represent both petrol and diesel emissions. The consequence of this is that in some locations values of zero (or one) are used to effectively turn models 'off' in situations where they would be inappropriate.

Hot versus Cold Emissions

One of the major influences on the level of emissions produced from vehicles is that of engine and catalyst temperature. Once an engine is warm, its efficiency improves resulting in a cleaner burn of the fuel. Catalytic converters also require a high temperature (300 to 500^{o}C) to operate efficiently, although current research is aimed at reducing the lower end of operating conditions. The initial start-up phase of an engine therefore produces the most emissions on a unit basis and has the lowest ability to treat these in the catalytic converter. The SNRA (1995) estimate the proportion of emissions from cold start in Swedish cars as:

- 18 per cent of HC;
- 37 per cent of CO; and,
- 3 per cent of NOx.

In testing vehicles for the effect of cold starts the EFRU (1997) established the ratio of emissions during the first 3 minutes to those once the engine is warm (after 6 minutes of operation). The ratio is equivalent to the ratio of cold start to hot engine emissions and are given below for petrol fuel injected engines with catalytic converters:

- CO = 6.2;
- HC = 8.0; and,
- NOx = 1.7.

It was noted that for non-catalyst equipped vehicles, emissions of NOx increase as the engine warms owing to the enrichment of the mixture during startup suppressing the formation of NOx (EFRU, 1997). For vehicles with catalysts, the efficiency of the catalyst improves at a greater rate than the increase in engine out emissions[4], thus yielding the above results.

For many applications, the duration of the journey is not known and hence the composition of engines running hot and cold is also unknown. Given that this proportion would be largely unaffected by most road investment projects—except where there is likely to be significant route shortening — the emissions models are based on hot engine emissions.

The peculiarity of cold engine emissions and evaporation (refer below), although often significant quantities in themselves, are specifically excluded from this research. If cold engine emissions are considered important in a project then the project should be analysed using a dedicated emissions model, such as Mobile 5 produced by the USA Environmental Protection Agency (EPA, 2003).

[4] Engine out emissions equate to the quantity of the various compounds being emitted from the engine, prior to treatment by the catalytic converter if present.

Evaporation

When considering vehicle emissions, not all of the pollutants are emitted from the vehicle's exhaust. As is readily observed when petrol is spilt on the ground, it quickly evaporates into the atmosphere. A similar process occurs within vehicles, whereby the production of HC from evaporation is often significant.

The rate of evaporation of fuel is directly related to two items:

- The air temperature; and,
- The level of vapour pressure in the fuel.

To minimise evaporation, fuel companies have the ability to alter the vapour pressure level as the ambient temperature alters during the year. SNRA (1995) indicate that this is standard practice in Sweden, where a lower vapour pressure is utilised in winter than during the warm summer period.

Evaporation is primarily a concern for the production of HC, with the SNRA (1995) estimating that evaporation accounts for approximately 43 per cent of the total production. The proportion of evaporation from the various modes is estimated as follows (SNRA, 1995):

- Diurnal (losses during the day) 45 per cent;
- Running losses (losses while vehicle is in operation) 33 per cent; and,
- Hot soak (during cool down period after use) 22 per cent.

It is interesting to note that a significant proportion of HC production takes place in parked vehicles. As with cold start conditions, the impact of road investment alternatives on evaporation is minimal, and hence it is considered appropriate to exclude the modelling of this component from a model such as is being developed here.

Effect of Legislation

Unlike fuel consumption, the level of emissions is closely regulated in many countries of the world. Where emissions legislation is enforced, in spite of differences in the physical characteristics of the vehicles, the level of emissions exiting the tailpipe tend to be very uniform—dictated by the legislation. Consequently, vehicles that may have differing fuel consumption levels for a given power demand, will often have similar emission rates with the use of appropriate catalytic converters.

Two Stroke Engines

Two stroke engines are considered to be cheap to run – as is evident by their high representation in the vehicle mix in most developing nations of the world. However, despite consuming relatively little fuel, what fuel they do consume is not utilised efficiently. In particular, there is a high percentage of the fuel that bypasses the combustion process completely and simply exits the exhaust pipe as a vapour. Sheaffer, *et al. (*1998) state that as much as 30 to 40 per cent of the air-fuel mixture at wide open throttle is short circuited unburned to the atmosphere.

Catalysts for two stroke engines are not common, but can achieve reductions in CO of 94 per cent and HC of 90 per cent. Such potential reductions, in combination with legislation may well see dramatic changes in the emissions from two stroke engines in the near future.

NOx production from two stroke engines is in general very low owing to the lack of either high temperatures or high engine pressures.

Predictive Models

Predicting vehicle emissions has proved to be more difficult than that of fuel consumption owing to the greater variability in results. Factors such as ambient air temperature and journey length (*ie* proportion of trip with hot engines) play pivotal roles in determining emissions yet are largely beyond the control of vehicle manufacturers and drivers. Vehicles that appear to be the same can also have vastly different emission output levels.

For this research project, it was necessary to provide models that could be used to evaluate one road project against another, as opposed to models that can evaluate one vehicle relative to another. Thus, models that predict average emission levels for each vehicle type were adopted.

To enable comparisons of emissions from one vehicle to another, manufacturers and researchers have resorted to the use of typical drive cycles. These cycles are deemed to represent the various types of driving undertaken either in urban or rural conditions. Although these results are of use in comparing one vehicle with another under 'average' conditions, they do not enable one roading option to be compared with another, as only those options resulting in a shortened route would show any benefits.

The EPA (1997) state that 18 per cent of on-road driving conditions are not modelled within the standard FTP (Federal Test Procedure) drive cycles, therefore even questioning the reliability of using such results in the comparison of one vehicle to another. In particular the FTP drive cycle is not considered to account for the following driving conditions (EPA, 1997):

- High engine loads;
- Hard accelerations;
- Climbing grades;
- Warm starts; and,
- Accessory use.

As emissions typically increase under high loading conditions, the results produced from the test cycles could be considered as lower bounds of the on-road results.

For use in analysing road investment projects on vehicle emissions, it is necessary to be able to compare the average level of vehicle emissions under the different operating conditions. To do this, a relationship is required to predict emissions either as a function of operating conditions (road geometry, roughness, vehicle speed and total power), or as a function of another variable (such as fuel consumption).

Many vehicle emissions can be expected to have a high degree of correlation with fuel consumption owing to fuel being one of the primary agents in the combustion process. In support of this approach, An, *et al*. (1997) states *"analysis indicates a strong correlation between fuel use and engine-out emissions under specific conditions"*.

The SNRA produced a range of parameters and statistics for a simple linear model between fuel consumption and the various emissions. The SNRA (1995) state that the R-squared values "*could be considered high enough to accept a simple model describing exhaust emissions as linear functions of fuel consumption."*

ETSU (1997) state that *"The emissions of nitrogen oxides do not depend on fuel consumption, however, and are more directly linked to engine speed and temperature of combustion."* They then go on to state *"The disadvantage of the fuel consumption model* [to model emissions] *is that in several cases the emission of a specific pollutant is not physically dependent on the level of fuel consumed."* ETSU (1997) present the following equation form for predicting the vehicle speed dependent emissions:

$$EOE_i = a1 + a2\,S + a3\,S^{a4} + a5\,e^{a6\,S} \qquad (2.3)$$

where EOE_i is the engine out emission in g/km for emission i
i is the emission type (*ie* HC, CO, NOx, SO_2, Pb, PM or CO_2)
a1 to a6 are model parameters varying by emission type and vehicle
S is the vehicle speed in km/h

ETSU (1997) defined 64 sets of parameters for Equation 2.3, however, only one utilised the exponential term. Therefore, the model could well be simplified to exclude the final component. This simplified model form is similar to the early empirical fuel consumption models discussed previously. Therefore, although the ETSU (1997) state that the emission of some pollutants are not related to fuel, the form of the predictive models tends to suggest that a moderate level of correlation would in fact exist—supporting the findings of other researchers.

In using any model it is necessary to consider the transportability of the results to differing vehicles and/or countries. To this end ETSU (1997) state:

> *"the data for deriving the empirical relationships between fuel consumption and pollutant emissions have been measured by laboratories in the developed world. It is not clear how suitable these relationships would be under different climatic conditions, with different vehicle types and levels of maintenance."*

ETSU (1997) recommend the use of what they term the "Detailed Traffic Flow/Engine Power Calculations" method. This method uses detailed information from a range of driving conditions, including parking manoeuvres and the like. However, owing to the data requirements being beyond those readily available in practice, ETSU (1997) state that this would *"undermine the accuracy of the method".* Therefore it is considered that the use of such models are inappropriate for use within most

systems and where such information is available then consideration should be given to a dedicated emission model such as Mobile5 (EPA, 2003).

Based on the above work, it is concluded that the most appropriate emissions model to adopt is one that predicts most emissions as a function of fuel use. The exception is carbon dioxide, which is modelled as a carbon balance equation, wherein any carbon not consumed by the other emissions, by default is emitted as CO_2. The method of modelling each of the emissions is shown in Table 2.6.

Table 2.6: Selection of Estimation Method by Emission

Emission	Fuel Consumption	Carbon Balance
Hydrocarbons (HC)	✓	
Carbon monoxide (CO)	✓	
Oxides of nitrogen (NOx)	✓	
Particulates (PM)	✓	
Carbon dioxide (CO_2)		✓
Sulphur dioxide (SO_2)	✓	
Lead (Pd)	✓	

2.10 Representative vehicles

2.10.1 Introduction

Due to the large number of vehicle makes and models available, it is not practical (and barely possible) to model all vehicle types on the road. Instead, practitioners resort to the use of representative vehicles. The concept of representative vehicles is rather simple, with a given vehicle chosen to represent all like vehicles. For example a single small passenger car may be chosen to represent all small passenger cars on the road.

There are two methods available to obtain a representative vehicle, one of adopting a particular make and model to represent all like vehicles (e.g. a Ford Laser to represent all small cars), or secondly create an average vehicle based on the attributes of all vehicle models within a given class.

While the second method may give a better representation of the nominated vehicle class, it does have the disadvantage that all vehicle parameters must be known about every model within that class. By adopting the first method, data collection and analysis is greatly simplified and thus this method is the most commonly used in practice. Furthermore, some average values are meaningless, for example if 90 percent of the vehicles are front wheel drive and 10 per are rear wheel drive, then an average has no real use.

Bennett (1994) utilised a 44 vehicle classification system for his research into vehicle speeds, although he commented that normally between two and eighteen vehicles are used. Bennett (1994) goes on to state that:

> *"While using a large number of vehicles to describe the vehicle fleet may initially seem to be an improvement, the intrinsic difficulties associated with accurately describing the characteristics of vehicles and the continually changing composition of traffic means that there will always be errors."*

Technically, it is possible to split vehicles into groups based on any parameter value. However, the difficulty is in the collection of data - especially large quantities of data - and the associated analysis. For instance, it may be desirable to split cars from other light 2-axle vehicles.

However as illustrated in Figure 2.9, even when considering only a sample of the total vehicle fleet, there is no clearly definable value of length that would make this distinction. Therefore, unless manual methods are employed to classify vehicles, dissemination of a stream of vehicles into highly detailed groups is not feasible.

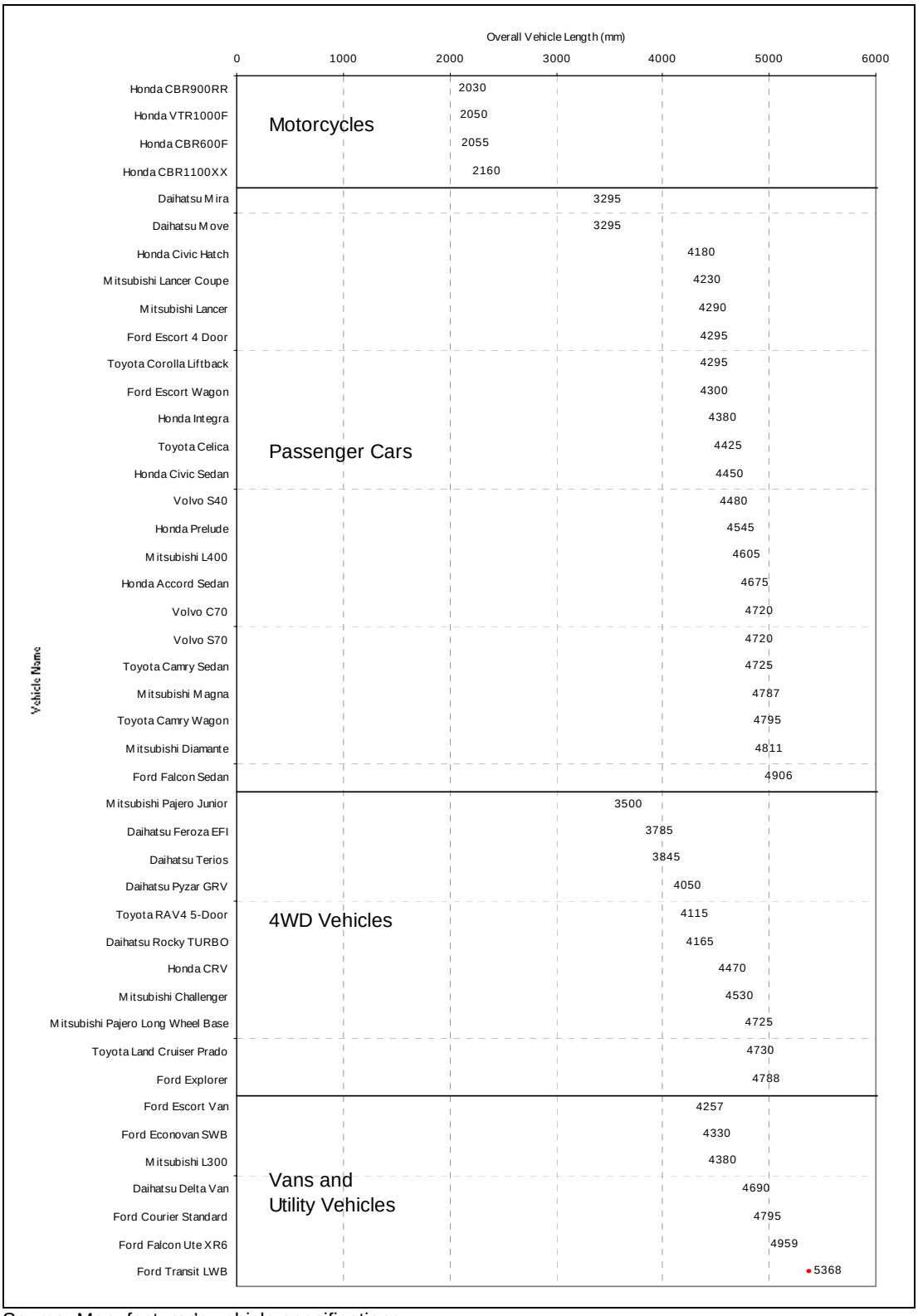

Source: Manufacturer's vehicle specifications

Figure 2.9: Variation in Vehicle Lengths

2.10.2 Selected Vehicle Types

The passenger car forms the majority (82 per cent) of the traffic stream during periods of high congestion according to the Transfund New Zealand Project Evaluation Manual (PEM) (1997). Table 2.7 shows the vehicle classes utilised within the PEM and their proportion of the traffic stream on New Zealand arterial roads during the morning peak period.

Table 2.7: Transfund New Zealand PEM Vehicle Classes and Composition of Traffic Stream in Morning Peak, Arterial Roads

Transfund New Zealand PEM Vehicle Classes	Percentage of Traffic Stream
Passenger Car (PC)	82
Light Commercial Vehicle (LCV)	10
Medium Commercial Vehicle (MCV)	3
Heavy Commercial Vehicle, Type I (HCV-I)	2
Heavy Commercial Vehicle, Type II (HCV-II)	3
Bus	0

Within HDM-4 (Bennett and Greenwood, 2001), 16 representative vehicle types were utilised. Details of these are given in Table 2.8

Table 2.8: HDM-4 Representative Vehicle Classes

Code	Vehicle Description
MC	Motorcycle
PC-S	Small passenger car
PC-M	Medium passenger car
PC-L	Large passenger car
LDV	Light delivery vehicle
LGV	Light goods vehicle
4WD	Four wheel drive
LT	Light truck
MT	Medium truck
HT	Heavy truck
AT	Articulated truck
MiniBus	Mini bus
LB	Light bus
MB	Medium bus
HB	Heavy bus
Coach	Coach bus

Source: Bennett and Greenwood (2001)

Based on the high percentage of cars, it was decided that the data collection and modelling exercise should focus on these vehicles, as this would offer the maximum benefit. The results from the passenger car data collection would then be related to the other vehicle classes using available information.

2.11 Summary and Conclusions

This chapter has presented the results of a review of literature to provide a background for the work contained within the remainder of this thesis. It has been shown that although numerous researchers have looked at the speed-flow effects of congestion, the consequences of utilising steady-state speeds rather than varying speeds has not been covered in such depth.

The review of speed-flow models included the adoption of the HDM-4 three-zone model, which simplifies the application of the congestion model in later work owing to its discrete change points.

This chapter has also provided a background to various measures of traffic flows in use, including comments on their respective drawbacks and assumptions. A discussion on the measurement of vehicle headways was made, along with the issue of measurement and the impact that vehicle length has on the measured value. It was concluded that the effect of gap size and vehicle type could be expected to have a significant impact on vehicle accelerations.

The review of fuel consumption models included both empirical and mechanistic models, along with a discussion on methods commonly utilised to reduce fuel consumption. Key requirements included the need for the fuel model to be able to predict accurately under congested conditions, plus be of a mechanistic type model. On the basis of the review, it was concluded that the ARFCOM model was appropriate for inclusion into this research project.

Acceleration noise (the standard deviation of accelerations) was decided upon as the most appropriate measure of non-steady speed driving. Other options ranging from maximums of accelerations, through to positive kinetic energy approaches were considered but found to be inappropriate for this project.

Vehicle emission modelling frameworks were reviewed, along with a discussion on many of the factors that influence the amount of emissions produced. It was concluded that although not all vehicle emissions are directly related to fuel consumption, that such a model would offer the best overall results for this research.

In order to model the traffic stream, it is standard practice to adopt representative vehicles. A review of approaches to selecting representative vehicles was made, along with the recommendation to adopt actual vehicles to represent various vehicle classes, as opposed to the use of average vehicles. Based on a review of vehicle lengths, it was concluded that it is not possible to split the traffic stream into different classes based on vehicle length alone.

Further discussions on many of the issues raised in this chapter are contained in the remainder of this thesis.

3 THEORY OF ACCELERATION NOISE

3.1 Introduction

As noted in the literature review (refer to Section 2.8) it was concluded that the most appropriate unit of measure for describing the non-steady component of driving for the purpose of this project was that of acceleration noise, which equates to the standard deviation of accelerations. This approach is in line with that of previous work by Bester (1981) and is considered the best means of representing the unsteadiness in travel speeds within a modelling process such as that being undertaken here.

This chapter presents the theory of the acceleration noise parameter, including discussions on the time impact of measurement, and models to predict acceleration noise.

3.2 Time Period of Measure

An important consideration in developing any measures is that of model calibration. In particular, the number of readings that can be practically made per time interval will have a direct bearing on the usefulness and magnitude of the end result. In general, the result of adopting a longer measuring interval are as follow:

- improved accuracy of measurement (relative error is decreased)
- lower cost measuring equipment
- less data to analyse
- lower value of variation owing to the smoothing effect of the time interval

The last of the above points is important in that if a long interval is adopted, then much of the variation in speeds will be lost to the averaging effect of time, thereby resulting in an underestimation of the impacts of traffic congestion. In fact, taken to the extreme a single average value will yield the basic speed-flow curve wherein zero variation occurs.

Another consideration is that of enabling a single period of data collection to fit in with more than one model calibration – therefore decreasing the cost of using the model. With respect to traffic models and data collection tools, the common time interval in use is 1 second (eg. PARAMICS for reporting, ROMDAS refer to Section 4.3) and it is this time interval that has been adopted for this project.

By adopting a 1 second interval, the following events will be averaged into a single measurement:

- around 14 m of travel at 50 km/h
- around 50 engine revolutions (based on an engine speed of 3000 rpm)

It is considered that the above averaging is acceptable for the modelling of traffic congestion and therefore a 1 second time interval has been adopted for this project.

3.3 Acceleration Noise

3.3.1 Introduction

A platform to account for the non-steady state effects was presented by Bester (1981), who utilised the concept of *acceleration noise*. Bester (1981) defined acceleration noise as the standard deviation of vehicle accelerations, and thus it had the units of m/s². Bester (1981) derived the following relationship between acceleration noise and traffic density based on the results of following-car surveys:

$$\sigma a = \sqrt{\sigma at^2 + \sigma an^2} \qquad (3.1)$$

where σa is the total acceleration noise in m/s²
σat is the traffic acceleration noise in m/s²
σan is the natural acceleration noise in m/s²

The form of the above equation is based on the concept that accelerations form a Normal Distribution and therefore it is valid to add variances, but not standard deviations. Bester (1981) gave the following relationship for predicting the traffic acceleration noise as a function of traffic density:

$$\sigma at = \sigma atmax\ (1-6.75\ RELDEN + 13.5\ RELDEN^2 - 6.75\ RELDEN^3) \qquad (3.2)$$

where $\sigma atmax$ is the maximum total traffic acceleration noise in m/s²
RELDEN is the relative density of traffic on the road

The relative density can be predicted as:

$$RELDEN = \frac{k}{kjam} \qquad (3.3)$$

where, k is the traffic density in veh/km
kjam is the jam density in veh/km

Equation 3.2 is a basic pseudo-sine wave function, which increases to a maximum value of 1 at a relative density of 1 as is illustrated in Figure 3.1. What is of interest is that the function has a minimum value at a relative density well above zero.

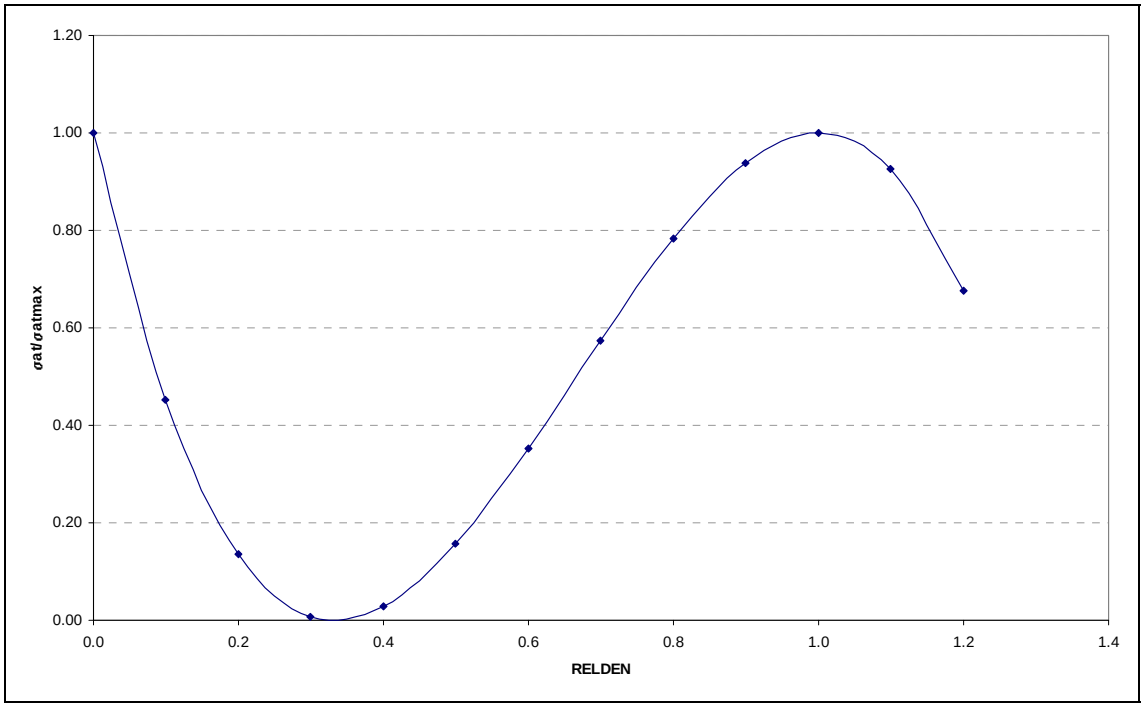

Figure 3.1: Form of Bester's Acceleration Noise Function

Differentiating Equation 3.2 with respect to relative density indicates that Equation 3.2 has a minimum value obtained at a relative density of 0.33 as illustrated below.

$$\frac{d\sigma at}{dRELDEN} = -6.75\,\sigma at\,max + 27.0\,\sigma at\,max\,RELDEN - 20.25\,\sigma at\,max\,RELDEN^2 \quad (3.4)$$

Setting Equation 3.4 to zero and solving for RELDEN yields the following solutions for the minimum and maximum turning points of Equation 3.2:

RELDEN = 0.33 or 1.00 (3.5)

It is concluded that below this minimum Bester (1981) assumed the effect of traffic acceleration noise can be ignored, as any other conclusion would yield unreasonable predictions. Similarly it is assumed that "over capacity" situations cannot occur, wherein the relative density would exceed a value of 1.

Research by Greenwood and Bennett (1995b) suggested that the model form proposed by Bester (1981) was not appropriate as it predicted that the effects of congestion did not begin until the road system was at approximately 90 per cent of its capacity. Figure 3.2 illustrates this situation utilising the proposed HDM-4 speed-flow model (refer to Section 2.2), using the basic relationship between speed, flow and density, to yield the density curve.

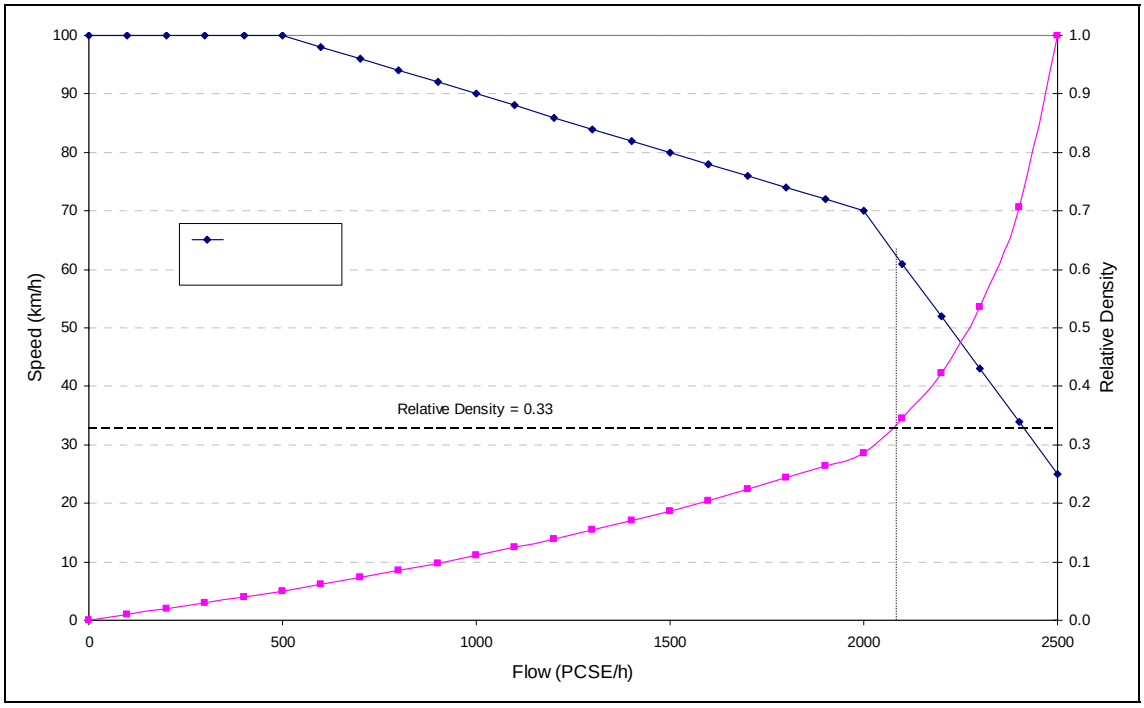

Figure 3.2: Speed-Flow and RELDEN-Flow Relationship

The concept of congestion not impacting until 90 per cent of capacity is in contrast to the results obtained by Greenwood and Bennett (1995b) and Greenwood (1999) where congested effects began to be manifested at much lower levels of flow. Further to this, the first change in the form of the speed-flow model is in theory where traffic interactions start to become significant, so it would be expected that this flow level would also correlate to the manifestation of acceleration noise above the natural noise level.

3.3.2 Components of Acceleration Noise

The work of Bester (1981) that is represented in Equation 3.2 did not indicate any variation depending upon the type of road the congestion was occurring on. This is in contrast to a number of speed-flow models (Hoban, et. al., 1994) that suggest that the effects of congestion, as observed by reduced speeds, begin to be noticed at different flow levels, depending upon the type of road under review.

Further work by Greenwood and Bennett (1995b) identified that if the term RELDEN in Equation 3.2 was replaced by the volume to capacity ratio of the road section, then more appropriate predictions are realised.

The magnitude of vehicle interactions is represented in HDM-4 (Bennett and Greenwood, 2001) by the acceleration noise. Figure 3.3 illustrates the different acceleration distributions that arise with congested and uncongested conditions.

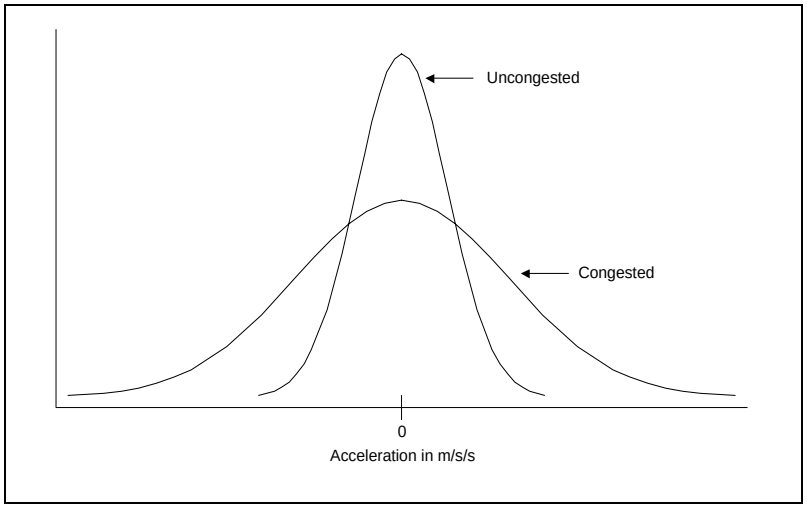

Figure 3.3: Congested and Uncongested Acceleration Distributions

The natural noise can be described as:

$$\sigma an = f(\sigma adr, \sigma aal, \sigma asf, \sigma anmt, \sigma airi) \quad (3.6)$$

where σadr is the noise due to natural variations in the driver's speed in m/s^2
σaal is the noise due to the road alignment in m/s^2
σasf is the noise due to road side friction in m/s^2
$\sigma anmt$ is the noise due to non-motorised transport in m/s^2
$\sigma airi$ is the noise due to roughness in m/s^2

In the HDM-4 model (Bennett and Greenwood, 2001), traffic noise is caused by motorised transport only, with all other components forming part of the natural acceleration noise. On the basis of previous research and experiments conducted by the ISOHDM HTRS team in Malaysia, the following equation was developed which gives the traffic noise as a function of the volume to capacity ratio (NDLI, 1995):

$$\sigma at = \sigma atmax \frac{1.04}{1+e^{(a0+a1\ VCR)}} \quad (3.7)$$

$$VCR = \frac{Q}{Qult} \quad (3.8)$$

where VCR is the volume to capacity ratio
a0 and a1 are regression coefficients quantified as:

$$a0 = 4.2 + 23.5 \left(\frac{Qo}{Qult}\right)^2 \quad (3.9)$$

$$a1 = -7.3 - 24.1 \left(\frac{Qo}{Qult}\right)^2 \quad (3.10)$$

Bennett and Greenwood (2001) combined the driver noise (σadr) and the alignment noise (σaal) into a single value as it is difficult to differentiate between these two components. The other three components of natural noise — roadside friction (σasf), non-motorised transport (σanmt) and roughness (σairi) — are modelled as linear functions such as those shown in Figure 3.4. The maximum values preliminarily estimated for these components are:

- σasf = 0.20 m/s^2
- σanmt = 0.40 m/s^2
- σairi = 0.30 m/s^2

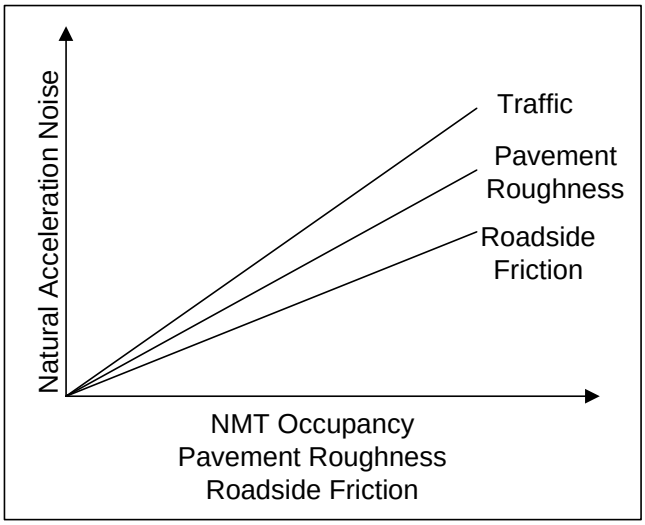

Figure 3.4: HDM-4 Natural Noise Models

These maxima apply at side friction and non-motorised transport ratios of 1.0 and a roughness of 20 IRI m/km.

The total natural noise is given by:

$$\sigma an = \sqrt{\max((\sigma adr^2 + \sigma aal^2), \sigma asf^2, \sigma anmt^2, \sigma airi^2)} \quad (3.11)$$

Using the above equations, the total acceleration noise at any relative flow can be characterised by the natural noise (σan) and the maximum traffic noise (σatmax).

The maximum traffic noise is calculated as:

$$\sigma atmax = \sqrt{\sigma a max^2 - \sigma an^2} \quad (2.12)$$

3.3.3 Typical Values of Acceleration Noise

Experiments conducted in Malaysia with cars, medium trucks and buses, led to a value of 0.60 m/s^2 being recommended for the maximum total acceleration noise (σamax) and a minimum value of 0.10 m/s^2 for the natural noise (refer to Section 5.2). These were adopted as the default parameters in HDM-4 for all vehicle classes (Greenwood and Bennett 1995b). A plot of the predicted acceleration noise level, for a range of volume to capacity ratios is contained in Figure 3.5 (refer to Section 2.2 for definitions).

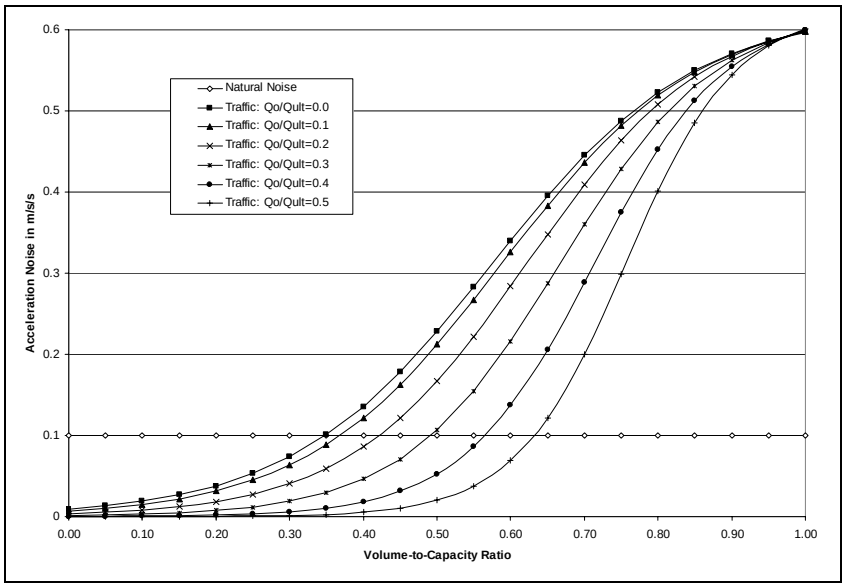

Figure 3.5: Acceleration Noise Versus Volume To Capacity Ratio

Only the total acceleration noise level can be measured. It is not possible to distinguish what portion of the accelerations recorded are due to traffic interactions and what portion is the natural noise component while collecting the data. To separate the recorded data into the two components it is necessary to refer to the predictive equations and the basic assumption that the natural noise is independent of traffic flow. By recording the natural noise at very low traffic flows (where it can be assumed no traffic noise occurs) and using the basic relationship between total acceleration noise and the two components, the traffic noise at other flows can be calculated.

3.3.4 Formal Definition of Acceleration Noise

Although Bester (1981) does not give a formal definition of the time basis of acceleration noise, both Greenwood and Bennett (1995b) and Greenwood (1999) have adopted a 1 second base.

For this research work the following definition of acceleration noise is adopted:

> *Acceleration Noise: Standard deviation of accelerations of a vehicle calculated under nominally uniform operating conditions from average acceleration readings measured over 1 second intervals.*

In practice, the measurement recorded at 1-second intervals is most commonly vehicle speed or travelled distance. Accelerations, and acceleration noise, are then calculated later from these raw data values.

Of interest in the above definition is the inclusion of the term "under nominally uniform operating conditions". Although a value of acceleration noise can be calculated from any series of acceleration readings, it is considered that only those values recorded from operating under a nominally uniform condition of traffic, geometry etc, have any real meaning.

3.3.5 Acceleration Noise Distribution

Bester (1981) found that although the acceleration noise distribution was reported in the literature to follow a Normal distribution, his experimental data were not Normally distributed. The data collected by NDLI (1995) also showed that the acceleration noise does not follow a Normal distribution, with the distribution skewed to the left (*ie* the deceleration tail is longer than that of the acceleration).

This finding was confirmed by Hine and Pangihutan (1998) who found in Indonesia that the maximum deceleration exceeded the maximum acceleration and was also confirmed by Greenwood (1999). This finding also makes logical sense as the deceleration tail is limited by driver behaviour whereas the maximum acceleration rate is a function of the vehicle power-to-weight ratio.

A typical plot of acceleration noise is shown in Figure 3.6, with the observed distribution overlain by the Normal Distribution with equal mean and standard deviation. NDLI (1995) found that although the acceleration noise distributions failed tests for Normality, the data were approximately Normally distributed over much of the range, with most of the error occurring within 0.05 m/s^2 of the mean value or at the tails.

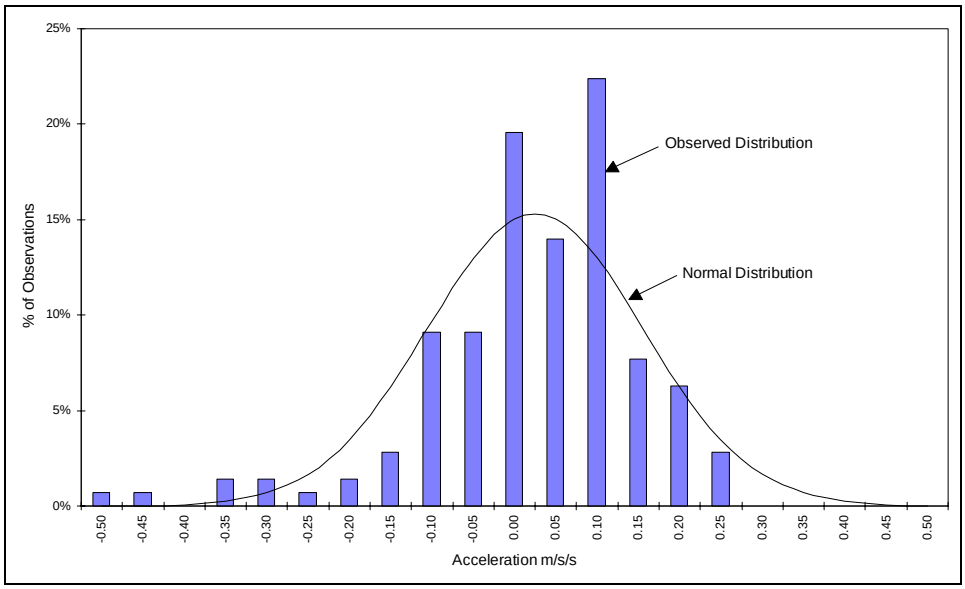

Figure 3.6: Distribution of Acceleration Noise Under Free Flow Conditions for Passenger Car

Since the majority of the error was at such a low acceleration rate, and the error was within the accuracy of the measurement system, it was considered by NDLI (1995) that the assumption of the acceleration noise being Normally distributed would not significantly influence the analysis results. The assumption of Normality greatly simplifies the modelling process and the majority of the difference occurs at very low accelerations where the overall impact on fuel consumption is minor.

3.4 Data Collection Requirements

Given the above definition of acceleration noise, and the requirement to be able to distinguish between values obtained under various operating conditions, it is possible to calculate what accuracy the distance travelled each second (and hence speed and acceleration) must be measured. Bennett and Greenwood (2001) calculated that acceleration noise ranges over a typical range of 0.1 - 0.6 m/s².

Based on the work of NDLI (1995), Greenwood and Bennett (1995b), Bester (1981) and Greenwood (1999), acceleration noise levels should ideally be distinguishable at a 0.01 m/s² level such that the accuracy of measurement is not effecting the analysis to a significant level. Figure 3.7 illustrates the flow-on effects of errors in the measurement of distance, and the impact on the confidence of the acceleration readings. To obtain the ±0.01 m/s² acceleration accuracy, the distance therefore needs to be measured at ±0.005 m.

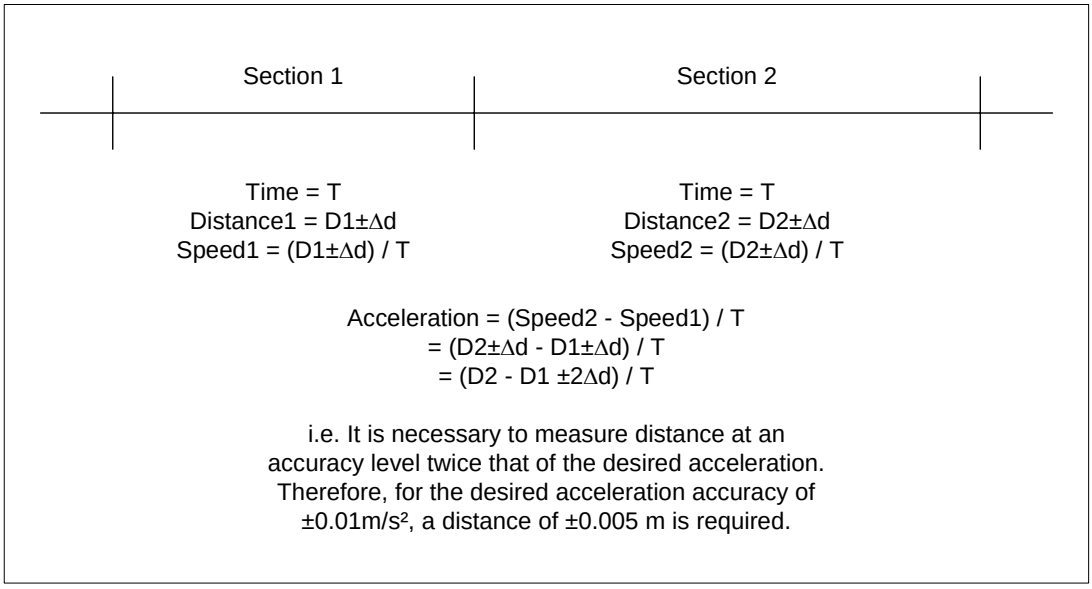

Figure 3.7: Errors Within Data Collection

As the acceleration is measured over a 1 second interval, the accuracy of the base distance measurement needs to be within ± 0.005 m. Based on a nominal car tyre diameter of 0.6 m, this then equates to 377 readings per revolution. Data collection equipment that reports 360 readings per revolution is readily available to general practitioners and for this reason was considered to be sufficiently close to the above desired 377 readings to be acceptable. Back calculating the above process, this equates to an overall accuracy of the accelerations of ± 0.0104 m/s², which is considered sufficient for this purpose.

Further discussions on the data collection equipment is contained in Section 4.3.

3.5 Summary and Conclusions

This chapter has presented a discussion on the various possible measures of the non-steady component of vehicle speeds. Based on this, “acceleration noise”, which equates to the standard deviation of accelerations, has been adopted for this research project.

A standard recording interval of 1 second has been adopted for the measurement of accelerations. This time unit simplifies application of the end results and also corresponds with the time interval used in various other studies and data collection systems.

Overall the following definition of acceleration noise has been adopted:

> *Acceleration Noise: Standard deviation of accelerations of a vehicle calculated under nominally uniform operating conditions from average acceleration readings measured over 1 second intervals.*

It is hypothesised that a relationship exists between acceleration noise and the volume to capacity ratio of the road. This is in contrast to the work of Bester (1981) who related acceleration noise to the relative density of the traffic stream.

The work of Bester (1981) indicated that acceleration noise levels remained constant until around 90 per cent of capacity. This is contrary to the findings of the author, wherein acceleration noise commenced at very low traffic flows.

Acceleration noise was concluded to consist of a traffic component and a natural component, with the latter consisting of parameters that account for all impacts apart from vehicle-to-vehicle interactions. It is noted that only the total acceleration noise can be measured, and from this various components can be estimated.

To measure the natural acceleration noise, experiments are required to be conducted at very low traffic flows, wherein vehicle interactions can be assumed to be negligible.

It was concluded that although acceleration noise data were not Normally Distributed, that it were sufficient to assume the data as Normal. This was based on the combined impact of the data approximating a Normal Distribution, and the simplifications such an assumption has on the application of the results.

In order to have data of sufficient accuracy to identify accelerations over all traffic conditions, it was considered necessary to record the distance travelled to within $\pm$0.005m per second, resulting in confidence that accelerations could be reported to the nearest 0.01 m/s^2.

4 DATA COLLECTION SYSTEMS

4.1 Introduction

Modelling congestion effects requires data collection equipment that can measure both the cause of the driving style and the impact on the vehicle and associated fuel consumption and emission volumes. While not the key focus of the research, an understanding of the data collection methods utilised does provide a background to explain the results later within the research project.

4.2 Traffic Stream Data

Information on the traffic stream in terms of flow rates, mean speeds and densities were collected from several different sources depending on the location of the data collection run. These methods included:

- manual surveys at the roadside using data loggers (flow and headways)
- temporary traffic counters installed on the road
- permanent traffic counters installed in the road
- subjective measures of flow and density.

These data sources were then related to the test vehicle location to determine the appropriate traffic stream data to apply to the test vehicle. The collection of data from the traffic counters (either temporary or permanent) was undertaken by a separate project and the results supplied to this study. Calibration of the system and error testing was not possible, but confirmation was received from those supplying the data that all calibration was undertaken.

The last method of measurement noted above, relied on the visual assessment of flows as being either free flow conditions or in highly congested conditions.

4.3 Acceleration and Fuel Consumption Data Collection

In order to model the effects of congestion on driver behaviour, vehicles were equipped with a data logger capable of recording the following:

- average pulse width per second of fuel entering the injectors
- number of pulses per second
- distance travelled during the second.

For this project two separate pieces of information were generally used to collect the data. These sensors were then connected to a ROMDAS[5] unit. This summarised electronic pulse information from both an engine sensor and a wheel sensor before sending the information to a computer for storage. Figure 4.1 illustrates schematically the ROMDAS system as used on this project.

The ROMDAS system consists of:

[5] ROad Measurement Data Acquisition System, see www.ROMDAS.com for further information.

- ROMDAS Hardware Interface (RHI). This contains a circuit board and associated technologies to enable the recoding of pulses from the various sensors, and the output of a text string to a computer that summarises all information every second.
- Distance Measurement Instrument (DMI). The DMI is attached to the rear wheel and is used to establish the distance travelled. The unit was custom made for this research project.
- Fuel Sensor. This is connected to a fuel injector to establish the fuel consumption. It consists of various electronic filters, to enable the electronic pulse that is fed to the fuel injector to be passed to the RHI without overloading the circuitry. The unit was custom made for this research project.
- Connectors. Power cables, interface and computer connections.

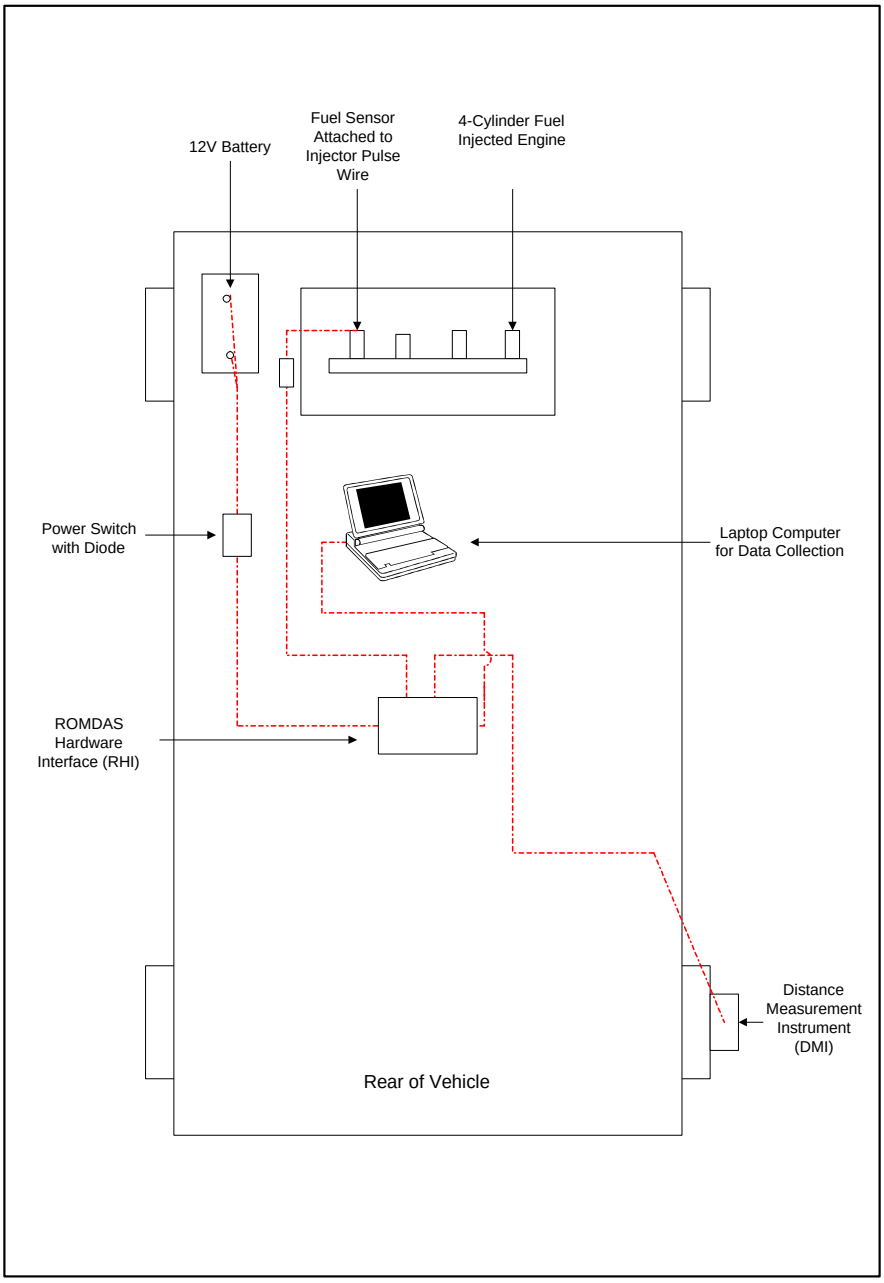

Figure 4.1: Schematic of Data Collection Unit and Connections

4.3.1 Principles of The System

The centre of the data collection system is the ROMDAS Hardware Interface (RHI). It is to this unit that the fuel and distance sensors send their information for processing, and from this unit that the processed pulses are sent to the computer. The RHI receives the data continuously from the fuel and distance sensors, summarises the data to 1-second intervals and then sends a fixed format text string to the computer for storage.

The fuel sensor records the number of pulses and the length of the pulse of fuel entering the fuel injectors every second. The number of pulses directly relates to the engine speed[6], while the combination of number of pulses and pulse length yields a measure of the fuel consumed (refer to calibration in Section 4.4.1).

By relating the pulse length to fuel consumed it is possible to yield the fuel consumption during on-road tests without directly connecting to the fuel line. Many systems that use flow meters installed in the fuel line require significant amounts of equipment and fuel bypasses, which besides being relatively difficult and intrusive to install, can potentially result in abnormal engine operating conditions. By comparison, the ROMDAS system is simple to use, robust and has no effect on engine operation.

Under heavy deceleration or while traversing a steep downgrade the fuel consumption of modern vehicles can drop to zero. In these situations the engine speed recorded from the unit will also be zero as no fuel pulses will be entering the injectors. However, by analysing the vehicle speed data from the distance sensors and a knowledge of the gear ratios of the vehicle, it is possible to back calculate the engine speed at all times.

The distance sensor consists of a mounting plate that attaches to the rear wheel of the vehicle and an electrical unit with a rotating spigot. This unit records 360 pulses per revolution of the wheel. By knowing the distance travelled per pulse, the traversed distance can be easily calculated (refer to Section 4.4.2 for calibration of this device).

4.3.2 Installation of Equipment

Fuel Sensor

The fuel consumption sensor consists of a small custom built unit (electrical components are sealed in a plastic canister) as shown in Figure 4.2. The cable with the circular plug is inserted into the RHI (refer below), while the other wire (thin orange coloured wire) connects to the pulse wire of the fuel injectors and sends information on the length and timing of the fuel that is entering the injectors (the equipment is only suitable for fuel injected vehicles).

[6] With 1 pulse of fuel for every 2 engine revolutions on the engines tested and the data summarised at 1 second intervals, the reported number is 1/120th of the engine speed in rpm.

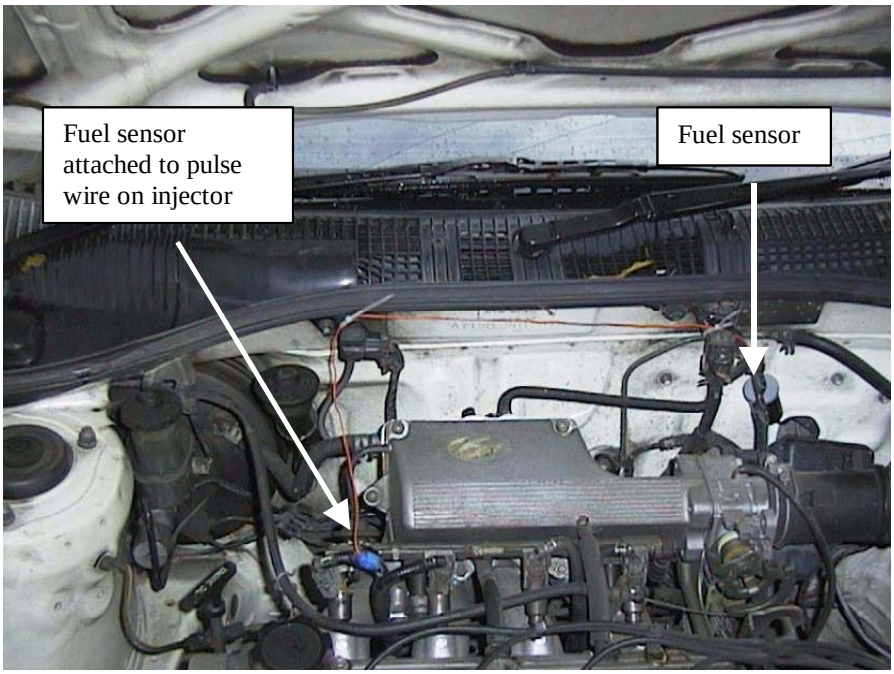

Figure 4.2: Fuel Consumption Data Collection Equipment

Distance Measuring Interface (DMI)

The DMI has three components:

- a wheel plate that connects to the rear wheel of the vehicle
- an electronic sensor
- cabling to connect the sensor to the RHI.

The wheel plate is connected to the vehicle for the duration of the surveys. The electronics and wiring (the wiring is permanently fixed to the electronic sensor) are removed when surveys are not in progress.

Figure 4.3 shows the wheel plate connected to the wheel. The unit is installed by replacing the wheel nuts of the rear wheel with the longer ones provided. A total of four wheel nuts are provided and may be used, although a total of three are sufficient for attaching the mounting plate. The mounting plate is then installed on these new wheel nuts using the lock bolts provided that screw into the end of the provided wheel nuts. Note that the unit is self-centering when 3 or more bolts are used.

Figure 4.3: Mounting Plate for the DMI Attached to the Rear Wheel

Once the wheelplate is mounted the electronics are attached by inserting the spigot of the electronics into the tube on the mounting plate and inserting the lock bolt. Figure 4.4 shows the electronics installed on the mounting plate. To stop the unit from rotating, stretch cords are attached from the unit to the body of the car. Typically these are attached to the boot and rear door of the car. The computer cable is then connected to the data collection unit and to the cable that runs to the rear window as shown in Figure 4.5.

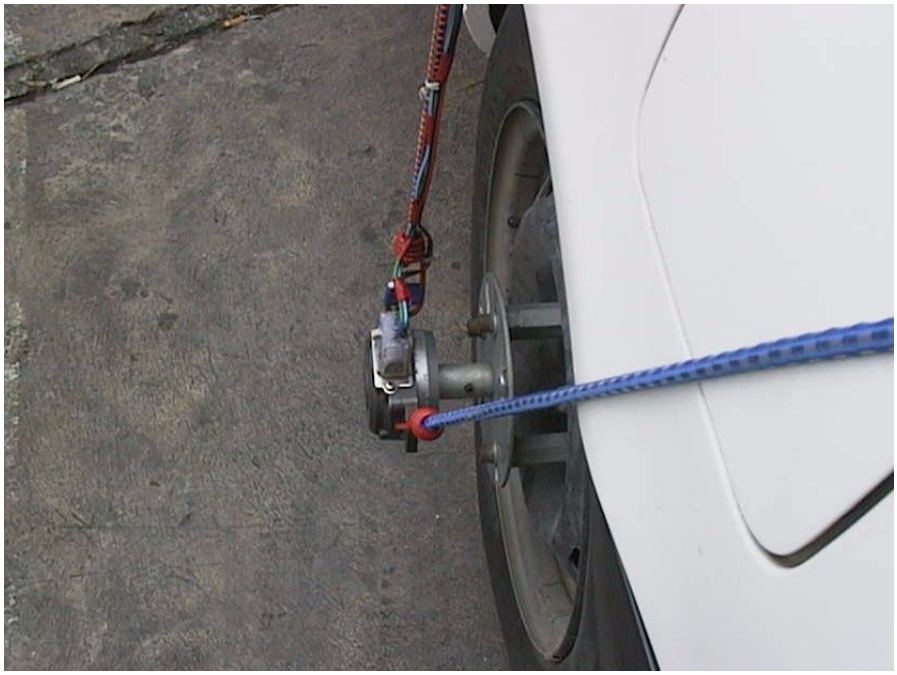

Figure 4.4: Distance Unit Installed on Rear Wheel

Figure 4.5: Side view of Distance Sensor showing Stretch Cords

4.3.3 ROMDAS Hardware Interface (RHI) Output

The format of the data sent from the RHI to the computer is as described below. A sample of a file is contained in Figure 4.6 below. The format of the data file is such that when imported as a comma delimited file into a package such as Excel, it will insert each field into a separate column. The contents of the data file is as follows:

Line 1:	Data and time that the menu option Start Recording was pressed
Line 2:	Road name as entered when requested
Line 3:	Drivers name as entered when requested
Line 4:	Vehicle type and registration number as entered when requested
Line 5+:	Data as received from the ROMDAS unit and processed by the software. The fields are:
F	code to identify pulse width string
ffff	pulse width string
E	code to identify engine speed string
eeee	engine speed string
S	code to identify speed/distance string
ssss	speed/distance string
L	code to identify start of data from second port
LComPort2	default value when second port not used
T	code to identify start of time string
hh:mm:ss	time in hours, minutes and seconds
K	code to identify start of keyboard entry
k	keyboard string when pressed
Last Line:	Date and time that the menu option End was selected.

```
"X1111",#1998-11-18#,#1899-12-30 14:47:50#
"Road Name","3215-2 lane undivided"
"Drivers Name","amnuay"
"Vehicle Type and Reg Number","1.6 L corona"
F,0372,E,0020,S,1370,L,ComPort2,T,4:55:26 PM,K,
F,0306,E,0012,S,1394,L,ComPort2,T,4:55:27 PM,K,
F,0563,E,0016,S,1530,L,ComPort2,T,4:55:28 PM,K,
F,0528,E,0018,S,1789,L,ComPort2,T,4:55:29 PM,K,
F,0368,E,0020,S,1963,L,ComPort2,T,4:55:30 PM,K,
F,0295,E,0022,S,2051,L,ComPort2,T,4:55:31 PM,K,
F,0171,E,0006,S,2008,L,ComPort2,T,4:55:32 PM,K,
F,0430,E,0013,S,1974,L,ComPort2,T,4:55:33 PM,K,
F,0556,E,0014,S,2054,L,ComPort2,T,4:55:34 PM,K,
F,0514,E,0014,S,2095,L,ComPort2,T,4:55:35 PM,K,
F,0307,E,0015,S,2126,L,ComPort2,T,4:55:36 PM,K,1
F,0457,E,0014,S,2142,L,ComPort2,T,4:55:37 PM,K,
F,0559,E,0016,S,2277,L,ComPort2,T,4:55:38 PM,K,
F,0538,E,0017,S,2436,L,ComPort2,T,4:55:39 PM,K,
F,0516,E,0018,S,2596,L,ComPort2,T,4:55:40 PM,K,
F,0507,E,0018,S,2741,L,ComPort2,T,4:55:41 PM,K,
F,0400,E,0019,S,2858,L,ComPort2,T,4:55:42 PM,K,
F,0178,E,0008,S,2858,L,ComPort2,T,4:55:43 PM,K,
F,0278,E,0013,S,2806,L,ComPort2,T,4:55:44 PM,K,
F,0464,E,0015,S,2798,L,ComPort2,T,4:55:45 PM,K,
F,0583,E,0015,S,2863,L,ComPort2,T,4:55:46 PM,K,
F,0387,E,0016,S,2936,L,ComPort2,T,4:55:47 PM,K,
F,0195,E,0015,S,2904,L,ComPort2,T,4:55:48 PM,K,
F,0157,E,0005,S,2813,L,ComPort2,T,4:55:49 PM,K,
F,0000,E,0000,S,2697,L,ComPort2,T,4:55:50 PM,K,
F,0000,E,0000,S,2582,L,ComPort2,T,4:55:51 PM,K,
F,0000,E,0000,S,2469,L,ComPort2,T,4:55:52 PM,K,
F,0197,E,0006,S,2357,L,ComPort2,T,4:55:53 PM,K,
F,0321,E,0012,S,2292,L,ComPort2,T,4:55:54 PM,K,
F,0333,E,0013,S,2296,L,ComPort2,T,4:55:55 PM,K,
F,0468,E,0012,S,2322,L,ComPort2,T,4:55:56 PM,K,
F,0475,E,0013,S,2397,L,ComPort2,T,4:55:57 PM,K,
F,0414,E,0013,S,2458,L,ComPort2,T,4:55:58 PM,K,2
F,0257,E,0013,S,2473,L,ComPort2,T,4:55:59 PM,K,
F,0160,E,0013,S,2419,L,ComPort2,T,4:56:00 PM,K,
F,0280,E,0013,S,2365,L,ComPort2,T,4:56:01 PM,K,
F,0535,E,0013,S,2397,L,ComPort2,T,4:56:02 PM,K,
F,0285,E,0013,S,2449,L,ComPort2,T,4:56:03 PM,K,
F,0427,E,0013,S,2460,L,ComPort2,T,4:56:04 PM,K,
F,0483,E,0013,S,2523,L,ComPort2,T,4:56:05 PM,K,
F,0252,E,0014,S,2563,L,ComPort2,T,4:56:06 PM,K,
"X9999",#1998-11-26#,#1899-12-30 16:56:07#
```

Figure 4.6: Sample Output Data

4.4 Calibration

4.4.1 Fuel Sensor

As noted above, it is necessary to relate the pulse information received from the unit to actual fuel consumed. For this purpose the recommended procedure is to temporarily install a fuel flow meter in the fuel line (following the manufacturers instructions) and then run both the ROMDAS and this fuel meter together under controlled conditions. It is recommended that where possible a chassis dynamometer be used for this purpose as it improves the overall calibration accuracy.

It is necessary to obtain fuel flow rates that correspond to the full range of pulse widths and engine speeds encountered during driving conditions. It is therefore recommended that once the electrical fuel meter is installed the vehicle is driven on the road over a range of traffic and geometric conditions to give these data. Failure to cover the full range of pulse widths can lessen the reliability of the calibration and thus the prediction of fuel consumption.

From the author's experience, the value of the pulse width ffff will range from 100 to 700 counts (equivalent of 3 to 12 msec), although values outside of this range may be valid. It is noted that under rapid acceleration or deceleration, values significantly outside this range are possible with lows of 0 recorded. However, as noted above the calibration is undertaken under controlled steady state conditions and such values are in general not sustainable.

Figure 4.7 illustrates the results for 3 different cars - two in Thailand and one from New Zealand. Although all three cars are Toyota make cars, and two are Coronas, the figure illustrates the need to calibrate each individual vehicle.

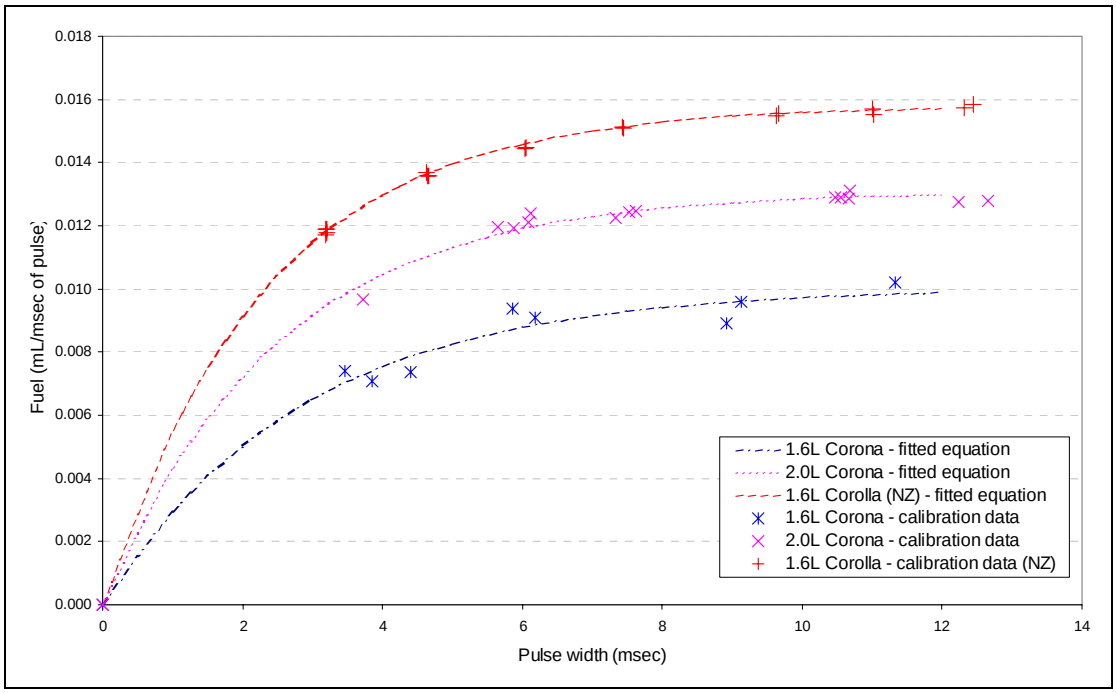

Figure 4.7: Relationship Between Pulse Width and Fuel Consumption

The calibration involves recording the actual fuel consumption from the flow meter and comparing this data to the electronic records over the same time period. The form of the model to be calibrated is as given below. The model essentially comprises two components; the fuel for a given pulse width (mL/msec of pulse), and the total pulse width per second (msec/sec).

$$IFC = \frac{a0\left(1-\exp\left(a1.Pulse\right)\right)}{1000}.Pulse.eeee \tag{4.1}$$

$$Pulse = \frac{ffff.12.16}{11.0592.10^{3}} \tag{4.2}$$

where

IFC	is the fuel consumption in mL/s
Pulse	is the pulse width in msec/engine cycle
a0, a1	are the coefficients to be calibrated
eeee, ffff	are the values output from the ROMDAS

The relationship indicates that for short to medium pulse widths there is a significant loss of throughput, and it is not until reasonably high pulse widths that the fuel being consumed per msec of pulse approaches a constant value.

The results of the calibration runs are contained in Table 4.1 and Table 4.2 for two of the test vehicles. The results were then analysed in a statistical regression package in order to obtain the value of the two variables a0 and a1. The results of this process and the associated statistical values are reported in Table 4.3. All coefficients were significant at the 99% level of confidence. For the purposes of calibrating the model, a data point at the origin was included to ensure the correct form of the model was achieved.

Table 4.1: Results of Fuel Sensor Calibration for Vehicle 1 (2.0 L Toyota Corona)

Run	Fuel (mL)	ROMDAS eee	ROMDAS fff	Pulse width (msec)	Engine Speed (rpm)	Test Length (secs)	Fuel per msec of Pulse	comment
a		7	215	3.7	788			too low flow for meter
b	19	18	214	3.7	2172	36.4	0.0097	1st gear
c	25	11	352	6.1	1372	34.6	0.0124	1st gear
d	38	18	325	5.6	2180	34.6	0.0120	1st gear
e	53	24	350	6.1	2932	34.0	0.0121	1st gear
f	70	33	338	5.9	3916	35.5	0.0119	1st gear
g	70	25	433	7.5	2964	33.6	0.0124	2nd gear
h	91	33	439	7.6	3932	32.2	0.0125	2nd gear
i	47	17	423	7.3	2088	32.8	0.0122	2nd gear
j	68	16	615	10.7	1956	32.8	0.0131	3rd gear
k	73	18	615	10.7	2152	32.5	0.0129	3rd gear
l	100	25	607	10.5	2992	32.4	0.0129	3rd gear
m	121	30	603	10.5	3560	32.4	0.0129	3rd gear
n		7	264	4.6	890			idle with A/C on - not steady
o		6	208	3.6	768			idle without A/C - flow too low
p		8	202	3.5	948			abandoned run - not steady
q	96	17	755	13.1	2036	33.7	0.0144	4th gear - not steady
r	100	21	729	12.7	2464	32.7	0.0128	4th gear
s		25	722	12.5	2956			abandoned run - not steady
t	115	24	705	12.2	2896	32.4	0.0128	4th gear
	0	0	0	0	0		0	default value for calibration

Table 4.2: Results of Fuel Sensor Calibration for Vehicle 2 (1.6 L Toyota Corona)

Run	Fuel (mL)	ROMDAS eee	ROMDAS fff	Pulse width (msec)	Engine Speed (rpm)	Test Length secs	Fuel per msec of Pulse	Comment
a	13.7	6.6	253.3	4.4	795	63.8	0.00737	idle test
b	23.7	26.2	199.2	3.5	3148	35.4	0.00739	1st gear
c	33.7	18.1	337.4	5.9	2172	33.9	0.00937	2nd gear
d	57.5	26.1	356.5	6.2	3128	39.2	0.00910	2nd gear
e	98.7	32.5	514.0	8.9	3900	38.3	0.00890	2nd gear
f	90	28.4	525.5	9.1	3404	36.3	0.00958	3rd gear
g	80	20.9	652.6	11.3	2512	33.1	0.01019	3rd gear
h	51.2	18.7	663.9	11.5	2248	32.9		not steady – excl from calibration
I	10	8.0	320.0	5.6	960	32.8		idle - with A/C
j	6.2	7.0	222.0	3.9	840	32.5	0.00708	idle - without A/C
	0	0	0	0	0		0	default value for calibration

Table 4.3: Results of Calibration Tests on Fuel Consumption Meter

Vehicle Number	Description	a0	a1	R-squared (adjusted)	Std Err
1	2.0 L Toyota Corona	13.0884 (116.68)	0.4018 (20.62)	0.995	0.0002
2	1.6 L Toyota Corolla	10.0476 (25.89)	0.3471 (7.79)	0.977	0.0007

Note: values in brackets below coefficients are t-statistics.

4.4.2 Distance Sensor

Calibration of the distance sensor consists of determining how far the vehicle travels per pulse received from the DMI. The vehicle is driven along a straight section of road that is then accurately measured. By dividing this known distance by the total pulses received, a conversion factor can be ascertained. It is recommended that a length of at least 200 m is utilised for this purpose. For most car tyres a result in the vicinity of 0.005 m or 5 mm per pulse should be expected.

This test should be repeated whenever the tyre pressure is changed or if a significant amount of time (and hence tyre tread wear) has occurred since the previous calibration. Furthermore, the test needs to be undertaken with warm tyres, as cold tyres will have a different pressure.

As a check, dividing the circumference of the tyre by 360 yields an approximate measure of this value. However, as tyres deform during rotation the “rolling diameter” and “static diameter” are often different. This process does however provide a useful “ballpark” value to ensure gross errors have not been made.

The results of the calibration process for two cars used during this research are reported in Table 4.4 below.

Table 4.4: Results of Calibration of Distance Meter

Vehicle Number	Description	Calibration length (m)	Total pulses	Distance per pulse (m)	Effective Wheel Diameter[1] (m)	Static Wheel Diameter[2] (m)
1	2.0 L Toyota Corona	243.2	47052	0.00517	0.592	0.59
2	1.6 L Toyota Corolla	200.5	39417	0.00509	0.583	0.60

Notes: 1 The effective wheel diameter is calculated as the distance per pulse * 360 / pi
2 The static wheel diameter was calculated from the tyre description and not directly measured.

As can be seen from the results within Table 4.4, there is a good comparison between the effective tyre diameter from the distance sensor and the static tyre diameter. This comparison acts as an independent check on the calibration of the wheel sensor. As the tyre pressure was not altered during the study and the interval over which the data were collected was short, the process of calibration was not repeated.

4.4.3 Speed Sensitivity of Device

A 500 m length of level and straight road was marked out. The vehicle was then driven along this length at a range of speeds between 20 and 100 km/h. To ensure that the exact distance was travelled, it was necessary to both start and end the test length at low speeds, so the vehicle speeds represent maximum speeds and not a constant speed. The data did not show any variation with vehicle speed, therefore no additional corrections needed to be made to account for vehicle speed.

4.5 Summary and Conclusions

This chapter has provided an overview of the data collection equipment utilised to collect the vehicle speed and fuel consumption data, along with comments on the calibration of the equipment.

Traffic stream information (flow, average speed etc) have been collected from a range of sources, including permanent counters imbedded in the road, through to manual surveys and visual assessment.

The in-vehicle data collection system was based around the ROMDAS data processing unit, with one sensor feeding in distance information and another yielding fuel consumption and engine speed data. Fuel consumption data were collected by monitoring the electronic pulses that control the fuel injector system of the engine. In this way, fuel consumption data could be collected without interfering with the operation of the engine performance. The fuel consumption data collection system required calibration through the use of traditional inline fuel meters and a chassis dynamometer.

Vehicle speeds were recorded via a unit attached to the rear wheel of the car. This unit then fed electronic pulses (360 per revolution of the wheel) to the central processing unit. Calibration of the distance sensor was achieved by driving a known distance along a section of road and dividing this by the number of pulses generated. Calibration included testing to ensure no speed bias was present in the results.

An example of the calibration of the equipment is provided along with commentary on the potential errors within the results.

5 ACCELERATION NOISE

5.1 Introduction

Acceleration noise has been adopted as the method of reporting the impacts of traffic congestion on driver and vehicle behaviour (refer to Chapter 3). This chapter presents the research into the relationship between acceleration noise and speed or flow.

As the data were collected and analysed in three distinct phases, each with differing data collection devices, the reporting below is also split into these three stages. Section 5.2 relates to the work completed in Malaysia during 1995 as part of the HDM-4 HTRS study. Section 5.3 covers the work completed as part of the Thailand Motorway Project where calibration of the HDM-4 models was being undertaken in 1998. The New Zealand work completed since 1999 is presented in Section 5.4.

Finally a section presents an approach trialled to identify a relationship between acceleration noise and the following distance. Although unsuccessful in identifying any relationship, the section does present the results of the data collected.

5.2 Malaysian Study

5.2.1 Background

In Malaysia, the nature of the experiments was such that only limited information was gained. Data were collected for a range of vehicle types (cars, vans and trucks) and various drivers. Acceleration data were collected using an accelerometer, with average vehicle speed recorded from the vehicle's speedometer at regular intervals. The volume to capacity ratio was estimated from observations[7].

5.2.2 Methodology

In order to quantify the acceleration noise model parameters for HDM-4 (NDLI 1995), experiments were undertaken under different operating conditions. By measuring traffic noise on a high standard motorway, at low traffic flows the natural noise due to drivers could be directly quantified. Similarly, by collecting data under stop-start conditions (heavily congested), information on the traffic-induced acceleration noise were obtained.

Three cars; one 4WD, one mini-van and two medium trucks (one laden and one unladen) were tested. Multiple runs were made with the same vehicle using different drivers. A total of 10 different drivers were tested in the study. Figure 5.1 is an example of a speed profile gained during a test run consisting of driving on congested local roads (leading up to the motorway) and non-congested motorway driving.

[7] The data collection runs were undertaken in either very high or very low traffic flows, such that it could be assumed that the resulting acceleration noise represented the maximum or natural noise repesectively.

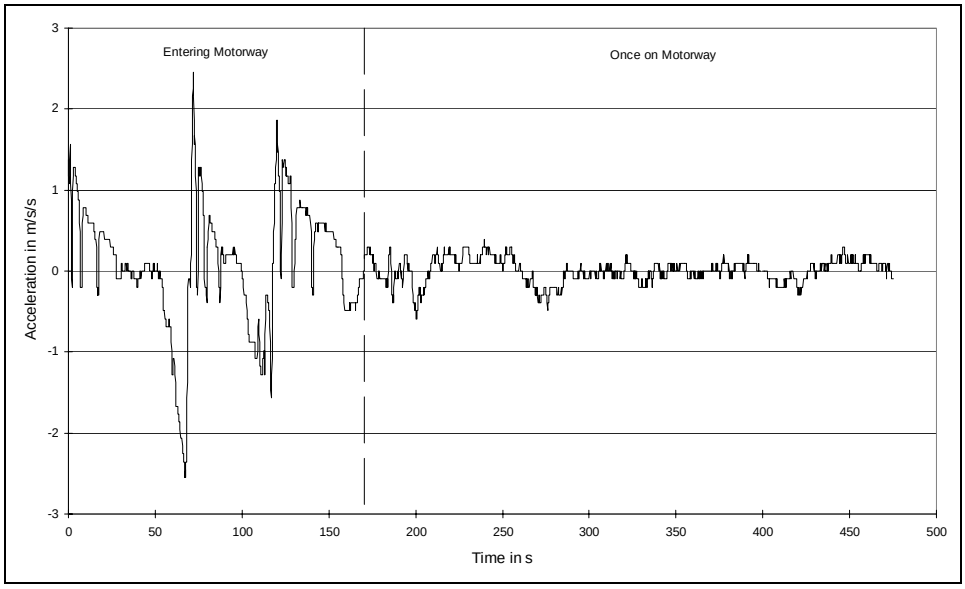

Figure 5.1: Example of Acceleration Data on Motorway - Pajero 4WD

A typical data collection journey took between 1 to 2 hours and traversed the full range of traffic and road conditions. All data were electronically recorded onto a notebook computer for later processing.

5.2.3 Impact of Data Collection Equipment

The acceleration data were collected using an accelerometer, which records gradients (and cross-fall) as well as accelerations (either positive or negative). Therefore, when processing data over a long interval it is possible that a net change in speed would be recorded even if such a change did not occur in reality.

To account for this anomaly in the measuring equipment, speeds were recorded from the vehicle speedometer at regular intervals (nominally every 5 minutes or at significant locations on the route) such that the accelerations could have an overall adjustment made to correct the resulting speeds to the appropriate value. This process, while resulting in a correct speed does not alter the underlying acceleration noise level, as the standard deviation remains the same.

5.2.4 Results

The natural noise was deemed to be that observed along the motorway under free flow conditions. This was quantified for all the vehicles and drivers. Typically, the natural noise was around 0.1 m/s^2, with vehicles having higher power-to-weight ratios resulting in higher values than those with a lower power-to-weight ratios.

The natural traffic noise is defined as a function of the noise due to the driver, alignment, roadside friction, non-motorised traffic and roughness (refer to Section 3.3). The motorway standards were such that the only components present were the driver noise and the traffic noise.

As the traffic noise is a function of the volume-to-capacity ratio, and this is difficult to accurately quantify except at either extreme (*ie* either at free flow or capacity), the traffic noise could not be accurately related to different levels of congestion. The data collection therefore focused on collecting data at jam flow when the volume-to-capacity ratio equals (or approaches) a value of 1.0.

Table 5.1 gives the values for the natural, traffic and acceleration noise for each of the vehicles tested by NDLI (1995), averaged for the different drivers. From Table 5.1 it can be seen that the maximum acceleration noise is approximately 0.6 m/s^2 for all the tested vehicles, and this value has been adopted for HDM-4 (Bennett and Greenwood, 2001).

Table 5.1: Measured Natural and Traffic Acceleration Noises by Vehicle Type

Vehicle Type	Natural Acceleration Noise (m/s^2)	Maximum Traffic Acceleration Noise [1] (m/s^2)	Maximum Total Acceleration Noise (m/s^2)
Passenger Car	0.11	0.57	0.58
4WD Diesel	0.15	0.61	0.63
Van	0.11	0.59	0.60 [2]
MCV – Unladen	0.21	0.48	0.52
MCV – Laden	0.02	0.57	0.57

Notes: 1/ The maximum traffic noise was not directly measured and was calculated using Equation 3.1
2/ This value was not measured and was assumed to equal 0.60.
Source: NDLI (1995)

The natural noise appears to be related to the power-to-weight ratio of the vehicle, with a higher ratio leading to a higher natural noise level. Neither of these observations is surprising given that at jam density the entire traffic stream has similar start-stop patterns, while under free flow conditions those vehicles that are under-powered (low power-to-weight ratio) have very little available power to accelerate. Hine and Pangihutan (1998) found a strong relationship between acceleration noise and truck loads in their study in Indonesia. However, since data are lacking for establishing this relationship, a constant value of 0.10 m/s^2 has been adopted for the natural noise.

5.3 Thailand Study

5.3.1 Introduction

As part of the Thailand Motorway Project undertaken by Dessau-Soprin Consultants for the Thailand Department of Highways (Greenwood, 1999), it was necessary to calibrate the HDM-4 congestion model to Thailand roads, vehicles and drivers.

For this work the author was employed to calibrate the model and provide the default parameter values. Data collection was undertaken to calibrate the congestion model on a wide range of road standards, as well as providing vehicle parameters for the HDM-4 fuel consumption model.

The work consisted of fitting a data collection system (refer to Chapter 4) to two passenger cars and operating the vehicles on various roads with different levels of congestion and different design standards, ranging from two lane roads to multilane highways.

5.3.2 Parameters Obtained From Other Sources

There is a strong interaction between the congestion model and the speed-flow model. Bennett (1999) in calibrating the speed-flow model recommends the following parameter values for use in Thailand:

Table 5.2: Parameter Values Calculated by Bennett (1999)

Parameter	2 Lane Roads (<9 m in width)	Multi-Lane Roads
Qo (pcse/hr)	300	500 / lane
Qnom (pcse/hr)	2520	2140 / lane
Qult (pcse/hr)	2800	2300 / lane
Snom (km/h)	55	75
Sult (km/h)	25	40

Source: Bennett (1999)

5.3.3 Data Collection Process

Representative Vehicles for Calibration of the Congestion Model

For this study, the calibration has been limited to passenger cars since our traffic studies showed that passenger cars form an overwhelming majority of the traffic stream in locations where traffic congestion occurs. Two cars were used within the calibration exercise, a 1.6L and a 2.0L Toyota Corona. For vehicle types other than cars, values have been recommended based on the results of previous studies.

The use of a 1.6L and 2.0L vehicle is considered to represent the majority of vehicles in the passenger car fleet in Thailand. It is noted that there are very few large cars (greater than 3.0L engine size) within the traffic stream and therefore calibration of such vehicles was considered unwarranted.

Congestion Survey Sites

In order to fully calibrate the congestion model it is necessary to undertake measurements on a range of road standards and conditions. For this project, emphasis was placed on calibration over the full range of road standards as opposed to the road conditions. The road standards used within the speed-flow study (Bennett, 1999) were also used in the congestion study. These covered the following road classes:

- 2 lane undivided
- 4 lane undivided
- 4 lane divided
- 6 lane divided
- 6 lane divided motorway
- 8 lane divided

Table 5.3 contains a list of where the calibration sites were, their lengths and some general comments. To enable confirmation that the sites chosen would be congested, it was decided to utilise test sections that span one of the speed-flow sites. Table 5.3 indicates the nominal length of the test section. This nominal test length varied slightly depending on traffic levels and the available turning locations (particularly for divided carriageways) but is indicative of the actual test length used.

Table 5.3: Calibration Sites for the Congestion Model

Road standard	Speed-flow site number and route number/name	Nominal testing length (km)	Comments
2 lane undivided	2 – 3215	3.0	Relatively high level of side friction along most of length. Manual traffic count. Site reaches high traffic flows.
	3 - 345		A second site with lower roadside friction. Site reaches high traffic flows.
4 lane undivided	23 – Onnut	3.0	MetroCount traffic flow data. Site did not get heavily congested.
4 lane divided	24 – 3 Sukhumvit (Samut Prakan)	4.5	MetroCount traffic flow data. Site had moderate congestion levels.
6 lane divided	9 – 304	2.0	Lane configuration controlled by Police during periods of congestion. Site has moderate congestion levels.
	22 – Patanakarn	2.0	MetroCount traffic flow data. Site has low-moderate congestion levels.
6 lane motorway	19 – 31	5.0	Central 6 lanes of motorway. Road also consists of 2*2 lane service roads and elevated expressway above. Manual traffic count, 5 min alternative directions. Site has moderate-high congestion levels.
8 lane divided	-	-	Not tested due to unsuitable sites. Values adopted from 6 lane divided data collection exercise.

For the shortest length of 2km, a sample of around 100 data points is still achieved at a speed of 70 km/h. As is noted in Table 5.3, data for an 8 lane divided road was not collected owing to the unsuitableness of the identified speed-flow sites for the purpose of calibrating the congestion model. Further details of the test locations are given within Bennett (1999).

Congestion Model Data Collection Procedure

Prior to commencing the data collection, a site visit was made to determine the extent of the road length to be traversed in each run. This site visit also identified which physical locations would be located in the files through the pressing of keys.

The ends of the data collection runs were always coded, along with some intermediary point such as the location of the traffic count, a bridge or an intersection. Two vehicles and two drivers were used for the data collection exercise, with each fully equipped with all the necessary data collection equipment. After approximately 2 hours of data collection the drivers switched vehicles to enable a comparison of driving styles to be made.

For each site it was endeavoured to undertake at least 4 hours of data collection with each vehicle (a total of 8 hours of data per site), with the period spanning the afternoon/evening peak period. For those sites where very low flows were not encountered during the period, it was necessary to undertake further data collection at night. These night visits were to enable calculation of the natural noise to be made. The surveys were designed to span various flow levels to confirm the basic form of the relationship between traffic noise and traffic flow.

The SERIAL CAPTURE software was installed on to notebook computers and used as detailed in Greenwood (1999). For some of the early data collection, the clocks on both the notebooks were not the same, thus the data had to be corrected to ensure the same time was present on all systems to enable matching with the traffic flow data.

Traffic flows were obtained by either manual traffic counts or from undertaking the data collection exercise while the counters for the speed-flow sites were installed. In the case of the former of these two methods, a PSION data logger was utilised that enabled the user to simply press a key each time a vehicle went past. The PSION saved the data to file and was then downloaded to a computer for analysis. When the speed-flow sites were used, the data was first processed for the speed-flow modelling (Bennett, 1999). The resulting file, with flow by time of day is then used to yield the flow for each data collection period.

5.3.4 Data Processing

Congestion Model Data Processing

The resulting text files from the data collection exercise were loaded into a spreadsheet package for analysis. The fuel consumption was then determined for each second of travel from the fuel sensor data, while the distance travelled (and hence speed and acceleration) was calculated from the distance sensor readings. The data was then plotted to yield a graph similar to Figure 5.2 to enable a visual inspection of the data to be made. Figure 5.2 is for a number of runs back and forth along a given section of road.

From this graph and the keys pressed during the data collection exercise, it is possible to determine which variations in speed are genuine acceleration noise effects and which are caused by the start and end of each run (the start/end effects are shaded in Figure 5.2). Sections of the data are then extracted and the calculation of the acceleration noise and fuel consumption are made.

The traffic flow for the selected period is then estimated from the average speed or matched to field results to yield a flow under which the acceleration noise was recorded. By using the maximum traffic flow from the speed-flow modelling, it is then possible to establish a volume to capacity ratio for each acceleration noise level. The maximum flows (Qult) that were used for this purpose are given in Table 5.2.

The model assumes that no net acceleration takes place along a section of road, with the speed-flow relationship predicting the same mean speed regardless of location along the section length. Therefore, in order to be compatible with the speed-flow model into which the parameter values are to be used, the periods identified for analysis must also have no net acceleration.

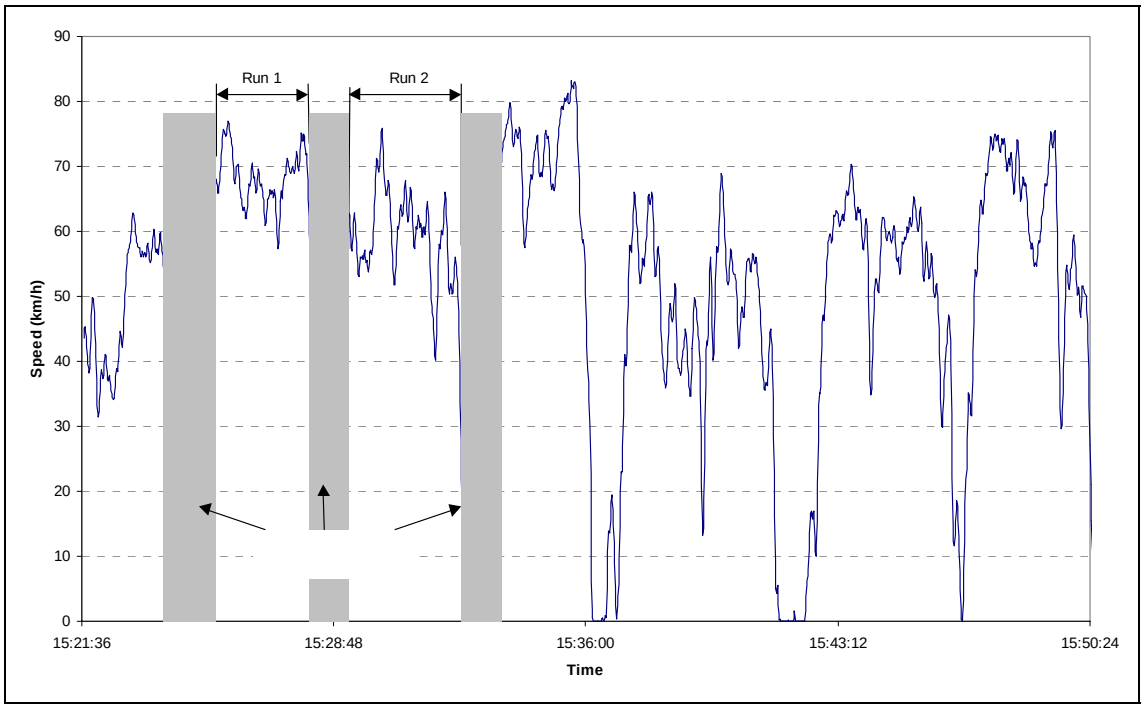

Figure 5.2: Speed-Time Profile on Two-Lane Undivided Road

As a result of the analysis methodology, 328 recordings were available to calibrate the congestion model. The breakdown of this total number into the various road types is given below.

Table 5.4: Distribution of Survey Sites

Road Type	Number of records
2 lane undivided	112
4 lane undivided	62
4 lane divided	47
6 lane divided	62
6 lane highway/motorway	45
Total	328

As noted previously, the maximum length of the test runs ranged from 2.0 to 5.0 km. However, owing to a variety of causes the actual test length within each record was often below this range. Such causes included:

- a change in lane configuration mid-way along the test length owing to police enforcement
- a change in the level of side friction along the test length
- a change in cross-section to reduce non-motorised traffic effects
- a substantial change in mean speed mid-way along the test length that could not be ascribed to one of the previous factors

Figure 5.3 below illustrates the distribution of the length of the test runs in km. Figure 5.4 illustrates similar data but based on the duration of each run. Figure 5.3 and Figure 5.4 indicate an average test run length of around 1.78 km and an average duration of just under 2 minutes.

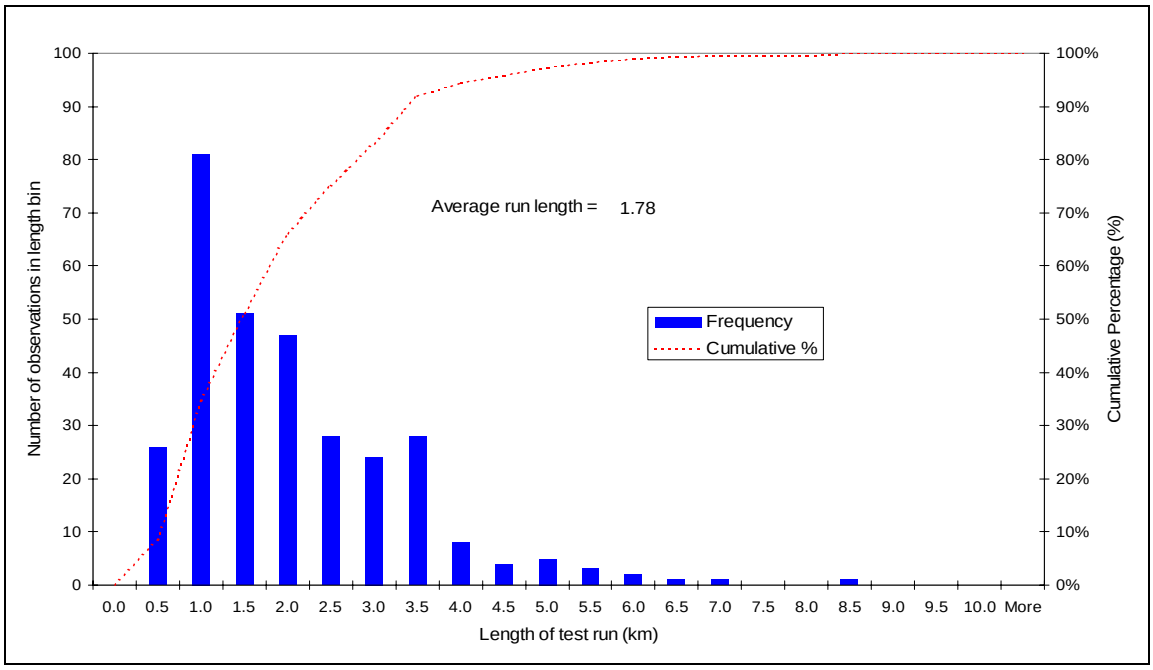

Figure 5.3: Distribution of Length of Test Runs

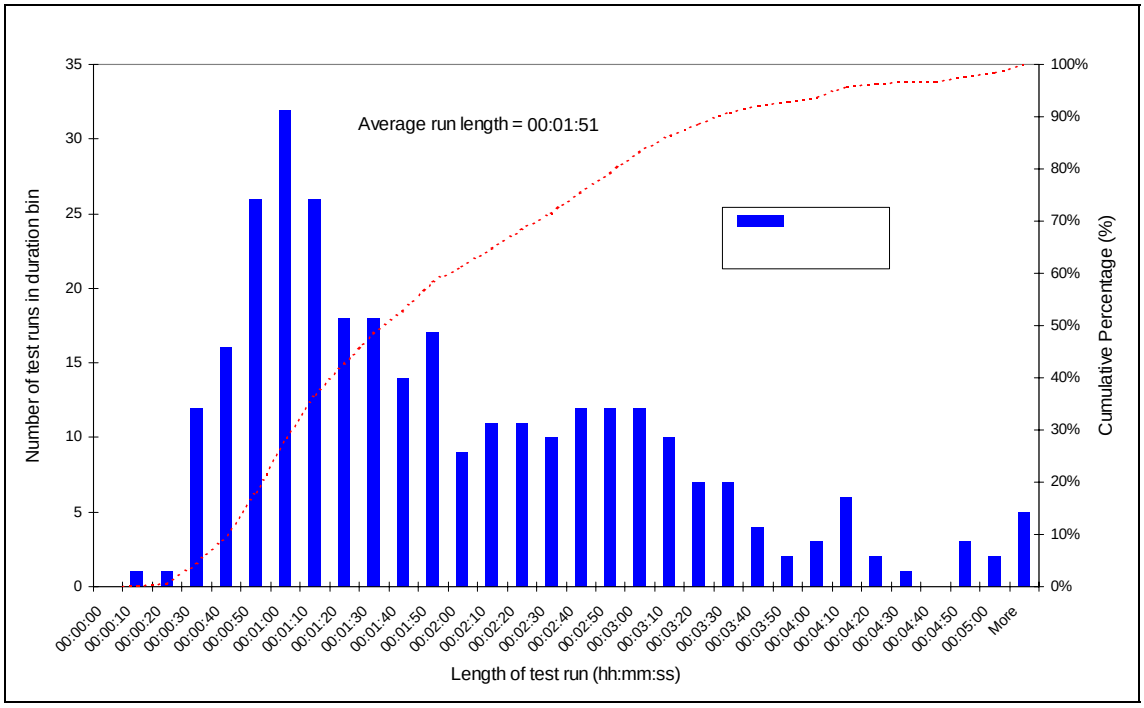

Figure 5.4: Distribution of Duration of Test Runs

Congestion Model Parameters

Overview

The following section presents the results of the acceleration noise experiments. The primary aim of this section is to provide parameter values for the natural noise and the maximum traffic noise for the two vehicles monitored. Separate sections are presented on the effects of traffic flow and drivers on acceleration noise.

Variations with Traffic Flow

An important part of the analysis of acceleration noise revolves around the ascribing of traffic volumes to each test run. As is detailed in Chapter 3, acceleration noise is considered to be related to the volume to capacity ratio and once this is known, only the natural noise and maximum traffic noise remain to be calibrated.

It is noted that vehicle flows are generally measured at a point in space and then applied over a length of road under the assumption that all points on the road have the same flow profile. The issue then raised from this is what is the flow that vehicles are operating under when analysing the results. Two alternative methods are considered for this purpose:

- Utilise the average speed on the link during the test run and back-calculate a flow from the speed-flow relationship (also measured at a point but assumed to hold constant along a homogeneous link)
- Measure flow at some point (either the start of the section or at some intermediary location) along the link and ascribe the measured flow to the road section.

When undertaking the data collection exercise, the focus was on model calibration as opposed to model development and validation. The assumption behind this is that the basic form of the model developed within HDM-4 (Greenwood and Bennett, 1995b and Bennett and Greenwood, 2001) is correct. However, it was of interest to confirm that the model form is correct; therefore data collection runs were undertaken over a range of traffic flows.

In considering which of the above methods to determine flows to use, it is important to keep in mind the utilisation of the resulting flow. For the purposes of calibrating the acceleration noise parameters, it is only necessary to determine those test runs that were undertaken in either very congested conditions (maximum acceleration noise) or very low traffic (natural noise). The actual quantification of whether the flow is 0.5 or 0.6 of capacity on a test run is of use only to validate the overall model form.

It was therefore considered that the adoption of the former of the two methodologies above would yield results sufficient to determine which runs were undertaken at (or very near to) a volume to capacity ratio of 0 or 1. This method was also considered to yield results sufficiently accurate to validate the overall model form. By utilising this method of back-calculating the flow, it is possible to account for the actual flow level observed by the driver, as opposed to some average flow level. This method was also more adept at accounting for the influence of localised changes in the traffic patterns owing to police enforcement, as often lane utilisation and/or direction of travel was heavily affected during the peak periods.

For each road type, the data were plotted of acceleration noise versus mean test run speed. Figure 5.5 to Figure 5.9 illustrate the results of this plotting and confirm that a wide range of traffic conditions were included within the data collection exercise.

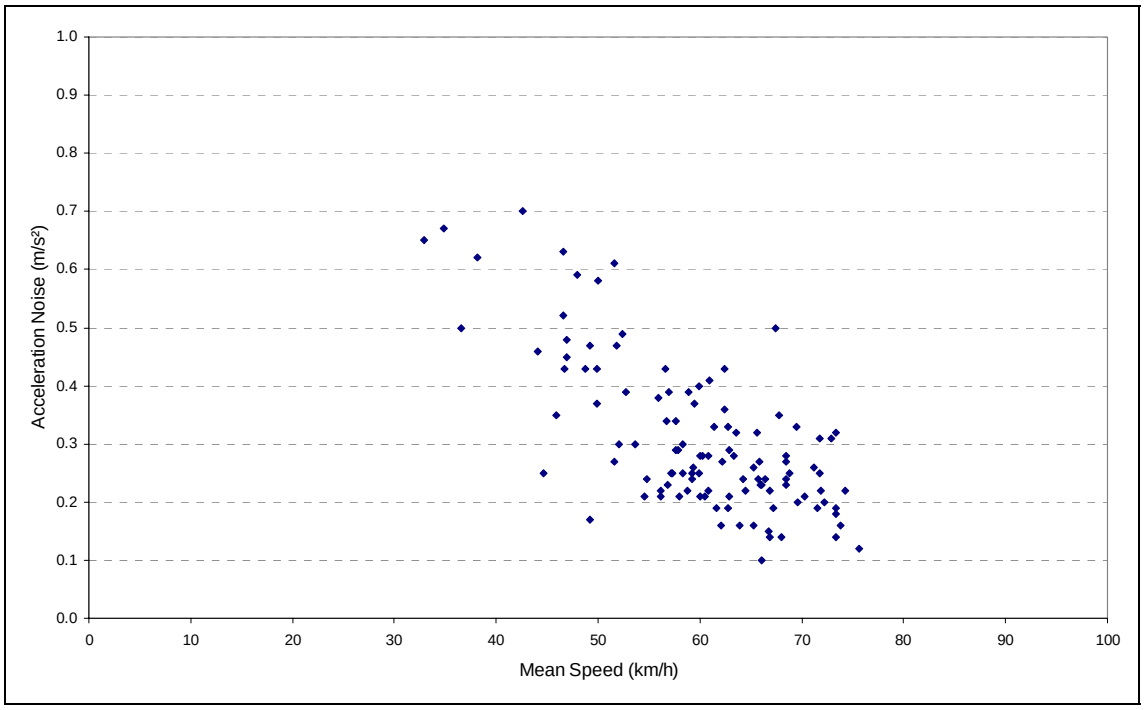

Figure 5.5: Acceleration versus Speed for 2 Lane Undivided Road

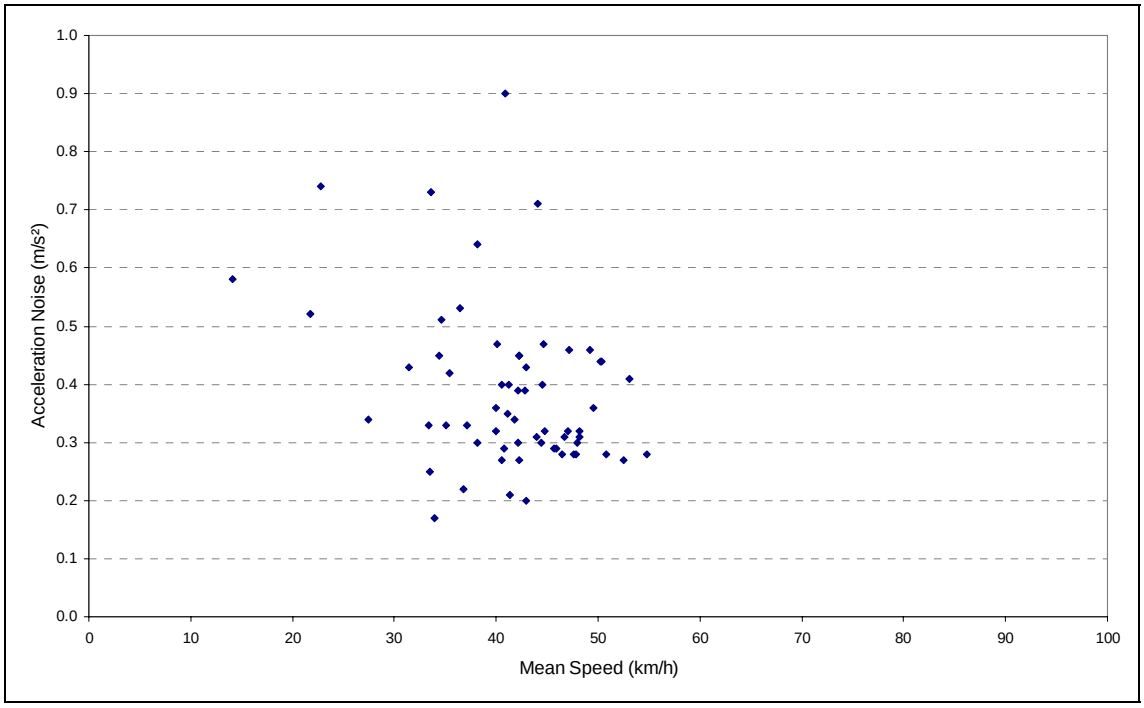

Figure 5.6: Acceleration versus Speed for 4 Lane Undivided Road

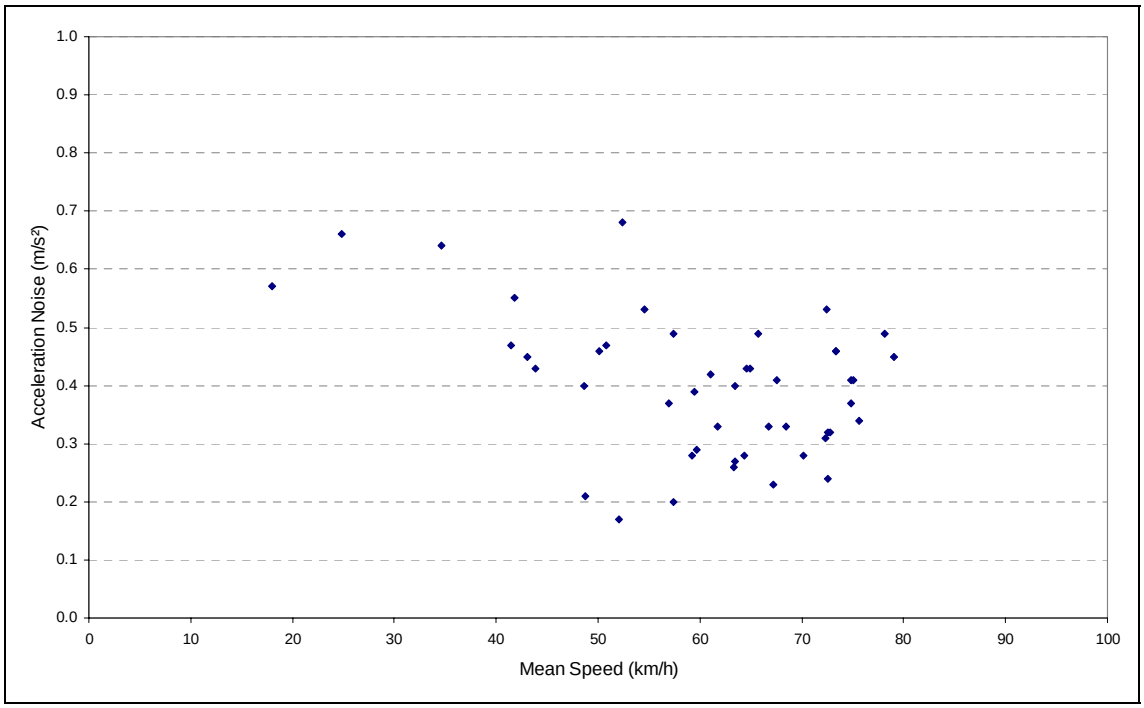

Figure 5.7: Acceleration versus Speed for 4 Lane Divided Road

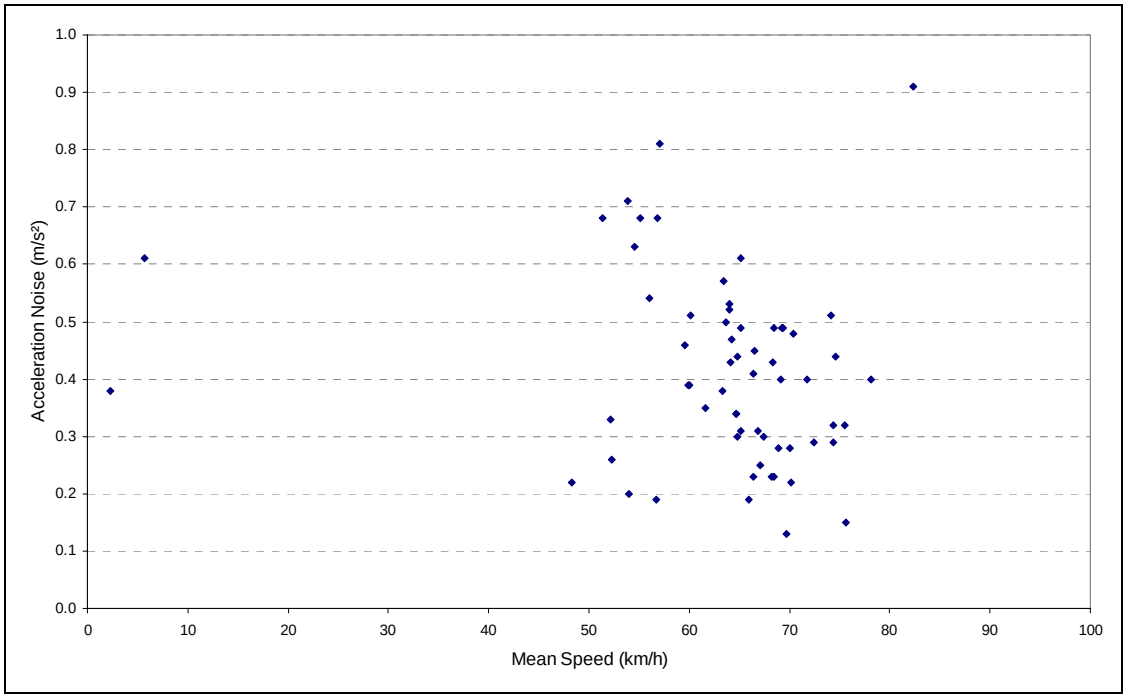

Figure 5.8: Acceleration versus Speed for 6 Lane Divided Road

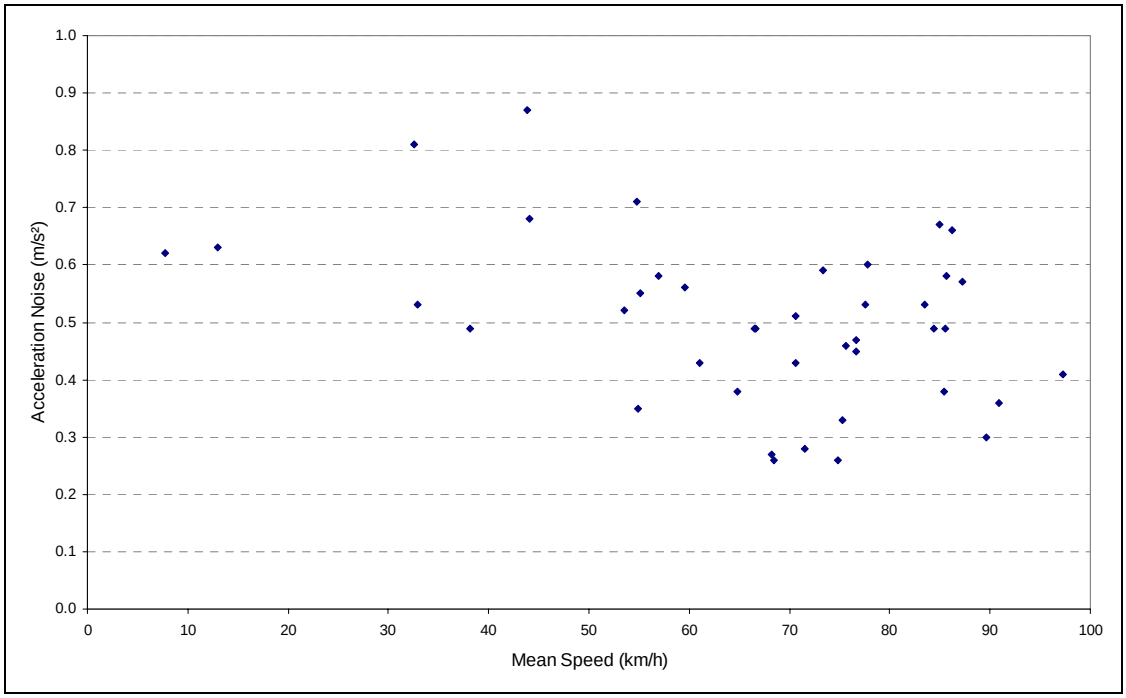

Figure 5.9: Acceleration versus Speed for 6 Lane Highway/Motorway

There is some argument for simply taking the maximum recorded acceleration noise and the minimum recorded acceleration noise levels as the values representing the maximum acceleration noise and the natural acceleration noise respectively. However, it is necessary to utilise values that are considered representative of the acceleration noise level observed at each flow (presented as speed above) level.

In order to obtain values for the maximum traffic noise it is necessary to only include those results measured under highly congested conditions. Figure 3.5 indicates that the acceleration noise level plateau's at high levels of congestion and it was therefore considered that any recording that had a mean speed below that of the nominal capacity speed (Snom) would be considered (values of Snom are given in Table 5.2). From this analysis, the proposed natural noise, maximum traffic and maximum acceleration noise levels proposed for the various road types are given in Table 5.5

Table 5.5: Resulting Acceleration Noise Parameters for Passenger Cars by Road Type

Road Type	Natural Acceleration Noise (m/s^2)	Maximum Traffic Acceleration Noise (m/s^2)	Maximum Total Acceleration Noise (m/s^2)
2 Lane Undivided	0.20	0.62	0.65
4 Lane Undivided	0.20	0.57	0.60
4 Lane Divided	0.20	0.57	0.60
6 Lane Divided	0.15	0.58	0.60
6 Lane Highway/Motorway	0.15	0.58	0.60

Of note in Table 5.5 is that the natural noise level of the 2 and 4 lane roads are higher than the 6 lane roads. It is hypothesised that this is the result of the higher level of side friction typically present on these roads. As expected, the 2 lane road has the highest total acceleration noise level. The maximum acceleration noise levels on the 6 lane roads is in line with the results found by the author in Malaysia (NDLI 1995) and New Zealand.

Figure 5.5 to Figure 5.9 indicate a reasonable spread of test runs in relation to mean speed. However, when plotted as a distribution of volume to capacity ratio as in Figure 5.10, the spread of conditions under which data was collected was found not to be well distributed. As a result of this, it was decided that model validation was not possible as less than 3 per cent of the results span the range of 0.0 to 0.60.

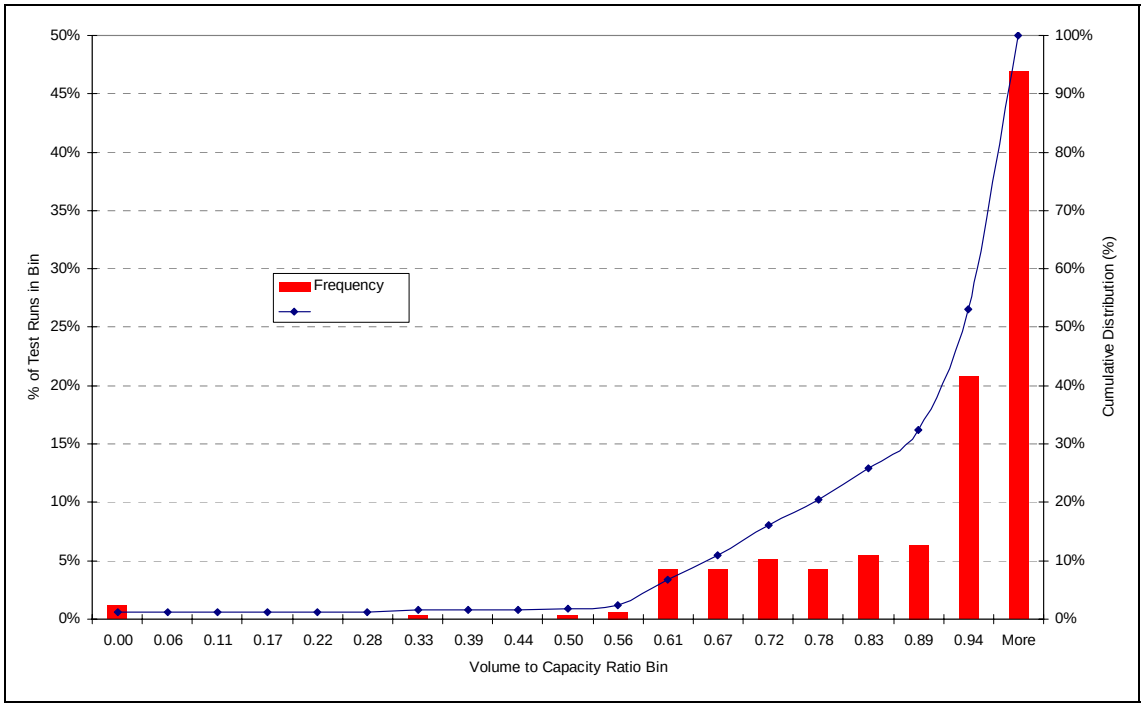

Figure 5.10: Distribution of Volume to Capacity Ratios from Test Runs

Variations between Vehicles and Drivers

This study has included two different vehicles and two drivers as noted previously. It has been postulated (Greenwood and Bennett, 1995b) that the vehicles power to weight ratio plays a significant role in determining the acceleration noise. The two vehicles used within this study were a 1.6L and a 2.0L Toyota Corolla. The power to weight ratios of the two vehicles are given in Table 5.6 below.

Table 5.6: Power to Weight Ratio

Vehicle	Power (kW)	Tare Weight (kg)	Loading[1] (kg)	Power/Weight (kW/kg) * 10^{-3}
1.6L Corolla	85	1150	250	60.7
2.0L Corolla	99	1230	300	64.7

Notes: 1. Loading is an estimate of the load of the driver, surveyor, fuel and cargo

With a difference in the power to weight ratios being under 7 per cent, it is not anticipated that clear results on the effect of the power to weight ratio will be evident. This is especially so for those results recorded at very low flows. It is noted that the comparison between vehicles at very low flows are of little interest, as the level of accelerations are such that the two vehicles would be expected to operate almost the same. Additionally, any difference in driving styles and the accuracy of the back-calculation of the flow from the speed would be expected to 'swamp' the effect of the difference in the power to weight ratios at low flows.

Although it is not possible to enter a range of driving styles within ACCFUEL (refer to Section 5.6) for any single vehicle, the variation between drivers under similar traffic conditions yields some indication as to the need to use representative drivers when undertaking the data collection exercise.

To study the effect of vehicle and driver on the acceleration noise, the results were summarised according to the mean speed of the test run. The average acceleration noise within each 10 km/h mean speed bin and for each vehicle-driver combination was then compared. No data were available for some vehicle-driver-speed combinations. The results of this analysis are shown in Figure 5.11 and Figure 5.12. Both these figures show that driver 2 has a consistently higher acceleration noise level than driver 1. There was not a consistent variation between the two vehicles, which as noted above is thought to be the result of the limited difference in the power to weight ratios of the two vehicles.

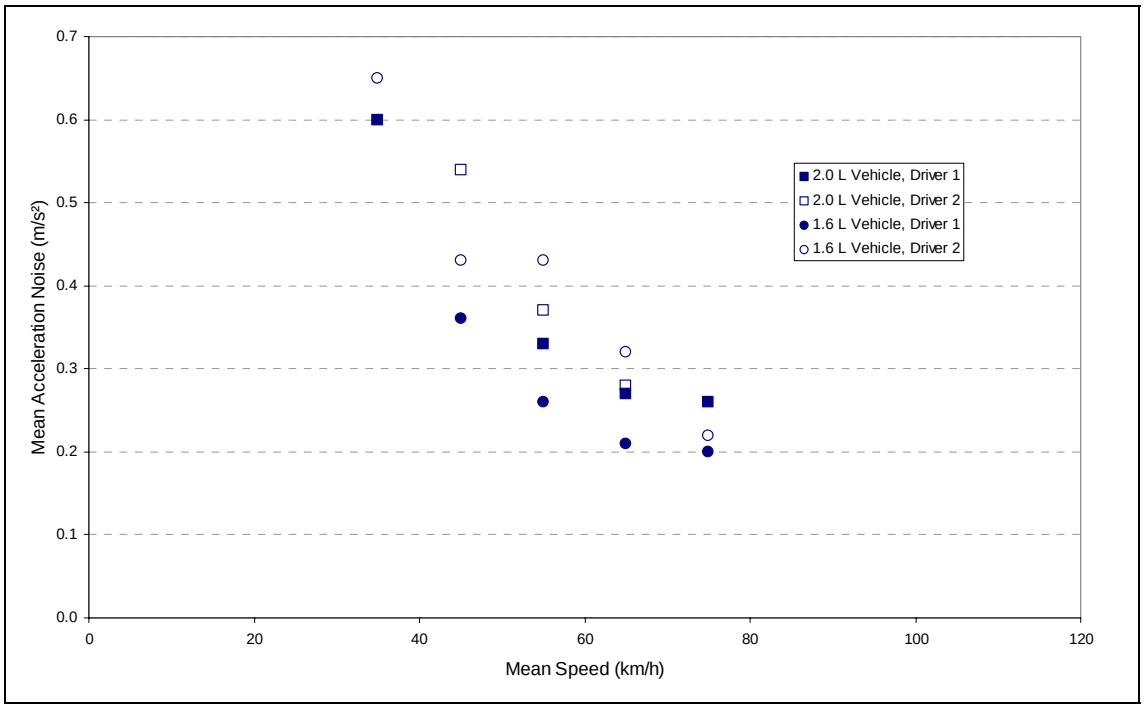

Figure 5.11: Effect of Vehicle-Driver Combinations on 2 Lane Roads

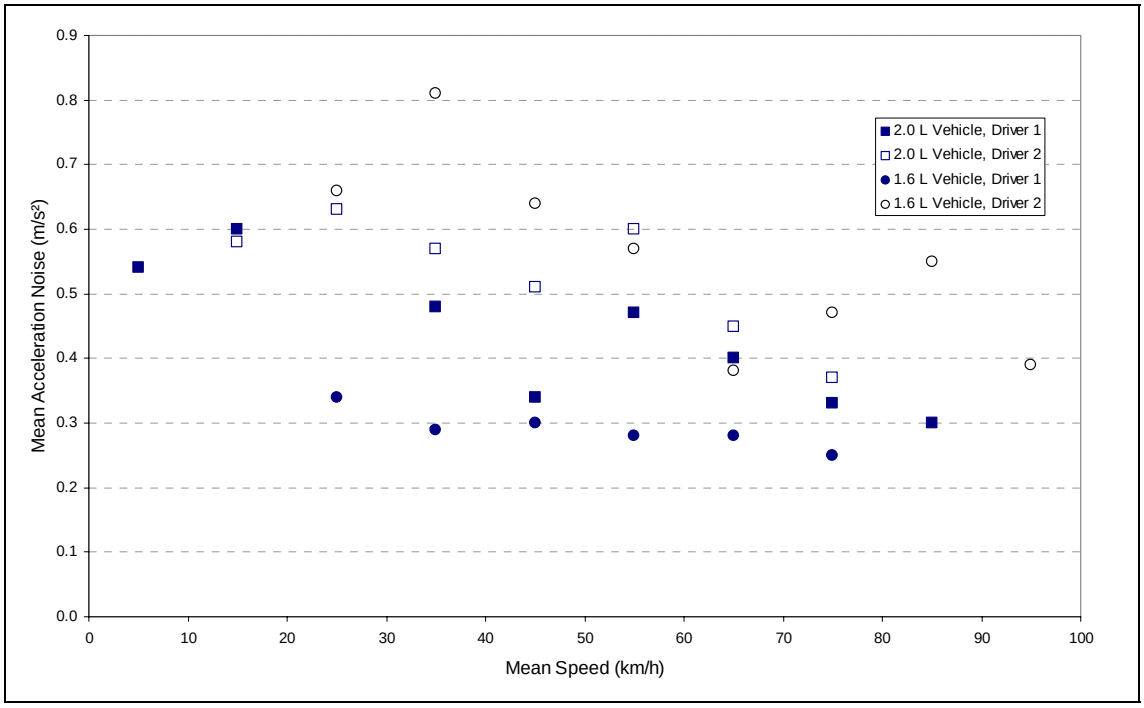

Figure 5.12: Effect of Vehicle-Driver Combinations on Multi-Lane Roads

5.4 New Zealand

5.4.1 Introduction

Following the research in Malaysia and Thailand, a data collection exercise was completed in New Zealand to ensure the results of the Asian countries studied were appropriate outside of the Asian region. The process involved collecting acceleration noise data for a number of drivers under different traffic flow conditions on the Auckland motorway network (central motorway junction to Takanini interchange).

Data collection was restricted to only passenger cars, rather than the wider range of vehicles tested in Malaysia, with the equipment utilised being the same as that employed in Thailand, with traffic count information extracted from induction loops imbedded into the road surface[8].

5.4.2 Methodology

The data collection exercise was designed to provide sufficient evidence to support the previous research in Malaysia and Thailand, rather than to create new relationships. Consequently, the data collection was limited to two passenger cars and three drivers, with data collection runs spanning the full range of traffic conditions.

[8] The author wishes to thank Transit New Zealand for their approval to utilise this data.

5.4.3 Acceleration Noise Versus Flow and Driver Impacts

Figure 5.13 illustrates the consistency between different test drivers over a range of traffic flow conditions (as represented by the average vehicle speed). Of note is that the minimum acceleration noise is in the order of 0.1 m/s², while the maximum is around 0.5 m/s². With the minimum speed under congested conditions being around 10 to 20 km/h as opposed to the 30 km/h surveyed, then extrapolation of the trend would indicate an upper value of approximately 0.6m/s², in line with the value obtained in Malaysia and Thailand (Sections 5.2 and 5.3 respectively).

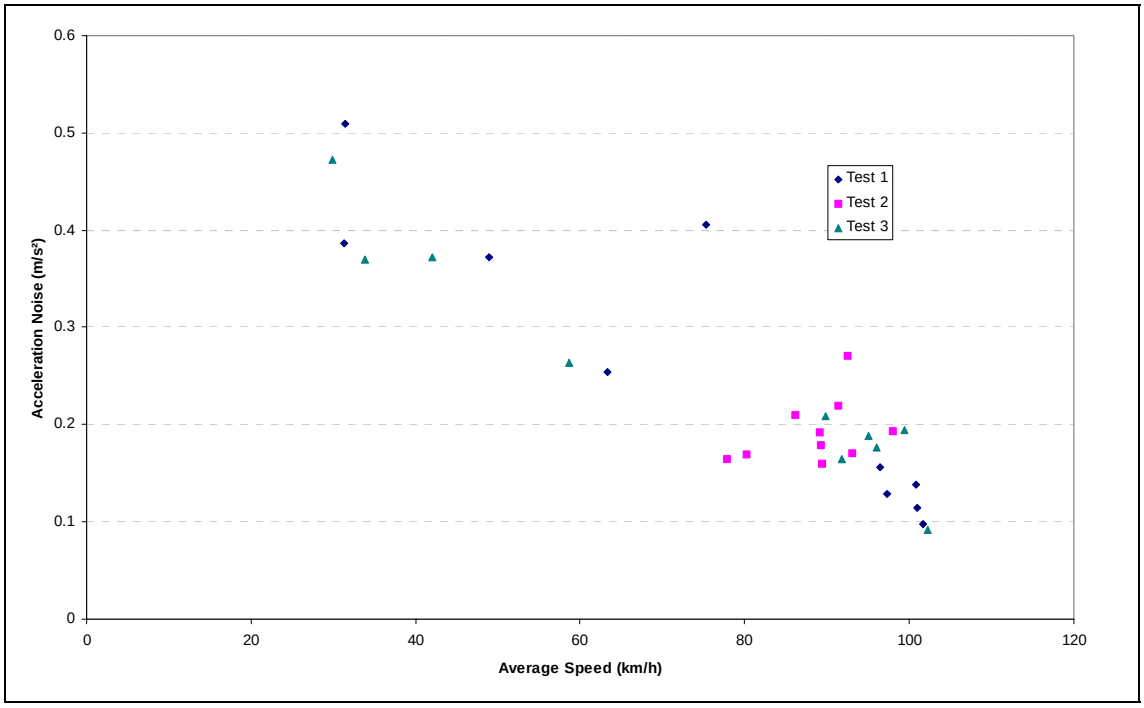

Figure 5.13: Acceleration Noise versus Average Speed from New Zealand Surveys

These values also compared with those collected by EFRU (1997) wherein values of 0.13 m/s² for free flow and 0.66 m/s² for congested conditions on the Auckland motorway system were reported. The EFRU (1997) also indicate a value of 0.31 m/s² corresponding to a mean speed of 70 km/h, which is also in agreement with the results in Figure 5.13.

5.5 Acceleration Noise vs Following Distance and Speed

5.5.1 Introduction

It was postulated that the following distance could well be a significant factor in the determination of acceleration noise, especially when considered in conjunction with the type of vehicle being followed.

The results of the New Zealand data collection tasks indicated that following distance increased depending on the size of the vehicles involved, but no method of relating this information to acceleration noise was performed. Figure 5.14 presents the results of the analysis for data collected on the Auckland motorway network.

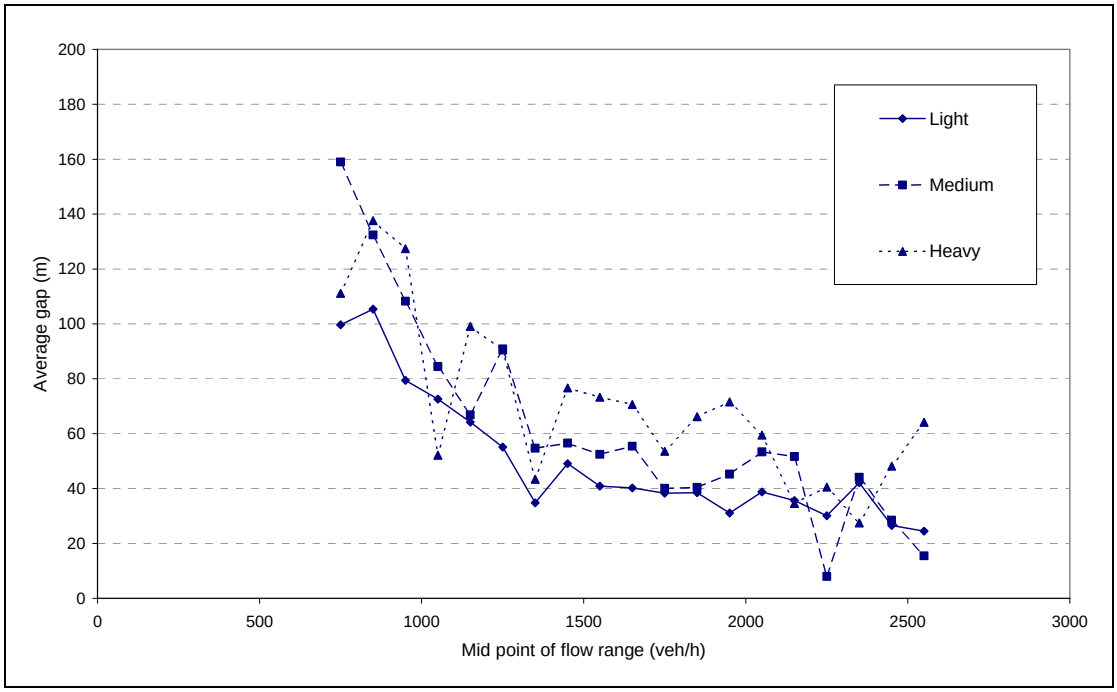

Figure 5.14: Impact of Lead Vehicle Size on Following Distance

Although there is significant variation in the data (especially at lower flows) there exists a general trend that the larger the lead vehicles (the dashed lines), the greater the gap between vehicles. A more detailed examination of the impact of the size of the following vehicle, in conjunction with the lead vehicle (refer to Figure 5.15), also supports the trend but contains a significant level of variation in results.

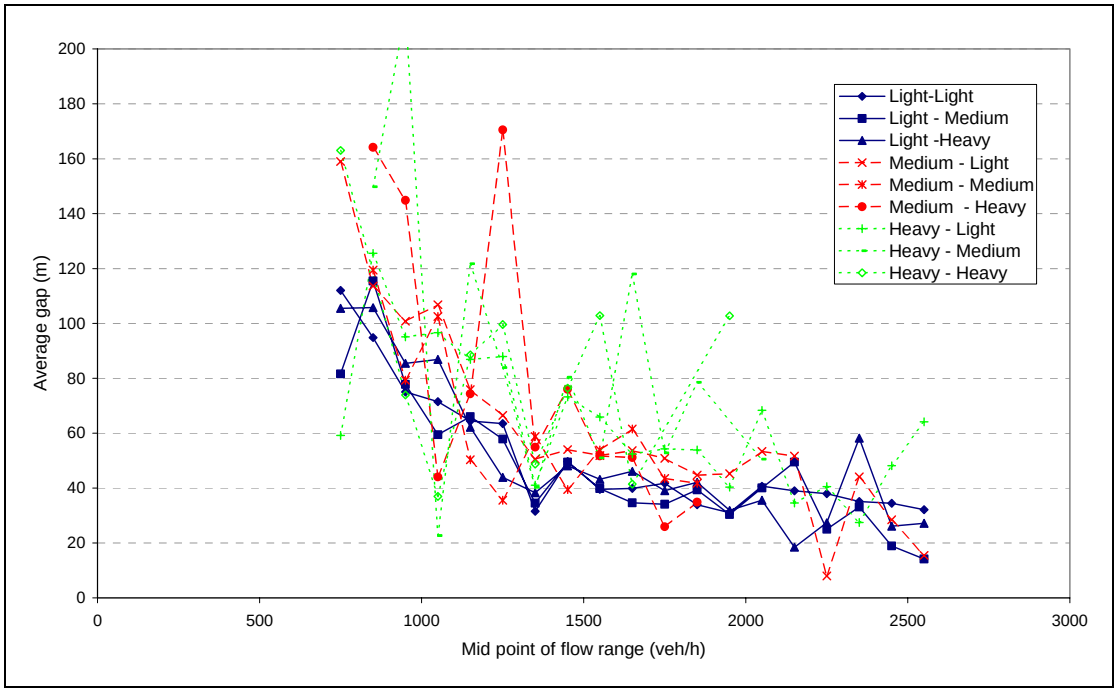

Figure 5.15: Impact of Vehicle Size Combinations on Following Distance

These findings are consistent with those of Wasielewski (1981) who studied the impact of vehicle combination size on headways. Wasielekski (1981) indicated that the size of the headway would increase by 14 per cent if a car was following a truck rather than another car.

On the basis of these findings, it was decided to attempt to record data that could be utilised in refining the acceleration noise model.

5.5.2 Method of Data Collection

The aim with the collection of any data is to do it in a manner that the act of collecting the data has the smallest possible impact on the results. With this in mind, it was considered that trying to equip a pair of vehicles and monitor these throughout the traffic stream was inappropriate as it would lead to very real changes in driving style owing to the fact that each driver would be aware of the other half of the pair.

It was therefore decided to trial a system wherein the existing data collection equipment (refer to Chapter 4) would be supplemented by a device that could record the distance to the vehicle in front. After discussion with various manufacturers it was decided to trial a laser based, distance-measuring device for this purpose.

Upon trial however, it proved to be unreliable in that as the vehicles travelled along the following issues were identified:

- the laser continually picked up different locations on the vehicle, thereby reporting erroneous changes in following distance
- the laser sometimes failed to pick up a measurement off certain areas of the car ahead

As a result of these problems and upon further discussion with the manufacturers of the systems, it was decided to halt this portion of the data collection programme and concentrate on the relationship with flow as discussed in the previous section.

This stance is further supported in terms of the application of the results in the real world. While data on vehicle speeds and flows is generally readily available, information on the distance between vehicles is often more difficult to obtain and it may be that a model built around following distance would not have a practical use.

5.6 Acceleration Noise Simulation Program – ACCFUEL

5.6.1 Introduction

The acceleration noise theory with the parameters derived and presented in Table 5.8 can be used to calculate the effects of congestion on fuel consumption (refer to Chapter 6) and vehicle emissions (refer to Chapter 7). The nature of acceleration noise is such that the application of the theory does not lend itself to a deterministic approach. Instead, a Monte-Carlo simulation was used to establish effects of congestion. The output from this simulation can be used to establish deterministic relationships for the various VOC components – namely fuel consumption and vehicle emissions.

ACCFUEL is a Monte-Carlo simulation program written by the author to simulate the effects of congestion. It was developed specifically for fuel consumption, but it can be used for any other mechanistically predicted VOC component. A flow chart of the simulation program is given in Figure 5.16.

5.6.2 Program Logic

The program is designed to integrate the three-zone speed-flow model (refer to Section 2.2) with the acceleration noise model, to enable prediction of the fuel consumption (or any mechanistic VOC component) at any relative flow. It analyses the congestion effects for relative flows in the range of 0 to 1.0. For each flow, it establishes the mean initial speed from the speed-flow model. Using a coefficient of variation to generate a starting speed for a given mean fleet speed, it then calculates the initial speeds for a number of individual vehicles about this mean.

The simulation is completed by having the vehicles travel along an idealised road, with the acceleration calculated on an instantaneous basis from the acceleration noise distribution. This is added to the previous speed to obtain the speed on the next interval. On the basis of the vehicle speeds and the acceleration, the instantaneous fuel consumption (in mL/s) is established (refer to Chapter 6).

The simulation is conducted so that the vehicle travels a minimum of 10 km and it ends when the average speed over the simulation interval converges within 1 per cent of the initial speed. The additional fuel consumed is the difference between the fuel from the simulation and that to travel the same distance at the initial speed without any accelerations.

The nature of the simulation is such that vehicles may either accelerate or decelerate at any time. To prevent vehicle speeds deviating excessively from the initial speed, restrictions are placed on the speeds. The minimum and maximum velocities used within the programs are calculated as:

$$maxvel = velinit + deltavel \quad (5.3)$$

$$minvel = \max(0, velinit - deltavel) \quad (5.4)$$

where
- maxvel is the maximum allowable velocity for any given initial velocity in m/s
- minvel is the minimum allowable velocity for any given initial velocity in m/s
- velinit is the initial velocity in m/s
- deltavel is the maximum deviation from the initial velocity in m/s

The relationship between the maximum deviation (deltavel) and the initial speed was constructed from a visual analysis of the data.

The maximum deviation at 90 km/h (25 m/s) was approximately 5 km/h (1.4 m/s), while at 20 km/h (5.6 m/s) the maximum deviation was approximately 20 km/h. Between 20 and 90 km/h a quadratic was fitted to give the graph presented as Figure 5.17. The resulting mathematical expression for the allowable velocity deviation is given as Equation 5.5.

$$deltavel = \begin{cases} 0.009\, velinit^2 - 0.485\, velinit + 7.97 & \text{if } velinit < 27.8 \text{ m/s} \\ 1.44 & \text{otherwise} \end{cases} \quad (5.5)$$

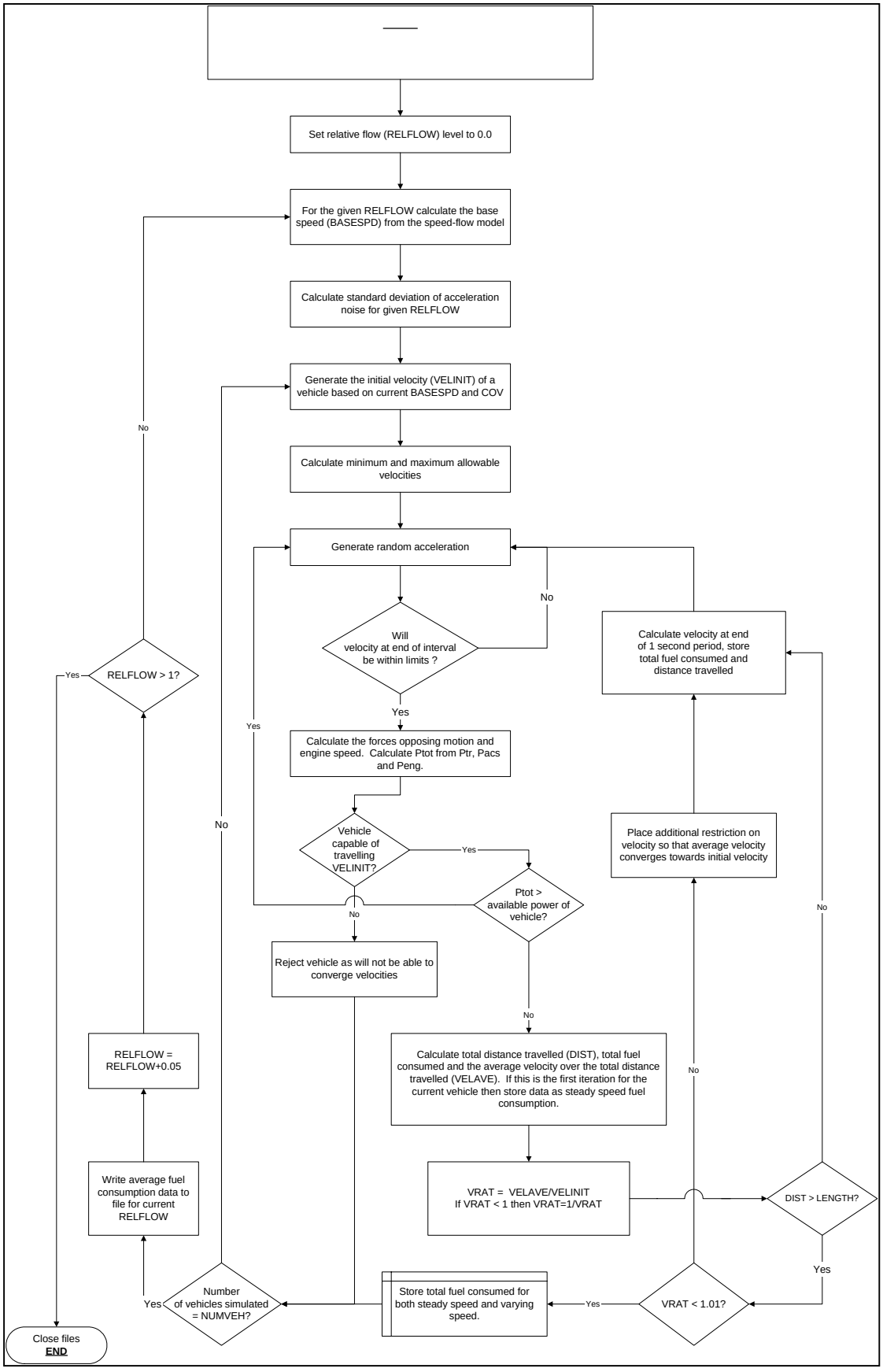

Figure 5.16: Flow Chart of Simulation Methodology for ACCFUEL

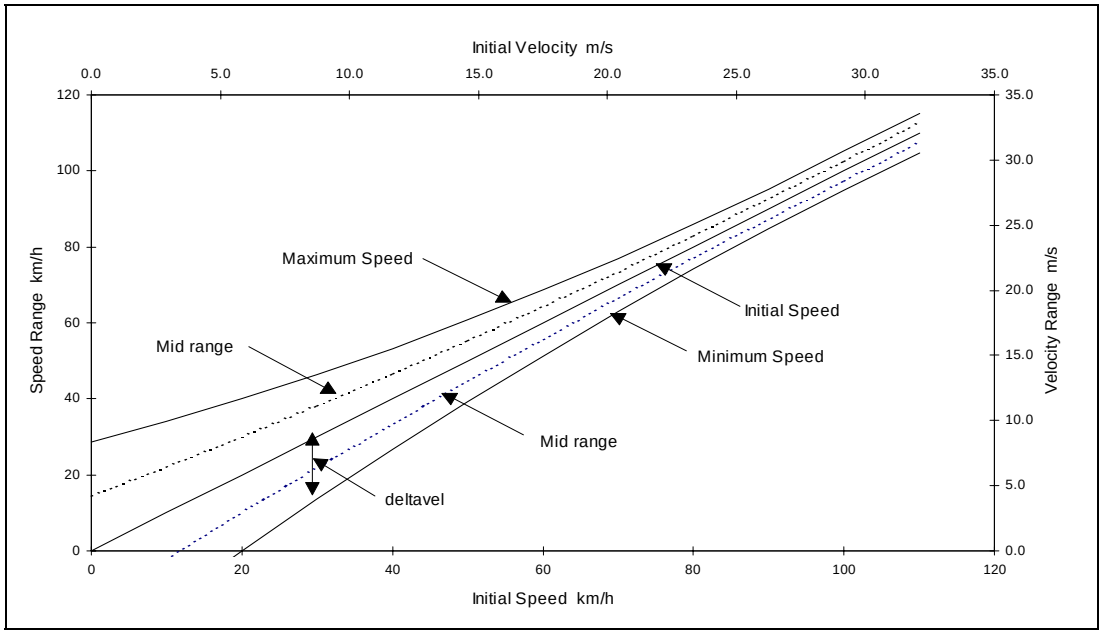

Figure 5.17: Minimum and Maximum Vehicle Speeds

Since the fuel consumption is calculated on an instantaneous basis, it was necessary to use a numerical integration technique. The trapezoidal technique as described by Rajasekaran (1992) was adopted. The instantaneous fuel consumption was calculated at the start of every second, from which the total fuel consumption was calculated.

A typical acceleration profile for a simulation with a minimum length of 1000 m is illustrated in Figure 5.18 (note that a shorter run of 1 km is used for clarity in the following graphs and that in practice a minimum of 10 km is used). The corresponding velocity profile is illustrated in Figure 5.19, which also shows the average velocity. It can be observed in Figure 5.19 that after the minimum simulation length has been reached, the velocities change until the average is within 1 per cent of the initial velocity, at which time the simulation ends.

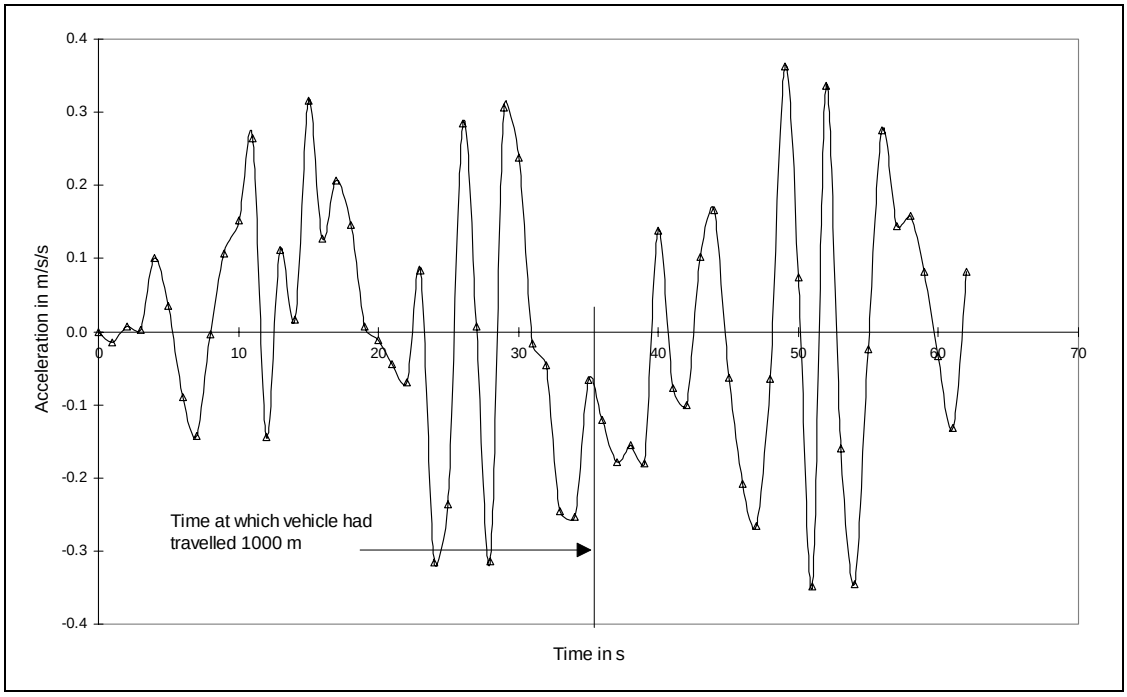

Figure 5.18: Typical Acceleration-Time Profile from Simulation

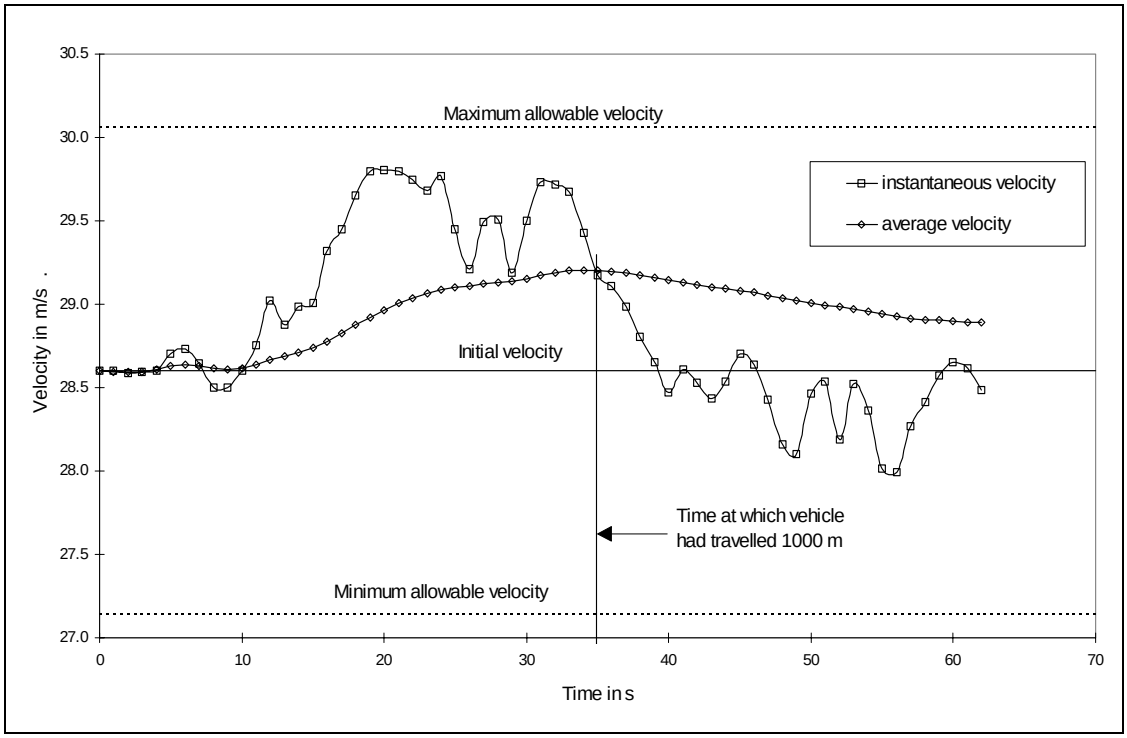

Figure 5.19: Typical Velocity-Time Profile from Simulation

Although there are continuous fluctuations in the velocity, they are of relatively small magnitude. This is illustrated in Figure 5.20, which shows the time-distance profile for the above simulation as an almost straight line.

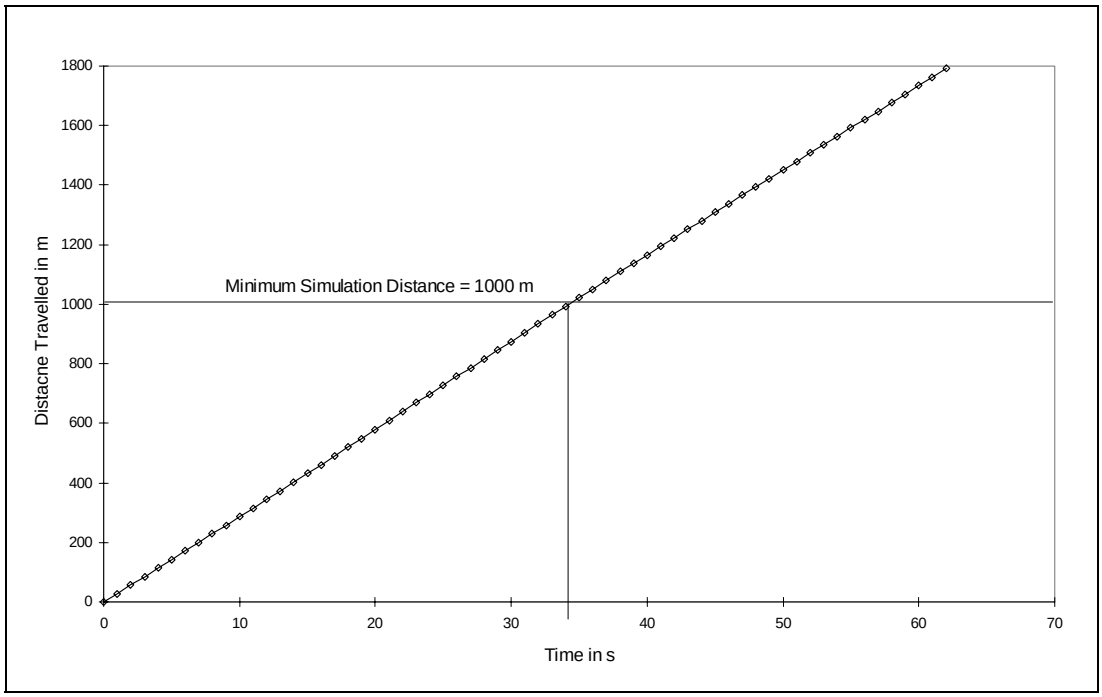

Figure 5.20: Typical Distance-Time Profile from Simulation

5.6.3 ACCFUEL Outputs

The ACCFUEL simulation program outputs a single table of results for each vehicle type analysed. The table contains the parameter DFUEL, which is defined as:

$$\text{DFUEL} = \frac{\text{CongFuel}}{\text{SteadyFuel}} - 1 \qquad (5.6)$$

where DFUEL is the proportionate increase in fuel consumption due to acceleration noise
CongFuel is the fuel consumption rate (mL/s) with congestion impacts
SteadyFuel is the fuel consumption rate (mL/s) without congestion impacts

The simulation program outputs DFUEL for a matrix of acceleration noise (0 to 1 m/s² in 0.05 m/s² increments) and mean speeds (10 to 100 km/h in 5 km/h increments). A sample output for a single vehicle class is given in Table 5.7.

Table 5.7: Sample Output From ACCFUEL Program

VEH_NUM	VEH_NAME	SPEED	ACC_000	ACC_005	ACC_010	ACC_015	ACC_020	ACC_025	ACC_030	ACC_035	ACC_040	ACC_045	ACC_050	ACC_055	ACC_060	ACC_065	ACC_070	ACC_075	ACC_080	ACC_085	ACC_090	ACC_095	ACC_100
3	PC-M	10	0.005	0.005	0.010	0.017	0.027	0.038	0.048	0.058	0.068	0.078	0.087	0.097	0.109	0.121	0.133	0.143	0.160	0.170	0.184	0.193	0.209
3	PC-M	15	0.007	0.008	0.011	0.014	0.020	0.026	0.033	0.042	0.049	0.057	0.068	0.082	0.096	0.105	0.120	0.130	0.148	0.158	0.175	0.190	0.203
3	PC-M	20	0.007	0.008	0.009	0.013	0.018	0.025	0.028	0.036	0.044	0.052	0.062	0.069	0.082	0.095	0.109	0.125	0.134	0.158	0.172	0.187	0.199
3	PC-M	25	0.010	0.011	0.013	0.017	0.021	0.027	0.034	0.041	0.050	0.061	0.070	0.081	0.096	0.110	0.127	0.143	0.156	0.174	0.193	0.212	0.226
3	PC-M	30	0.013	0.013	0.016	0.021	0.028	0.031	0.039	0.048	0.057	0.072	0.083	0.100	0.115	0.136	0.154	0.171	0.187	0.210	0.231	0.249	0.274
3	PC-M	35	0.017	0.017	0.021	0.025	0.030	0.035	0.044	0.059	0.069	0.076	0.095	0.116	0.132	0.151	0.176	0.193	0.223	0.246	0.265	0.289	0.308
3	PC-M	40	0.025	0.024	0.024	0.028	0.037	0.041	0.043	0.060	0.072	0.088	0.104	0.126	0.147	0.172	0.191	0.212	0.242	0.260	0.290	0.315	0.336
3	PC-M	45	0.030	0.027	0.033	0.035	0.038	0.048	0.049	0.065	0.079	0.090	0.111	0.132	0.153	0.179	0.201	0.231	0.252	0.276	0.302	0.325	0.355
3	PC-M	50	0.037	0.039	0.039	0.042	0.044	0.051	0.059	0.068	0.080	0.097	0.119	0.132	0.161	0.183	0.207	0.229	0.261	0.286	0.305	0.339	0.372
3	PC-M	55	0.037	0.040	0.045	0.046	0.051	0.054	0.060	0.068	0.083	0.099	0.121	0.140	0.158	0.182	0.215	0.238	0.271	0.294	0.309	0.344	0.370
3	PC-M	60	0.051	0.050	0.055	0.053	0.057	0.064	0.062	0.078	0.092	0.097	0.123	0.140	0.162	0.178	0.207	0.236	0.262	0.286	0.319	0.350	0.364
3	PC-M	65	0.056	0.056	0.059	0.059	0.066	0.068	0.072	0.087	0.089	0.101	0.119	0.144	0.153	0.182	0.211	0.236	0.257	0.287	0.318	0.340	0.351
3	PC-M	70	0.070	0.066	0.069	0.068	0.070	0.079	0.074	0.082	0.102	0.101	0.121	0.145	0.169	0.183	0.207	0.220	0.246	0.267	0.295	0.320	0.345
3	PC-M	75	0.072	0.078	0.071	0.080	0.089	0.083	0.085	0.096	0.102	0.114	0.132	0.136	0.160	0.172	0.195	0.225	0.233	0.260	0.296	0.303	0.340
3	PC-M	80	0.080	0.088	0.080	0.094	0.094	0.087	0.101	0.099	0.101	0.109	0.131	0.144	0.155	0.171	0.192	0.221	0.241	0.252	0.269	0.298	0.328
3	PC-M	85	0.095	0.091	0.093	0.097	0.103	0.094	0.106	0.104	0.118	0.126	0.142	0.146	0.158	0.177	0.188	0.210	0.224	0.239	0.271	0.276	0.297
3	PC-M	90	0.099	0.104	0.103	0.105	0.102	0.103	0.117	0.120	0.123	0.119	0.133	0.154	0.168	0.166	0.187	0.212	0.216	0.245	0.261	0.268	0.299
3	PC-M	95	0.105	0.115	0.112	0.111	0.115	0.113	0.112	0.127	0.128	0.129	0.146	0.140	0.154	0.169	0.202	0.205	0.227	0.226	0.252	0.272	0.278
3	PC-M	100	0.117	0.106	0.111	0.126	0.120	0.126	0.120	0.139	0.136	0.136	0.144	0.165	0.169	0.179	0.177	0.205	0.222	0.230	0.249	0.264	0.272

5.7 Summary and Conclusions

This chapter has presented the findings of three separate studies aimed at identifying the relationship between acceleration noise and traffic flow. The data were collected in New Zealand, Malaysia and Thailand using a combination of drivers and vehicles.

As a result of the work, Table 5.8 contains the recommended model parameters predicting acceleration noise:

Table 5.8: Recommended Acceleration Noise Values

Vehicle Class	Road Class	Natural Acceleration Noise[1] (m/s^2)	Maximum Traffic Acceleration Noise (m/s^2)	Maximum Total Acceleration Noise (m/s^2)
Motorcycles	All	0.20	0.57	0.60
Private Passenger Cars and Taxis	2 Lane Undivided	0.20	0.62	0.65
	4 Lane Undivided	0.20	0.57	0.60
	4 Lane Divided	0.20	0.57	0.60
	6 Lane Divided	0.15	0.58	0.60
	6 Lane Highway /Motorway	0.15	0.58	0.60
Light Truck	All	0.10	0.59	0.60
Medium Truck	All	0.10	0.59	0.60
Heavy Truck	All	0.10	0.59	0.60
Heavy Truck Towing	All	0.10	0.59	0.60
Mini-Bus	All	0.20	0.57	0.60
Medium Bus	All	0.20	0.57	0.60
Coach	All	0.10	0.59	0.60

Source: For non-passenger cars is Bennett and Greenwood (2001)

The Malaysian research also indicated that the power to weight ratio of the vehicle played a significant role in the acceleration noise level, although insufficient data were available to develop this theory further. It does however make logical sense that with a low power to weight ratio, very little “spare” power is available to accelerate the vehicle. The use of multiple vehicle classes also negates the need for such refinement to a certain extent, as the different power to weight ratios are implicit in the different vehicle classes.

The New Zealand data collection exercise has established that the parameter values obtained from the extensive work in Malaysia and Thailand are relevant also to the Auckland motorway network.

Analysis of the data available from the traffic counting loops indicates a relationship between the following distance and the size of the vehicles in the combination. Data were not available to establish if the change in following distance also resulted in a change to the acceleration noise level (refer to Section 5.5).

Various methods were tried in the attempt to establish a relationship between acceleration noise and following distance. However, the methods tested proved to be unreliable and were therefore halted. The New Zealand data provided evidence that drivers also maintain different gaps depending on the size of the vehicle they are following, with the larger the vehicle the larger the gap.

A simulation program – ACCFUEL – has been developed to apply the acceleration noise concepts to determine the additional fuel consumed from congestion impacts. The output is a parameter termed DFUEL, which is the proportionate increase in fuel consumption caused by the acceleration noise. ACCFUEL simulates a number of vehicles travelling along a section of road, and for each second uses Monte Carlo techniques to select an acceleration from the appropriate acceleration noise distribution.

6 FUEL CONSUMPTION MODELLING

6.1 Introduction

Fuel consumption is one of the primary vehicle operating costs impacted by traffic congestion. Section 2.7 presented a review of fuel consumption models, with this section focussing on the calculation of the many inputs.

As part of the data collection discussed in Chapter 5, fuel consumption data were available for a range of vehicles under different driving conditions and in a laboratory environment.

This chapter commences with a discussion of the forces acting upon a vehicle, then moves through to determining the power requirements of the vehicle and finally on to the prediction of the fuel consumed to meet the power requirements.

The chapter also includes a comparison of observed versus predicted fuel consumption values.

6.2 Forces Opposing Motion

6.2.1 Introduction

When modelling vehicle operating costs (VOCs), two approaches are available — empirical and mechanistic. Traditionally researchers used coarse empirical data (de Weille, 1966) and analysed using some form of regression. The result was often a model with a high degree of complexity and accuracy but a complete lack of mobility, i.e. it could not be applied to any other location. The recent approach has been to use mechanistic models that relate the VOC components to the forces opposing motion. This approach has many benefits over the earlier empirical models, especially in the area of transportability of the resulting models.

Given the many benefits of mechanistic modelling (NDLI 1995), this approach has been adopted for this research. Mechanistic models predict that the VOC are proportional to the forces acting on the vehicle (refer to Section 2.7). Thus, by quantifying the magnitude of the forces opposing motion one can establish, for example, the fuel consumption.

The forces acting on a vehicle as it ascends a grade of angle θ to the horizontal, are shown in Figure 6.1. These forces are:

Fa	Aerodynamic drag resistance in N
Fg	Gradient resistance in N
Fi	Inertial resistance in N
Fr	Rolling resistance in N
Ftr	Tractive forces in N

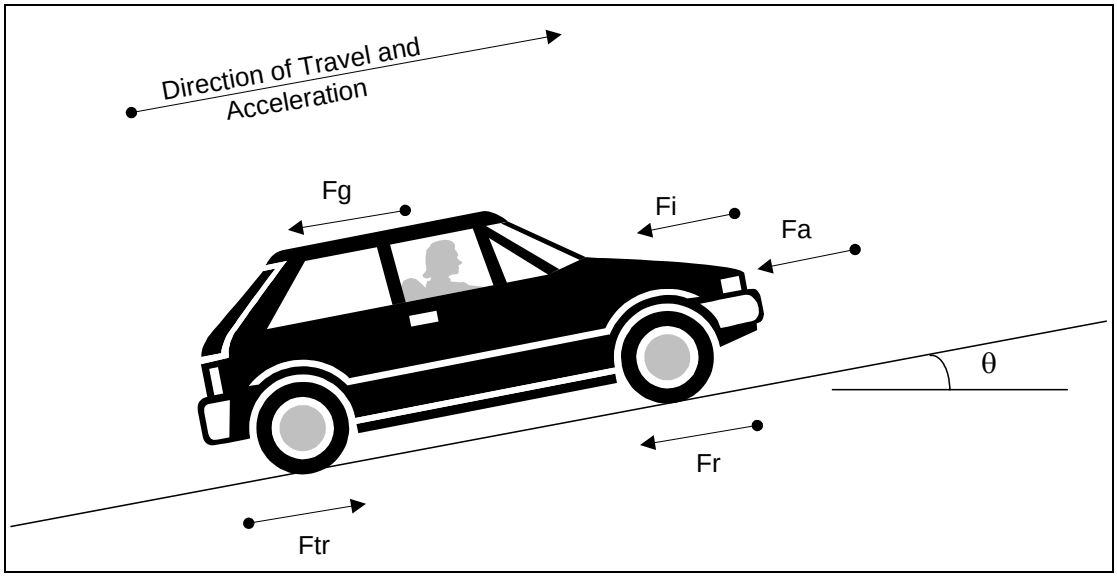

Figure 6.1: Forces acting on a Vehicle on a Gradient

An additional force is applied to the vehicle when it traverses a curve, which is called the curvature resistance (Fcr). This force is also present on straights owing to the cross-fall of the road, but is generally ignored from calculations owing to the small impact on results.

The tractive force, Ftr, applied to the wheels by the engine opposes the sum of these forces. Each of these forces is described in the following sections, along with how they are quantified.

6.2.2 Aerodynamic Resistance

Introduction

The aerodynamic resistance represents the force required to push an object through the air. It is calculated as:

$$Fa = 0.5\ \rho\ CD\ AF\ vr^2 \qquad (6.1)$$

where	Fa	is the aerodynamic force opposing motion in N
	ρ	is the mass density of air in kg/m^3
	CD	is the aerodynamic drag coefficient
	AF	is the projected frontal area of the vehicle in m^2
	vr	is the speed of the vehicle relative to the wind in m/s

The remainder of this section quantifies the various components of this equation.

Mass Density of Air

The mass density of air varies with pressure and temperature. Hess (1959) shows that for the troposphere (sea level to 10.769 km), the temperature decreases at a constant rate of 6.5°C/km. Hess (1959) also proves that the relationship between air pressure and temperature for the troposphere is:

$$P = P_o \left(\frac{T}{T_o} \right)^{g/R\gamma} \tag{6.2}$$

where P is the pressure at temperature T in kPa
Po is the standard pressure at sea level in kPa (101.325 kPa)
T is the temperature at a selected altitude in K
To is the standard air temperature at sea level in K (288.16 K)
R is the gas constant (286.934 $m^2/s^2/K$)
g is the acceleration due to gravity in m/s^2

The relationship between temperature and altitude is given in Hess (1959) as:

$$T = T_o - \gamma \, ALT \tag{6.3}$$

where γ is the rate of change in temperature in K/m (0.0065 K/m)
ALT is the altitude above sea level in m

Air density is related to pressure and temperature by:

$$\rho = \frac{P}{R\,T} \tag{6.4}$$

Combining equations 6.2 to 6.6 yields the following equation for predicting air density at any given altitude up to 10.769 km.

$$\rho = \frac{P_o}{R\,T_o} \left(1 - \frac{\gamma \, ALT}{T_o} \right)^{\left(g/R\gamma\right)-1} .1000 \tag{6.5}$$

Substituting the standard values for the variables as given above yields the following simplified relationship:

$$\rho = 1.225 \, (1 - 2.26 \times 10^{-5} \, ALT)^{4.26} \tag{6.6}$$

Figure 6.2 illustrates the above equation, showing an almost straight line over the range of likely values, with a decrease in density of approximately 25 per cent between sea level and 3000 m.

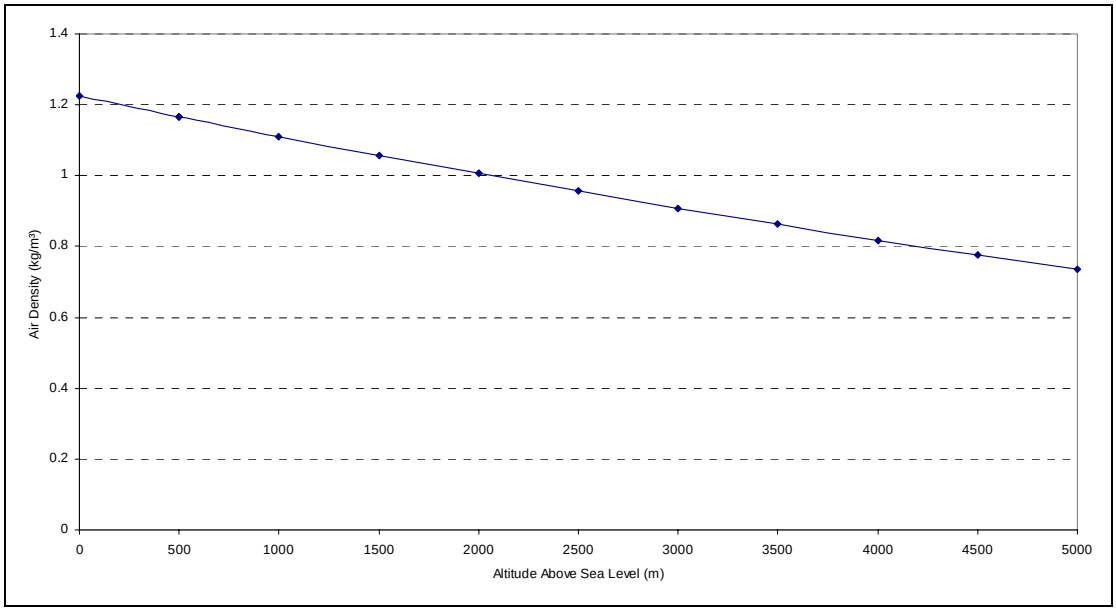

Figure 6.2: Air Density Versus Altitude

This is very similar to the relationship reported in St John and Kobett (1978), which only has the exponent value different by a small amount as shown below.

$$\rho = 1.225 (1 - 2.26 \times 10^{-5} ALT)^{4.225} \quad (6.7)$$

Biggs (1987) gives the density of air at 15 ^{o}C and 200 m as 1.20 kg/m^3. Substituting an altitude of 200 m into Equation 6.6 yields a density of 1.20kg/m^3, which supports the methodology presented.

Within HDM-4 (NDLI,1995), the effect of air temperature has been double counted by combining various relationships from different research.

For the remainder of this research, a density of air equalling 1.20 kg/m^3 has been used.

Aerodynamic Drag Coefficient and Relative Velocity

The aerodynamic drag coefficient (CD) is a measure of three sources of air resistance:

- form drag caused by turbulent air flow around the vehicle;
- skin friction between the air and the vehicle;
- interior friction caused by the flow of air through the vehicle.

Form drag and skin friction make up approximately 85 per cent and 10 per cent respectively of the total air resistance (Mannering and Kilareski, 1990). Square shaped vehicles have higher CD values than rounded vehicles due to the increased turbulence caused as they pass through the air. The desire for a low aerodynamic drag coefficient is seen in many of todays streamlined cars.

The CD is a function of vehicle direction relative to the wind and the relative velocity of the vehicle to the wind. The apparent direction of the wind, which is the vector resultant of the vehicle direction and the wind direction, is termed the yaw angle (ψ) and is illustrated in Figure 6.3. The values of CD reported in the literature are usually from wind tunnel tests conducted with a 0 degree yaw (i.e. front on to the wind) and accordingly are the minimum for the vehicle.

The following notation applies to Figure 6.3:

Vw	velocity of the wind in m/s
χ	angle between direction of vehicle and wind in degrees
ψ	yaw angle in degrees
vr	relative velocity in m/s
v	vehicle velocity in m/s

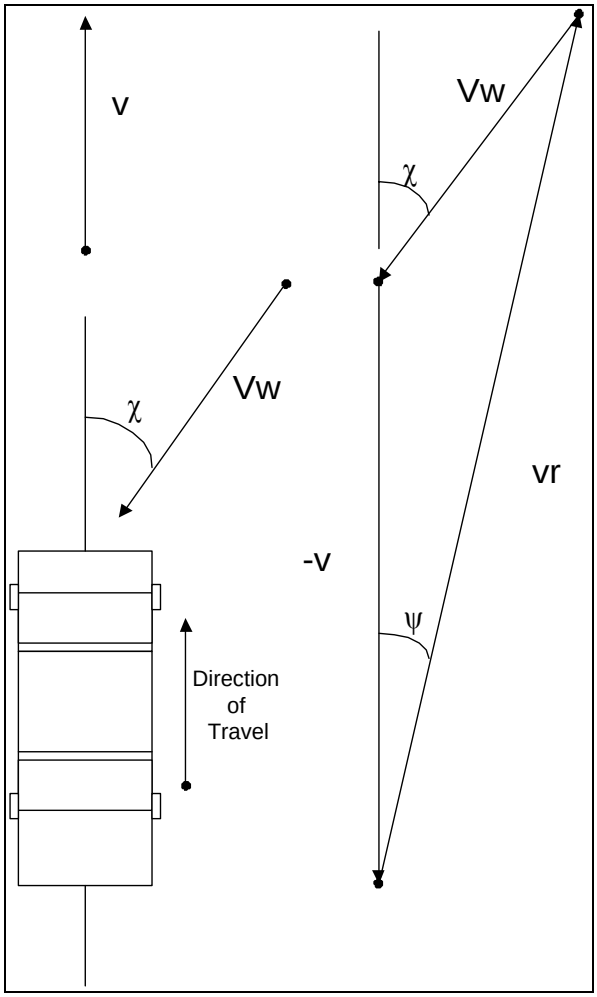

Figure 6.3: Wind Forces Acting on a Vehicle

To obtain typical values of CD that would be found on roads, it is therefore necessary to adjust for the variation in wind direction. This can be done using a "typical" wind angle which increases the 0 degree yaw CD, leading to wind averaged CD, or CD(ψ). The ratio of CD(ψ)/CD is termed the CD multiplier (CDmult). Equation 6.1 can therefore be rewritten as:

$$Fa = 0.5\ \rho\ CD(\psi)\ AF\ vr^2 \quad (6.8)$$

$$Fa = 0.5\ \rho\ CDmult\ CD\ AF\ vr^2 \quad (6.9)$$

where CD(ψ) is the wind averaged CD
CDmult is the CD multiplier

Biggs (1988) presented an approach for calculating CDmult, however Biggs (1995) recommends the use of the methodology presented by Sovran (1984). The Sovran (1984) approach gives a value of zero for CDmult when the yaw angle is 90°, whereas the method presented by Biggs (1988) gives a non-zero value. The Sovran (1984) approach for calculating CDmult is as follows:

For $0 < \psi < \psi c$

$$CDmult = 1 + h\left[\sin\left(\frac{90\psi}{\psi c}\right)\right]^2 \quad (6.10)$$

For $\psi c < \psi < 180 - \psi c$

$$CDmult = (1+h)\cos\left[\frac{90(\psi - \psi c)}{90 - \psi c}\right] \quad (6.11)$$

For $180 - \psi c < \psi < 180$

$$CDmult = -\left(1 + h\left[\sin\left(\frac{90(180 - \psi)}{\psi c}\right)\right]^2\right) \quad (6.12)$$

where ψc is the yaw angle in degrees at which CDmult is a maximum
ψ is the yaw angle (i.e. the apparent direction of the wind)
h is the proportionate increase in CD at angle ψc (see Figure 6.4)

The yaw angle is given by:

$$\psi = \sin^{-1}((Vw \sin(\chi))/vr) \quad (6.13)$$

The velocity of the vehicle relative to wind can be calculated from Figure 6.3 as:

$$vr^2 = v^2 + Vw^2 + 2\ v\ Vw \cos(\chi) \quad (6.14)$$

Sovran (1984) gives the value of ψc as 30^o and h as 0.4 for passenger cars. Figure 6.4 is a plot of CDmult for $\psi c = 30^o$ and h=0.4. Wong (1993) indicates that ψc is approximately 30^o for heavy vehicles also. Biggs (1995) gives the following values of h for trucks, which compare well with the data in Wong (1993).

0.6	rigid trucks
0.8	single trailer trucks
1.2	double trailer trucks

In order to calculate an average value for CDmult it is necessary to allow for the distribution of wind directions acting on a vehicle.

Ingram (1978) calculated wind-averaged values of CD for heavy goods vehicles by establishing the distribution of wind speeds and directions imposed on a vehicle on various motorways around Britain. He compared his detailed values with those that would have arisen under the assumption that on a network there is an equal probability of wind arriving at all angles relative to the centre line of the roads. He concluded that:

[using] *"the approximation reached by assuming that the national average wind speed is equally probable from all directions is quite adequate, giving an error of less than one per cent"*.

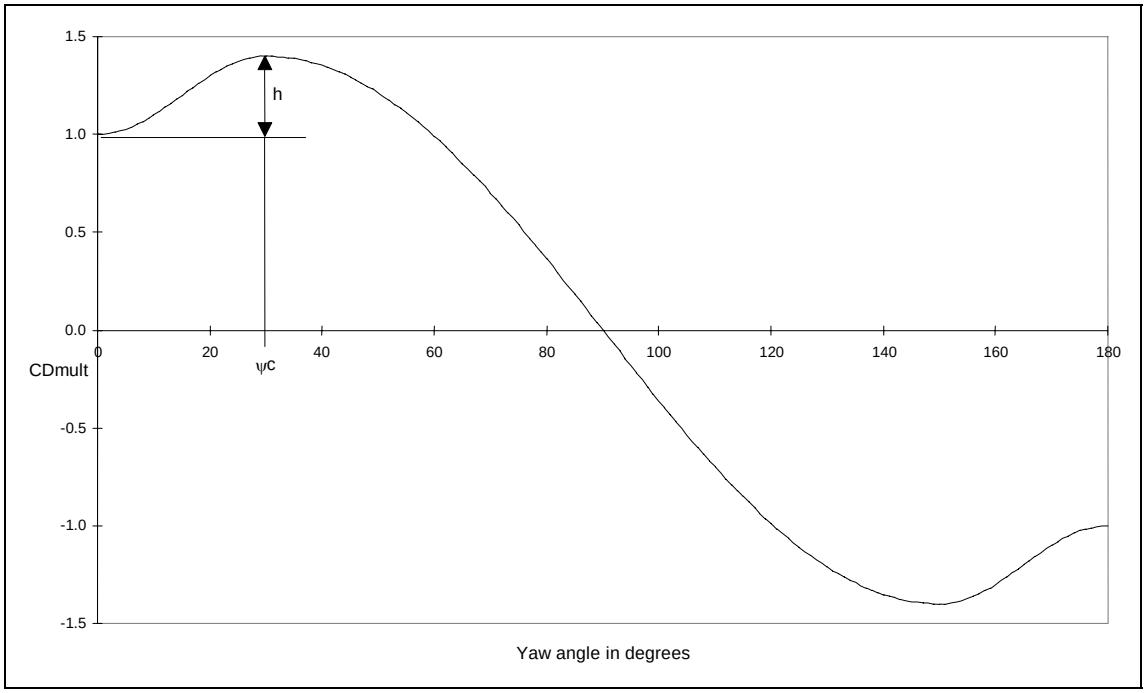

Figure 6.4: CDmult versus Yaw Angle

This does not imply that the wind has an equal probability of arriving from all directions, as most localities have predominant wind patterns, but rather that the combined distribution of wind and road angles is equally distributed. Consequently,

there is little utility in undertaking a detailed analysis of wind direction, such as that done by Ingram (1978).

Using the approximation that wind has an equal probability of arriving at any angle relative to the centre line of the road within a network, in conjunction with Equations 6.10 through 6.12, a wind-averaged CD multiplier can be ascertained. By considering the relative velocity of the vehicle in these calculations it is possible to rewrite Equation 6.9 as:

$$Fa = 0.5\ \rho\ CDmult\ CD\ AF\ v^2 \qquad (6.15)$$

Thus, the value of CDmult implicitly models the ratio of vr^2/v^2.

Under the assumption that ψc is a constant value of 30^o for all vehicle classes, a series of calculations were performed using a program written in Visual Basic to calculate the CD multiplier. Appendix B contains a listing of the code. As ψc is assumed to be a constant (30 degrees) for all vehicle types, the value of CDmult is a function of 3 variables - vehicle velocity, wind velocity and h.

Table 6.1 is a plot of CDmult for a range of vehicle and wind velocities with a value of 0.4 (passenger car) for h. It is noted that wind has a greatest effect when vehicle velocities are low. This is due to the dominance of the relative wind vector by the actual wind velocity at these lower vehicle speeds. Further to this, it is important to note that under normal operating conditions one would expect vehicle speeds to be typically much higher than the average wind speed.

Table 6.1: CDMult versus Wind and Vehicle Speeds

		Vehicle Speed (m/s)						
		1	**5**	**10**	**15**	**20**	**25**	**30**
Wind Speed (m/s)	**0**	1.00	1.00	1.00	1.00	1.00	1.00	1.00
	2	6.33	1.36	1.10	1.05	1.03	1.02	1.01
	4	21.64	2.04	1.36	1.18	1.10	1.07	1.05
	6	47.16	3.06	1.67	1.36	1.22	1.15	1.10
	8	82.89	4.49	2.04	1.56	1.36	1.24	1.18
	10	128.82	6.33	2.50	1.78	1.51	1.36	1.26
	12	184.96	8.58	3.06	2.04	1.67	1.48	1.36
	14	251.31	11.23	3.73	2.34	1.85	1.60	1.45
	16	327.87	14.29	4.49	2.68	2.04	1.74	1.56

A regression analysis was undertaken to allow prediction of CDmult for any combination of v, Vw and h. The resulting function is:

$$CDMult = \left[(0.5106\ h + 0.9821)\ V^{(0.0082\ h\ -\ 1.9919)}\right] Vw^2 + \left[(-0.004\ h - 0.0001)\ V + (0.1372\ h + 0.0015)\right] Vw + 1 \qquad (6.16)$$

The predictive ability of Equation 6.16 is illustrated in Figure 6.5. Figure 6.5 indicates that there is a slight over prediction of CDMult values at lower values – as indicated by the non-zero intercept value of the equation. However, this is considered acceptable within the context of this research project.

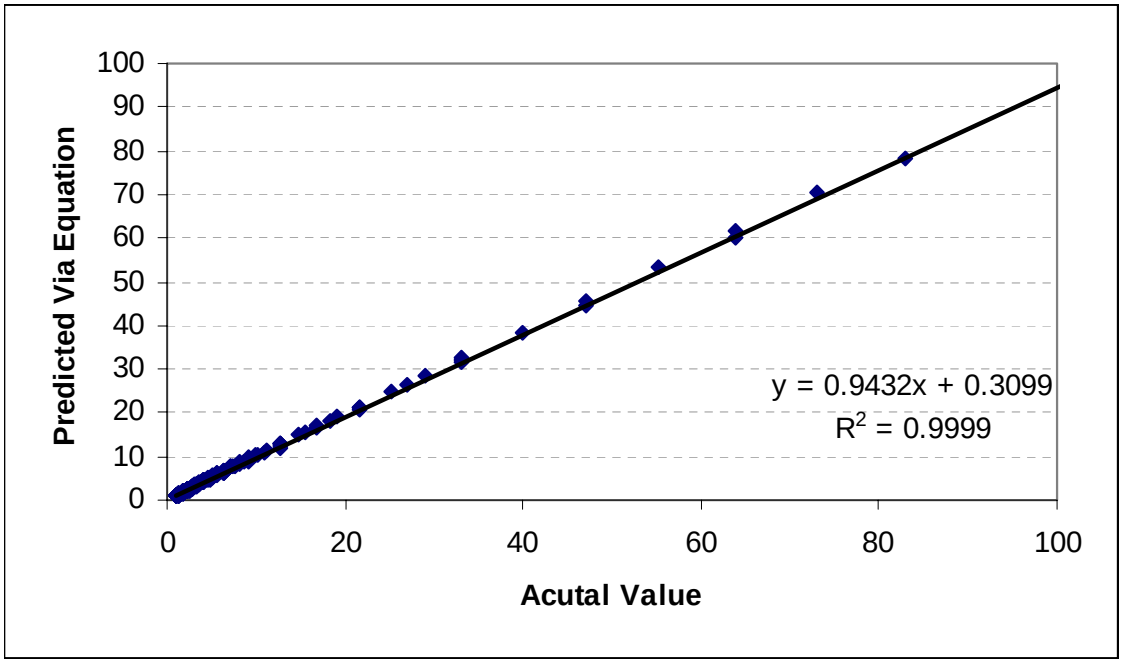

Figure 6.5: Predicted versus Actual CDMult Values

A wind velocity of 4 m/s has been chosen as the default value when required for the remainder of this research work. This value of 4 m/s is at the mid-range of the predominant wind speeds found by Ingram (1978).

This assumption results in a slight under prediction of the aerodynamic resistance at low vehicle speeds and a slight over prediction at high vehicle speeds. At low vehicle speeds, the tractive force is dominated by rolling resistance, whereas at high vehicle speeds aerodynamic resistance dominates due to the v^2 term. Hence, it is more important to accurately model aerodynamic resistance at higher vehicle speeds.

Appendix A presents the recommended default values of CD and CDmult for use with Equation 6.15 based on the default vehicle and wind velocities. Where the average driving speed is well above 21 m/s (75 km/h) or the wind velocity is significantly different to the default value of 4 m/s, the methodology detailed above should be used to calculate a more appropriate value for CDmult.

Projected Frontal Area

The projected frontal area (AF), is calculated as the product of the maximum width of the vehicle by the maximum height less the area under the axles. Biggs (1988) indicates that the area under the axles is between 5 and 15 per cent for most vehicles. While Wong (1993) indicates a 16 to 21 per cent reduction for the axle area is appropriate for passenger cars. An analysis of vehicle specification data suggests that for typical modern vehicles found on New Zealand roads, the area under the axle accounts for approximately 10 per cent of the total frontal area.

This suggests that the New Zealand vehicle fleet is closer to the Australian than the North American, which is not surprising. The figure of 10 per cent is also observed for many of the 4WD recreational vehicles and motorcycles found in New Zealand. An approximate equation for predicting the frontal area of passenger cars (and other light vehicles) in the New Zealand fleet is therefore calculated as:

$$AF = 0.9 \, Hmax \, Wmax \quad (6.17)$$

where Hmax is the maximum overall height of the vehicle in m
Wmax is the maximum overall width of the vehicle in m

Wong (1993) gives the following approximation for calculating the frontal area of a passenger car from the vehicle mass. As with Equation 6.17, Equation 6.18 is only an estimated value, and more reliable values are gained from vehicle specifications.

$$AF = 1.6 + 0.00056 \, (M - 765) \quad (6.18)$$

where M is the vehicle mass in kg

An analysis of vehicle specification data, for modern vehicles found in New Zealand, resulted in the following relationship between vehicle mass and frontal area:

$$AF = 1.947 + 0.000481 \, (M - 765) \quad (6.19)$$

Over the typical range of car vehicle masses (1000-1500 kg), Equation 6.18 predicts frontal areas some 10 - 15 per cent lower than Equation 6.19. This would suggest that the typical North American vehicles thought to have been analysed in Wong (1993) are built heavier than the New Zealand fleet of predominantly Japanese origin vehicles.

As with the aerodynamic drag coefficient, the projected frontal area is proportional to the yaw angle. However, these considerations have been included with the wind averaged aerodynamic drag coefficient so are not repeated here.

6.2.3 Rolling Resistance

Introduction

The rolling resistance is described by Biggs (1988) as:

> *"... the total of all forces, apart from aerodynamic drag, acting on a free-wheeling vehicle (i.e., with the clutch disengaged). Thus, it includes all frictional forces from the output of the gear box to the wheels and tyre resistance forces."*

The rolling resistance of tyres on hard surfaces is caused by the following factors (Wong,1993):

- hysteresis in the tyre material due to deflections while rolling,

- friction between the tyre and the road,
- resistance due to air circulating inside the tyre, and
- fan effect of the rotating tyre on the surrounding air.

Hysteresis is the primary determinant of rolling resistance as indicated in Figure 6.6, whereby 92 per cent of rolling resistance is caused by hysteresis in the various parts of the tyre.

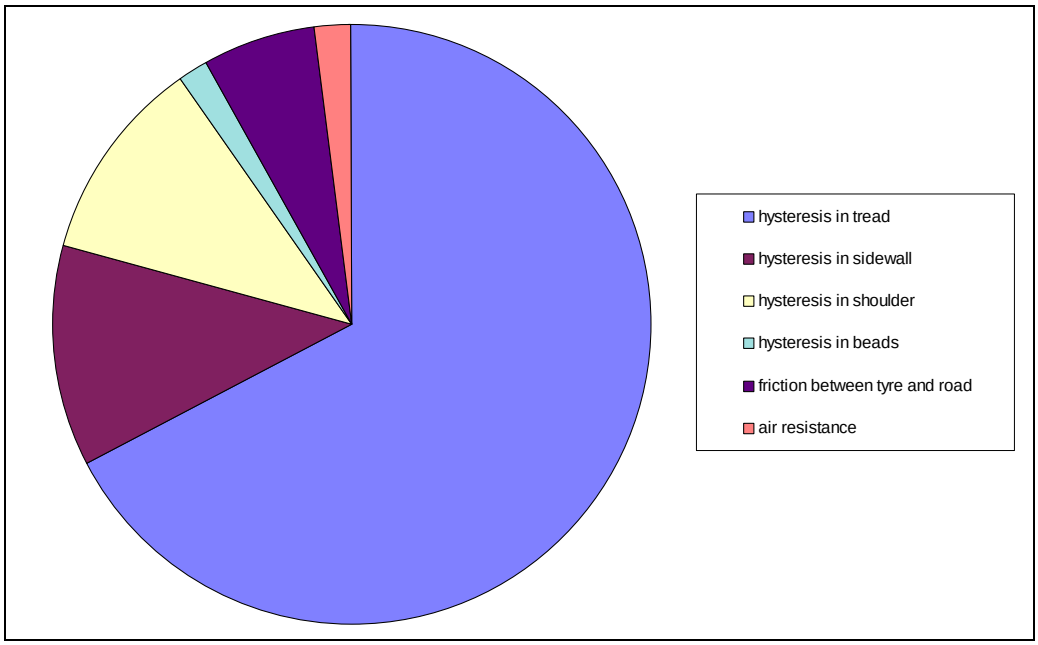

Figure 6.6: Breakdown of Rolling Resistance (Wong, 1993)

Review of available methods of calculation

Introduction

Traditionally the rolling resistance is calculated as:

$$Fr = M\ g\ CR \qquad (6.20)$$

where Fr is the rolling resistance in N
g is the acceleration due to gravity in m/s^2
CR is the coefficient of rolling resistance

There is an alternative formulation for this equation which takes into account vehicle lift. This aerodynamic effect serves to reduce the normal load on the pavement and therefore reduce the rolling resistance. However, for a model such as this it was considered that the additional sophistication and data requirements of such a formulation were not warranted.

HDM-III Methodology

In HDM-III (Watanatada, et al., 1987a), only roughness was considered to influence CR. This led to the following equations:

$$CR = 0.0218 + 0.00061\ IRI \quad \text{for cars and LCVs} \tag{6.21}$$

$$CR = 0.0139 + 0.00026\ IRI \quad \text{for buses and HCVs} \tag{6.22}$$

where IRI is the roughness in IRI m/km

New Zealand - Cenek

Cenek (1994) presents a detailed review of rolling resistance characteristics of roads. He shows that most studies (e.g. Bester, 1981; St. John and Kobett, 1978; CRRI, 1985; Brodin and Carlsson, 1986) have found that there is a speed dependence on CR. The common form of equation is:

$$CR = (Co + Cv\ v^{Cm}) \tag{6.23}$$

where Co is the static coefficient of rolling resistance
Cv is the dynamic coefficient of rolling resistance in $1/(m/s)^{Cm}$
Cm is an exponent

The values reported for Cm are usually 2 for light vehicles and 1 for all other vehicles[9].

The importance of texture in rolling resistance is highlighted by Cenek (1994) who states:

> *"[a 4 per cent reduction] in fuel consumption will be achieved by reducing surface texture depth from 2.2 mm to 1.4 mm [the same] as by reducing the roughness from 5.7 IRI to 2.7 IRI."*

ARFCOM Rolling Resistance Model

Biggs (1988) presented the following formula for the calculation of rolling resistance within ARFCOM:

$$Fr = CR2\ (b11\ Nw + CR1\ (b12\ M + b13\ v^2)) \tag{6.24}$$

where CR1 is a rolling resistance tyre factor
CR2 is a rolling resistance surface factor
b11, b12, b13 are rolling resistance parameters
Nw is the number of wheels

[9] Cenek (1994) indicates that the value of 1 for Cm with heavy vehicles arises because with increasing speed there is an increase in the vertical stiffness of the tyre due to the centrifugal force increasing the vertical tension on the belt.

The coefficient CR1 is a function of tyre type and was given by Biggs (1988) as:

CR1 = 1.3 for cross-ply bias
= 1.0 for radial
= 0.9 for low profile tyres

Biggs (1988) indicates that coefficients b11 to b13 are a function of wheel diameter:

$$b11 = 37\ Dw \quad (6.25)$$

$$b12 = 0.067/Dw \quad \text{for old model tyres} \quad (6.26)$$

$$= 0.064/Dw \quad \text{for latest model tyres} \quad (6.27)$$

$$b13 = 0.012\ Nw/Dw^2 \quad (6.28)$$

where Dw is the diameter of the wheels in m

Biggs (1988) presented values for CR2 for several surface types. Information from Cenek (1995) led to the values for CR2 in Table 6.2. These are based on the work of Walter and Conant (1974) and Knoroz and Shelukhin (1964), which are similar to those given by Biggs (1988).

Table 6.2: Proposed Values for CR2

Type of Surface	CR2
Rigid Pavement	$CR2 = 0.89 + 0.03\ IRI\ (0.38 + 0.93\ Tdsp)^2$ $M \leq 2500$ kg $CR2 = 0.64 + 0.03\ (Tdsp + IRI)$ $M > 2500$ kg
Flexible Pavement	$CR2 = 0.89 + 0.03\ IRI\ (0.38 + 0.93\ Tdsp)^2$ $M \leq 2500$ kg $CR2 = 0.84 + 0.03\ (Tdsp + IRI)$ $M > 2500$ kg
Packed gravel	$CR2 = 1.0 + 0.075\ IRI$
Hard packed soil	$CR2 = 0.8 + 0.1\ IRI$
Cobblestones	$CR2 = 2.0$
Loose dirt	$CR2 = 2.2$ (Range: 1.8 - 2.7)
Sand	$CR2 = 7.5$ (Range: 4.0 - 11.0)

Notes: Tdsp is the sand patch derived texture depth in mm

Bias-Ply versus Radial Tyres

Wong (1993) published data which indicates that for vehicles operating with speeds between 5 and 100 km/h, bias-ply tyres have an average of 28 per cent higher rolling resistances than radial tyres. This is similar to a value of 30 per cent reported by Biggs (1987). Accordingly, it will be assumed that there is a 30 per cent increase in rolling resistance for passenger car bias ply tyres over radials.

Effect of Surface Type

Wong (1993) presented data on the coefficient of rolling resistance (CR) for various surface types. Figure 6.7 illustrates the effect of tyre diameter on the rolling resistance of various surfaces. This figure shows that tyre diameter has a greater effect on deformable or soft ground.

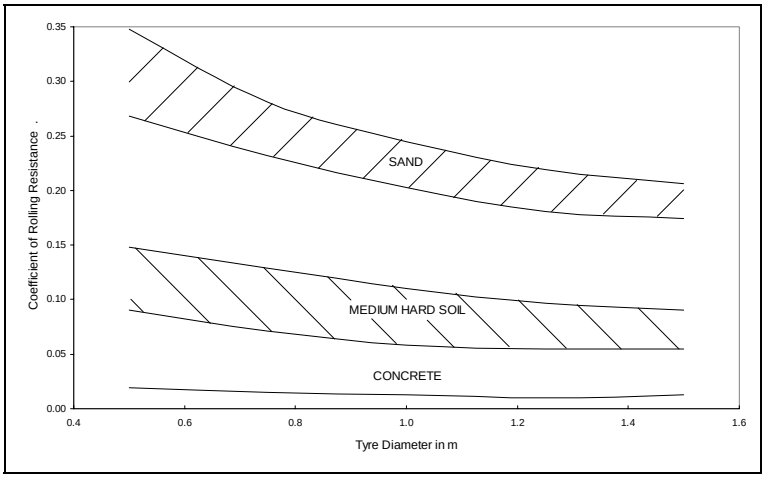

Source: Wong (1993)

Figure 6.7: Coefficient of Rolling Resistance for Various Surface Types

Research in the USA supports Wong (1993) that pavement type has a significant influence on rolling resistance. Francher and Winkler (1984) multiplied the rolling resistance (CR) by the following factors as a function of pavement type:

Smooth concrete	1.0
Worn concrete, cold blacktop	1.2
Hot blacktop	1.5

Rolling Resistance of Truck Tyres

There has been much less work into truck tyre rolling resistance than with passenger car tyres. In South Africa, du Plessis, et al. (1990) developed a model that used the roughness and tyre pressure as independent variables. Substituting in a standard value of 640 kPa results in the following equation:

$$Co = 0.00874 + 0.00043\ IRI \qquad (6.29)$$

Cenek (1994) concluded that truck tyres are not as sensitive to texture as passenger car tyres based on a study in the UK. This found that whereas texture would increase rolling resistance by 44 per cent for passenger cars, there would only be a 6 per cent increase in truck tyre resistance. This is probably due to the larger dimensions and higher inflation pressures of truck tyres.

Effect of Water and Snow on Rolling Resistance

Biggs (1995) indicates that the effect of snow is to increase CR2 by 20 to 40 per cent. Cenek (1995) suggests an increase in CR2 of 20 per cent for wet surfaces.

6.2.4 Gradient Resistance

The gradient resistance is the force component in the direction of travel necessary to propel a vehicle up a grade (positive resistance) or down a grade (negative resistance). Figure 6.8 is a force resolution diagram for a vehicle on a gradient. The weight of the vehicle can be resolved into both a parallel and perpendicular component with respect to the direction of travel. Therefore, the gradient resistance is given as:

$$Fg = M\ g\ \sin(\theta) \tag{6.30}$$

where Fg is the gradient force in N
θ is the angle of incline in radians

Since θ is typically small, $\theta \approx \sin(\theta) \approx \tan(\theta)$, and $\tan(\theta) = GR/100$, where GR is the gradient as a percentage.

Using this approximation Fg can be written as:

$$Fg = M\ GR\ g\ 10^{-2} \tag{6.31}$$

The approximation that $\theta \approx \sin(\theta) \approx \tan(\theta)$ introduces a 1.1 per cent error on a gradient of 15 per cent.

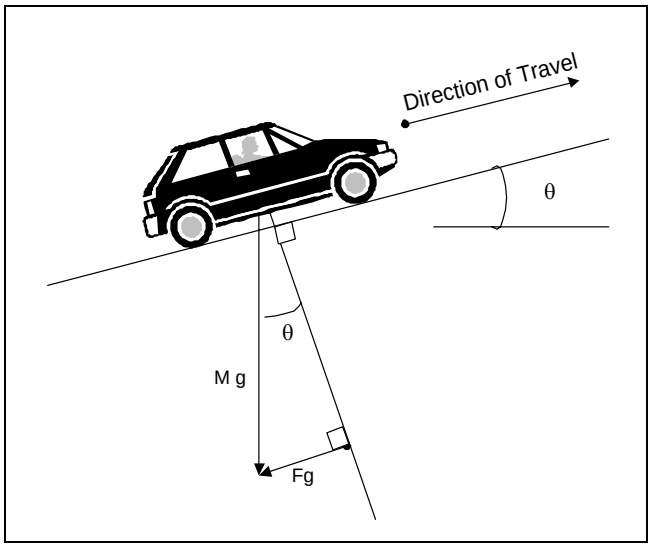

Figure 6.8: Resolving Forces on a Gradient

6.2.5 Curvature Resistance

Introduction

When a vehicle traverses a curve or travels along a straight section of road with a cross-fall, the tyres deform by a finite amount resulting in a small angle (slip angle) occurring between the direction of travel and the direction of the wheels. Due to this slip angle, an additional force against motion (the curvature resistance) is placed on the vehicle.

As noted this force also occurs while travelling along a section of road with a cross-fall, however this case results in a much smaller force than that on curves and hence is commonly ignored by researchers.

This curvature resistance is proportional to the side force applied to the wheels and the slip angle, i.e.:

$$Fcr = Ff \tan(\Phi) \tag{6.32}$$

where Fcr is the curvature force in N
Ff is the side friction force in N
Φ is the slip angle

Since Φ is small, $\tan(\Phi) \approx \Phi$ and hence the curvature resistance can be written as:

$$Fcr = Ff\ \Phi \tag{6.33}$$

Calculation of the Side Friction Force

The basic equation for the balance of forces as a vehicle traverses a curve is:

$$M \frac{v^2}{R} = M\ g\ e + M\ g\ f \tag{6.34}$$

where R is the radius of the curve in m
e is the superelevation in m/m
f is the side friction factor

Rearranging the above gives:

$$M\ g\ f = M \frac{v^2}{R} - M\ g\ e \tag{6.35}$$

Thus,

$$M\ g\ f = Ff = \frac{Fcr}{\Phi} \tag{6.36}$$

Calculation of the Side Friction Factor

The above equations suggest that it is possible to calculate the side friction force directly from the side friction factor f. However, there are two different views of the side friction factor. One is that drivers select a side friction factor and then adjust their speed accordingly to fit with this. The other is that drivers select a speed appropriate for the curve, and that the side friction factor is merely an outcome of this.

The HDM-III Brazil free speed model (Watanatada, et al., 1987a) viewed the side friction factor as limiting the curve speed. However, research in several countries (Bennett, 1994) demonstrated that it is more appropriate to view the side friction factor as the result of the speed adopted. This approach is embodied in several geometric design guides, such as that published by AUSTROADS (1989).

Hence, the formula for calculating the side friction factor of a vehicle traversing a curve is:

$$f = \frac{\frac{Mv^2}{R} - Mge}{Mg} \tag{6.37}$$

which can be simplified to:

$$f = \frac{v^2}{Rg} - e \tag{6.38}$$

Calculation of the Slip Angle

The slip angle Φ is a measure of the amount of roll (or deformation) in the tyres. Moore (1975) indicates that the slip angle is dependent upon the magnitude of the side force applied to each wheel and inversely to the stiffness of the tyre.

By dividing the side force Ff by the number of wheels and the stiffness of the tyres, the slip angle Φ can be calculated as:

$$\Phi = \frac{\left(\frac{Mv^2}{R} - Mge\right)}{NwCs} 10^{-3} \tag{6.39}$$

By rearranging Biggs (1987) equation for the calculation of Fcr, it can be seen that this is equivalent to his formulation for the slip angle. Typical values for tyre stiffness coefficient, Cs (in kN/rad) are as follows (Biggs, 1988):

Cars

Cs =	54	for high performance/low resistance tyres
	43	for standard radial tyres
	30	for bias ply tyres

Trucks

$$Cs = 8.8 + 0.088\ M/Nw - 0.0000225\ (M/Nw)^2 \qquad \text{for } 0.7<Dw\leq 0.9 \qquad (6.40)$$

$$Cs = 0.0913\ M/Nw - 0.0000114\ (M/Nw)^2 \qquad \text{for } Dw > 0.9 \qquad (6.41)$$

6.2.6 Inertial Resistance

Introduction

When a vehicle accelerates it needs to overcome inertial resistance of the rotating components of the vehicle. The inertial effects of the various rotating parts (engine, wheels and drivetrain) serves to increase the vehicles dynamic mass over its static mass. This increased mass is termed the *effective mass*. Thus, inertial resistance is given by:

$$Fi = M' a \qquad (6.42)$$

where Fi is the inertial resistance in N
M' is the effective mass in kg
a is the acceleration in m/s^2

Watanatada, et al. (1987b) defined the effective mass as:

$$M' = M + Mw + Me \qquad (6.43)$$

where Mw is the inertial mass of the wheels in kg
Me is the inertial mass of the engine and drivetrain in kg

The following sections consider each of these contributors to effective mass.

Inertial Mass of the Wheels

Watanatada, et al. (1987b) gave the following equation for the calculation of the inertial mass of the wheels:

$$Mw = \frac{Iw}{r^2} \qquad (6.44)$$

where Iw is the moment of inertia of the wheels in kg-m^2
r is the rolling radius of the tyres in m

The moment of inertia of a wheel is given by the product of its mass and radius of gyration. Thus, the total inertial effects for all the wheels on the vehicle is:

$$Mw = TMW \frac{rg^2}{r^2} \quad (6.45)$$

where TMW is the total mass of the wheels in kg
rg is the radius of gyration of the tyre in m

Inertial Mass of the Engine and Drivetrain

Watanatada, et al. (1987b) gave the following equation for the calculation of inertial mass of the engine:

$$Me = \frac{IeH^2}{r^2} \quad (6.46)$$

where Ie is the moment of inertia of the engine in kg-m^2
H is the total gear reduction

Bester (1981) gave the following formula for the moment of inertia of a truck engine:

$Ie = 0.169 + 0.0188\ D^2$ for a petrol truck engine (6.47)

$Ie = 0.169 + 0.0251\ D^2$ for a diesel truck engine (6.48)

where D is the engine displacement in L

Total Effective Mass

From combining the above calculations for Mw and Me, M' can be written as:

$$M' = M + \frac{Iw}{r^2} + \frac{IeH^2}{r^2} \quad (6.49)$$

which equates to:

$$M' = M + TMW \frac{rg^2}{r^2} + \frac{IeH^2}{r^2} \quad (6.50)$$

The ranges of Iw and Ie for a passenger car as reported by Burke, et al. (1975) and Watanatada, et al. (1987b) are given in Table 6.3.

Table 6.3: Moment of Inertia Values for Passenger Cars

	Burke, et al. (1975)	**Watanatada, et al. (1987b)**
Iw (kg-m^2)	1.223 to 1.495	0.89 to 1.01
Ie (kg-m^2)	0.543 to 0.678	not supplied

The Effective Mass Ratio

Another method of representing the effective mass is through the ratio of effective mass to the static mass, which is termed the "effective mass ratio" (EMRAT = M'/M). Due to the gearing of vehicles, the EMRAT would be expected to decrease as speed increases. Bester (1981) indicates that EMRAT would be expected to equal 1.082 for a car and between 5.0 (<1.8 m/s) and 1.033 (27.8 m/s = 100 km/h) for a truck. Bennett (1993) applied a constant value of EMRAT = 1.10 across all speeds.

In order to calculate a representative value for EMRAT it is necessary to take into account the influences of speed. This is because EMRAT is inversely proportional to speed due to the general reduction in gears with increasing speed. While it is possible to calculate the effects for a single vehicle, the value for the traffic stream is more applicable for applications such as this.

Accordingly, EMRAT was calculated using a Monte-Carlo simulation for a stream of vehicles with a Normal Distribution about a mean speed with a coefficient of variation in speeds of 0.15 (Bennett, 1994). Appendix B gives the listing for this simulation program. The mean vehicle speeds were incremented in steps of 5 km/h over the range of 5 km/h to 100 km/h, with 1000 vehicles simulated at each speed increment.

Wong (1993) indicates that vehicle manufacturers select gear ratios such that the driver can always operate the vehicle at or very near to the optimal engine power. This idealised gear selection is shown in Figure 6.9 for a four-speed vehicle.

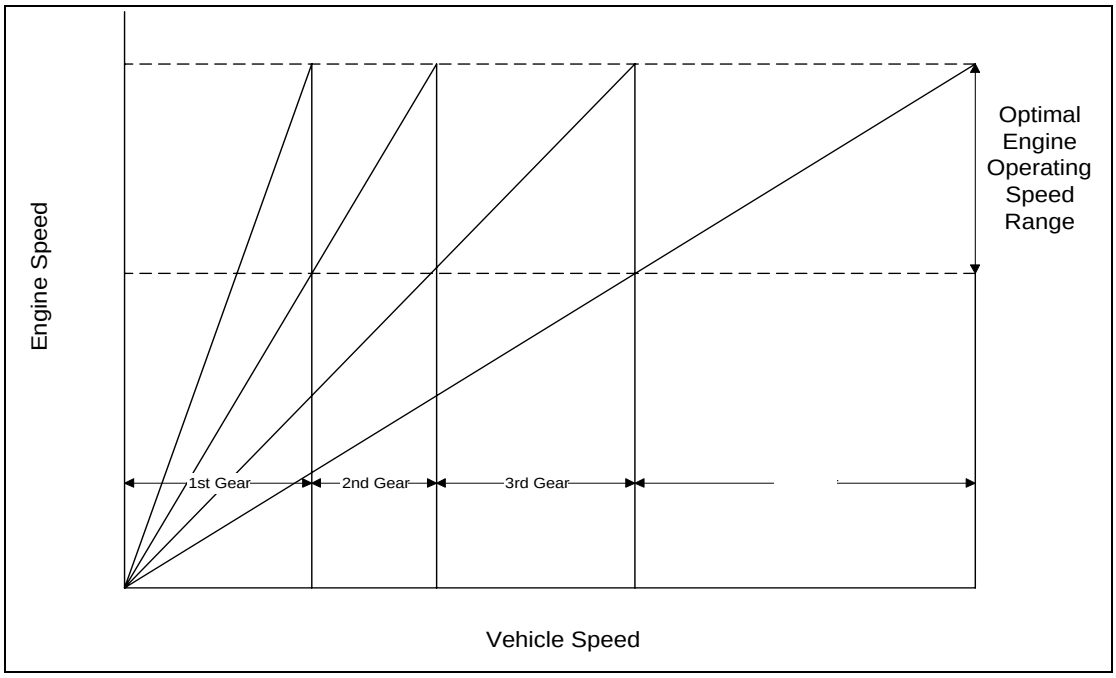

Source: Wong (1993)

Figure 6.9: Manufacturers Idealised Gear Selection

In reality drivers do not maintain the engine speed in the optimal range, and hence there is overlap in the use of the gears at the same speed.

Ideally, the simulation would be based on data that explicitly represented driver gear selection. However, such data were not available. Instead, the gear selection was predicted based on the vehicles not travelling with an engine speed less than 15 percent higher than the idle speed (except for 1st gear), or more than 85 per cent of the engine speed at maximum power of the engine. The maximum speed a vehicle could travel at in a gear was further restricted by power requirements. This primarily affected the higher gears, as in the lower gears the maximum engine speed was the primary restriction.

From these restrictions on engine speed, the range of speeds at which a vehicle could travel in any gear was determined based on the vehicles characteristics. Figure 6.10 illustrates the relationship between vehicle speed and engine speed for each of the gears in a 1995 Ford Laser passenger car.

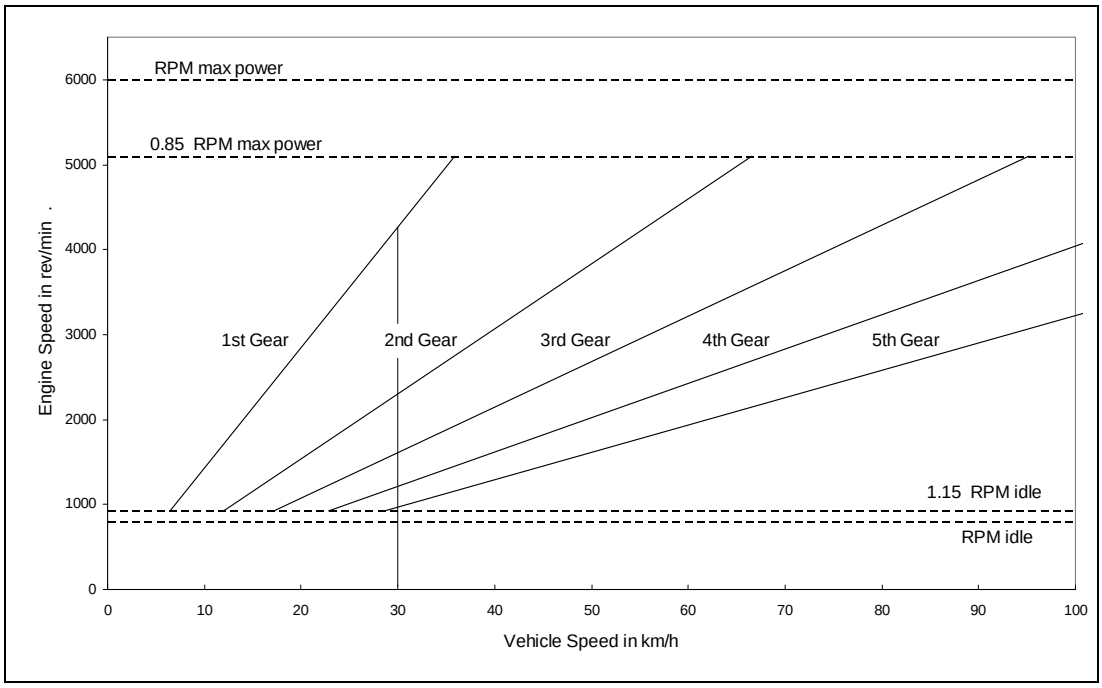

Figure 6.10: Engine Speed Versus Vehicle Speed for a Ford Laser Passenger Car

As shown in Figure 6.10, there is often a range of gears a driver can choose for a particular vehicle speed. For example at 30 km/h the Ford Laser could theoretically be in any of the 5 gears. It was therefore necessary to model this is in simulation. Over the range of speeds where a driver has a choice of gears, a straight-line distribution of percentage of drivers in the higher gear was applied (see Figure 6.11).

In the upper half of Figure 6.11, the dashed horizontal lines indicate the restrictions imposed on engine speed for the simulation. By use of these restrictions, the assumed distribution of gear selection (represented by the dark solid line in the lower half of the figure) was obtained.

In the simulation, for any speed the gear was established by generating a random number and then applying it to the assumed function (e.g. Figure 6.11). This

approach was followed for the simple case, when there were only two gears, or for the complicated case when the drivers could select from several gears.

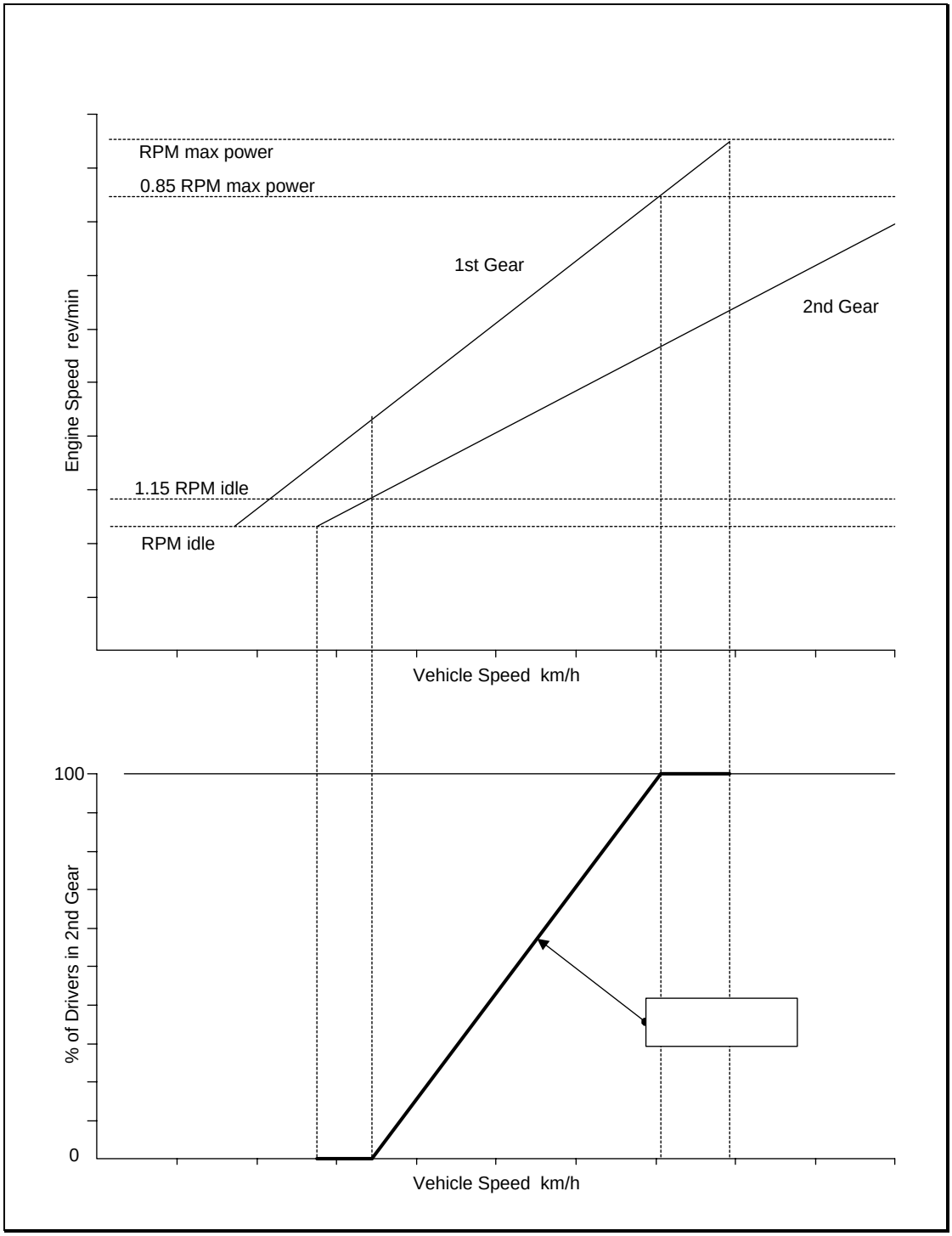

Figure 6.11: Driver Gear Selection

Figure 6.12 illustrates the observed distribution of speed by gear selected for a drive cycle on a 6-lane road in Thailand. As predicted above, there are some vehicle

speeds whereby a range of gears are utilised depending upon driving conditions and styles. For instance, at 40 km/h only 1st gear has not been utilised.

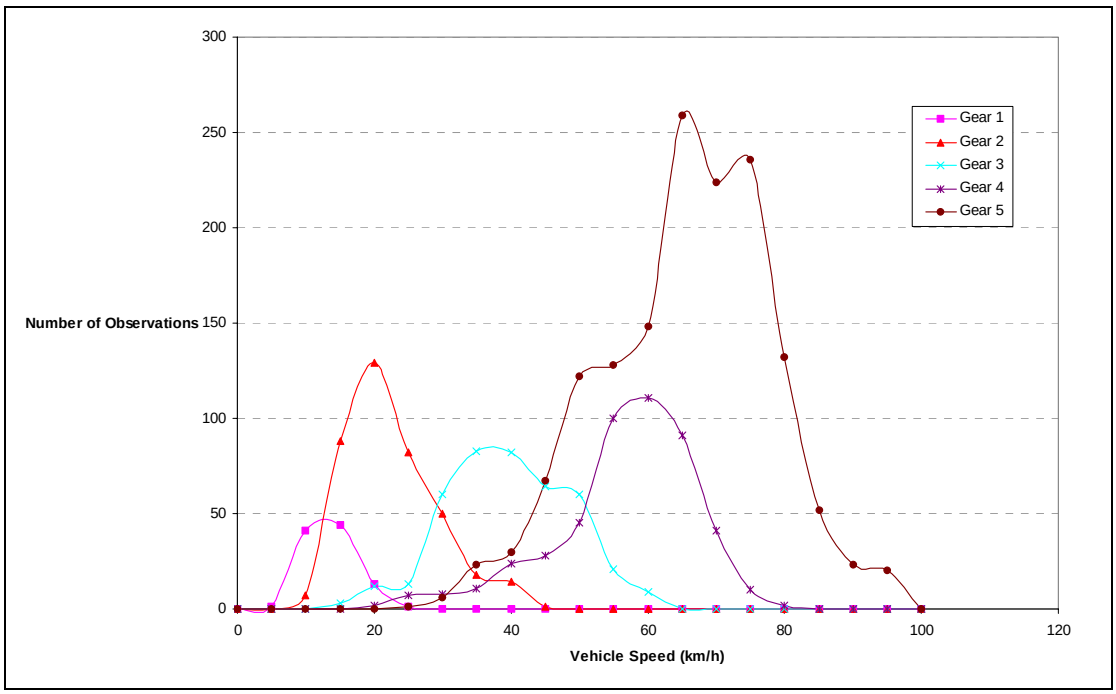

Figure 6.12: Observed Gear Selection Distribution

A simulation programme (GEARSIM) was run to generate an equivalent plot based on the previously discussed gear selection logic. The results of this are presented in Figure 6.13 and indicate a general matching trend. Considering that the actual results in Figure 6.12 are from a single driver, the results of the simulation are considered to be of an appropriate accuracy.

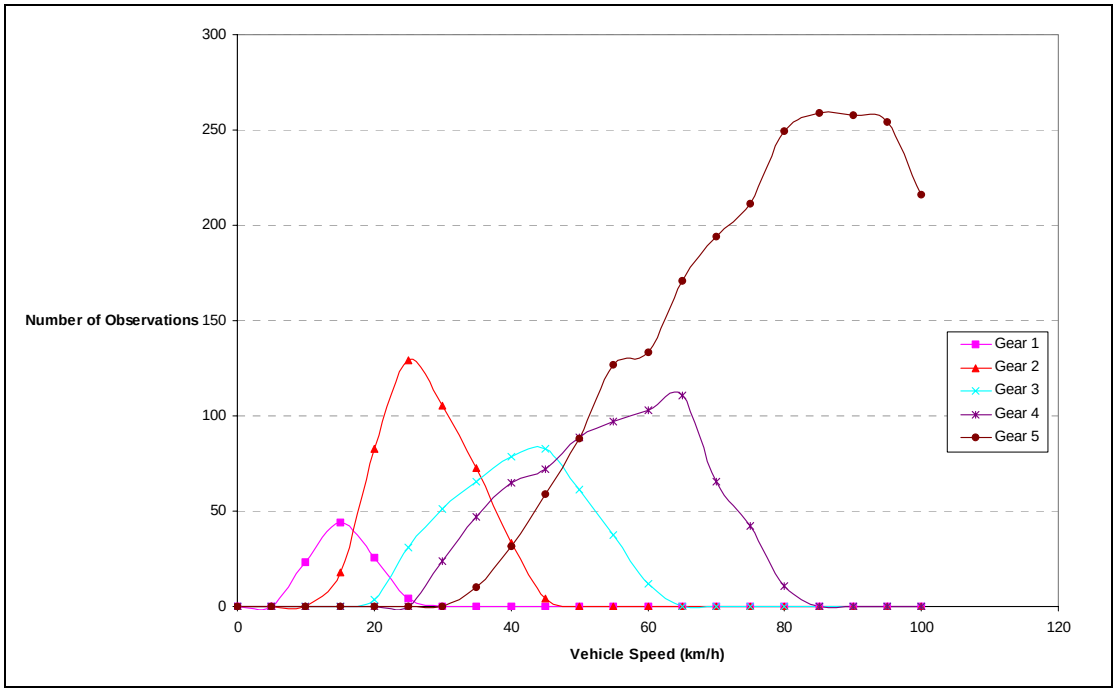

Figure 6.13: Simulated Gear Selection Distribution

Vehicle characteristics were obtained from Watanatada, et al. (1987a), Biggs (1988) and 1995 motor vehicle manufacturers specifications. The weight distributions for different vehicle classes were obtained from Bennett (1994). Using these data with the above methodology, the average values of EMRAT were calculated for each average vehicle speed. The results for a Mitsubishi FV402 heavy truck, a Ford medium truck, Ford Telstar and Laser cars and a Mitsubishi Pajero 4WD are shown in Figure 6.14.

The asymptotic nature of some vehicles at low speeds is due to the fact that they are in their top gear, and only that gear, at these speeds. By comparison, the heavy truck gearing is so high that even at low speeds there are still several gears to choose from.

Trucks exhibit a lower value of EMRAT at higher speeds than do the light vehicles because of their higher static masses. While the magnitude of the effective mass for the light vehicles is much lower than for trucks, relative to their static mass it is higher.

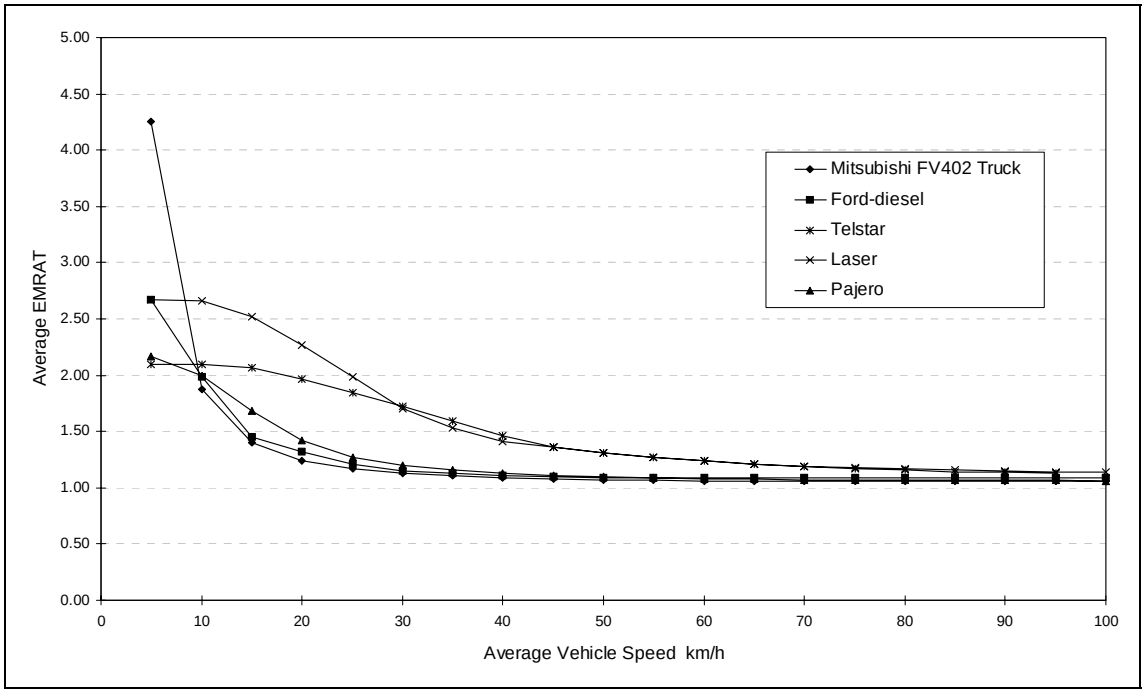

Figure 6.14: Average EMRAT versus Average Vehicle Speed for Selected Vehicles

From the data generated from the simulation the following model was fitted which expresses the effective mass ratio as a function of velocity:

$$EMRAT = a0 + a1 \cdot \tan\left(\frac{a2}{v^3}\right) \qquad (6.51)$$

where atan is the arc tan in radians
a0 to a2 are regression coefficients

Appendix A gives the values for the regression coefficients for the representative vehicle types for use in the above model. For all vehicle types the r-squared values of the equations were greater than 0.88 and the standard error less than 0.13.

6.2.7 Summary and Conclusions – Forces Opposing Motion

The forces opposing motion can be quantified in terms of the vehicle characteristics. Wherever possible, VOC should be predicted using mechanistic principles since they allow for the extrapolation and application of the VOC equations to vehicles with different characteristics to those upon which the relationships were based.

On the basis of the discussion in this chapter the following are the recommended models for calculating the forces opposing motion.

Aerodynamic Resistance

The aerodynamic resistance model for HDM-4 is:

$$Fa = 0.5\ \rho\ CDmult\ CD\ AF\ v^2 \quad (6.52)$$

Mass Density of Air

Given the range of climatic conditions over which HDM-4 is anticipated to be used, it is proposed that HDM-4 include a default value for the mass density of air which may be modified according to local conditions. The recommended default value is 1.20 kg/m^3, which is based on an air temperature of 15^oC and an altitude of 200 m. Equation 6.7 can be used to adjust this value for other altitudes.

Aerodynamic Drag Coefficient and Relative Vehicle Velocity

The aerodynamic drag coefficient at zero degrees yaw and the CDmult should be input by the user to correct for wind effects. Appendix A lists the recommended default values for the default vehicle types. The approach proposed by Sovran (1984) is recommended for dealing with the different approach angles of the wind.

A wind speed of 4 m/s has been chose as the default value for use in the analysis.

Projected Area

The projected frontal area should be calculated from the actual vehicle characteristics. Values for the representative vehicles are given in Appendix A. In the absence of other data, Equations 6.17 and 6.19 may be used to approximate the frontal area.

Rolling Resistance

The ARFCOM approach to rolling resistance has been adopted, with modifications to account for different surface types and water/snow as outlined previously. This yields the following formula for calculating the average rolling resistance of vehicles:

$$Fr = CR2\ FCLIM\ (b11\ Nw + CR1(b12\ M + b13\ v^2)) \quad (6.53)$$

$$FCLIM = 1 + 0.003\ PCTDS + 0.002\ PCTDW \quad (6.54)$$

where FCLIM is a climatic factor related to the percentage of driving done in snow and rain
PCTDS is the percentage of driving done on snow covered roads
PCTDW is the percentage of driving done on wet roads

It is recommended that the default values of PCTDS and PCTDW are both zero. It is noted that the sum of PCTDS and PCTDW has a theoretical upper limit of 1. However, in practice it is not expected that the sum of these two parameters will approach anywhere near this limit.

Appendix A lists the recommended parameter values for the various rolling resistance model coefficients, except CR2 whose values are established based on

the information in Table 6.2. The values of CR1 are dependent on the tyre type and these are also given for each representative vehicle.

Gradient Resistance

The gradient resistance is given as:

$$Fg = M\ g\ \sin(\theta) \tag{6.55}$$

where Fg is the gradient force in N
θ is the angle of incline in radians

Since θ is small, $\theta \approx \sin(\theta) \approx \tan(\theta)$, and $\tan(\theta) = GR/100$, where GR is the gradient as a percentage.

Using this approximation Fg can be written as:

$$Fg = M\ GR\ g\ 10^{-2} \tag{6.56}$$

Curvature Resistance

The cornering force can be calculated as:

$$Fcr = Ff\ \Phi \tag{6.57}$$

Substituting in the equations for the side friction force and the slip angle gives:

$$Fcr = \frac{\left(\frac{Mv^2}{R} - Mge\right)^2}{NwCs} 10^{-3} \tag{6.58}$$

Equation 6.58 is applicable for both instances when tyres deform due to a side force, namely on curves and sections of road with crossfall.

Inertial Resistance

On the basis of the above discussion, the recommended formula for the calculation of inertial resistance is:

$$Fi = M\ EMRAT\ a \tag{6.59}$$

Substituting for EMRAT with the function whose parameter values are given in Appendix A yields:

$$Fi = M\left[a0 + a1a\tan\left(\frac{a2}{v^3}\right)\right]a \tag{6.60}$$

The parameter values for the term EMRAT have been developed from a regression of the output of a gear selection simulation program (GEARSIM). This program has been tested against observed gear selection data and is considered to give appropriate results.

Total Tractive Force

The total tractive force can therefore be written as:

$$Ftr = Fa + Fr + Fg + Fcr + Fi \tag{6.61}$$

$$Ftr = 0.5\,\rho\,CD\,CDmult\,AF\,v^2 + CR2\,(1 + 0.003\,PCTDS + 0.002\,PCTDW)\,(b11\,Nw + CR1(b12\,M + b13\,v^2)) + M\,g\,GR\,10^{-2} + \frac{1}{NwCs}\left(\frac{Mv^2}{R} - Mge\right)^2 10^{-3} + M\left[a0 + a1\,a\tan\left(\frac{a2}{v^2}\right)\right]a \tag{6.62}$$

6.3 Total Power Requirements

6.3.1 Introduction

It was decided that mechanistic modelling techniques would be adopted for use wherever possible within the research owing to their greater flexibility. The total power requirements, in conjunction with the efficiency of the engine, directly determines the fuel consumption of a vehicle.

The power demand on the engine from a vehicle varies with grade, with a steep downgrade often resulting in a negative power demand on the engine. It is within this region of operation that many electric vehicles use generators to recharge their batteries.

Figure 2.7 illustrated how the total power requirements within ARFCOM (Biggs, 1988) are based on the tractive forces, the power required to run accessories, and internal engine friction. The fuel consumption (refer to Chapter 7) is calculated to be proportional to the total power requirements.

This chapter presents the model for calculating the total power requirements for a vehicle. The reviewed models for predicting the accessories power and engine drag were found to have some deficiencies and hence a new model was formulated.

6.3.2 Tractive Power

The tractive power is calculated as the product of vehicle speed and the total tractive forces as calculated in Section 6.2. This power however, does not account for inefficiencies in the drivetrain, and hence a modification to account for inefficiencies is required to yield the power required from the engine to overcome the forces opposing motion.

The efficiency (less than 100 per cent) of the drivetrain, requires greater power to be supplied by the engine than that required at the wheels, with the excess power being lost to the system as heat and noise in the bearings and other moving parts.

In circumstances where a vehicle is descending a steep grade or decelerating hard, it is possible that the forces opposing motion will become negative. In these cases power is supplied from the wheels to the motor to assist in powering the engine accessories etc. Again the efficiency of the drivetrain has an effect, which in this case serves to decrease the power supplied to the engine from the wheels. The resulting formula for calculating the tractive power therefore has two conditions, one when the tractive forces are positive, and when they are negative.

$$Ptr = \frac{Ftr\,v}{edt\,1000} \qquad Ftr \geq 0 \qquad (6.63)$$

$$Ptr = edt\ Ftr\ v / 1000 \qquad Ftr < 0 \qquad (6.64)$$

where Ptr is the tractive power as observed by the engine in kW
edt is the efficiency of the drive train
Ftr is the tractive force in W
v is the vehicle velocity in m/s

6.3.3 Accessories Power and Engine Drag

Within ARFCOM (Biggs, 1988), accessories power and engine drag were accounted for in two separate equations, given below as Equations 6.65 and 6.66 respectively. With reference to the engine drag equation Biggs (1988) noted that the estimation of model parameters was problematic, with quite low coefficients of determination and high standard errors. Small petrol engines were reported as being particularly difficult.

$$Pacs = EALC\frac{RPM}{TRPM} + ECFLC\,P\max\left(\frac{RPM}{TRPM}\right)^{2.5} \qquad (6.65)$$

where EALC is the accessories load constant in kW
ECFLC is the cooling fan constant
TRPM is the load governed maximum engine speed in rev/min

$$Peng = ceng + beng\left(\frac{RPM}{1000}\right)^{2} \qquad (6.66)$$

where ceng is the speed independent engine drag parameter
beng is the speed dependent engine drag parameter
RPM is the engine speed in rev/min

When the fuel use due to engine drag from the ARFCOM equations were compared to values from other passenger car sources (e.g. Bester, 1981), it was found that the equations were predicting a much higher rate of fuel usage than was found by other

researchers (NDLI, 1995). In some circumstances up to 40 per cent of engine power was predicted to be required to overcome engine drag. This apparent overestimation arose over all speeds so was not considered to be a result of the HDM-4 engine speed assumptions (refer to Section 6.3.4).

As a consequence of this finding, it was decided that a new model should be formulated. As in HDM-III, the engine drag and accessories power has been assumed to follow a linear[10] relationship with engine speed (Watanatada, et al., 1987a). The resulting formula for calculating the combined engine drag and accessories power is given below, with the appropriate parameter values for the different vehicle classes given in Appendix A.

$$Pengacc = Prat\left[a0+(a0-a1)\frac{RPM-RPMidle}{RPM100-RPMidle}\right] \quad (6.67)$$

where Pengacc is the total engine and accessories power in kW
Prat is the rated engine power in kW
a0 and a1 are parameter values given in Appendix A
RPM is the engine speed in rev/min
RPMidle is the idle engine speed in rev/min
RPM100 is the engine speed while travelling at 100 km/h (refer to Section 6.3.4)

As can be observed from Equation 6.67, the model contains a constant component and an engine speed dependent component. The product of the rated engine power and a0, yields the power usage at idle, while the product of the rated engine power and a1 yields that at an engine speed equating to a vehicle speed of 100 km/h. This is represented graphically in Figure 6.15.

[10] Although the HDM-III generic model included a squared term, the coefficient for this term was equal to zero for all but one vehicle class.

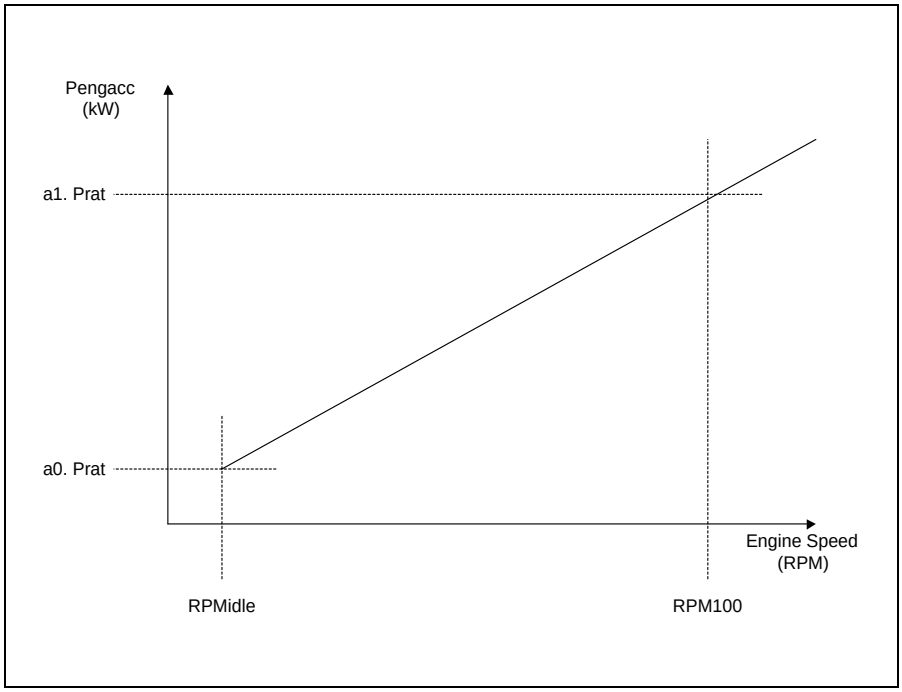

Figure 6.15: Relationship between Engine Speed and Pengacc

When a vehicle is at idle, the fuel consumption is solely that due to engine drag and accessories power. By substituting the formulated equation for engine and accessories power into the fuel consumption formulae presented in Section 6.4 and then solving using the quadratic formula, the following formula for the parameter a0 can be ascertained.

$$a0 = \frac{-b + \sqrt{b^2 - 4ac}}{2a} \qquad (6.68)$$

where $a = \zeta b \; ehp \; Prat^3 \; (1 - PRPPeng)$
$b = \zeta b \; Prat$
$c = -\alpha$

and ζb is the base fuel efficiency factor (refer to Section 6.4.3) in mL/kW/s
PRPPeng is the proportion of Pengacc ascribable to engine drag.

From an analysis of data in Biggs (1988) and Watanatada, et. al (1987a) the parameter values for all representative vehicle types were ascertained. Appendix A lists the recommended values for the parameters required to predict the engine and accessories power for all vehicle types.

6.3.4 Predicting Engine Speed

Predicting engine speed has presented problems to many researchers, yet as it is a fundamental component of both the accessories power and engine drag it is important that this parameter be aptly modelled.

The ARFCOM model utilised a two-stage model for predicting engine speed — one for when a vehicle is in top gear and the other for all lower gears. However, as described in Bennett and Dunn (1989), the ARFCOM engine speed equation lead to a discontinuous relationship between vehicle speed and engine speed when the vehicle shifts into top gear. Such discontinuities lead to inconsistent fuel consumption predictions and so must be avoided. While one solution would be to adopt a constant engine speed, such as was done for HDM-III, this creates a bias in the predictions and was also considered unsuitable.

Accordingly a Monte-Carlo simulation was undertaken to develop a continuous function between vehicle speed and engine speed. Using the same methodology as described in Section 6.2.6 for calculating the effective mass ratio (EMRAT) values, an average engine speed for each average vehicle speed was calculated.

For each vehicle, the simulation was run for speeds from 5 to 100 km/h in 5 km/h increments, with 250 vehicles being simulated for each increment. The mean speed was then established for each increment. The results for a 1995 Ford Laser passenger car are shown in Figure 6.16, with the individual discrete gears overlaid.

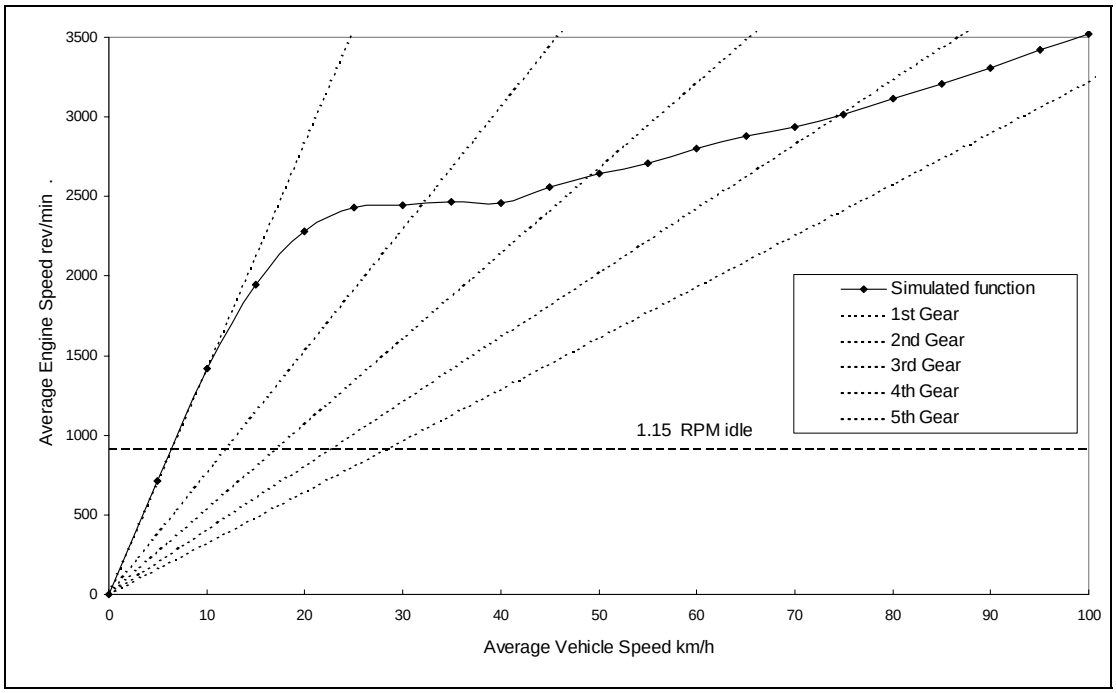

Figure 6.16: Simulated Vehicle Speed vs Engine Speed for Ford Laser Car

It can be seen from Figure 6.16 that the engine speed is dominated by 1st gear at low speeds, and is asymptotic to top gear at higher speeds. Justification of the appropriateness of the simulation results, along with further details of the gear selection methodology are given in Section 6.2.6.

Figure 6.17 illustrates the relationship for the different types of cars. It is particularly noteworthy that the slope is essentially consistent between vehicles of the same type above approximately 30 km/h.

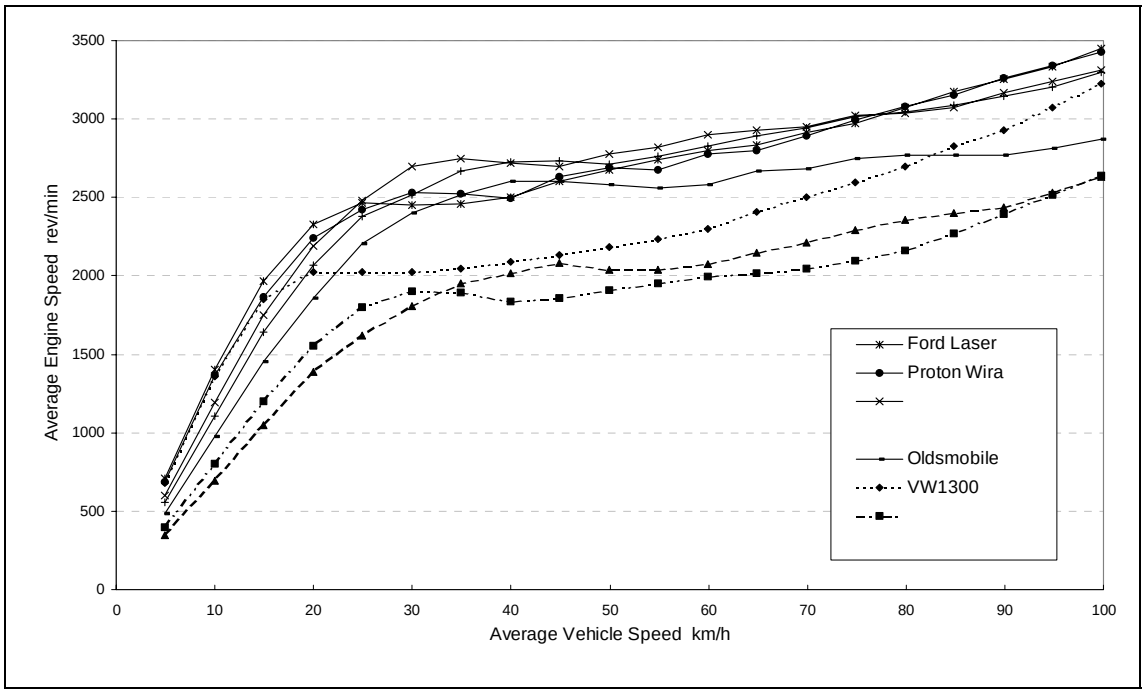

Figure 6.17: Simulated Average Vehicle Speed vs Average Engine Speed for Passenger Cars

To test the above methodology, it was applied to the heavy truck reported by Pan (1994). Pan (1994) gives the distribution of engine speeds for a range of vehicle speeds. By simulating a set of vehicle speeds that match those of Pan (1994) and applying the above methodology to determine the gear selection, a check was made on the assumptions used.

In the comparison, 5000 vehicles were simulated, with a distribution of speeds and vehicle characteristics matching that given by Pan (1994). Pan (1994) was conducting fuel consumption tests and it was therefore decided that the full range of engine speeds should be used in the analysis, as opposed to the 15 per cent upper and lower cut offs normally employed. This was done because it would be expected that more time would be spent at the extreme ranges of engine speed for each gear than would be expected under normal driving conditions.

The results of the comparison are shown in Figure 6.18, which indicates a good comparison between the distribution reported by Pan (1994) and those derived from the simulation, especially when using the “0 % cut off” engine speeds. As was expected the comparison is not quite as good when the 15 per cent upper and lower limits were used. However, given that the simulation assumes a distribution of driving habits, as opposed to the single driver thought to have been used by Pan (1994), the simulation and its assumptions appear to be valid and give reasonable results.

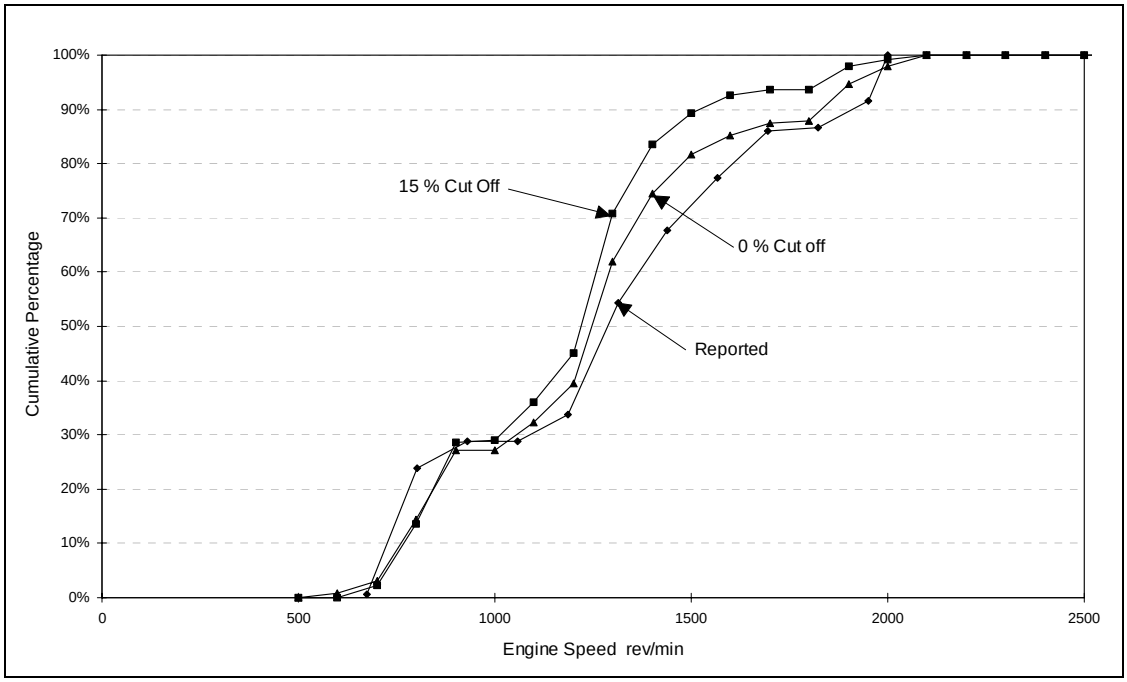

Figure 6.18: Comparison of actual and simulated data

From the simulation of gear selection, it was confirmed that a continuous function existed between average vehicle speeds and average engine speed for the vehicle stream. This simulation does not support the relationship from ARFCOM, where there is a discontinuity when the vehicle changes into top gear, nor does it support the assumption of constant engine speed in HDM-III.

There are three regions to the engine speed relationship:

Low speeds	Dominated by 1st gear
Intermediate Speeds	Continuous function
High Speeds	Dominated by top gear

The low speed region presents a particular problem since it will lead to a discontinuity in the fuel modelling. Accordingly, for HDM-4 (NDLI, 1995) it has been assumed that the minimum engine speed of the continuous function applies at low speeds. For most vehicles this minimum engine speed coincides with a vehicle speed of approximately 20 km/h. Thus, the HDM-4 (NDLI, 1995) engine speed equation can be written as:

$$RPM = a0 + 5.6\,a1 + 31.36\,a2 \quad \text{for } v \le 5.6 \text{ m/s (20 km/h)} \tag{6.69}$$

$$RPM = a0 + a1\,v + a2\,v^2 \quad \text{for } 5.6 < v \le a3 \text{ m/s} \tag{6.70}$$

$$RPM = \left(a0 + a1\,a3 + a2\,a3^2\right)\frac{v}{a3} \quad \text{for } v > a3 \text{ m/s} \tag{6.71}$$

where a0 to a3 are constants

The parameter a3 indicates the velocity at which vehicles are in top gear. The slope of the continuous function at velocity a3 is related to top gear as shown by Equation 6.72.

$$a1 + 2\,a2\,a3 \approx \frac{60\,Htop}{\pi\,Dw} \qquad (6.72)$$

where Htop is the total gear reduction (gearbox plus differential) in top gear

Bennett and Greenwood (2001) revised the above set of equations to a single regression curve of the following form, using the justification that it *"gives equivalent predictions and is simpler to apply so it has been recommended as a replacement for the NDLI (1995) model".*

$$RPM = a0 + a1\,SP + a2\,SP^2 + a3\,SP^3 \qquad (6.73)$$

$$SP = \max(20, S) \qquad (6.74)$$

where a0 to a3 are model parameters
S is the vehicle road speed in km/h

6.3.5 Total Power

The total power requirement for a vehicle is given as the sum of the three individual components — tractive, accessories and engine. Due to the fact that the tractive power component has two different functions, the total power is appropriately written as:

$$Ptot = \frac{Ftr\,v}{edt\,1000} + Pengacc \qquad Ftr \geq 0 \qquad (6.75)$$

$$Ptot = edt\,Ftr\,v / 1000 + Pengacc \qquad Ftr < 0 \qquad (6.76)$$

where Ptot is the total output power required of the engine in kW

6.3.6 Summary and Conclusions – Total Power Requirements

This chapter has presented the power demand model, which forms the basis of the fuel consumption model presented in Section 6.4 below. The approach adopted is that as utilised within ARFCOM (Biggs, 1988). The total power requirements are comprised of the power to overcome the tractive forces (refer to Section 6.2), that required to overcome engine drag and finally a component to power vehicle accessories.

As has been shown, the reviewed model forms did not predict the engine drag and accessories power adequately and hence a new model has been formulated. This

model is linear in nature, with the appropriate model parameter values given in Appendix A.

An important part of predicting the engine drag and accessories power is the calculation of engine speed. As a result of no suitable engine speed model being available, a simulation program was written that predicted driver gear selection based on Monte-Carlo principals.

The simulation program compared favourably with independently sourced data, thereby justifying the logic of the gear selection process assumed. An analysis of the output from the simulation program resulted in a three-stage model with respect to vehicle speed being developed.

6.4 Fuel Consumption

6.4.1 Introduction

Fuel consumption is a significant component of VOC and is one component that is directly affected by driving conditions. Traffic congestion, road condition and alignment influence fuel consumption, so it is sensitive to road investment decisions.

This section describes the fuel consumption model utilised for this research. It commences with a summary of the various types of fuel models available from the literature. On the basis of these, a modelling approach and fuel model is recommended for the remainder of this research project. The implementation of this fuel model for predicting steady state fuel consumption is given.

As described in Section 2.7, it was decided to adopt a mechanistic fuel consumption model as the basis for the fuel model. The model is based on the ARFCOM (Biggs, 1988) approach and offers the greatest flexibility and scope for fuel modelling without going into extremely detailed models such as those based on engine maps.

ARFCOM predicts that the fuel consumption is proportional to the vehicle power requirements (Biggs, 1988):

$$IFC = \max(\alpha, \zeta\ Ptot) \tag{6.77}$$

where IFC is the fuel consumption in mL/s
α is the idle fuel consumption in mL/s
ζ is the fuel efficiency factor in mL/kW/s
Ptot is the total power requirements in kW

The earlier portions of this section addressed the issue of predicting the power requirements of a vehicle. Once the total power requirements have been calculated, this is multiplied by the fuel efficiency factor to give the required fuel consumption to meet the power demand. As Equation 6.77 indicates, the fuel consumption is then the maximum of this product and the idle fuel rate. Equation 6.77 is modified in Section 6.4.6 to account for zero fuel consumption under negative power loading.

Equation 6.77 indicates that three parameters are required before the fuel consumption can be calculated. As the calculation of the total power has already

been discussed, only estimation of the idle fuel consumption and the fuel efficiency factor are addressed in this section.

6.4.2 Idle Fuel Consumption

Introduction

The idle fuel consumption can play an important role in determining the fuel consumption for a given journey. This is especially so for routes heavily congested, where a significant amount of time is spent idling or under negative power, or for routes involving steep downgrades, where tractive power may be such that the total power is negative or very small.

Bowyer, et. al (1986) performed a regression analysis to calculate the idle fuel rate as a function of engine capacity. Their resulting equation (R^2 = 0.67, SE = 0.086 mL/s) was:

$$\alpha = 0.220\ D - 0.0193\ D^2 \qquad (6.78)$$

where D is the engine capacity in litres

For passenger cars, typical values for the idling fuel consumption rate are in the vicinity of 0.5 mL/s, which equates to an engine capacity of around 3 Litres within Equation 6.78. Large trucks may consume over 1 mL/s while idling. Appendix A lists the recommended default values for α used within this research.

Measuring the Idle Fuel Consumption

For a description of the data collection system and calibration utilised in the measurement of fuel consumption, refer to Section 4.3.

The idle fuel consumption was obtained by running the vehicle at idle speed for an extended period of time. For the purpose of the model, only a single idle fuel consumption value is used, therefore requiring a decision on whether the consumption associated with a cold or warm engine should be used.

Data were collected to yield a relationship between time since engine start up and idle fuel consumption. This was undertaken to determine the length of time for the idle fuel consumption to stabilise, thus enabling a decision on what parameter values to adopt.

The results of the tests on idle fuel consumption for the two passenger cars in the Thailand study are shown in Figure 6.19 and Figure 6.20. The data, although collected at 1 second intervals, were aggregated to 10, 20 and 30 second intervals in order to eliminate some of the minor variation in the results[11]. As can be seen, very little change results from the longer averaging period, suggesting that the data is reasonably stable.

[11] When recording at 1 second intervals, the number of fuel pulses is around the 8 per second value at idle. Owing to this low number, any slight variation can have a significant impact on predicted results from 1 second to the next. The data were therefore averaged to reduce some of this scatter.

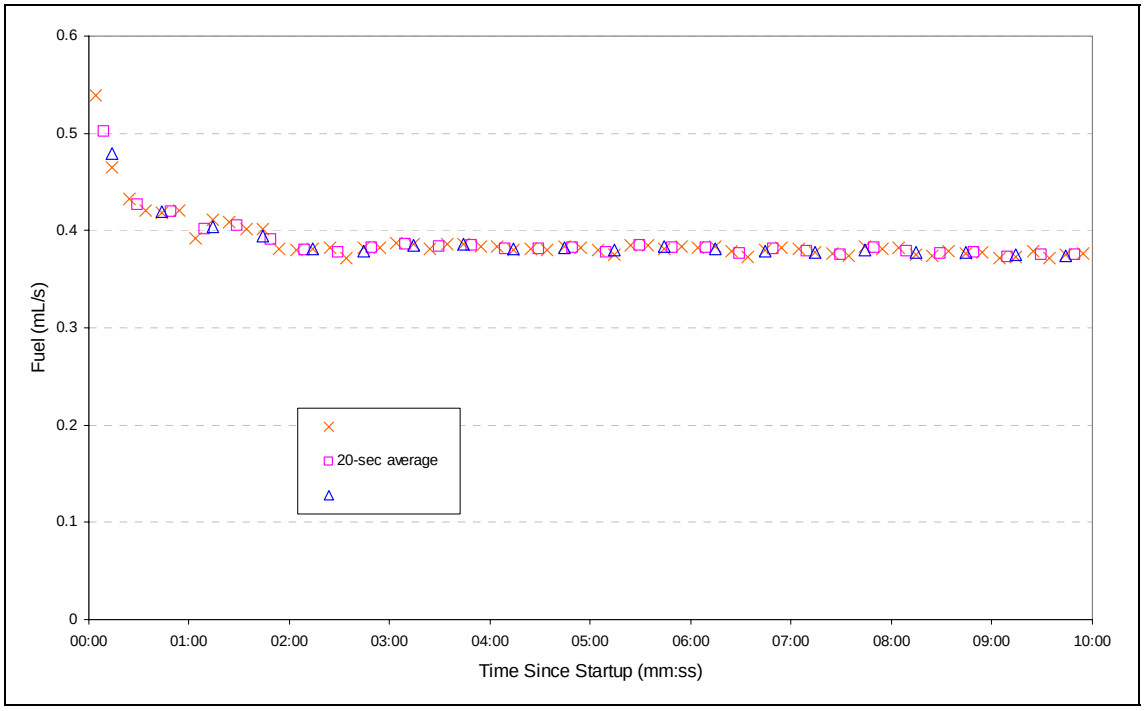

Figure 6.19: Variation of Idle Fuel Consumption with Time Since Startup for 2.0L Toyota Corona with Air Conditioning On

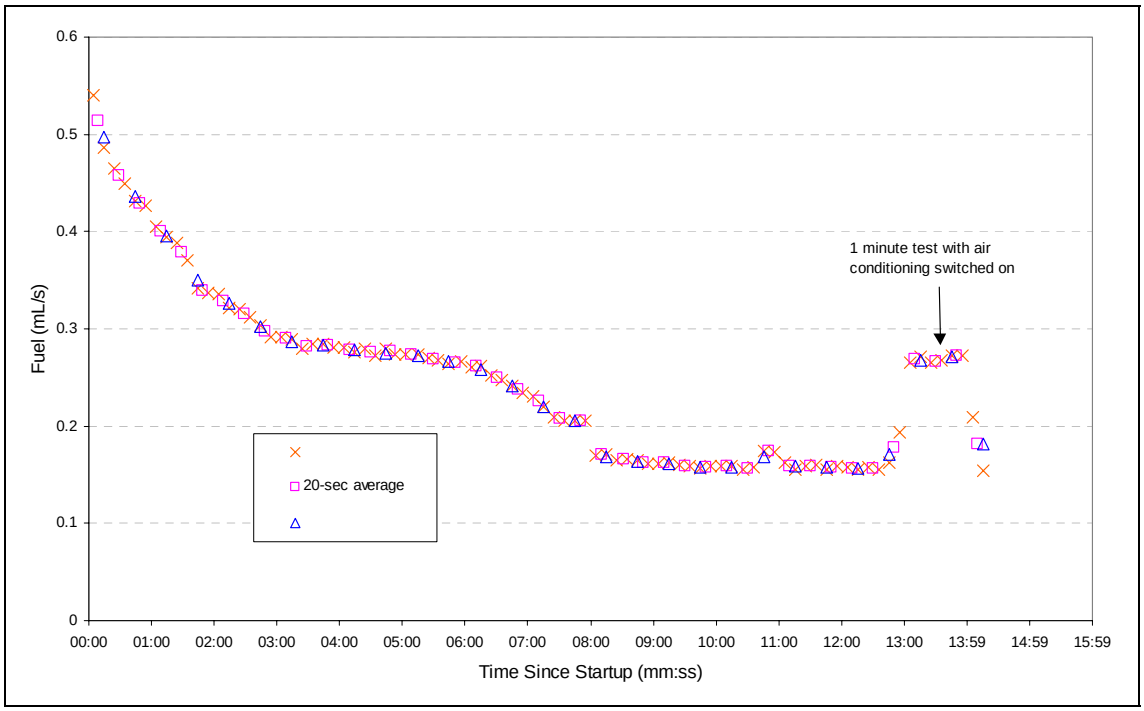

Figure 6.20: Variation of Idle Fuel Consumption with Time Since Startup for 1.6L Toyota Corona with Air Conditioning Off

As can be seen from the data in the above figures, the idle fuel consumption steadies after a period of approximately 2 minutes and 8 minutes for the 2.0L and 1.6L cars respectively when the engine is left to warm up under idle conditions. In reality, vehicles tend to be driven almost immediately upon being started, which decreases the length of time for the engine to warm up and the idle fuel consumption to steady. Given that the higher of these two times of 8 minutes is significantly shorter than many journeys within congested periods, it is considered appropriate to utilise the idle fuel consumption for a warm engine.

The second issue regarding idle fuel consumption is that of what accessories are assumed to be utilised during normal driving periods. Air conditioning, headlights, rear window heater and other electrical appliances can cumulatively have a significant impact on the idle fuel consumption. As shown in Figure 6.20, turning on the air conditioning unit results in an almost doubling of the idle fuel consumption.

It is therefore concluded that the idle fuel consumption of the two vehicles presented above once the engine is warm is:

2.0 L Toyota Corona, 0.38 mL/s
1.6 L Toyota Corolla, 0.27 mL/s

These values compare reasonably closely with those predicted from Equation 6.78, where values of 0.36 and 0.30 are obtained respectively.

6.4.3 Fuel Efficiency Factor

Introduction

The fuel efficiency of vehicles varies with changes in engine speed and power (Smith and Hawley, 1993). In general, efficiency forms a 'U-shaped' relationship with power, with the most efficient range being at about half the maximum power output. For a constant power demand, increasing the engine speed generally leads to a decrease in fuel efficiency. A decrease in efficiency results in an increase in the fuel efficiency factor, ζ and thus an increase in fuel consumption.

ARFCOM Fuel Efficiency Model

Biggs (1988) uses the following relationship to account for the variation in efficiency with power. As engine drag is related to engine speed, this term is implicitly included within the relationship. Table 6.4 lists the engine efficiency factors given by Biggs (1988).

$$\xi = \xi b\ (1 + ehp\ (Ptot\text{-}Peng)/Prat) \qquad (6.79)$$

where ξb is the base engine efficiency in mL/kW/s
ehp is the proportionate decrease in efficiency at high output power
Prat is the rated engine power in kW

Table 6.4: Engine Efficiency Parameters

Engine Type	ξb		ehp
Diesel	0.059	Old technology engines	0.10
	0.058 - [Pmax 10^{-5}]	New technology engines	
Petrol	0.067		0.25

Source: Biggs(1988)

It is noted that the model proposed by Biggs (1988) does not show a decrease in efficiency at both low and high power outputs, nor does it show a decreased efficiency with increasing engine speed.

This is a significant problem when constructing a congestion model, as a large portion of travel is done at low power while idling or decelerating.

Relationships Derived From Engine Maps

Engine maps, which show the engine efficiency as a function of power and engine speed, yield good data for the development of a fuel efficiency model. Unfortunately, the data do not enable simple relationships to be developed that are transferable from one engine to another.

Smith and Hawley (1993) present a graph of fuel efficiency versus power for a range of engine speeds. This graph is reproduced as Figure 6.21 below and clearly illustrates the change in efficiency with increasing power and engine speed as noted earlier.

Measured Fuel Efficiency

To accurately measure the fuel efficiency of a vehicle requires a level of data significantly greater than that available to this project and is a significant study within its own right. Vehicle and engine manufacturers produce engine maps showing performance levels as engine speed, power and torque vary based on extensive data sets.

However, the data that was collected as part of the congestion modelling can be used to confirm the general appropriateness of the recommended fuel efficiency values. The fuel efficiency of the two test vehicles was confirmed using the steady state test results and the idle fuel consumption presented in the previous sections.

Two parameters are involved in describing the fuel efficiency of a vehicle. The first is the base fuel efficiency (ξb) and the second the change in efficiency at high engine loading (ehp).

To estimate the base efficiency, it is possible to use the idle fuel consumption level previously ascertained. Under idle conditions, the total power usage is purely that of engine drag and accessories power. As the total power used will be a small proportion of the rated engine power at idle, the change in efficiency at high power can be ignored resulting in the following simplified form:

$$\alpha = (\text{Peng} + \text{Pacc})\,\xi\text{b} \qquad (6.80)$$

where Pacc is the power required to run the accessories in kW

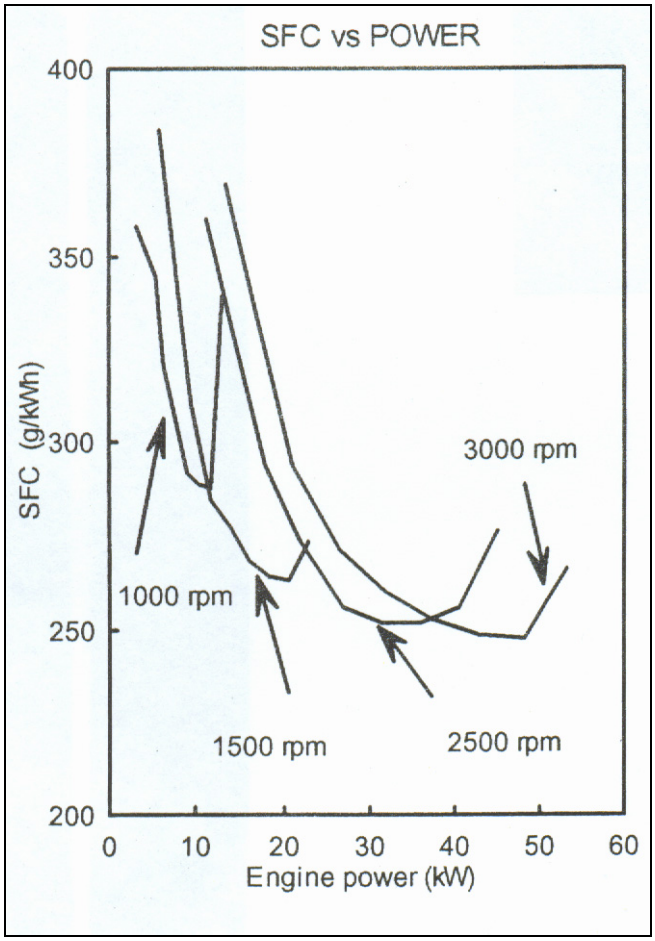

Source: Smith and Hawley (1993)

Figure 6.21: Fuel Efficiency versus Power

Under idle conditions the combined engine and accessories power is typically around 5 per cent of the rated engine power (NDLI, 1995a). Substituting this assumption into the above equation and the previously obtained idle fuel consumption values yields the following values for the base fuel efficiency.

- 1.6 L $\xi b = 0.0635$ mL/kW/s = 0.27 / (0.05 * 85)
- 2.0 L $\xi b = 0.0768$ mL/kW/s = 0.38 / (0.05 * 99)

These values compare favourably with the recommended HDM-4 (Bennett and Greenwood, 2001) default value of 0.067 mL/kW/s.

Alternatively, assuming that the HDM-4 default efficiency of 0.067 mL/kW/s is appropriate for the tested vehicles, then back calculating for the percentage of the rated power being consumed at idle, indicates that the 1.6 L vehicle uses around 4.7 per cent and the 2.0 L vehicle around 5.7 per cent of the rated engine power.

Calibration of the parameter ehp is more difficult with the data collected. In particular, at these higher speeds it is necessary to accurately know the contribution of the accessories and engine drag to the total fuel consumption. In calibrating the ACCFUEL model it was found that the default value of 0.25 gave appropriate results.

6.4.4 Steady State On Road Fuel Consumption Tests

Although not an input to the fuel model, the calculation of base on-road fuel consumption for a given speed is a useful figure in confirming the magnitude of additional fuel predicted by the ACCFUEL program (refer to Section 5.6). For this project, test runs were performed on sections of road that were in flat terrain and of a good condition. The tests were undertaken at speeds from 30 to 150 km/h, with the results illustrated in Figure 6.22 for both the 1.6 L and 2.0 L vehicles.

Greenwood and Bennett (1995a) in reviewing various empirical models found that the most common form fitted is as given below (the equation has been converted to mL/s and the terms relating to gradient and roughness have been excluded as they were not measured in the tests[12]):

$$IFC = a0 + a1S + a2S^3 \qquad (6.81)$$

The above model form was found to give poor predictions at low speeds (below 20 km/h) and was therefore not used within this project. Instead a simple quadratic model was fitted and used as illustrated within Figure 6.22. Note that the intercept value was forced through the previously established idle fuel consumption values (refer to Section 6.4.2)

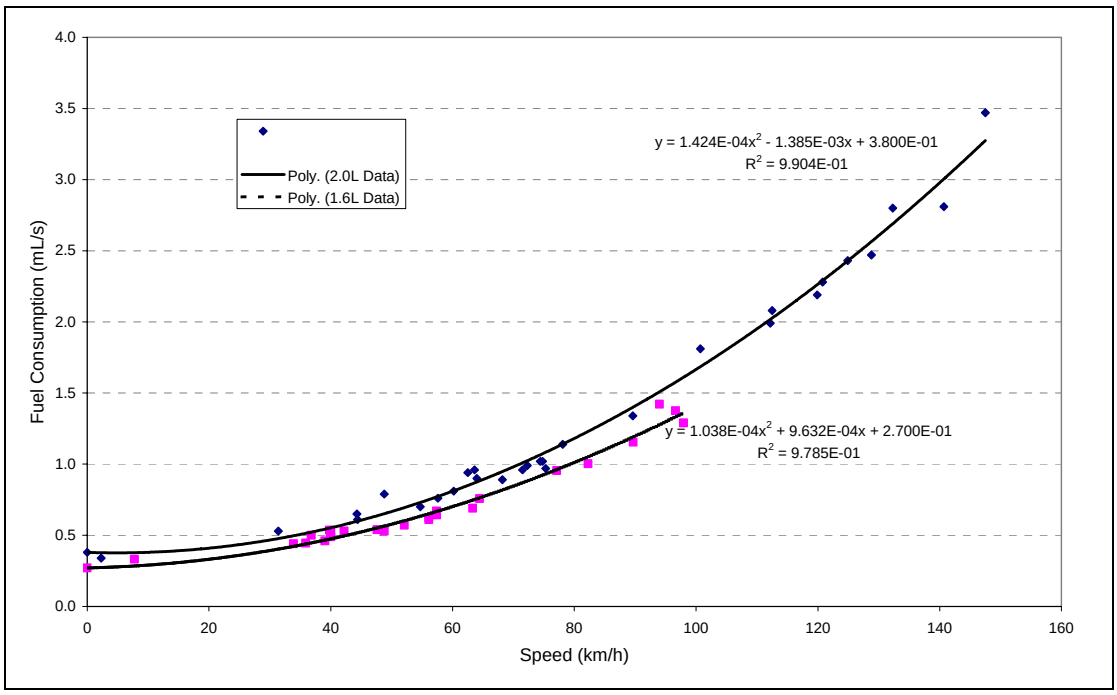

Figure 6.22: On-road Steady Speed Fuel Consumption Tests

[12] The tests sites were chosen such that the gradient was essentially zero. Roughness effects were considered to be minimal (and constant) on the test sections and can therefore be included within the constant term a0.

The parameter values ascertained for the two vehicles are given below. Note that the values are based on speeds in kilometres per hour. To convert the formula to metres per second the coefficient a1 needs to be divided by 3.6 and the coefficient a2 divided by 12.96.

Table 6.5: Steady Speed Fuel Model Parameters

Term	1.6 L Vehicle	2.0 L Vehicle
a0	0.27	0.38
A1 (S)	$9.632*10^{-4}$	$1.385*10^{-3}$
a2 (S^2)	$1.038*10^{-4}$	$1.42*10^{-4}$

If the test runs were "ideal" then there would be no scatter in the data. However, as noted previously the results are from on-road situations and will therefore have a level of variation in driving speeds owing to the natural noise level of the driver/road combination. Fuel consumption higher than the minimum indicates a certain level of acceleration noise occurring during the test run or variation in the test conditions (wind, gradient, texture, roughness etc).

Although Figure 6.22 shows a quadratic function regressed through the data points, the minimum fuel consumption at each speed is the technically correct value that should be used in comparisons. Effectively, the desired relationship would form an efficiency envelope around the minimum values. However, as noted previously, the prediction of the minimum fuel consumption is not a direct input to the fuel consumption model and has only been calculated to allow for a broad check on the output from the congestion model (ACCFUEL).

6.4.5 Model Validation

Introduction

In order to test the validity of the outputs, it is necessary to consider the two distinct parts of the process, namely;

- Predicting the driving style (acceleration noise modelling)
- Predicting the impact of the driving style (fuel and vehicle emission modelling)

This section firstly calculates some basic parameters for use in the comparison, then covers the ability of the fuel model to predict actual fuel consumption given a known drive cycle, before finally looking at total fuel consumption from a simple input of acceleration noise value.

Calibrating ACCFUEL Parameters

Although not given as output from the standard ACCFUEL software, the source code was altered to enable a comparison of the base fuel versus speed relationship. The input parameters were then adjusted[13] until there was close comparison between the

[13] Rather than perform a multi variable regression analysis it was opted to perform a manual calibration. Owing to the interaction of many of the variables it was considered that this approach was the better option to ensure that the resulting values retained a logical inter-relationship.

observed fuel versus steady speed relationship discussed in Section 6.4.4 and the predicted relationship from ACCFUEL.

Comparison of Observed and Predicted Fuel Consumption

Speed and acceleration data for two hours was fed directly into the calibrated ACCFUEL program to test the ability of the fuel consumption prediction models. In this mode of operation, ACCFUEL does not utilise the concept of acceleration noise, as the known speed profile is an input.

Figure 6.23 illustrates the results of the second-by-second predictions from ACCFUEL against the observed readings. The significant number of readings along the x-axis indicates that the model is predicting zero fuel consumption (negative power requirements) in more cases than occurs in practice.

Figure 6.24 illustrates the differences between the observed and predicted values with time. Both this figure and Figure 6.23 indicate a level of variation about the line of equality, with the typical range of variation being within 0.5 mL/s (standard deviation of 0.25 mL/s). This is further testified by the distribution of errors illustrated in Figure 6.25.

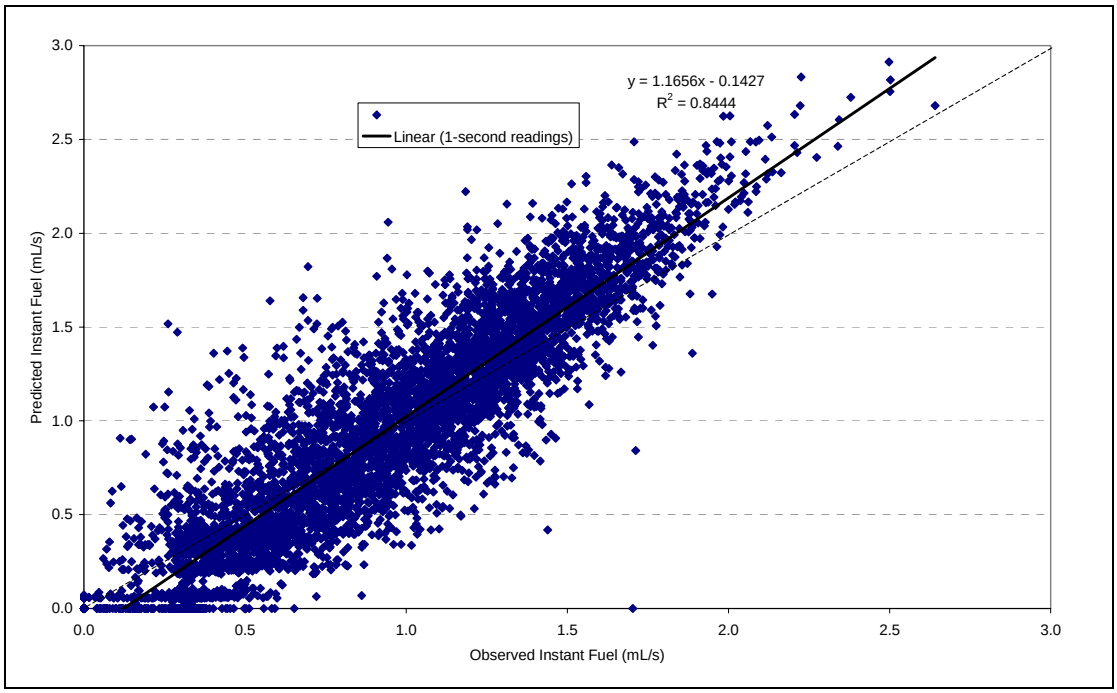

Figure 6.23: Observed versus Predicted Fuel Readings

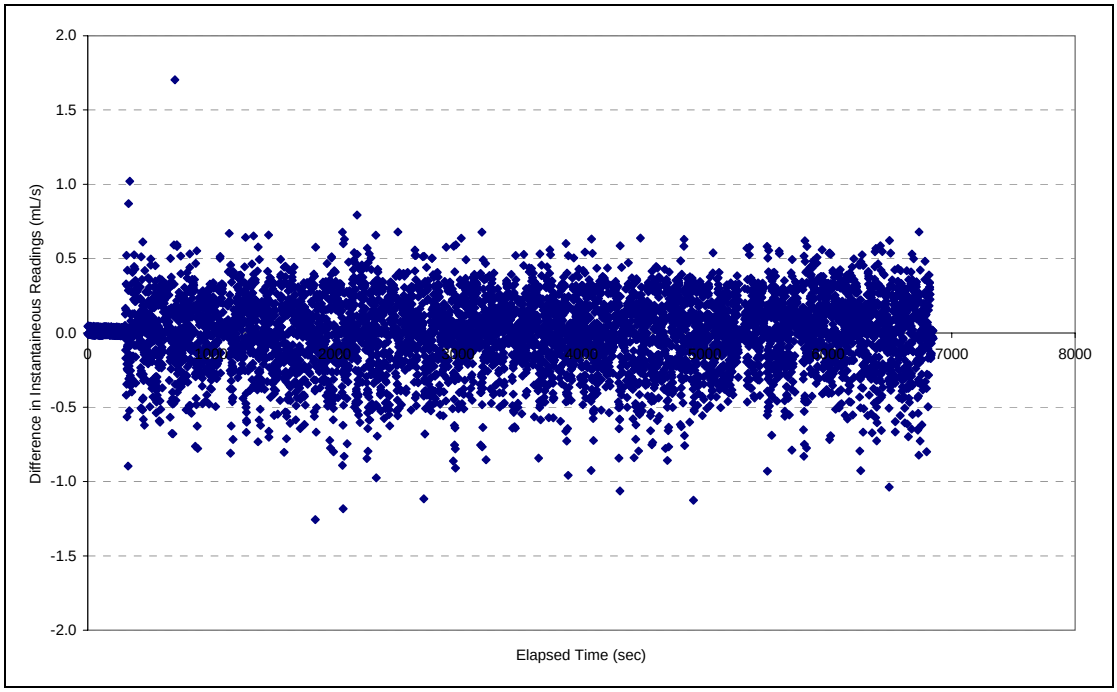

Figure 6.24: Variation Between Observed and Predicted With Time

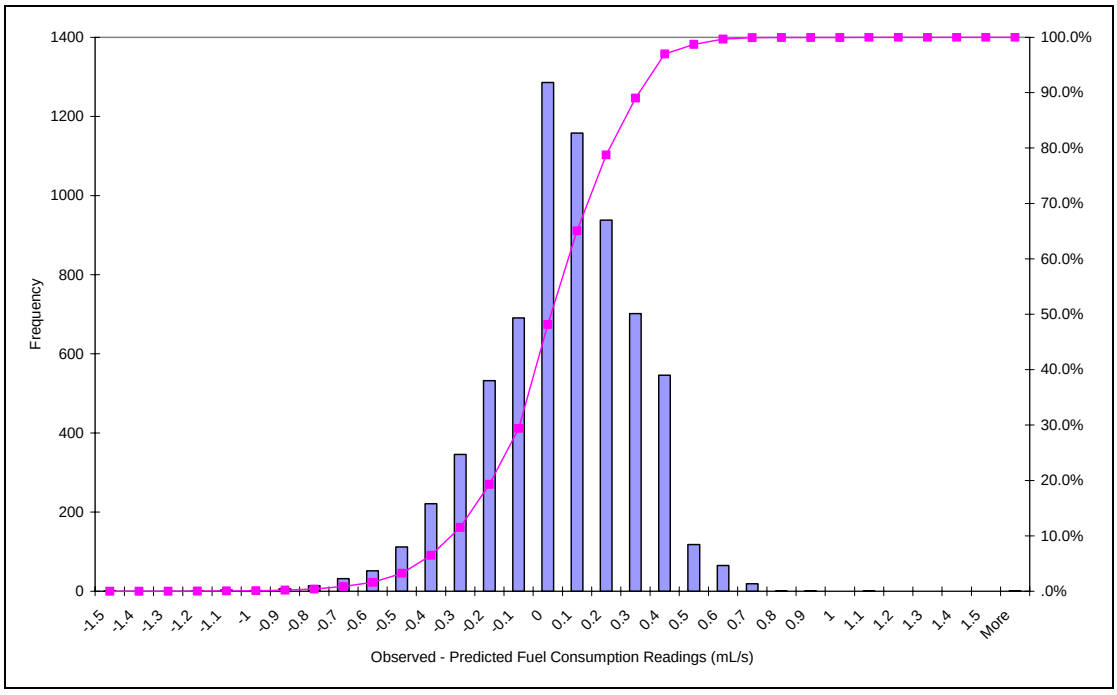

Figure 6.25: Distribution of Errors in the Prediction of Fuel Consumption

Figure 6.26 illustrates the cumulative difference in fuel consumption with time and the percentage of the observed fuel consumption that this makes up. Although there is a reasonably high level of variation (up to 4 per cent) in the early stages of the test run, this reduces to a level of around 0.2 per cent for the longer term predictions.

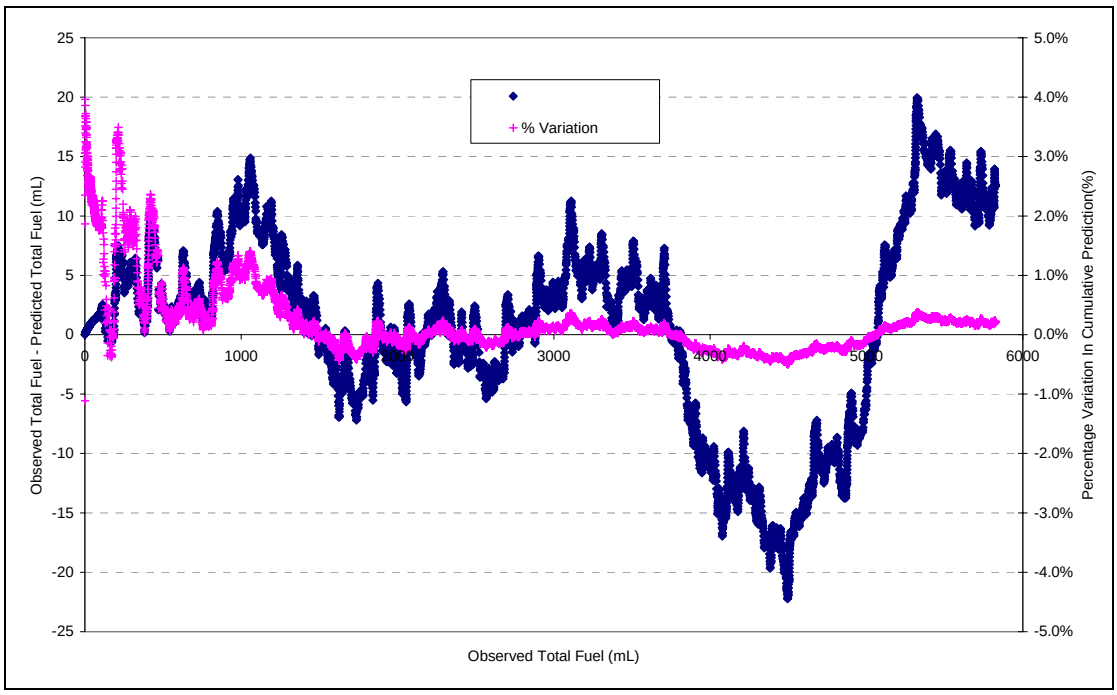

Figure 6.26: Variation and Percentage Variation In Fuel Consumption

As a result of these tests, it is concluded that the fuel consumption model will not provide a significant level of bias to any predictions within ACCFUEL. The standard deviation of error in the fuel predictions (0.25 mL/s) equates to approximately 5 per cent of all readings.

Comparison of Observed versus Predicted Increases

Utilising the results of the identified periods from the congestion analysis, a comparison has been made between the predicted value of DFUEL from the ACCFUEL program and that observed from the on-road tests.

The results of the comparison for each test run are given in Appendix C. A plot of the observed versus predicted values of DFUEL is shown in Figure 6.27. As is shown in the plot, there is a reasonably high level of bias in the overall predictions, with the predicted value of DFUEL being consistently lower than that observed. For observed values of DFUEL in the order of 2, the predicted value is some 25 per cent low.

The R-squared value of 0.49 indicates that although a moderate level of correlation exists between the observed and predicted value, there is a large amount of variation as yet unexplained by the modelling process.

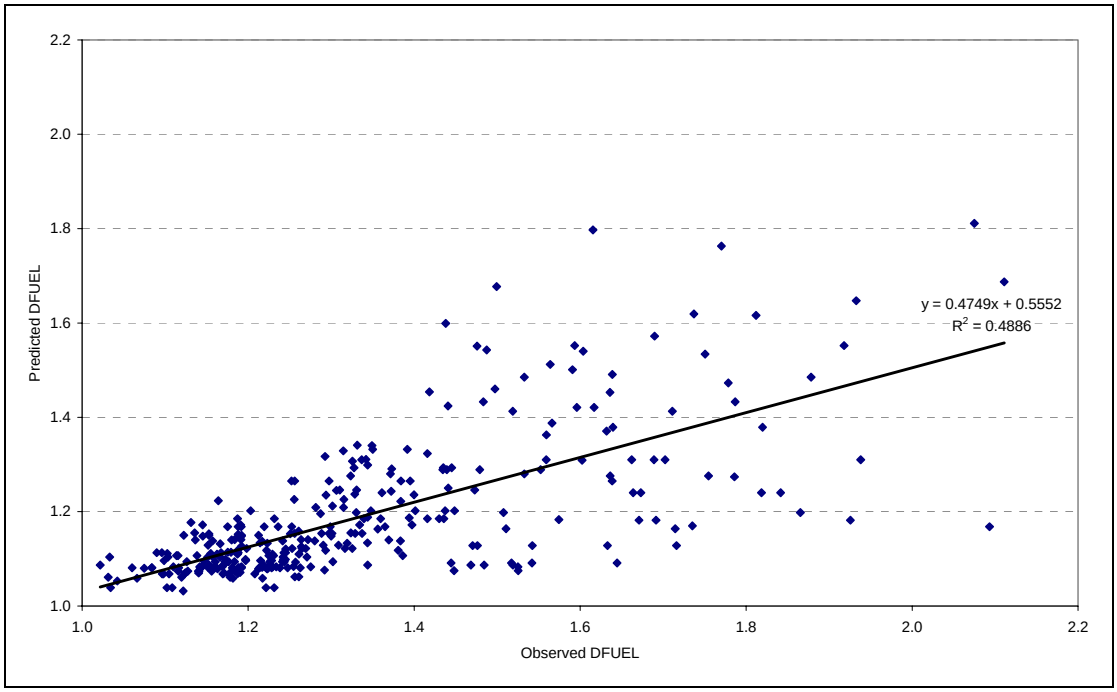

Figure 6.27: Observed vs Predicted Values of DFUEL

It is important to note that the ACCFUEL program assumes that the acceleration noise distribution is Normal. Both Greenwood and Bennett (1995) and NDLI (1995) discuss the implications and validity of this assumption. For those test runs that are shorter in duration, there is a higher likelihood that a non-normal distribution of accelerations is measured, thus reducing the probability of achieving an exact match. The distribution of test run length (both time and distance) is given in Figure 5.3 and Figure 5.4.

For the majority of the test runs, the data is negatively skewed in the order of one standard deviation. The kurtosis factor for many of the data sets indicates that the distribution is not Normal in shape. Combined, these two measures suggest that the underlying assumption of Normality may need to be reviewed in order to improve the predictive accuracy of the model.

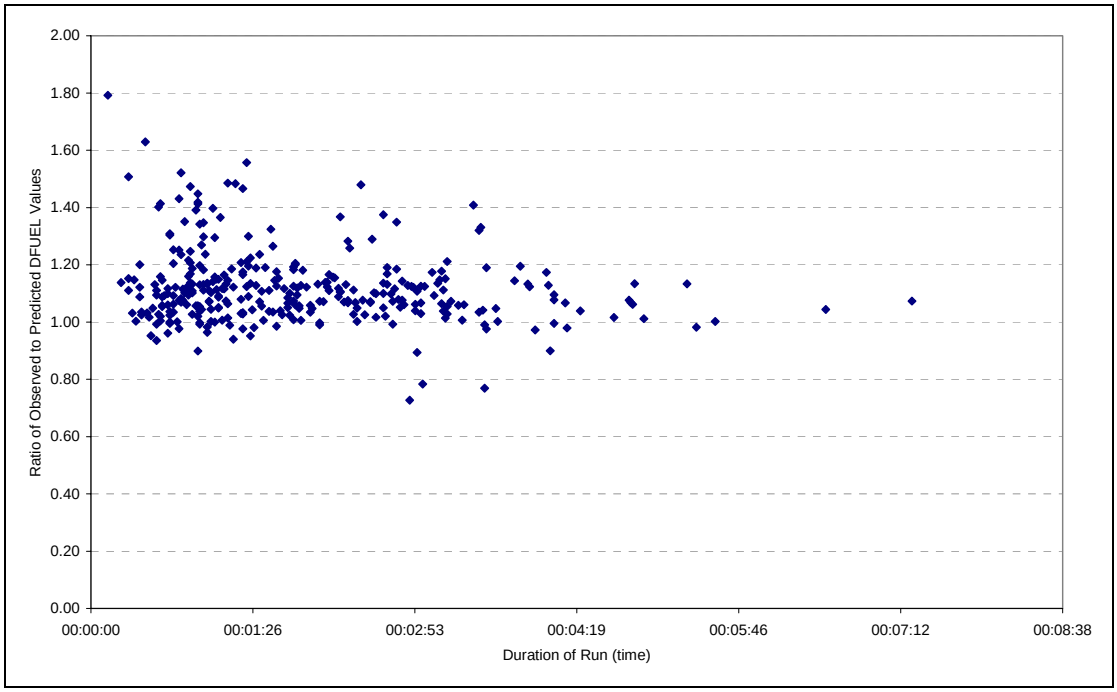

Figure 6.28: Impact of Duration of Run on Predictive Ability

Summary

Although there is a reasonably high level of variation between the observed and predicted values of DFUEL, the overall relationship is on-average predicting an increase in fuel consumption of the correct magnitude when the model is appropriately calibrated, although there is significant variation in the results.

The impact of the assumption of Normality in the underlying acceleration noise distribution may require further consideration given that many of the data sets are both skewed and have a kurtosis value other than unity. It is postulated that the short duration of many of the test runs is partly responsible for this finding and that test runs of a much greater duration than those currently recorded are required to justify a shift away from the assumption of normality.

6.4.6 Minimum Fuel Consumption

Historically, engines did not have the ability to shut off fuel to the engine completely, such that even under heavy deceleration the engine was still consuming fuel at the idle fuel rate. With the advent of fuel injected engines (particularly more recent models) the engine now has the ability to reduce fuel consumption to zero during such events. Therefore Equation 6.77 can be rewritten to:

$$IFC = \max(\alpha, \xi\ Ptot) \quad \text{if } Ptot \geq 0 \qquad (6.82)$$

$$MinIFC \quad \text{otherwise} \qquad (6.83)$$

For modern vehicles the value of MinIFC will be zero, while for older carburettor type engines a value equal to the idle fuel consumption would be appropriate.

6.4.7 Summary and Conclusions – Fuel Consumption Model

This section has presented the fuel consumption model. The model adopted is based on the ARRB ARFCOM mechanistic model. Some modifications have been made to the basic model parameters and equations in the standard model. In particular, the inclusion of a minimum fuel consumption parameter for the negative power component, which accounts for the ability of some engines to operate at zero fuel consumption during such periods.

The fuel model predicts that fuel is proportional to the power requirements of the vehicle. It can be expressed as:

$$IFC = \max(\alpha, \xi\ Ptot) \quad \text{if } Ptot \geq 0 \qquad (6.84)$$

$$MinIFC \quad \text{otherwise} \qquad (6.85)$$

where
- IFC is the instantaneous fuel consumption in mL/s
- α is the idle fuel consumption in mL/s
- ξ is the fuel-to-power efficiency factor in mL/kW/s
- Ptot are the total vehicle power requirements
- MinIFC is the minimum fuel consumption under negative power loading (default =0) in mL/s

The total power requirements comprise the power to overcome the tractive forces, to overcome engine drag and to power vehicle accessories. Calculation of these are covered in Section 6.3.

Engine efficiency is dependent upon the output power and engine speed. The following relationship is utilised to account for this decreased efficiency:

$$\xi = \xi b\ (1 + ehp\ (Ptot\text{-}Peng)/Pmax) \qquad (6.86)$$

The predictive ability of the fuel consumption model was tested against data collected from on road drive cycles. The findings of the test are contained within Section 6.4.5 and indicate that for a known drive cycle, the fuel consumption model is predicting to an acceptable level with errors in the 0.25 per cent range once the model has stabilised.

The test of the total ACCFUEL program indicates an under prediction of the impact of congestion on fuel consumption in the order of 3 to 12 per cent – with extreme values of 25 per cent. Given that the fuel consumption model has been demonstrated to give reliable predictions, the reason for the mismatch is that the assumed distribution of accelerations does not match that observed in the various test runs.

An examination of the distribution of the accelerations in the test runs concluded that they were not Normally Distributed. In many cases, the number of readings in the test runs were too short to confirm if the underlying distributions were Normal.

6.5 Summary

This chapter has presented the detailed methodology adopted for estimating the fuel consumption of a vehicle. The method is based on the ARFCOM model and requires the estimation of all forces acting on the vehicle, along with an assessment of the engine drag and accessories power.

Models were presented for the estimation of all forces, based on mechanistic principals. A simulation program (GEARSIM) was written to estimate gear selection in order to identify the inertial mass of the vehicle when accelerating. A summary of the recommended model forms for predicting the forces opposing motion is contained in Section 6.2.7.

Changes were made to the ARFCOM engine and accessory power models. These were primarily to address areas that the original research for ARFCOM had identified as having a very low confidence level. A key input to the fuel consumption model was that of engine speed, with the same simulation program (GEARSIM) as utilised to model gear selection, also utilised for this purpose.

The minimum fuel consumption of some modern vehicles was found to drop to zero during periods of heavy deceleration. To take this into account it was necessary to modify the resulting ARFCOM model to include a minimum fuel constant as opposed to the use of the idle fuel consumption.

On road tests were undertaken to produce a set of steady speed curves for the test vehicles, against which the impact of congestion could be measured. These curves were then utilised to test the overall predictive ability of the models against an actual drive cycle. Overall the fuel model predicted total fuel consumption within 0.25 per cent of that observed, with a maximum deviation of 4 per cent.

Prediction of the increase in fuel consumption caused by traffic congestion resulted in a lower level of confidence. As the fuel consumption model is generating appropriate results, it is concluded that the cause of errors is that the assumption that the acceleration data are Normally distributed does not hold for all the data sets tested. This could be a result of two issues:

- the population data is not Normal
- the population data is Normal, but the sample is too small to accurately reflect this.

Indications are that the longer the test run (the larger the sample) the better the predicted impact of congestion is, which suggests that the latter of the two causes may be correct.

7 VEHICLE EMISSION MODELLING

7.1 Introduction

Section 2.9 provided an overview of various approaches to the modelling of vehicle emissions, along with discussions on the impact of fuel type, engine temperature and the like. On the basis of the information reviewed, a modelling approach has been adapted from that proposed by An et al (1997).

No data collection exercises have been completed to validate the form or predictive ability of the models, although the resulting models have been tested in Chapter 8.

7.2 Modelling Approach

For this report, all models have been presented such as they predict emissions in g/km, where this is not the format of the models in their original formulation, appropriate conversions have been made. The basic model form is:

$$TPE_i = EOE_i * CPF_I \quad (7.1)$$

where TPE_i is the Tailpipe Emissions in g/km for emission i

EOE_i is the engine out emissions in g/km for emission i

CPF_i is the Catalyst Pass Fraction for emission i

Diagrammatically this can be represented as shown in Figure 7.1, which is a modification of a similar plot presented by An et al (1997). In essence, the engine out emissions are estimated based on the fuel consumption rates, with CO_2 being calculated from carbon balance assumptions. These engine out emissions are then treated by the catalytic converter, if present, to yield the tailpipe emissions observed by the environment.

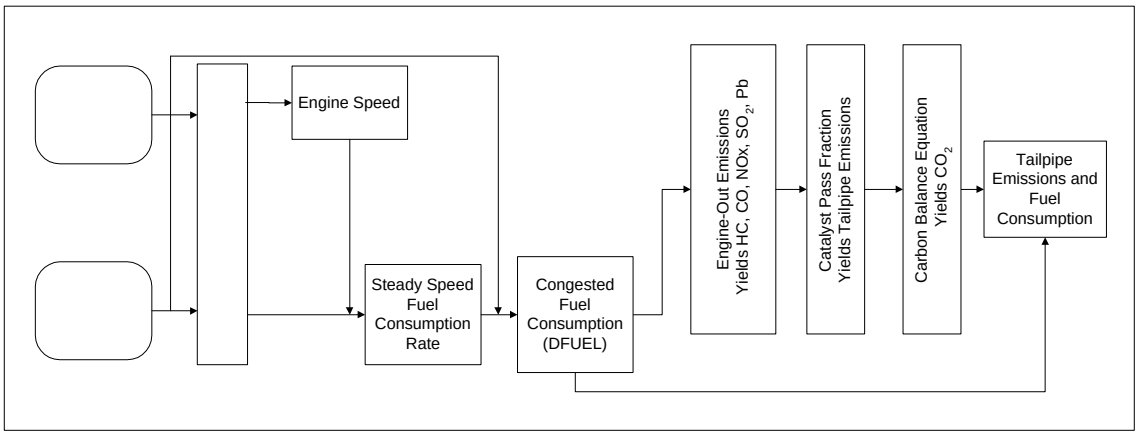

Figure 7.1: Calculation of Vehicle Emissions

This section of this report first presents models for predicting the various engine out emissions that are related to fuel consumption. It then provides functions for the catalytic converter performance and finishes with the carbon balance equation for predicting CO_2.

7.3 Fuel Dependent Emissions

7.3.1 Introduction

Before relating emissions to fuel consumption, it is necessary to review the fuel consumption model presented in Section 6. In essence, the model firstly predicts the steady speed fuel consumption, which is then adjusted to account for acceleration cycles through the use of the term DFUEL. DFUEL takes into account the proportional increase in fuel consumption caused by non-steady speed driving.

Two alternatives are available for predicting vehicle emissions as a function of fuel consumption; the first is to predict emissions as a function of the congested fuel consumption (*i.e.* the steady state plus DFUEL). Alternatively, we could predict them as a function of the steady state fuel consumption, then use a factor to increase for congestion.

The former of these two approaches results in a much simpler model, and on the basis of the work in An et al. (1997), it is this technique that has been adopted for developing the emissions model. In addition, the prediction of certain emissions requires the actual fuel consumption to be utilised, which can only be through the use of the congested fuel consumption.

In relating emissions to fuel consumption, the assumption is primarily one of chemical balance. Therefore, the production of emissions is considered to be directly proportional to the fuel consumed, resulting in a nominal model form as given below. As is illustrated in the remainder of this chapter, for the prediction of some emissions a slightly modified form of this model is utilised, although the base component is still evident.

$$EOE_i = FC\left(\frac{g_{emissions}}{g_{fuel}}\right)_i \tag{7.2}$$

$$FC = \frac{IFC \quad DensFuel \quad 1000}{V} \tag{7.3}$$

where

FC	is the fuel consumption (including congestion effects) in g/km
$(g_{emissions}/g_{fuel})_i$	is the ratio of engine-out emissions per gram of fuel consumed for emission i
IFC	is the instantaneous fuel consumption (including congestion effects) in mL/s
DensFuel	is the density of fuel in g/mL
V	is the vehicle speed in m/s

As part of the ISOHDM work, the SNRA (1995) presented a vehicle emissions model similar in form to that shown in Equation 7.2, with the exception that a constant component was also included and no explicit allowance for catalytic converters was made.

The work of An et al (1997) included an allowance for the fuel/air equivalence ratio (ϕ) in emission production[14]. The form of the fuel consumption model adopted does not incorporate the modelling of this term and hence an adjustment was necessary. An et al. (1997) state that the fuel/air equivalence ratio varies between 0.98 and 1.02 during stoichiometric operating conditions (normal conditions) and increases up to a value of 1.3 during "rich" operating conditions, when power demand exceeds the available engine power under stoichiometric conditions.

For the range of conditions that the emissions model is expected to cover, rich operating conditions will be minimal and thus it has been assumed that the air/fuel ratio can be assumed as a constant. During the remainder of this work on emissions modelling, the fuel/air equivalence ratio has therefore been set equal to 1.0

7.3.2 Swedish Emission Models

In the SNRA (1995) work mentioned earlier, relationships were presented for urban and rural driving, and new and old vehicle technologies, based on a linear regression analysis.

The form of the model used in the regression analysis is (SNRA, 1995) given below (note that the prediction is in terms of g/s and not g/km):

$$\text{Emissions (g/s)} = a + b * \text{fuel consumption (mL/s)} \quad (7.4)$$

The analysis based on the combined rural and urban data yielded unexpected results in that some of the emissions were shown to decrease with increasing fuel consumption, despite both the individual urban and rural relationships showing that the emissions increased. It is postulated that this anomaly is due to the fact that the range of fuel consumption flows over which the measurements were taken in the urban and rural studies were not the same, and thus the average results are distorted and thus considered invalid. The SNRA (1995) note that for general driving conditions reasonable values would be obtained, however in some situations such as steep downgrades, negative emission levels would be predicted unless appropriate modifications were made to the models.

Table 7.1 contains the various coefficients from the Swedish work (SNRA, 1995) including R^2 values for the new technology vehicles. From a pure theoretical view point, the value of the constant for the various emissions, should always be zero, as when no fuel is being consumed, no emissions can be produced.

[14] A fuel/air equivalence ratio of 1.0 is deemed to be operating under stoichiometric conditions.

Table 7.1: Coefficients from Swedish Study for New Technology Vehicles

Vehicle Type	Area	HC			CO			NOx			Particulates		
		a	b	R^2	a	b	R^2	a	b	R^2	a	b	R^2
Car	Rural	-0.000113	0.000436	0.877	-0.00200	0.00512	0.655	-0.00182	0.00340	0.992			
	Urban	0.0000349	0.000357	0.622	-0.00206	0.00467	0.200	-0.00150	0.0024	0.580			
	Total	-0.000272	0.000394	0.847	-0.00291	0.00554	0.658	-0.00314	0.00400	0.895	-1.48×10^{-5}	3.92×10^{-5}	0.758
Light Duty	Rural	-0.00691	0.000866	0.949	-0.00886	0.0145	0.620	-0.000839	0.00251	0.835			
	Urban	0.000150	0.000235	0.470	-0.00728	0.0126	0.687	-0.000269	0.00152	0.417			
	Total	-0.00533	0.000780	0.913	-0.00968	0.0148	0.713	-0.00166	0.00283	0.838	-2.16×10^{-5}	6.85×10^{-5}	0.560
Truck	Rural	0.0156	0.000808	0.140	0.0215	0.00623	0.830	0.0185	0.0185	0.886			
	Urban	0.0261	-0.000977	0.063	0.0454	0.00186	0.051	-0.0126	0.0332	0.961			
	Total	0.0233	-0.000785	0.038	0.0383	0.00275	0.106	0.0205	0.0187	0.842	-5.25×10^{-4}	1.40×10^{-3}	0.862
Artic-Truck	Rural	0.0106	0.00129	0.484	-0.00165	0.00921	0.982	0.0860	0.0178	0.974			
	Urban	0.0156	0.00208	0.592	0.0225	0.00573	0.365	0.0340	0.0306	0.971			
	Total	0.0244	0.000345	0.189	0.00776	0.00814	0.838	0.100	0.0175	0.783	2.81×10^{-3}	2.10×10^{-4}	0.164

Emissions (g/sec) = a + b * IFC (mL/s)
Source: SNRA (1995)

From an examination of the R-squared values in Table 7.1, clearly some of the relationships are tenuous, with the simple linear equation accounting for less than half of the variation in over 30 per cent of the equations.

As the work of SNRA (1995) does not explicitly consider the impact of catalytic converters, the results of the SNRA model are best considered as equivalent to the tailpipe emissions rather than engine out emissions. To use these model coefficients within the emissions model, the appropriate adjustment to account for the impact of catalytic converters and a change in units to g/km would be required.

7.3.3 US Emission Models

An et al. (1997) present the following models for predicting vehicle emissions. As noted earlier, the fuel/air equivalence ratio (ϕ) is not modelled within the fuel consumption model used and has been assumed to be equal to unity (1.0). For those predictive models within An et al. (1997) that do include this variable, a value of 1.0 has been substituted and the resulting equation simplified.

Carbon Monoxide (CO)

For the prediction of CO, it is assumed that a direct relationship exists between fuel consumption and the production of CO in the engine.

$$EOE_{CO} = a_{CO}\, FC \tag{7.5}$$

where EOE_{CO} is the engine-out CO emissions in g/km
a_{CO} is a constant = g_{CO}/g_{fuel}

Hydrocarbons (HC)

Hydrocarbons are generated from two sources within a combustion engine. The first is from the burning of the fuel, while the second is from incomplete combustion. Therefore, the model for the prediction of HC being emitted from the engine is as follows.

$$EOE_{HC} = a_{HC}\, FC + \frac{r_{HC}}{V} 1000 \tag{7.6}$$

where EOE_{HC} is the engine-out HC emissions in g/km
a_{HC} is a constant = g_{HC}/g_{fuel}
r_{HC} is a constant to account for incomplete combustion in g/s
V is the vehicle speed in m/s

Oxides of Nitrogen (NOx)

Oxides of nitrogen are possibly the emission that is least related directly to fuel consumption. As a result of this, the model used to relate NOx production as a function of fuel consumption is more complex that the others presented in this chapter. The model form proposed by An et al (1997) is:

$$EOE_{NOx} = \max\left[a_{NOx}\left(FC - \frac{FR_{NOx}}{V} 1000 \right), 0 \right] \tag{7.7}$$

where EOE_{NOx} is the engine-out NOx emissions in g/km

a_{NOx} is a constant = g_{NOx}/g_{fuel}
FR_{NOx} is the fuel threshold below which NOx emissions are very low in g/s

Values for the constants contained in Equations 7.5 to 7.7 are given in Table 7.2. Table 7.2 also contains some basic attributes of the different vehicles for which the parameter values were produced, such as mass and engine size.

Table 7.2: Constants for Prediction of Vehicle Emissions

Variable	1981 Toyota Celica	1986 Buick Century	1995 Honda Civic
Engine Capacity (litres)	2.4	2.8	1.6
Mass (kg)	1361	1531	1247
Pmax (kW)	78	84	76
a_{CO}	0.16	0.11	0.10
a_{HC}	0.013	0.013	0.012
r_{HC}	0.006	0.008	0.000
a_{Nox}	0.03	0.016	0.055
FR_{Nox}	0.39	0.49	0.17

Source: An et al. (1997)

7.3.4 English Models (ETSU)

The ETSU (1997) present fuel dependent emission models for SO_2 and Pb. The models presented are of the same form as Equation 2.3.

Sulpur Dioxide (SO_2)

The quantity of SO_2 produced is related directly to the quantity of sulphur present in the fuel. Estimation of the model coefficient is made by assuming that all the sulphur in the fuel is converted to SO_2 (ETSU, 1997). Based on this assumption, the following relationship is derived for predicting SO_2 engine out emissions.

$$EOE_{SO_2} = 2\,a_{SO_2}\,FC \qquad (7.8)$$

where EOE_{SO2} is the engine-out SO_2 emissions in g/km
a_{SO2} is a constant = g_{SO2}/g_{fuel}

A default value of a_{SO2} is estimated by ETSU (1997) from a variety of fuel supplies as:

- 0.0005 for petrol vehicles
- 0.005 for diesel vehicles

Lead (Pb)

The quantity of Pb produced is related directly to the quantity of lead present in the fuel, which in recent years has been dramatically decreased (or eliminated) in many

countries over health concerns. Estimation of the model coefficient is made by assuming that a proportion (default = 75 %) of the lead in the fuel is converted to lead emissions (ETSU, 1997). Based on this assumption, the following relationship is derived for predicting Pb engine out emissions.

$$EOE_{Pb} = Prop\_Pb\, a_{Pb}\, FC \qquad (7.9)$$

where EOE_{Pb} is the engine-out Pb emissions in g/km
Prop_Pb is the proportion of lead emitted (default = 0.75)
a_{Pb} is a constant = g_{Pb}/g_{fuel}

A default value of a_{Pb} is estimated by ETSU (1997) from a variety of fuel supplies as:

- 0.000537 for petrol vehicles
- 0 for diesel vehicles (i.e. diesel fuel should contain no lead)

7.4 Catalytic Converters

Catalytic converters aim to reduce certain harmful emissions into chemical compounds that are less harmful to both human life and the environment. Primarily catalytic converters aim to convert any carbon (found in CO, HC and particulate matter) into CO_2, and NOx into ammonia, nitrogen and CO_2 depending on operating conditions prevailing at the time (An et al., 1997). Significant changes have been made to the efficiency of the catalyst technology since the early oxidising catalysts. Current catalysts are made up of a range of materials in order to address a wider range of emissions, with current research focusing on the improved efficiency during cold start conditions (Heywood, 1997).

The effectiveness of catalytic converters in reducing emissions is modelled through the term Catalyst Pass Fraction (CPF). The effectiveness of catalysts is dependent on the temperature of the catalytic converter, with significant variances often observed between hot-stabilised and cold-start conditions. For the model being developed only the hot-stabilised portion is required.

An et al. (1997) present the following equation for the prediction of CPF, with the relevant constants contained in Table 7.3. As with the emission prediction models described above, the air/fuel equivalence ratio has been set equal to 1.0 and the appropriate simplifications made. An et al. (1997) note that the form of Equation 7.10 represents a decreasing probability for oxidation with increasing fuel consumption. An et al. (1997) state that the form of the CPF equation for the prediction of NOx is not good, and that only an average CPF for these emissions is used[15].

$$CPF_i = 1 - \varepsilon_i \exp\left[-b_i\, IFC\, MassFuel\right] \qquad (7.10)$$

where CPF_i is the catalyst pass fraction for emission I
ε_i is the maximum catalyst efficiency for emissions ei
b_i is the stoichiometric CPF coefficient

[15] An et al. (1997) do not include the prediction of NOx into an equation, but rather state that it is a constant value. However, for consistency across emissions, the appropriate constants in Equation 7.10 have been set to zero to enable one form of model for all emissions.

Table 7.3: Catalyst Pass Fraction Constants

Vehicle	CO		HC		NOx	
	ε_{CO}	b_{CO}	ε_{HC}	b_{HC}	ε_{NOx}	b_{NOx}
1981 Toyota Celica	.279	1.60	.474	1.30	0.000	0.0
1986 Buick Century	.999	0.46	.999	0.11	0.753	0.0
1995 Honda Civic	.999	0.05	.999	0.03	0.812	0.0

Source: An et al. (1997)

Lead poisons catalytic converts, such that they are only suitable for use with unleaded fuels. There is therefore no reduction in lead emissions ($\varepsilon_{Pb} = 0$) from the installation of a catalytic converter as these are mutually exclusive occurrences.
In a similar manner to lead, SO_2 also poisons the catalyst. SO_2 is also not converted or absorbed by catalytic converters, such that the engine out emission of SO_2 equals the tailpipe emissions.

Particulate matter is unaffected by catalysts and is simply emitted from the tailpipe in the same quantity as it is emitted from the engine[16]. Therefore CPF factors of $\varepsilon_{PM} = 0$ and $b_{PM} = 0$ are utilised.

Catalysts serve to convert CO and HC into CO_2, and do not treat CO_2 in itself. As is indicated in Equation 7.12 within the next section, the prediction of CO_2 already includes this effect by utilising tailpipe emissions in the carbon balance equation. Therefore, as there is a direct prediction of the tailpipe emissions for CO_2 there is no CPF.

It is evident from the constants in Table 7.3 that significant variation occurs between vehicles, with the newer model cars performing significantly better than the older models. To assist in understanding the values within Table 7.3, the CPF ratios have been plotted over a range of typical fuel consumption rates.

Figure 7.2 illustrates the variation of CPF with fuel consumption for the 1995 Honda Civic. The form of the equation for predicting CPF within An et al. (1997) contains an additional variable in the exponential portion of Equation 7.10. This additional component dealt with periods of rich operation. As noted elsewhere, only the stoichiometric conditions are being modelled within this research. Subsequent to this, Figure 7.2 shows that the variation in CPF is essentially linear over the typical range of fuel consumption observed.

[16] It is noted that particulate traps are being introduced on diesel vehicles and will result in a similar reduction in particulates as the catalytic converted does for the other emissions, although their method of operation are very different.

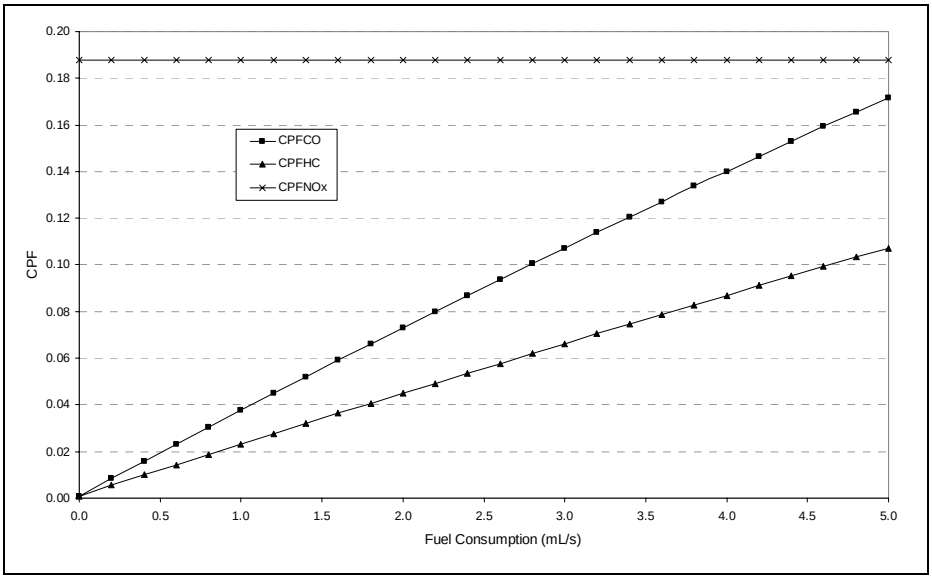

Figure 7.2: Variation of CPF with Fuel Consumption

Deterioration of the exhaust system is required to be modelled. The SNRA (1995) state that this is particularly important for new technology vehicles, where catalytic converters are present. The SNRA (1995) implemented a simple linear deterioration function with time to account for this deterioration. Although not included in either the model form in SNRA (1995) or the HDM-4 Technical Reference Manual (Odoki and Kerali, 1999), the SNRA (1995) state that the normal approach is to have an upper limit on the accumulated deterioration. A value of 10 for this upper limit is stated as normal practice for Sweden by SNRA (1995).

The addition of a deterioration component to the modelling of the CPF yields the following equation:

$$CPF_i = \left[1 - \varepsilon_i \exp\left(-b_i \, IFC \, MassFuel\right)\right] \min\left[\left(1 + \frac{r_i}{100} AGE\right), MDF_i\right] \qquad (7.11)$$

where r_i is the deterioration factor for emission i in %/year

AGE is the vehicle age in years

MDF_i is the maximum deterioration factor for emission i (default = 10)

Values for the deterioration factor, r_i, are given in Table 7.4. These values are extracted from SNRA (1995) and Hammarstrom (1999), and indicate a significant increase in the production of HC and CO for new technology vehicles. In particular, the emission of CO is predicted to double every four years and HC every 5 years. Deterioration is caused by a combination of poisoning (by lead or sulphur) or via thermal degradation, wherein the noble metals disintegrate under extreme heat, thereby reducing the effective surface area of the catalyst.

Table 7.4: Deterioration Factors r_i

Vehicle Technology	Substance			
	HC	CO	NOx	Particulates
Old[1]	7	6	2	
New[1]	20	25	5	
New[2]	20	4.8	11	4.8

Notes: 1. Source: SNRA (1995)
2. Source: Hammarstrom (1999)

Hammarstrom (1999) indicates that his values are based around a total travelled distance of 200,000 km over a period of 13 years. Hammarstrom (1999) states that the difference between the values he reports and those from the SNRA (1995) are that the newer values are from statistical data, while the older values are from a literature review at that time. The values of Hammarstrom (1999) could therefore be considered a more reliable source for a modern vehicle fleet.

7.5 Carbon Balance

The estimation of CO_2 production is undertaken by solving the carbon balance equation given below as Equation 7.12. This equation, extracted from ETSU (1997) yields the quantity of CO_2 based on the overall carbon consumed less that extracted by other forms. It is noted that this equation utilises the tailpipe emissions as the catalytic converter (refer to previous section) increases the output of CO_2 by converting CO and HC and particulate matter into CO_2. The equation as presented in ETSU (1997) has the denominator for HC as 0.01385, which is considered to be an error. A minimum value of zero is placed on the output of CO_2.

$$TPE_{CO_2} = \max\left[44.011\left(\frac{FC}{12.011+1.008\,a_{CO2}} - \frac{TPE_{CO}}{28.011} - \frac{TPE_{HC}}{12.011+1.008\,a_{CO2}} - \frac{TPE_{PM}}{12.011}\right), 0\right] \quad (7.12)$$

where a_{CO2} is a fuel dependent model parameter representing the ratio of hydrogen to carbon atoms in the fuel

In revising the denominator for the HC component, reference was made to the molar mass of the various substances. The molar mass for the various components is:

- CO_2 = 44.011
- CO = 28.011
- PM = 12.011 (assumption of carbon)
- HC = 13.018

On the basis of this, it became evident that the reported value for HC of 0.01385 was inconsistent with the other values. Similarly, the use of the reported value led to negative values of CO_2 production, prior to the minimum value of 0 being applied. Substituting a value of 1.8 for a_{CO2} yields a value of 13.825 for the molar mass for petrol powered vehicles.

7.6 Resulting Model Predictions

Based on the model formulation presented above, Figure 7.3 contains the predicted quantum of emission outputs as a function of vehicle speed. This is based on the vehicle parameters presented in Appendix A for a medium passenger car and steady speed conditions.

The U-shape is highly correlated to the fuel consumption trends (refer to Figure 2.6) as would be expected given the format of the equations to predict the vehicle emissions.

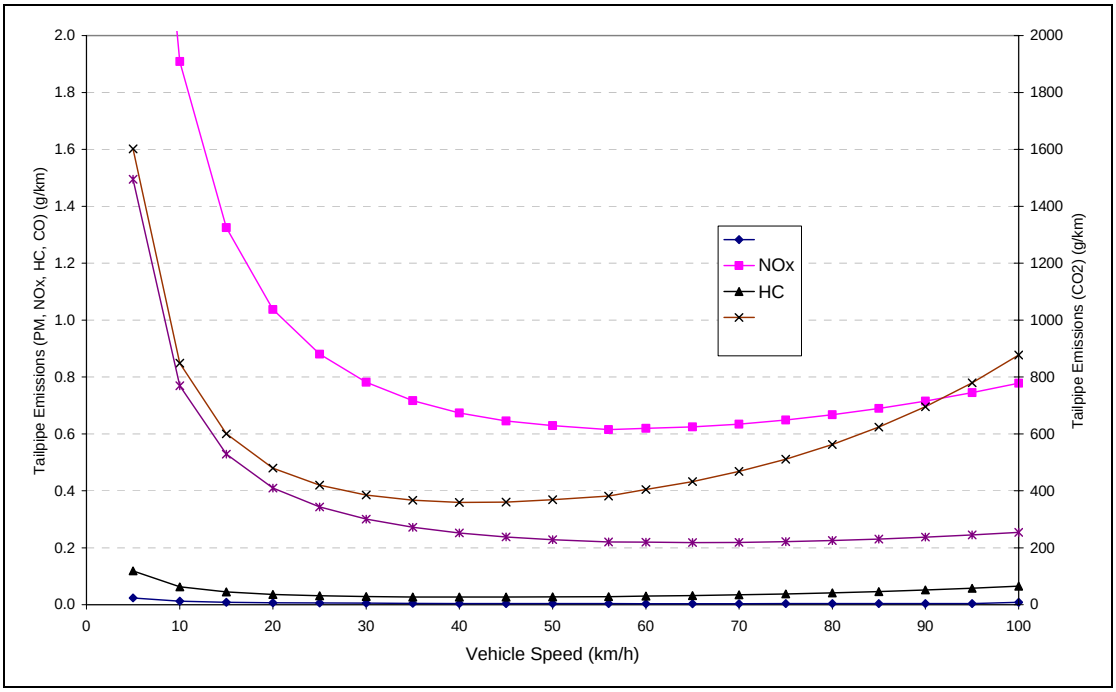

Figure 7.3: Predictions of Vehicle Emissions With Vehicle Speed

7.7 Summary and Conclusions

This chapter has presented the results of the investigation into vehicle emission modelling. A framework has been established that firstly models the emissions leaving the engine, then accounts for the impact of catalytic converts. Generically the prediction of vehicle emissions within this report utilises the following relationship:

$$TPE_i = EOE_i \, CPF_i \tag{7.13}$$

EOE_i is based on the emission under consideration as given below:

HC $$EOE_{HC} = a_{HC} FC + \frac{r_{HC}}{V} 1000 \tag{7.14}$$

CO $$EOE_{CO} = a_{CO} FC \tag{7.15}$$

NOx $$EOE_{NOx} = \max\left[a_{NOx} \left(FC - \frac{FR_{NOx}}{V} 1000 \right), 0 \right] \tag{7.16}$$

SO_2 $$EOE_{SO_2} = 2 a_{SO_2} FC \tag{7.17}$$

Pb $$EOE_{Pb} = Prop\_Pb\, a_{Pb}\, FC \quad (7.18)$$

PM $$EOE_{PM} = a_{PM}\, FC + \frac{r_{PM}}{V} 1000 \quad (7.19)$$

The catalytic pass fraction is given by:

$$CPF_i = \left[1 - \varepsilon_i \exp\left(-b_i\, IFC\, DensFuel\right)\right] \min\left[\left(1 + \frac{r_i}{100} AGE\right), MDF_i\right] \quad (7.20)$$

CO_2 is predicted based on the assumption of carbon balance utilising the following relationship:

$$TPE_{CO_2} = \max\left[44.011\left(\frac{FC}{12.011 + 1.008\, a_{CO2}} - \frac{TPE_{CO}}{28.011} - \frac{TPE_{HC}}{12.011 + 1.008\, a_{CO2}} - \frac{TPE_{PM}}{12.011}\right), 0\right] \quad (7.21)$$

Parameter values for the 16 default HDM-4 vehicles for the above equations are given in Table 7.5 and Table 7.6.

The density of fuel (DensFuel) may be taken as (Heywood, 1988):

- petrol: DensFuel = 0.75 g/mL
- diesel: DensFuel = 0.86 g/mL

Table 7.5: Default Emission Model Parameter Values for HDM-4 Representative Vehicle Classes

HDM-4 Vehicle	Fuel Type	HC		NOx		CO	SO_2	Pb		PM		CO_2
		a_{HC}	r_{HC}	a_{NOx}	FR_{NOx}	a_{CO}	a_{SO2}	Prop_Pb	a_{Pb}	a_{PM}	b_{PM}	a_{CO2}
MC	P	0.060	0	0.020	0.00	0.20	0.0005	0.75	0	0.0001	0.0	1.8
PC-S	P	0.012	0	0.055	0.17	0.10	0.0005	0.75	0	0.0001	0.0	1.8
PC-M	P	0.012	0	0.055	0.17	0.10	0.0005	0.75	0	0.0001	0.0	1.8
PC-L	P	0.012	0	0.055	0.17	0.10	0.0005	0.75	0	0.0001	0.0	1.8
LDV	P	0.012	0	0.055	0.17	0.10	0.0005	0.75	0	0.0001	0.0	1.8
LGV	P	0.012	0	0.055	0.17	0.10	0.0005	0.75	0	0.0001	0.0	1.8
4WD	D	0.040	0	0.027	0.00	0.08	0.005	0.75	0	0.0032	0.0	2.0
LT	D	0.040	0	0.027	0.00	0.08	0.005	0.75	0	0.0032	0.0	2.0
MT	D	0.040	0	0.027	0.00	0.08	0.005	0.75	0	0.0032	0.0	2.0
HT	D	0.040	0	0.027	0.00	0.08	0.005	0.75	0	0.0032	0.0	2.0
AT	D	0.040	0	0.027	0.00	0.08	0.005	0.75	0	0.0032	0.0	2.0
MNB	P	0.012	0	0.055	0.17	0.10	0.0005	0.75	0	0.0001	0.0	1.8
LB	D	0.040	0	0.027	0.00	0.08	0.005	0.75	0	0.0032	0.0	2.0
MB	D	0.040	0	0.027	0.00	0.08	0.005	0.75	0	0.0032	0.0	2.0
HB	D	0.040	0	0.027	0.00	0.08	0.005	0.75	0	0.0032	0.0	2.0
COACH	D	0.040	0	0.027	0.00	0.08	0.005	0.75	0	0.0032	0.0	2.0

Source: Base data from An et al (1997), ETSU (1997) and SNRA (1995)

Table 7.6: Default Emission Model Parameter Values for HDM-4 Representative Vehicle Classes

HDM-4 Vehicle	Fuel Type	HC			NOx			CO			SO_2			Pb			Particulates		
		ε_i	b_i	r_i	ε_i	b_i	r_i	ε_i	b_i	r_i	ε_i	b_i	r_i	ε_i	b_i	r_i	ε_i	b_i	r_i
MC	P	0	0	0	0	0	0	0	0	0	0	0	0	0	0	0	0	0	0
PC-S	P	0.999	0.03	20	0.812	0	11	0.999	0.05	4.8	0	0	0	0	0	0	0	0	4.8
PC-M	P	0.999	0.03	20	0.812	0	11	0.999	0.05	4.8	0	0	0	0	0	0	0	0	4.8
PC-L	P	0.999	0.03	20	0.812	0	11	0.999	0.05	4.8	0	0	0	0	0	0	0	0	4.8
LDV	P	0.999	0.03	20	0.812	0	11	0.999	0.05	4.8	0	0	0	0	0	0	0	0	4.8
LGV	P	0.999	0.03	20	0.812	0	11	0.999	0.05	4.8	0	0	0	0	0	0	0	0	4.8
4WD	D	0.900	0.00	20	0.250	0	11	0.900	0.00	4.8	0	0	0	0	0	0	0.5	0	4.8
LT	D	0.900	0.00	20	0.250	0	11	0.900	0.00	4.8	0	0	0	0	0	0	0.5	0	4.8
MT	D	0.900	0.00	20	0.250	0	11	0.900	0.00	4.8	0	0	0	0	0	0	0.5	0	4.8
HT	D	0.900	0.00	20	0.250	0	11	0.900	0.00	4.8	0	0	0	0	0	0	0.5	0	4.8
AT	D	0.900	0.00	20	0.250	0	11	0.900	0.00	4.8	0	0	0	0	0	0	0.5	0	4.8
MiniBus	P	0.999	0.03	20	0.812	0	11	0.999	0.05	4.8	0	0	0	0	0	0	0	0	4.8
LB	D	0.900	0.00	20	0.250	0	11	0.900	0.00	4.8	0	0	0	0	0	0	0.5	0	4.8
MB	D	0.900	0.00	20	0.250	0	11	0.900	0.00	4.8	0	0	0	0	0	0	0.5	0	4.8
HB	D	0.900	0.00	20	0.250	0	11	0.900	0.00	4.8	0	0	0	0	0	0	0.5	0	4.8
COACH	D	0.900	0.00	20	0.250	0	11	0.900	0.00	4.8	0	0	0	0	0	0	0.5	0	4.8

Source: Base data from An, et al (1997), Clean Cat (2000), Discount Converters Ltd (2000), Hammarstrom (1999) and SNRA (1995)

8 TESTING OF PREDICTIONS

8.1 Introduction

This chapter presents the results of two studies undertaken to test the predictions of this research. The first study provides an indication as to the overall impact of the study on a section of the Auckland motorway system. The second study compares the outputs to an independently sourced data set, also collected on the Auckland motorway system.

8.2 24-Hour Impact Predictions

8.2.1 Introduction

This section presents a study of a section of the Auckland motorway network with the aim of estimating the significance of the findings of the research. The site under examination is a section of six-lane motorway (3 lanes each direction) with a 24-hour traffic flow profile as indicated in Figure 8.1, indicating a total traffic at the site of around 140,000 vehs/day. The associated speed profile recorded at the site is presented in Figure 8.2. The data in Figure 8.1 and Figure 8.2 are recorded from induction loop counters imbedded into the road, with data supplied courtesy of Transit New Zealand.

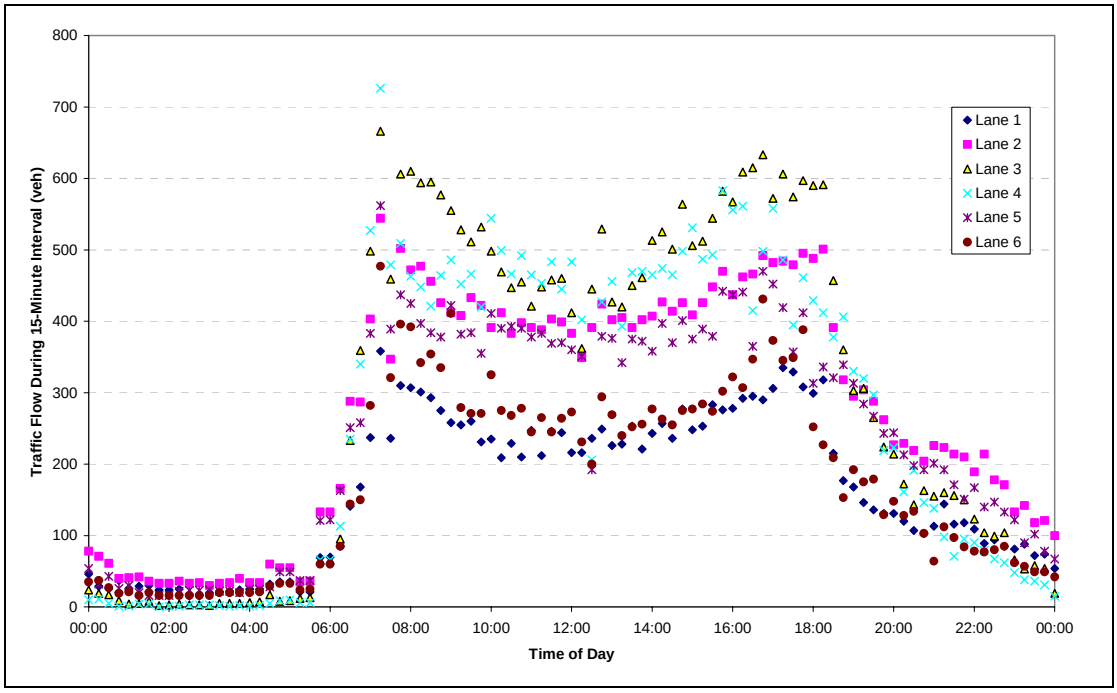

Figure 8.1: Distribution of Traffic

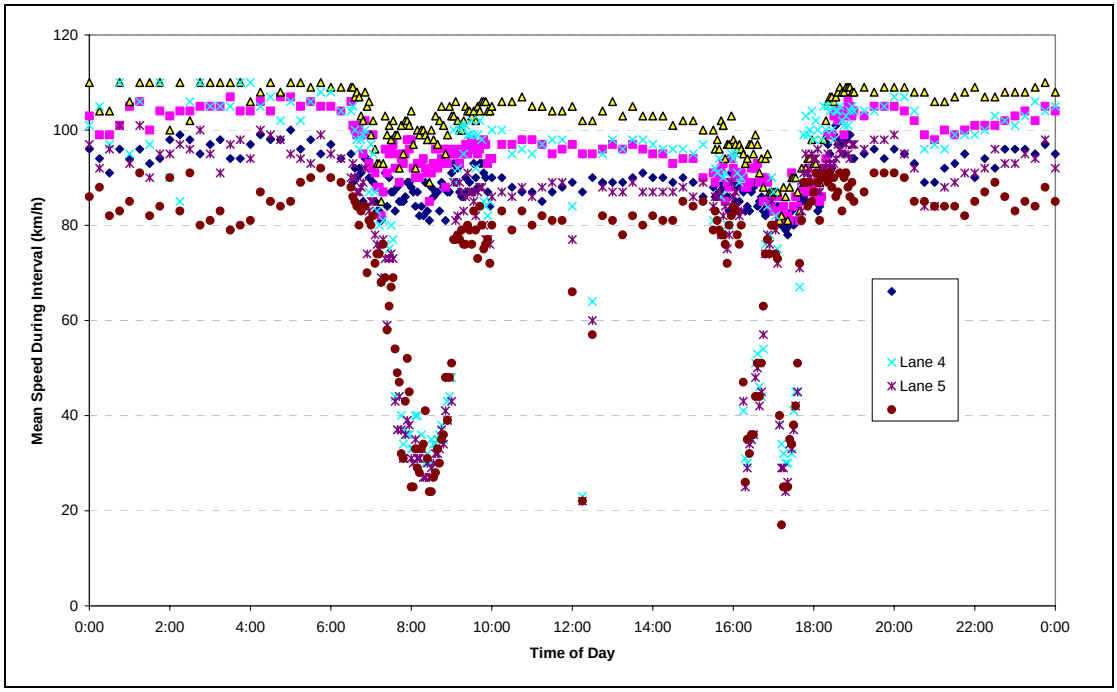

Figure 8.2: Measured Traffic Stream Speed-Time Profile

8.2.2 Methodology

The methodology adopted to test the significance of the findings is to analyse each 15-minute interval using the results of this research to estimate the additional fuel consumed and vehicle emissions, in comparison to a base case of steady speed travel. Each lane is analysed separately, with the results then combined to provide for the total impacts in terms of fuel consumption and vehicle emissions.

For the purpose of this testing, an assumption of all vehicles being medium sized passenger cars has been made, with the appropriate parameter values given in Appendix A. As heavy vehicles are more heavily influenced by traffic congestion, this assumption results in an under-estimate of the congestion impacts.

For each 15-minute interval, the volume to capacity ratio was calculated for each lane. The capacity for each lane was assumed to be equal to the maximum 15-minute value recorded throughout the day, which equated to 2200 veh/hr (550 veh/15-min). The resulting volume to capacity ratio and mean speed were then used to return the value of DFUEL for the current lane and time period.

The recommended default natural acceleration noise value of 0.1 m/s^2 was applied, as was a maximum total acceleration noise value of 0.6 m/s^2. These values also compare favourably to the values reported by EFRU (1997) such that the comparison in Section 8.3 is valid.

The values of DFUEL were estimated by running the simulation program ACCFUEL, with default parameters for a medium passenger car (refer to Appendix A). The output of ACCFUEL is only the increment of fuel consumption. For use with the vehicle emission model, it was necessary to also know the total fuel consumption. To achieve this, the increment of fuel consumption (DFUEL value) was multiplied by

the steady speed fuel consumption values for the same simulated vehicle characteristics.
As noted in Section 5.6, the output from the ACCFUEL program is a matrix of DFUEL values for discrete speed and acceleration noise values. For the purpose of this prediction test, no interpolation between values was undertaken. Instead the result chosen was that which was closest to the required speed and acceleration noise values. This simplification would not have a significant impact on the results over the 24-hour period.

For each 15-minute period, the total fuel consumption and vehicle emissions for both congested and un-congested conditions were calculated. Both the outputs per vehicle and the outputs per 15-minute period were calculated. These data sets were then utilised to calculate the increase in outputs as a result of traffic congestion.

The calculations have been completed in a large spreadsheet, with one sheet for the congested and one sheet for the steady speed conditions. With the 15-minute periods and 6-lanes, a total of 576 rows of calculations were required to analyse the total system for the 24-hour period.

8.2.3 Results

Table 8.1 illustrates the impact of congestion on the various emissions being modelled for a medium passenger car. While carbon monoxide and hydrocarbons have increased at a rate almost twice the predicted increase in fuel consumption, the other emissions have all undergone an increase about the same as that of the fuel consumption.

Table 8.1: Predicted Impact of Congestion on Vehicle Emissions

Pollutant	Percentage Increase		
	Minimum of 15-minute periods	**24-hour Average**	**Maximum of 15-minute periods**
Carbon monoxide – CO	+2%	+25%	+36%
Carbon dioxide - CO_2	+1%	+12%	+17%
Hydro carbons – HC	+2%	+25%	+36%
Oxides of nitrogen – NOx	+2%	+15%	+25%
Particulate matter – PM	+1%	+12%	+17%
Fuel consumption – FC	+1%	+13%	+17%

Based on the above methodology, the impact of the traffic congestion produces an overall 13 per cent increase in fuel consumption when compared with an assumption of steady speed driving over a 24-hour period. Individual 15-minute time periods have additional fuel consumption ranging in value from 1 to 17 per cent, with the lowest increase being during the low flow periods of the early morning hours and the high values during the peak periods of congestion.

Similarly, the vehicle emission models (refer to Chapter 7) were utilised to estimate the impact of the congestion on the various emission outputs, with 24-hour average increases between 12 and 25 per cent. All values are based on the parameter values given in Appendix A for a medium sized passenger car.

8.2.4 Conclusions

This study has estimated the additional fuel consumption and vehicle emissions for a medium sized passenger car, utilising the procedures presented in this thesis. Based on the traffic flow data extracted from loops on the Auckland motorway network, increases in all outputs (fuel and emissions) in the range of 12 to 25 per cent were predicted over a 24-hour period.

These fuel consumption and emission increases relate to the impact of applying acceleration noise impacts to the observed mean speeds and flow rates summarised at 15-minute intervals on the Auckland motorway system. It does not compare the impact of travelling under free flow conditions at 100 km/h with no acceleration noise, against the observed speed-time and flow-time profiles (i.e. changes in mean speed) and acceleration noise levels.

8.3 Comparison with Independent Data Set

8.3.1 Introduction

Data were sourced from the EFRU (1997) to compare the predictions of the methodology to an independent data set. The EFRU (1997) report contains data for a range of driving conditions including steady speed at 30 and 50km/h, and motorway free flow, interrupted flow and congested conditions, and for a total of 23 vehicles.

8.3.2 Methodology

The data were collected as follows (EFRU, 1997):

- Vehicle speed-time profile data were collected during test runs on the Auckland motorway network[17] using an instrumented vehicle under free flow, interrupted and congested conditions
- Fuel consumption and vehicle emission data were then collected for 23 vehicles during measurements on a chassis dynamometer using the representative vehicle speed-time profiles and at steady state speeds of 30km/h and 50 km/h.

Table 8.2 contains the resulting data from the above process for the 30km/h steady speed and the congested motorway run. The congested motorway run resulted in a mean speed of 32.9km/h and it is therefore considered that the difference in outputs (fuel and emissions) is an indication of the acceleration noise impacts and not speed change differences. Furthermore, the speeds of 30 km/h are a close match to the minimum speeds observed in Figure 8.2. The acceleration noise level of the congested run is 0.66 m/s², which further supports the comparison of numbers, given the assumed value of 0.6 m/s² in the ACCFUEL model.

Only the seven post 1990 vehicles reported by EFRU (1997) were selected for this comparison, as these are considered to best represent the attributes of the modelled medium passenger car (refer to Appendix A).

[17] Test runs were also completed on urban roads, suburban roads and rural state highways. However for the purpose of this comparison test, only the motorway data have been used.

Table 8.2: Pollutant Output Measurements

Model of Car	Pollutant	30km/h Steady Speed Driving	Congested driving	Percentage Change
Ford Falcon EF 4.0 Cat	CO	0.39	5.3	+1259%
	CO_2	195.2	285.3	+46%
	HC	0.16	0.19	+19%
	NOx	0.26	0.78	+200%
	FC	8.12	12.17	+50%
Toyota Corona ST 191 2.0i '94	CO	0.93	3.77	+305%
	CO_2	149.2	186.14	+25%
	HC	0.49	1.16	+137%
	NOx	0.46	1.47	+220%
	FC	6.29	8.09	+29%
Holden Vectra 2.0i Cat '96	CO	0.04	0.12	+200%
	CO_2	131.12	193.22	+47%
	HC	0.04	0.09	+125%
	NOx	0.01	0.06	+500%
	FC	5.43	8.01	+48%
Ford Festiva 1.3EFI '95	CO	3.36	5.03	+50%
	CO_2	112.74	141.2	+25%
	HC	0.74	1.3	+76%
	NOx	0.5	1.24	+148%
	FC	4.98	6.34	+27%
Mazda Familia 1.5 TRI '92	CO	1.01	11.64	+1052%
	CO_2	143.45	187.13	+30%
	HC	0.22	0.61	+177%
	NOx	0.13	0.52	+300%
	FC	6.03	8.57	+42%
Mazda Familia 1.5 MPI '94	CO	0.17	1.79	+953%
	CO_2	143.47	190.41	+33%
	HC	0.07	0.16	+129%
	NOx	0.01	0.08	+700%
	FC	5.95	8.01	+35%
Toyota Corona 2.0i '92	CO	1.44	7.85	+445%
	CO_2	163.32	187.11	+15%
	HC	0.68	0.99	+46%
	NOx	0.7	1.47	+110%
	FC	6.94	8.38	+21%
Averaged Results	CO	1.0	5.1	+384%
	CO_2	148.4	195.8	+32%
	HC	0.3	0.6	+88%
	NOx	0.3	0.8	+171%
	FC	6.2	8.5	+36%

CO=carbon monoxide (g/km), CO_2=carbon dioxide (g/km),
HC=hydrocarbons (g/km), NOx = oxides of nitrogen (g/km),
FC= fuel consumption (L/100km)
Steady speed: Average Speed = 30 km/h, Acceleration Noise = 0 m/s²
Congested: Average Speed = 32.9 km/h, Acceleration Noise = 0.66 m/s²
Source: EFRU (1997). Note only post-1990 vehicles included in above analysis.

As can be seen in Table 8.2, there was a wide range of impacts measured resulting from congested conditions, which in part represents the values under which the vehicle manufacturers have optimised their designs. Additionally, in many cases the denominators (that is the steady speed emissions) are very small, consequently any change in output represents a major percentage change.

8.3.3 Results

Table 8.3 summarises the results from Table 8.2, and aligns the results with the maximum impact results from Table 8.1. The comparison illustrates a good trend in the correlation for the production of CO_2, HC and fuel consumption, albeit that the predicted increase is only some 50 per cent of that observed by the EFRU (1997). The predictions for CO and NOx are low in comparison with the results provided by the selected vehicles observed by EFRU (1997).

Table 8.3: Summary of Results (percentage change)

Emission	EFRU (1997) Results For 7 Selected Vehicles			Predicted Impact
	Min	Max	Average	
CO	+50%	+1259%	+384%	+36%
CO_2	+15%	+47%	+32%	+17%
HC	+19%	+177%	+88%	+36%
NOx	+110%	+700%	+171%	+25%
FC	+21%	+50%	+36%	+17%

Note: Predicted impact deemed to equate to maximum of 15-min interval results
Only the 7 post 1990 vehicles from EFRU (1997) included in comparison

To check the predictions, it was considered necessary to also compare the absolute predictions, rather than just the percentage increases. The results of this for the steady speed mode of driving are displayed in Table 8.4. The table indicates that the quantum of all outputs apart from HC, are within the observed range for the seven vehicles tested.

Table 8.4: Summary of Results (absolute values)

Emission	EFRU (1997) Steady Speed Results For 7 Selected Vehicles		Predicted Values
	Min	Max	
CO (g/km)	0.04	3.36	0.08
CO_2 (g/km)	112.74	195.20	159.8
HC (g/km)	0.04	0.74	0.01
NOx (g/km)	0.01	0.70	0.24
FC (L/100km)	4.98	8.12	5.8

8.3.4 Conclusions

When comparing the estimated impact of congestion to that independently sourced for a range of vehicles, the values showed an acceptable level of agreement for fuel consumption, hydrocarbons and carbon dioxide production, albeit that the predictions are at the lower end of the observed values. The results in Table 8.4 indicate that the under-prediction observed in Table 8.3 is primarily a function of the under-estimation of the impacts of congestion, as the steady speed results are of an appropriate value.

It is well established (Heywood, 1988) that oxides of nitrogen, hydrocarbons and carbon monoxide emissions are strongly affected by rich operation conditions of the engine. The previously stated inability to model rich operating conditions in the current fuel model is a significant factor in the comparison of the predicted versus observed production of the emissions.

8.4 Summary

This chapter has presented the results of an application of the theory to a practical situation using measured speed-flow data on a section of motorway. Additionally, a comparison of the results to fuel consumption and vehicle emission data collected outside of this study, has been completed.

The 24-hour predictions indicated that fuel consumption and emissions would increase between 13 to 25 per cent, when compared against steady speed driving conditions.

The research results of the new modelling approach for emissions have been tested against an existing data set of seven vehicles sourced from independent research on Auckland's motorways. Vehicle emissions of carbon dioxide and hydrocarbons were under predicted by some 50 per cent in relation to the average tested vehicle, but were still well within the range of the seven observed results. Carbon monoxide and oxides of nitrogen were grossly under predicted and were below the minimum observed values.

9 SUMMARY

9.1 Introduction

The analysis of the impact of traffic congestion has traditionally been confined to the use of either simple speed-flow relationships or highly complex micro-simulation techniques. This research project has presented a methodology for assessing the impact of traffic congestion in the middle ground between these two extremes, with a methodology that gives improved predictions over the speed-flow approach, yet does not require the intensive inputs of the micro-simulation techniques.

The research goal, objective and intended use was stated in Section 1.2 as:

> *The intended use of the results of the research is for the evaluation of highway projects. Consequently, the model is not intended to be either a highly sophisticated traffic micro simulation model, nor is it intended to develop an engine performance model that could be used in vehicle design. Rather it is the middle ground between these detailed requirements and traditionally simple steady speed models that this research is targeting.*
>
> *The goal of the research is to develop fuel consumption and vehicle emission models that can estimate the impacts of traffic congestion for highway evaluation better than traditional assumptions of steady speed travel models.*
>
> *The objective is to have a model that significantly improves the predictive capability in comparison with current models, yet does not require the significant and detailed modelling associated with micro-simulation models.*
>
> *The focus is to accurately model mid-block congestion that occurs in uninterrupted conditions, and results in a series of stop/go waves (or similar speed change cycles). Interrupted flow, such as that which occurs at traffic signals or at other times where drivers make deliberate speed changes are not the focus of this work.*

It is concluded that overall the research project has been successful in achieving the goals and objectives stated above, in particular providing a method of estimating the marginal cost of congestion on fuel consumption and vehicle emissions.

The method presented first predicts the impact of congestion on driving style and from this, to the impacts on fuel consumption and vehicle emissions. The resulting model has been tested against field data collected in Thailand and New Zealand, and illustrates a good level of predictive ability.

The remainder of this chapter firstly presents a summary of the main conclusions from each chapter of the thesis, then provides an overview of the final methodology and an indication of the level of certainty in each step.

9.2 Summary of Research

Introduction (Chapter 1)

The context of the modelling approach was to formulate a model that could give reliable estimates of the impact of traffic congestion on fuel consumption and vehicle emissions, without the need for micro-simulation modelling of the traffic stream.

The work has been based on research undertaken in Malaysia, Thailand and New Zealand, with a primary focus on the passenger car owing to its dominance of the vehicle stream during periods of high congestion.

Background and Literature Review (Chapter 2)

The literature review established that while there were methods for examining traffic congestion at either end of the modelling spectrum (microscopic or macroscopic), there were not models available that reliably predicted congestion impacts at the middle level.

Speed-flow models were reviewed, with the HDM-4 three-zone model adopted for use when needed.

The discussion on vehicle headways and gaps between vehicles illustrated the difficulty in measurement of these parameters. It was noted that the gap between vehicles was expected to have a significant impact on the acceleration/deceleration behaviour of drivers.

A review of available fuel consumption models was completed, with the ARFCOM (Biggs, 1988) approach identified as the appropriate base to work from. This model was considered to offer the best potential for the modelling of congested conditions.

Various measures of unsteadiness were examined for the purpose of describing the driving conditions on a section of road. In light of those examined, the standard deviation of accelerations (acceleration noise) was deemed to be that which provided the best all round solution. The approach adopted was based on that utilised by Bester (1981).

Vehicle emission modelling was reviewed in the context of the research work presented in this thesis, with a focus on models that linked into the fuel consumption modelling work being proposed. The impact of various factors on vehicle emissions was reviewed.

The chapter also looked at the issue of representative vehicles for the purpose of modelling the vehicle fleet. It was concluded that the use of representative vehicles as opposed to “average” vehicles, was the better approach to take.

Theory of Acceleration Noise (Chapter 3)

The impact of the period of time measure was examined, with the conclusion that a 1-second interval was appropriate for the calculation of acceleration noise. This being a value that provided sufficient detail to model the vehicle performance, but was still readily collectable in the field.

Models for relating acceleration noise to traffic flow were presented, along with a discussion on the required accuracy of measurements.

The distribution of the acceleration noise values was reviewed, with the conclusion that although not technically Normally Distributed, that the approximation was sufficient for the purposes of this research.

Data Collection Systems (Chapter 4)
Based on the need to collect detailed vehicle performance parameters (vehicle speed, fuel consumption and engine speed) at 1-second intervals, it was decided to utilise an established data collection system called ROMDAS. This system enabled all sensors to be interfaced directly to a laptop computer for automatic recording of data.

Various means of collecting traffic stream data (flow rates and speeds) were employed depending on the location and facilities available. These included the use of pneumatic tube counters, manual surveys and induction loop systems.

Fuel consumption was measured by recording the electronic pulse of the wire controlling the opening and closing of the fuel injectors. This method was utilised as it measured directly the fuel entering the engine, without interfering with the engine performance.

This section also presented details on the setup and calibration of the system. Calibration included the bench marking of the fuel meter against traditional inline gauges through the use of a chassis dynamometer. This calibration indicated a function unique to each test vehicle.

Acceleration Noise (Chapter 5)
Acceleration noise data were collected in three countries; Malaysia, Thailand and New Zealand. The Thailand study had the greatest quantity of data available for analysis and model development, with the other two studies used primarily to confirm the transportability of the results generated.

The results of the three studies confirmed that acceleration noise levels under congested conditions were very similar regardless of the location where they were collected. Indications of a power to weight ratio impact on the acceleration noise level were noted, but insufficient data were available to confirm the magnitude or relationships involved (refer to Section 10.2).

The New Zealand data were also examined to identify the impact of vehicle size on following distance, with the expected trend that the larger the vehicle in front, the larger the gap left being confirmed.

An attempt was made to analyse the impact of the following distance on acceleration noise. This phase of the research did not progress, as it was not central to the research and a reliable means to collect the data without influencing the results was not readily available (refer to Section 10.2).

A traffic simulation program (ACCFUEL) was developed to apply the results. This used Monte Carlo simulation techniques to model a number of vehicles travelling along a section of road over a range of speeds and acceleration noise values. The output from the program is a table of DFUEL values. DFUEL is the proportional increase in fuel consumption caused by acceleration noise.

Fuel Consumption Modelling (Chapter 6)
The fuel consumption model employed in the research directly models the forces on the vehicle and accordingly, methods were presented to predict the total forces opposing motion.

The impact of the inertial resistance resulted in the need to perform a Monte Carlo simulation to predict driver gear selection and from this the inertial mass and engine speed for any given road speed. This program provided reasonable results when compared with on-road data.

A modified version of the ARFCOM (Biggs, 1988) fuel consumption model was decided upon as the basis for predicting the fuel consumption once all the forces opposing motion had been calculated. This model directly accounts for the need of tractive power, engine drag and the power-to-drive vehicle accessories.

The ability of many modern vehicles to operate under zero fuel consumption when in deceleration mode required the modification of expressions to ensure that the resulting calculations did not over estimate the quantity of fuel consumed during heavily congested periods.

The resulting fuel consumption model was tested against data collected from on-road drive cycles and was found to predict total fuel consumed almost exactly (within 0.25 per cent) of observed values for a known drive cycle (i.e. in the absence of the need to predict the acceleration noise level).

Similar examination of the ability to predict the resulting increase in fuel consumed from congestion impacts indicated a lower level of confidence (an under-prediction of some 25 per cent when compared to observed values). It is hypothesised that the underlying assumption that the acceleration data follows a Normal Distribution is the primary cause of this lower level of agreement. This is especially so for the shorter duration test runs wherein the data were observed to be both skewed and have a level of kurtosis. Further work in this area is suggested (refer to Section 10.2).

Vehicle Emission Modelling (Chapter 7)
A two-part methodology for the prediction of vehicle emissions was implemented, whereby firstly the engine out emissions were predicted, then the impact of catalytic converters was accounted for. Predictive models for hydrocarbons, carbon monoxide, oxides of nitrogen, sulphur dioxide, lead, particulate matter and carbon dioxide were presented. The basis of the approach is that presented by An et al. (1997).

The inability of the fuel consumption model adopted to identify periods of rich operating conditions was acknowledged as a problem in the prediction of emissions, as different relationships between emissions and fuel exist when operating under a non-stoichiometric condition.

Testing of Predictions (Chapter 8)
A two-phase test of the predictions presented was undertaken. Firstly, the models were used to estimate the impact of non-steady speed driving over a 24-hour period. This was followed by a comparison of independently sourced data to the model predictions.

The research results of the new modelling approach for emissions have also been tested against an existing data set of seven vehicles sourced from independent research on Auckland's motorways. Vehicle emissions of carbon dioxide and hydrocarbons were under-predicted by some 50 per cent in relation to the average tested vehicle, but were still well within the range of the seven observed results. Carbon monoxide and oxides of nitrogen were grossly under-predicted and were below the minimum observed values.

The research results of the new modelling approach have been applied to a section of the Auckland motorway system and indicate that the 24-hour predictions for fuel consumption and emissions would increase between 13 to 25 per cent, when compared against steady speed driving conditions.

The modelling framework, even with the above limitations, still has wide application in the prediction of highway performance. The patterns of fuel consumption and emissions are showing the appropriate changes in relation to traffic congestion, and therefore further calibration is required. Furthermore, the modelling framework developed readily lends itself to enhancement via adoption of some new sub-models.

9.3 Modelling Process and Estimated Level of Certainty

Figure 1.1 illustrated the overall concept of the research project. Figure 9.1 summarises this process and for each stage indicates the estimated relative level of certainty in the results, in addition to indicating which portion of the research deals with each step of the process.

Those areas that are identified as having a lower level of certainty are also those areas identified as potential areas of further research (refer to Section 10.2).

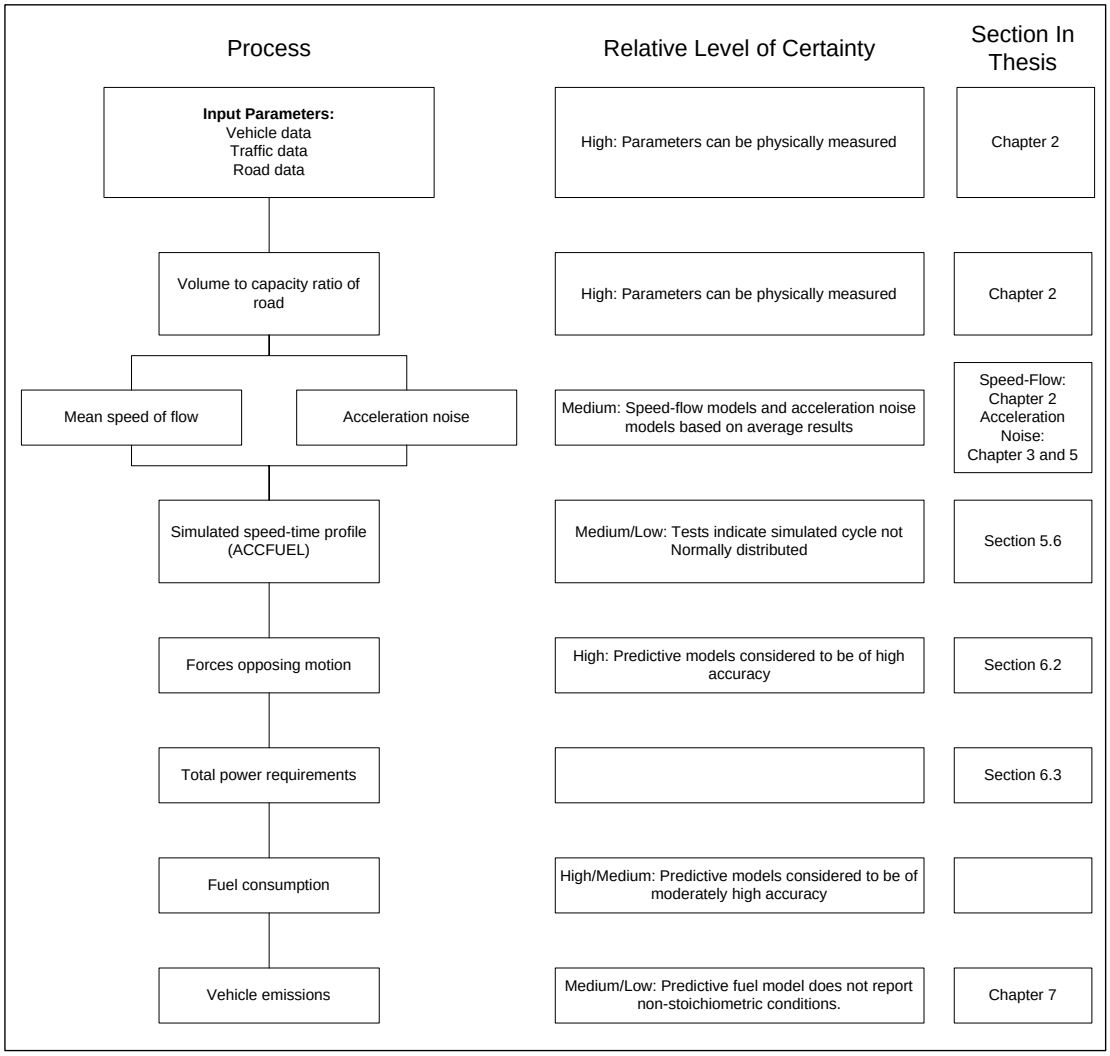

Figure 9.1: Summary of Process and Relative Levels of Certainty

10 CONCLUSIONS AND AREAS OF POTENTIAL FURTHER RESEARCH

10.1 Main Conclusions

The main conclusions of this research are:

- A methodology has been developed that models the effects of traffic congestion on fuel consumption and vehicle emissions, without the need for micro-simulation
- The methodology yields better results than traditional steady speed assumption models
- The methodology makes use of traditionally available data
- Parameter values for acceleration noise have been shown to be consistent in three countries and against independent measurements
- The methodology enables the estimation of the marginal costs of congestion on fuel consumption and vehicle emissions
- Fuel consumption predictions were found to be within 25 per cent of observed results when including the generation of a drive cycle, and within 0.25 per cent for a known drive cycle.
- Vehicle emission predictions were tested against independently sourced data for seven vehicles. Predicted emissions of carbon dioxide and hydrocarbons were within the observed range of values, while carbon monoxide and oxides of nitrogen were both grossly under predicted
- Applying the methodology to petrol powered vehicles for a section of the Auckland motorway system over a 24-hour period has indicated incremental fuel consumption and vehicle emission increases of between 12 and 25 per cent when compared with steady speed modelling.
- The research has been able to successfully link the traffic stream speed-flow effects with the vehicle dynamics of congestion

In addition to the above main conclusions, the following conclusions were made in the course of the research:

- The methodology utilises acceleration noise as a measure of congestion impacts
- Recording in-vehicle data at 1-second intervals was found to be practical and appropriate
- The acceleration data is assumed to be Normally Distributed, but data collected indicates that the data is skewed, with higher levels of deceleration than acceleration.

- The methodology has adapted established fuel consumption and vehicle emission models

- The emissions modelling is limited to stoichiometric conditions of engine operation, resulting in a less reliable estimation during periods of high acceleration and deceleration

The results have been incorporated into HDM-4 and other international road evaluation procedures.

10.2 Areas of Potential Further Research

The following issues were identified as areas of potential further research, but not progressed within this study:

- Relationship between acceleration noise and following distance

- Impact of vehicle power to weight ratio on acceleration noise

- Distribution of acceleration noise

- Fuel consumption and vehicle emission modelling under high accelerations when rich operating conditions occur

- Improved models for predicting oxides of nitrogen, with the use of models that do not directly relate to fuel consumption being a strong possibility

These areas were not refined further within this research as they were either seen as not been central to the focus of the project, or the increased level of detail was not considered warranted for the type of modelling framework desired from this research. These potential areas of future research are discussed further next.

Acceleration Noise Versus Following Distance

There is good justification to suspect that following distance would have a significant impact on acceleration noise. However, as discussed in Section 5.5, such an analysis has not been completed to date owing to the lack of data collection techniques that would support the formation of such a model framework.

There is also some reservation over the usefulness of such a model if it were formulated. How the results would be applied, without the use of a micro-simulation model would need to be considered.

Data collection indicated that there is a relationship between the following distance and vehicle size, which could possibly be utilised to estimate the impact of vehicle size on acceleration noise. This would require the use of a localised vehicle flow (i.e. that observed by the following vehicle) rather than the aggregated traffic stream vehicle speed-flow.

Power to Weight Ratio Impact on Acceleration Noise
From the Malaysian study, there is some evidence that the power to weight ratio has an impact on the acceleration noise value obtained. This certainly makes logical sense, wherein vehicles with a low power to weight ratio will usually have very little available power to create high accelerations (thereby yielding a lower acceleration noise). It is hypothesised that in addition to the reduction of the acceleration noise value as a result of decreased available power, the distribution of the acceleration noise may also become more skewed towards the deceleration end of the spectrum.

Distribution of Acceleration Noise
There is evidence that the distribution of accelerations is not truly Normal and that this is having an impact on the ability of the simulation program ACCFUEL to accurately replicate the true cost of congestion. With the methodology employed in this research and the associated ACCFUEL simulation program, the ability to incorporate a modified distribution is possible, without a rework of all other components of the congestion prediction model.

Fuel Consumption Model and Rich Operating Conditions
The fuel consumption model is based on the assumption of stoichiometric operating conditions and does not have the ability to output the fuel/air ratio, such that simplifications to the vehicle emissions models were required. Under heavy engine loading, such as high accelerations, there is the potential for rich operating conditions to occur.

Improved Emission Models
The production of oxides of nitrogen is only weakly correlated to fuel consumption and consequently to dramatically improve the predictions will require a new form of emission model to be implemented for this pollutant. Such a task should follow on from that above in case the introduction of an enhanced fuel consumption model (including rich operating conditions) can result in improved predictions of emissions within the current framework.

11 APPENDICES

11.1 Appendix A - Vehicle Characteristics

This appendix contains the vehicle characteristics utilised within this research but not defined elsewhere in the document. For completeness, it covers the full range of vehicle types as utilised by Bennett and Greenwood (2001) rather than just passenger cars as is the focus of this research.

Table 11.1: Default Vehicle Characteristics

Vehicle Number	Type	Description	Abbrev-iation	Fuel Type	Number of Axles	Number of Wheels	Aero-dynamic Drag Coeff.	CDmult	Projected Frontal Area (m^2)	Operating Weight (t)
1	Motorcycle	Motorcycle or scooter	MC	P	2	2	0.70	1.12	0.8	0.2
2	Small Car	Small passenger cars	PC-S	P	2	4	0.40	1.12	1.8	1.0
3	Medium Car	Medium passenger cars	PC-M	P	2	4	0.42	1.12	1.9	1.2
4	Large Car	Large passenger cars	PC-L	P	2	4	0.45	1.12	2.0	1.4
5	Light Delivery Vehicle	Panel van, utility or pickup truck	LDV	P	2	4	0.50	1.16	2.0	1.5
6	Light Goods Vehicle	Very light truck for carrying goods (4 tyres)	LGV	P	2	4	0.50	1.16	2.8	1.5
7	Four Wheel Drive	Landrover/Jeep type vehicle	4WD	P/D	2	4	0.50	1.16	2.8	1.8
8	Light Truck	Small two-axle rigid truck (approx. < 3.5 t)	LT	D	2	4	0.55	1.19	4.0	2.0
9	Medium Truck	Medium two-axle rigid truck (> 3.5 t)	MT	D	2	6	0.60	1.19	5.0	7.5
10	Heavy Truck	Multi-axle rigid truck	HT	D	3	10	0.70	1.22	8.5	13.0
11	Articulated Truck	Articulated truck or truck with drawbar trailer	AT	D	5	18	0.80	1.38	9.0	28.0
12	Mini-bus	Small bus based on panel van chassis (usually 4 tyres)	MNB	P	2	4	0.50	1.16	2.9	1.5
13	Light Bus	Light bus (approx. < 3.5 t)	LB	D	2	4	0.50	1.19	4.0	2.5
14	Medium Bus	Medium bus (3.5 - 8.0 t)	MB	D	2	6	0.55	1.22	5.0	6.0
15	Heavy Bus	Multi-axle or large two-axle bus	HB	D	3	10	0.65	1.22	6.5	10.0
16	Coach	Large bus designed for long distance travel	COACH	D	3	10	0.65	1.22	6.5	15.0

Source: Greenwood and Bennett (1995a)

Table 11.2: Rolling Resistance Model Parameters

Vehicle Number	Type	Number of Wheels	Wheel Diameter (m^2)	Type of Tyre	CR1	b11	b12	b13
1	Motorcycle	2	0.55	Bias	1.3	20.35	0.1164	0.0793
2	Small Car	4	0.60	Radial	1.0	22.20	0.1067	0.1333
3	Medium Car	4	0.60	Radial	1.0	22.20	0.1067	0.1333
4	Large Car	4	0.66	Radial	1.0	24.42	0.0970	0.1102
5	Light Delivery Vehicle	4	0.70	Radial	1.0	25.90	0.0914	0.0980
6	Light Goods Vehicle	4	0.70	Bias	1.3	25.90	0.0914	0.0980
7	Four Wheel Drive	4	0.70	Bias	1.3	25.90	0.0914	0.0980
8	Light Truck	4	0.80	Bias	1.3	29.60	0.0800	0.0750
9	Medium Truck	6	1.05	Bias	1.3	38.85	0.0610	0.0653
10	Heavy Truck	10	1.05	Bias	1.3	38.85	0.0610	0.1088
11	Articulated Truck	18	1.05	Bias	1.3	38.85	0.0610	0.1959
12	Mini-bus	4	0.70	Radial	1.0	25.90	0.0914	0.0980
13	Light Bus	4	0.80	Bias	1.3	29.60	0.0800	0.0750
14	Medium Bus	6	1.05	Bias	1.3	38.85	0.0610	0.0653
15	Heavy Bus	10	1.05	Bias	1.3	38.85	0.0610	0.1088
16	Coach	10	1.05	Bias	1.3	38.85	0.0610	0.1088

Source: Greenwood and Bennett (1995a)

Table 11.3: Coefficients for Predicting Effective Mass Ratio

Vehicle Number	Type	Effect Mass Ratio Model Coefficients		
		a0	a1	a2
1	Motorcycle	1.10	0	0
2	Small Car	1.14	1.010	399.0
3	Medium Car	1.05	0.213	1260.7
4	Large Car	1.05	0.213	1260.7
5	Light Delivery Vehicle	1.10	0.891	244.2
6	Light Goods Vehicle	1.10	0.891	244.2
7	Four Wheel Drive	1.10	0.891	244.2
8	Light Truck	1.04	0.830	12.4
9	Medium Truck	1.04	0.830	12.4
10	Heavy Truck	1.07	1.910	10.1
11	Articulated Truck	1.07	1.910	10.1
12	Mini-bus	1.10	0.891	244.2
13	Light Bus	1.10	0.891	244.2
14	Medium Bus	1.04	0.830	12.4
15	Heavy Bus	1.04	0.830	12.4
16	Coach	1.04	0.830	12.4

Source: Greenwood and Bennett (1995a)

Table 11.4: Default Fuel Model Parameters

Vehicle Number	Type	Engine Speed Model Parameters				RPMIdle	α	ξb	ehp	Prat	edt	Peng_a0	PctPeng
		a0 RPM	a1 RPM/(km/h)	a2 RPM/(km/h)²	a3 RPM/(km/h)³	rev/min	mL/s	mL/kW/s		kW			%
1	Motorcycle	-162	298.86	-4.6723	-0.0026	800	0.12	0.067	0.25	15	0.95	0.20	80
2	Small Car	1910	-12.311	0.2228	-0.0003	800	0.25	0.067	0.25	60	0.90	0.20	80
3	Medium Car	1910	-12.311	0.2228	-0.0003	800	0.36	0.067	0.25	70	0.90	0.20	80
4	Large Car	1910	-12.311	0.2228	-0.0003	800	0.48	0.067	0.25	90	0.90	0.20	80
5	Light Delivery Vehicle	1910	-12.311	0.2228	-0.0003	800	0.48	0.067	0.25	60	0.90	0.20	80
6	Light Goods Vehicle	2035	-20.036	0.3560	-0.0009	800	0.37	0.067	0.25	55	0.90	0.20	80
7	Four Wheel Drive	2035	-20.036	0.3560	-0.0009	800	0.48	0.057	0.10	60	0.90	0.20	80
8	Light Truck	2035	-20.036	0.3560	-0.0009	500	0.37	0.057	0.10	75	0.86	0.20	80
9	Medium Truck	1926	-32.352	0.7403	-0.0027	500	0.50	0.057	0.10	100	0.86	0.20	80
10	Heavy Truck	1905	-12.988	0.2494	-0.0004	500	0.70	0.056	0.10	280	0.86	0.20	80
11	Articulated Truck	1900	-10.178	0.1521	0.00004	500	0.70	0.055	0.10	300	0.86	0.20	80
12	Mini Bus	1910	-12.311	0.2228	-0.0003	800	0.48	0.067	0.25	60	0.90	0.20	80
13	Light Bus	2035	-20.036	0.3560	-0.0009	500	0.37	0.057	0.10	75	0.86	0.20	80
14	Medium Bus	1926	-32.352	0.7403	-0.0027	500	0.50	0.057	0.10	100	0.86	0.20	80
15	Heavy Bus	1926	-32.352	0.7403	-0.0027	500	0.60	0.057	0.10	120	0.86	0.20	80
16	Coach	1926	-32.352	0.7403	-0.0027	500	0.70	0.057	0.10	150	0.86	0.20	80

Source: Greenwood and Bennett (1995a)

Table 11.5: Default Emission Model Parameter Values

HDM-4 Vehicle	Fuel Type	HC		NOx		CO	SO_2	Pb		PM		CO_2
		a_{HC}	r_{HC}	a_{NOx}	FR_{NOx}	a_{CO}	a_{SO2}	Prop_Pb	a_{Pb}	a_{PM}	b_{PM}	a_{CO2}
MC	P	0.060	0	0.020	0.00	0.20	0.0005	0.75	0	0.0001	0.0	1.8
PC-S	P	0.012	0	0.055	0.17	0.10	0.0005	0.75	0	0.0001	0.0	1.8
PC-M	P	0.012	0	0.055	0.17	0.10	0.0005	0.75	0	0.0001	0.0	1.8
PC-L	P	0.012	0	0.055	0.17	0.10	0.0005	0.75	0	0.0001	0.0	1.8
LDV	P	0.012	0	0.055	0.17	0.10	0.0005	0.75	0	0.0001	0.0	1.8
LGV	P	0.012	0	0.055	0.17	0.10	0.0005	0.75	0	0.0001	0.0	1.8
4WD	D	0.040	0	0.027	0.00	0.08	0.005	0.75	0	0.0032	0.0	2.0
LT	D	0.040	0	0.027	0.00	0.08	0.005	0.75	0	0.0032	0.0	2.0
MT	D	0.040	0	0.027	0.00	0.08	0.005	0.75	0	0.0032	0.0	2.0
HT	D	0.040	0	0.027	0.00	0.08	0.005	0.75	0	0.0032	0.0	2.0
AT	D	0.040	0	0.027	0.00	0.08	0.005	0.75	0	0.0032	0.0	2.0
MNB	P	0.012	0	0.055	0.17	0.10	0.0005	0.75	0	0.0001	0.0	1.8
LB	D	0.040	0	0.027	0.00	0.08	0.005	0.75	0	0.0032	0.0	2.0
MB	D	0.040	0	0.027	0.00	0.08	0.005	0.75	0	0.0032	0.0	2.0
HB	D	0.040	0	0.027	0.00	0.08	0.005	0.75	0	0.0032	0.0	2.0
COACH	D	0.040	0	0.027	0.00	0.08	0.005	0.75	0	0.0032	0.0	2.0

Source: Base data from An et al (1997), ETSU (1997) and SNRA (1995)

Table 11.6: Default Emission Model Parameter Values (continued)

HDM-4 Vehicle	Fuel Type	HC			NOx			CO			SO_2			Pb			Particulates		
		ε_i	b_i	r_i	ε_i	b_i	r_i	ε_i	b_i	r_i	ε_i	b_i	r_i	ε_i	b_i	r_i	ε_i	b_i	r_i
MC	P	0	0	0	0	0	0	0	0	0	0	0	0	0	0	0	0	0	0
PC-S	P	0.999	0.03	20	0.812	0	11	0.999	0.05	4.8	0	0	0	0	0	0	0	0	4.8
PC-M	P	0.999	0.03	20	0.812	0	11	0.999	0.05	4.8	0	0	0	0	0	0	0	0	4.8
PC-L	P	0.999	0.03	20	0.812	0	11	0.999	0.05	4.8	0	0	0	0	0	0	0	0	4.8
LDV	P	0.999	0.03	20	0.812	0	11	0.999	0.05	4.8	0	0	0	0	0	0	0	0	4.8
LGV	P	0.999	0.03	20	0.812	0	11	0.999	0.05	4.8	0	0	0	0	0	0	0	0	4.8
4WD	D	0.900	0.00	20	0.250	0	11	0.900	0.00	4.8	0	0	0	0	0	0	0.5	0	4.8
LT	D	0.900	0.00	20	0.250	0	11	0.900	0.00	4.8	0	0	0	0	0	0	0.5	0	4.8
MT	D	0.900	0.00	20	0.250	0	11	0.900	0.00	4.8	0	0	0	0	0	0	0.5	0	4.8
HT	D	0.900	0.00	20	0.250	0	11	0.900	0.00	4.8	0	0	0	0	0	0	0.5	0	4.8
AT	D	0.900	0.00	20	0.250	0	11	0.900	0.00	4.8	0	0	0	0	0	0	0.5	0	4.8
MiniBus	P	0.999	0.03	20	0.812	0	11	0.999	0.05	4.8	0	0	0	0	0	0	0	0	4.8
LB	D	0.900	0.00	20	0.250	0	11	0.900	0.00	4.8	0	0	0	0	0	0	0.5	0	4.8
MB	D	0.900	0.00	20	0.250	0	11	0.900	0.00	4.8	0	0	0	0	0	0	0.5	0	4.8
HB	D	0.900	0.00	20	0.250	0	11	0.900	0.00	4.8	0	0	0	0	0	0	0.5	0	4.8
COACH	D	0.900	0.00	20	0.250	0	11	0.900	0.00	4.8	0	0	0	0	0	0	0.5	0	4.8

Source: Base data from An, et al (1997), Clean Cat (2000), Discount Converters Ltd (2000), Hammarstrom (1999) and SNRA (1995)

11.2 Appendix B – Code for Utility Software

The code listing below are part of a wider package of support software that is distributed under the collective title of HDMTools. The software, as compiled versions, are available for download from www.opus.co.nz/hdmtools.

11.2.1 CDMult – Aerodynamic Drag Multiplier

Note: The following code has been extracted from the HDMTools CDMULT program and modified for inclusion into an Excel spreadsheet.

```
Function CDMULT(Vw As Double, V As Double, h As Double, YawC As
Double) As Double
    Dim PI As Double
    Dim Rad As Double
    Dim Vr As Double
    Dim theta As Integer
    Dim dblTemp As Double
    Dim Yaw As Double
    Dim CDM As Double

    PI = 3.141592654
    Rad = PI / 180#

    theta = 0
    dblTemp = 0

    For theta = 0 To 359 Step 5

            Vr = Sqr(V * V + Vw * Vw + 2 * V * Vw * Cos(theta * Rad))

            If (V + Vw * Cos(theta * Rad)) = 0 Then
                Yaw = 90
            Else
                Yaw = 1 / Rad * Atn(Vw * Sin(theta * Rad) / Vr) '(V +
Vw * Cos(theta * Rad)))
            End If

            If Yaw < YawC Then
                CDM = 1 + h * (Sin((90 * Yaw / YawC) * Rad)) ^ 2
            ElseIf Yaw < (180 - YawC) Then
                CDM = (1 + h) * Cos(90 * (Yaw - YawC) / (90 - YawC) *
Rad)
            Else
                CDM = -(1 + h * (Sin(90 * (180 - Yaw) / YawC * Rad))
^ 2)
            End If

            dblTemp = dblTemp + CDM * Vr * Vr / V / V

            'Debug.Print theta, V, Vw, Yaw, CDM * Vr * Vr / V / V

    Next theta

        CDMULT = dblTemp / (360 / 5)


End Function
```

11.2.2 Gearsim

Note: The following code has been extracted from the HDMTools Gearsim programme and modified for inclusion into an Excel spreadsheet.

```
Private Sub Command1_Click()
    Dim std As Double
    Dim mean As Double
    Dim avgrpm(1 To 40) As Double
    Dim avgemrat(1 To 40) As Double
    Dim X As Double
    Dim t As Double
    Dim speed(1 To 2000) As Double
    Dim rand As Double
    Dim pi As Double
    Dim maxspd(1 To 16) As Double
    Dim minspd(1 To 16) As Double
    Dim ratio As Double
    Dim rpm As Double
    Dim emrat As Double
    Dim adjust As Boolean
    Dim i As Integer
    Dim j As Integer
    Dim k As Integer
    Dim l As Integer
    Dim dir As String
    Dim file1 As String
    Dim file2 As String
    Dim MaxVehSpd As Double
    Dim maxrpm As Double
    Dim minrpm As Double
    Dim numg As Integer
    Dim cov As Double
    Dim numveh As Long
    Dim RRow As Long
    Dim wheel_dia As Double
    Dim gr(5) As Double
    Dim differ As Double
    Dim wgt_oper As Double
    Dim ie As Double
    Dim minvehspd As Double
    Dim num_wheels As Integer
    Dim wheel_mass As Double

    Randomize



    RRow = 1
    MaxVehSpd = 100
    minvehspd = 10
    maxrpm = 3000
    minrpm = 800
    numg = 5
    cov = 0.05
    numveh = 1000
    wheel_dia = 0.6
    gr(1) = 3.42
    gr(2) = 1.84
```

```
    gr(3) = 1.29
    gr(4) = 0.97
    gr(5) = 0.78
    differ = 4.388
    wgt_oper = 1.04
    ie = 0.6
    num_wheels = 4
    wheel_mass = 15

    l = Val(MaxVehSpd) / 5
    'Graph1.NumPoints = l
    'Graph2.NumPoints = l

    'reset average values
    For i = 1 To l
        avgrpm(i) = 0
        avgemrat(i) = 0
    Next i

    'calculate the maximum and minimum speeds in each gear
    pi = 3.1415927
    For i = 1 To numg
        maxspd(i) = maxrpm * 3.6 * pi * wheel_dia / (60# * gr(i) *
differ)
        minspd(i) = (minrpm * 1.15) * 3.6 * pi * wheel_dia / (60# *
gr(i) * differ)
    Next i

   i = Val(minvehspd) / 5
    'loop about mean speeds
    'For mean = 5 To maxVehSpd Step 5
    For k = i To l
        mean = 5 * k
        std = mean * cov
        'curmeanspd = mean
        'curmeanspd.Refresh

        'this program firstly generates all the necessary speeds
        'then generates their gear selection, therefore there are
        '2 loops abount numveh.

        'generate speeds for current mean
        'Status = "Generating vehicle speeds"
        'Refresh

        For i = 1 To numveh
            'curvehnum = i
            'curvehnum.Refresh


            'trim ends of normal distribution
            rand = 0
            Do Until rand > 0.0228 And rand < 0.9722
                rand = Rnd
            Loop

            'calculate speed based on normal distribution
            If rand < 0.5 Then
                adjust = True
            Else
```

```
                rand = 1 - rand
                adjust = False
            End If

            t = rand * rand
            t = 1# / t
            t = Log(t)
            t = Sqr(t)
            X = t - ((t * 0.010328 + 0.802853) * t + 2.515517) / (((t
* 0.001308 + 0.189269) * t + 1.432788) * t + 1)

            If adjust = True Then
                speed(i) = mean - X * std
            Else
                speed(i) = mean + X * std
            End If

        Next i

        'this loop allocates gear selection
        'Status = "Simulating gear selection"
        'Status.Refresh

        For i = 1 To numveh
            'curvehnum = i
            'curvehnum.Refresh

            If speed(i) < minspd(1) Then
                j = 1
                GoTo foundgear
            End If


            rand = Rnd
            j = 1 'this is a counter for gear selection

nextgear:
            ratio = (speed(i) - minspd(j + 1)) / (maxspd(j) -
minspd(j + 1))

            If speed(i) > minspd(j) And speed(i) < maxspd(j) And rand
> ratio Then
                GoTo foundgear
            ElseIf j = numg - 1 Then
                j = numg
                GoTo foundgear
            Else
                j = j + 1
                GoTo nextgear
            End If

foundgear:


            rpm = 60 * speed(i) * gr(j) * differ / (wheel_dia * pi *
3.6)
            avgrpm(k) = avgrpm(k) + rpm

            emrat = wgt_oper * 1000# + num_wheels * wheel_mass * 0.56
+ ie * (gr(j) * differ) ^ 2 / (wheel_dia / 2) ^ 2
```

```
            emrat = emrat / (wgt_oper * 1000#)
            avgemrat(k) = avgemrat(k) + emrat


          RRow = RRow + 1
          Worksheets("sheet1").Cells(RRow, 1) = speed(i)
          Worksheets("sheet1").Cells(RRow, 2) = j
          Worksheets("sheet1").Cells(RRow, 3) = rpm



        Next i

        'compute averages for current mean speed
        avgrpm(k) = avgrpm(k) / numveh
        avgemrat(k) = avgemrat(k) / numveh



    Next k

    'Status = "Preparing plots"
    'Status.Refresh

    'Graph1.AutoInc = 0
    'Graph2.AutoInc = 0
    'For i = 1 To l
    '    Graph1.ThisPoint = i
    '    Graph1.XPosData = 5 * i
    '    Graph1.GraphData = avgrpm(i)
    '
    '    Graph2.ThisPoint = i
    '    Graph2.XPosData = 5 * i
    '    Graph2.GraphData = avgemrat(i)
    'Next i
    'Graph1.DrawMode = 2
    'Graph2.DrawMode = 2


    'Status = "Writing results to file"
    'Status.Refresh

    'file1 = gearsimdir & "\" & gearsimfile



    'Open file1 For Output As #1

    'k = Val(MinVehSpd) / 5
    'For i = k To l
    '    avgrpm(i) = Format(avgrpm(i), "0")
    '    avgemrat(i) = Format(avgemrat(i), "0.000")
    '    Print #1, 5 * i, avgrpm(i), avgemrat(i)
    'Next i
    'Close #1

   ' Status = "Simulation completed"
    'Status.Refresh

    'check = "done"
```

```
    'If check = "done" Then
    '    Title = "Data saved"
    '    Style = vbOKOnly
    '    msg = "The output data has been saved to file.  A regression
analysis is now required to determine the RPM and EMRAT parameter
values.  The file containing the data is called:"
    '    msg = msg + file1
    '    response = MsgBox(msg, Style, Title)
    'End If

End Sub
```

11.3 Appendix C – Data Analysis From Thailand Congestion Study

The following tables contain data collected in Thailand and previously published in Greenwood (1999).

Table 11.7: 2 Lane Undivided, Site 2 - 3215

Run No	Veh Eng Size	Driver	Time			Length (km)	Accel. Noise (m/s^2)	Mean Speed (km/h)	Calculated Traffic Volume (PCSE/hr)	Fuel Consumption Data			
			Start	End	Run (hh:mm:ss)					Actual Used (mL/s)	Computed at Mean Speed (mL/s)	DFUEL Calculated	DFUEL Simulated
1	2.0	1	15:22:59	15:23:53	00:00:54	0.9	0.21	58.0	2371	0.85	0.80	1.07	1.06
2	2.0	1	15:25:27	15:28:03	00:02:36	3.0	0.27	68.4	1861	0.98	0.97	1.01	1.08
3	2.0	1	15:29:17	15:31:55	00:02:38	2.6	0.40	59.9	2278	0.94	0.83	1.14	1.19
4	2.0	1	15:33:35	15:35:48	00:02:13	2.7	0.32	73.4	1614	1.11	1.07	1.04	1.11
5	2.0	1	15:37:12	15:40:58	00:03:46	3.1	0.58	50.0	2566	0.90	0.68	1.32	1.36
6	2.0	1	15:43:02	15:45:53	00:02:51	2.8	0.39	58.9	2328	0.89	0.81	1.10	1.15
7	2.0	1	15:47:22	15:49:28	00:02:06	2.4	0.35	67.8	1886	1.03	0.96	1.07	1.13
8	2.0	1	15:54:00	15:55:16	00:01:16	1.3	0.29	62.9	2128	0.90	0.88	1.03	1.08
9	2.0	1	15:57:24	15:58:52	00:01:28	0.9	0.50	36.6	2692	0.74	0.53	1.39	1.38
10	2.0	1	15:59:18	16:00:19	00:01:01	0.9	0.27	51.6	2552	0.80	0.70	1.14	1.09
11	2.0	1	16:02:32	16:03:19	00:00:47	0.5	0.67	34.8	2708	0.74	0.52	1.43	1.57
12	2.0	1	16:05:49	16:06:51	00:01:02	1.1	0.21	62.9	2130	0.91	0.88	1.04	1.08
13	2.0	1	16:08:21	16:08:48	00:00:27	0.5	0.22	60.8	2234	0.79	0.84	1.00	1.08
14	2.0	1	16:09:58	16:10:56	00:00:58	1.0	0.21	60.0	2271	0.80	0.83	1.00	1.08
15	2.0	1	11:55:54	11:58:14	00:02:20	2.8	0.31	71.7	1697	1.08	1.04	1.04	1.11
16	2.0	1	11:59:03	12:02:08	00:03:05	3.1	0.25	59.9	2277	0.86	0.83	1.04	1.08
17	2.0	1	12:03:51	12:06:29	00:02:38	2.9	0.27	65.8	1986	0.99	0.93	1.07	1.08
18	2.0	1	12:07:24	12:10:18	00:02:54	3.2	0.32	65.6	1997	0.96	0.92	1.04	1.11
19	2.0	1	12:12:16	12:13:53	00:01:37	1.6	0.30	58.3	2356	0.80	0.80	1.00	1.14
20	2.0	1	12:14:55	12:17:01	00:02:06	2.0	0.29	57.9	2378	0.83	0.79	1.04	1.08
21	2.0	1	12:22:03	12:25:06	00:03:03	3.1	0.33	61.4	2206	0.88	0.85	1.03	1.12
22	2.0	1	12:26:30	12:28:16	00:01:46	2.2	0.14	73.4	1613	1.08	1.07	1.01	1.08
23	2.0	1	12:30:23	12:31:19	00:00:56	1.0	0.24	64.2	2065	0.87	0.90	1.00	1.08
24	2.0	1	12:33:59	12:36:15	00:02:16	2.7	0.25	71.7	1695	1.06	1.04	1.02	1.07
25	2.0	1	12:37:35	12:39:30	00:01:55	1.9	0.21	60.5	2247	0.86	0.84	1.03	1.08
26	2.0	1	12:45:30	12:48:01	00:02:31	2.8	0.23	66.1	1973	0.94	0.93	1.01	1.08
27	2.0	1	12:49:06	12:51:42	00:02:36	3.0	0.25	68.8	1838	1.02	0.98	1.04	1.08

Run No	Veh Eng Size	Driver	Time			Length (km)	Accel. Noise (m/s²)	Mean Speed (km/h)	Calculated Traffic Volume (PCSE/hr)	Fuel Consumption Data			
			Start	End	Run (hh:mm:ss)					Actual Used (mL/s)	Computed at Mean Speed (mL/s)	DFUEL Calculated	DFUEL Simulated
28	2.0	1	12:52:42	12:55:14	00:02:32	2.8	0.24	65.7	1995	0.93	0.92	1.01	1.08
29	2.0	1	12:57:51	12:58:21	00:00:30	0.3	0.62	38.1	2678	0.71	0.55	1.30	1.49
30	2.0	1	13:08:35	13:11:33	00:02:58	3.1	0.27	62.2	2166	0.89	0.86	1.03	1.08
31	2.0	1	13:27:27	13:30:34	00:03:07	3.1	0.25	59.2	2311	0.88	0.82	1.08	1.08
32	2.0	1	13:31:42	13:34:38	00:02:56	3.0	0.36	62.4	2157	0.94	0.87	1.08	1.14
33	2.0	2	14:28:18	14:30:28	00:02:10	2.4	0.23	65.9	1983	0.98	0.93	1.06	1.08
34	2.0	2	14:31:43	14:33:52	00:02:09	2.3	0.32	63.5	2100	0.97	0.89	1.09	1.12
35	2.0	2	14:37:46	14:40:15	00:02:29	2.5	0.28	60.0	2274	0.81	0.83	1.00	1.08
36	2.0	2	14:48:54	14:52:01	00:03:07	3.1	0.28	60.2	2263	0.81	0.83	1.00	1.08
37	2.0	2	14:54:00	14:56:46	00:02:46	2.5	0.30	53.7	2532	0.80	0.73	1.09	1.13
38	2.0	2	14:59:05	15:01:07	00:02:02	2.0	0.34	57.6	2393	0.76	0.79	1.00	1.14
39	2.0	2	15:02:04	15:05:28	00:03:24	3.3	0.29	57.6	2392	1.02	0.79	1.29	1.08
40	2.0	2	15:07:50	15:09:38	00:01:48	1.8	0.22	58.8	2332	0.86	0.81	1.06	1.06
41	2.0	2	15:11:10	15:13:52	00:02:42	2.6	0.39	56.9	2428	0.85	0.78	1.09	1.15
42	2.0	2	15:17:39	15:19:14	00:01:35	1.2	0.45	46.9	2596	0.72	0.64	1.12	1.28
43	2.0	2	15:30:18	15:32:07	00:01:49	1.7	0.34	56.7	2435	0.90	0.78	1.16	1.14
44	2.0	2	15:33:36	15:35:37	00:02:01	1.6	0.43	46.7	2598	0.75	0.64	1.17	1.22
45	2.0	2	15:38:40	15:40:53	00:02:13	1.9	0.47	51.8	2550	0.82	0.71	1.16	1.24
46	2.0	2	16:02:04	16:05:58	00:03:54	3.4	0.61	51.6	2552	0.95	0.70	1.35	1.42
47	2.0	2	16:10:37	16:12:57	00:02:20	1.7	0.70	42.6	2636	0.80	0.59	1.35	1.55
48	2.0	2	16:27:43	16:30:20	00:02:37	1.9	0.46	44.1	2622	0.69	0.61	1.13	1.31
49	2.0	2	16:30:46	16:33:12	00:02:26	1.9	0.63	46.6	2598	0.81	0.64	1.27	1.46
50	2.0	2	16:35:34	16:39:38	00:04:04	3.3	0.59	48.0	2586	0.87	0.66	1.33	1.39
51	1.6	1	14:49:57	14:51:08	00:01:11	1.0	0.30	52.0	2548	0.72	0.59	1.21	1.13
52	1.6	1	14:52:31	14:54:04	00:01:33	1.7	0.22	66.9	1934	0.94	0.78	1.20	1.09
53	1.6	1	14:56:47	14:58:40	00:01:53	2.0	0.43	62.4	2157	0.88	0.72	1.22	1.12
54	1.6	1	15:01:36	15:02:39	00:01:03	1.1	0.22	64.5	2051	0.82	0.75	1.09	1.07
55	1.6	1	15:04:47	15:06:26	00:01:39	1.6	0.23	56.8	2432	0.73	0.65	1.12	1.04
56	1.6	1	15:17:41	15:19:29	00:01:48	1.3	0.25	44.6	2617	0.59	0.52	1.14	1.10
57	1.6	1	15:20:27	15:22:34	00:02:07	1.9	0.39	52.7	2541	0.75	0.60	1.25	1.16
58	1.6	1	15:38:19	15:40:24	00:02:05	1.7	0.37	49.9	2568	0.70	0.57	1.23	1.17
59	1.6	1	15:50:30	15:51:28	00:00:58	0.8	0.48	46.9	2596	0.76	0.54	1.41	1.28
60	1.6	1	15:55:18	15:57:01	00:01:43	1.6	0.25	57.3	2407	0.75	0.66	1.14	1.11

Run No	Veh Eng Size	Driver	Time			Length (km)	Accel. Noise (m/s²)	Mean Speed (km/h)	Calculated Traffic Volume (PCSE/hr)	Fuel Consumption Data			
			Start	End	Run (hh:mm:ss)					Actual Used (mL/s)	Computed at Mean Speed (mL/s)	DFUEL Calculated	DFUEL Simulated
61	1.6	1	16:00:40	16:02:30	00:01:50	1.8	0.26	59.3	2308	0.78	0.68	1.15	1.11
62	1.6	1	16:07:04	16:08:25	00:01:21	1.1	0.43	48.8	2577	0.72	0.56	1.29	1.20
63	1.6	1	16:09:22	16:10:37	00:01:15	1.2	0.24	59.2	2312	0.77	0.68	1.13	1.04
64	1.6	1	16:11:14	16:12:49	00:01:35	1.3	0.17	49.2	2574	0.61	0.56	1.08	1.06
65	1.6	1	16:23:44	16:26:13	00:02:29	2.0	0.47	49.2	2574	0.71	0.56	1.26	1.28
66	1.6	1	16:27:57	16:29:08	00:01:11	1.1	0.24	54.8	2522	0.68	0.63	1.09	1.06
67	1.6	1	16:31:44	16:32:57	00:01:13	1.2	0.19	61.6	2196	0.81	0.71	1.14	1.08
68	1.6	2	14:51:24	14:52:36	00:01:12	1.3	0.50	67.4	1907	1.02	0.79	1.29	1.24
69	1.6	2	14:55:40	14:57:05	00:01:25	1.6	0.33	69.5	1804	0.94	0.82	1.14	1.09
70	1.6	2	14:58:45	14:59:36	00:00:51	1.0	0.24	68.4	1857	0.91	0.81	1.13	1.09
71	1.6	2	15:03:27	15:04:52	00:01:25	1.1	0.52	46.6	2599	0.79	0.54	1.47	1.31
72	1.6	2	15:04:59	15:05:48	00:00:49	0.8	0.37	59.5	2296	0.80	0.68	1.17	1.14
73	1.6	2	15:09:33	15:10:07	00:00:34	0.7	0.18	73.4	1611	1.01	0.88	1.14	1.10
74	1.6	2	15:12:50	15:13:34	00:00:44	0.8	0.19	62.8	2135	0.79	0.73	1.09	1.08
75	1.6	2	15:15:43	15:16:49	00:01:06	1.3	0.26	71.2	1719	0.98	0.85	1.15	1.08
76	1.6	2	15:17:34	15:18:13	00:00:39	0.7	0.28	68.5	1853	0.89	0.81	1.10	1.10
77	1.6	2	15:28:44	15:30:33	00:01:49	1.5	0.43	49.9	2567	0.76	0.57	1.33	1.20
78	1.6	2	15:32:51	15:34:19	00:01:28	1.5	0.28	60.8	2235	0.79	0.70	1.13	1.09
79	1.6	2	15:36:46	15:37:46	00:01:00	0.9	0.49	52.4	2545	0.81	0.60	1.36	1.25
80	1.6	2	15:37:57	15:39:00	00:01:03	0.6	0.65	32.9	2727	0.67	0.42	1.60	1.62
81	1.6	2	15:39:21	15:41:09	00:01:48	1.4	0.35	45.9	2605	0.68	0.53	1.29	1.17
82	1.6	2	15:42:05	15:45:07	00:03:02	3.1	0.41	60.9	2230	0.85	0.70	1.21	1.12
83	1.6	2	15:46:40	15:48:01	00:01:21	1.3	0.43	56.6	2440	0.83	0.65	1.28	1.19

Table 11.8: 2 Lane Undivided, Site 3 - 345

Run No	Veh Eng Size	Driver	Time			Length (km)	Accel. Noise (m/s^2)	Mean Speed (km/h)	Calculated Traffic Volume (PCSE/hr)	Fuel Consumption Data			
			Start	End	Run (hh:mm:ss)					Actual Used (mL/s)	Computed at Mean Speed (mL/s)	DFUEL Calculated	DFUEL Simulated
1	1.6	1	15:54:32	16:00:05	00:05:33	6.0	0.26	65.3	2010	0.77	0.76	1.01	1.10
2	1.6	1	16:02:41	16:05:28	00:02:47	2.6	0.22	56.1	2464	0.65	0.64	1.01	1.04
3	1.6	1	16:05:53	16:09:30	00:03:37	3.9	0.16	63.9	2081	0.74	0.74	1.00	1.08
4	1.6	1	16:09:26	16:10:53	00:01:27	1.5	0.16	62.1	2169	0.70	0.72	1.00	1.08
5	1.6	1	16:18:18	16:24:50	00:06:32	6.1	0.38	55.9	2474	0.70	0.64	1.10	1.14
6	1.6	1	16:28:13	16:32:06	00:03:53	4.7	0.19	73.3	1615	1.01	0.88	1.15	1.10
7	1.6	1	16:37:12	16:39:09	00:01:57	2.4	0.31	72.9	1638	0.95	0.88	1.09	1.11
8	1.6	1	16:40:44	16:44:58	00:04:14	4.1	0.25	58.3	2355	0.67	0.67	1.00	1.11
9	1.6	1	16:49:11	16:51:02	00:01:51	2.3	0.12	75.6	1506	0.97	0.92	1.06	1.10
10	1.6	1	16:59:58	17:04:05	00:04:07	3.9	0.21	56.1	2467	0.61	0.64	1.00	1.04
11	1.6	1	17:05:56	17:08:37	00:02:41	3.1	0.20	69.6	1798	0.89	0.82	1.08	1.09
12	1.6	1	17:11:55	17:13:40	00:01:45	1.9	0.14	66.8	1940	0.81	0.78	1.03	1.07
13	1.6	1	17:15:15	17:17:19	00:02:04	2.4	0.23	68.4	1861	0.87	0.81	1.08	1.09
14	1.6	1	17:18:54	17:23:15	00:04:21	4.9	0.19	67.2	1920	0.81	0.79	1.03	1.07
15	1.6	1	17:25:26	17:30:15	00:04:49	5.4	0.15	66.7	1943	0.82	0.78	1.05	1.07
16	1.6	1	17:33:22	17:34:30	00:01:08	1.2	0.10	66.1	1974	0.80	0.77	1.03	1.07
17	1.6	1	17:35:55	17:37:40	00:01:45	2.0	0.14	68.0	1879	0.84	0.80	1.05	1.07
18	1.6	1	17:39:35	17:43:42	00:04:07	5.0	0.22	71.9	1685	0.92	0.86	1.07	1.08
19	1.6	1	17:45:56	17:48:32	00:02:36	2.8	0.16	65.3	2013	0.79	0.76	1.04	1.07
20	1.6	1	17:49:04	17:50:43	00:01:39	1.6	0.25	57.2	2413	0.66	0.65	1.01	1.11
21	1.6	1	18:25:14	18:30:02	00:04:48	5.0	0.33	62.7	2138	0.80	0.73	1.10	1.12
22	1.6	1	18:38:49	18:40:13	00:01:24	1.7	0.19	71.5	1705	0.94	0.85	1.10	1.10
23	1.6	1	18:44:50	18:49:37	00:04:47	5.1	0.28	63.3	2110	0.79	0.73	1.08	1.09
24	1.6	1	18:51:32	18:56:22	00:04:50	5.7	0.21	70.3	1766	0.94	0.84	1.13	1.08
25	1.6	1	19:02:18	19:07:36	00:05:18	6.6	0.22	74.3	1568	1.01	0.90	1.12	1.08
26	1.6	1	19:13:32	19:16:50	00:03:18	3.0	0.21	54.5	2525	0.61	0.62	1.00	1.06
27	1.6	1	19:18:54	19:23:01	00:04:07	5.0	0.20	72.2	1670	0.94	0.86	1.09	1.08
28	1.6	1	19:28:11	19:35:29	00:07:18	8.1	0.24	66.4	1956	0.84	0.78	1.08	1.09
29	1.6	1	19:46:59	19:51:12	00:04:13	5.2	0.16	73.8	1593	0.96	0.89	1.08	1.10

Table 11.9: 4 Lane Undivided, Site 23 - Onut

Run No	Veh Eng Size	Driver	Time			Length (km)	Accel. Noise (m/s^2)	Mean Speed (km/h)	Calculated Traffic Volume (PCSE/hr)	Fuel Consumption Data			
			Start	End	Run (hh:mm:ss)					Actual Used (mL/s)	Computed at Mean Speed (mL/s)	DFUEL Calculated	DFUEL Simulated
1	2.0	1	15:27:36	15:28:18	00:00:42	0.6	0.30	48.0	2264	0.82	0.66	1.25	1.13
2	2.0	1	15:29:01	15:30:37	00:01:36	1.2	0.28	46.5	2270	0.78	0.64	1.22	1.09
3	2.0	1	15:32:45	15:35:02	00:02:17	1.9	0.46	49.2	2258	0.93	0.67	1.38	1.28
4	2.0	1	15:37:31	15:38:44	00:01:13	0.8	0.40	40.5	2298	0.89	0.57	1.56	1.24
5	2.0	1	15:39:52	15:41:09	00:01:17	0.8	0.33	37.1	2300	0.79	0.54	1.47	1.17
6	2.0	1	15:43:35	15:44:28	00:00:53	0.7	0.30	44.4	2280	0.89	0.61	1.45	1.16
7	2.0	1	15:45:01	15:45:43	00:00:42	0.6	0.31	48.2	2263	0.82	0.66	1.24	1.13
8	2.0	1	15:46:24	15:46:44	00:00:20	0.3	0.28	47.8	2264	0.91	0.65	1.39	1.09
9	2.0	1	15:54:11	15:54:58	00:00:47	0.7	0.44	50.2	2253	0.98	0.68	1.43	1.18
10	2.0	1	15:57:13	15:59:49	00:02:36	2.0	0.46	47.2	2267	0.96	0.65	1.49	1.28
11	2.0	1	16:01:51	16:04:04	00:02:13	1.8	0.32	48.2	2262	0.86	0.66	1.31	1.13
12	2.0	1	16:05:25	16:06:25	00:01:00	0.7	0.21	41.3	2294	0.71	0.58	1.23	1.08
13	2.0	1	16:08:37	16:09:37	00:01:00	0.7	0.32	44.8	2278	0.79	0.62	1.28	1.16
14	2.0	1	16:10:29	16:11:50	00:01:21	0.9	0.40	41.2	2295	0.89	0.58	1.54	1.24
15	2.0	1	16:14:22	16:17:50	00:03:28	2.9	0.36	49.5	2256	0.90	0.68	1.33	1.18
16	2.0	1	16:18:28	16:19:16	00:00:48	0.6	0.31	46.7	2269	0.93	0.64	1.45	1.13
17	2.0	1	16:20:29	16:23:12	00:02:43	2.0	0.40	44.5	2279	0.87	0.61	1.42	1.24
18	2.0	1	16:25:27	16:26:04	00:00:37	0.5	0.44	50.3	2253	0.97	0.69	1.41	1.18
19	2.0	1	16:26:52	16:27:57	00:01:05	0.9	0.27	52.5	2243	0.92	0.72	1.29	1.09
20	2.0	1	16:31:23	16:32:20	00:00:57	0.7	0.20	42.9	2287	0.77	0.60	1.29	1.08
21	2.0	1	16:33:01	16:34:10	00:01:09	1.0	0.28	50.8	2251	0.87	0.69	1.26	1.09
22	2.0	1	16:36:21	16:37:11	00:00:50	0.8	0.28	54.8	2232	0.93	0.75	1.24	1.09
23	2.0	1	16:38:55	16:39:51	00:00:56	0.7	0.29	45.9	2273	0.81	0.63	1.28	1.09
24	2.0	1	16:42:19	16:44:37	00:02:18	1.6	0.39	42.1	2290	0.75	0.59	1.28	1.20
25	2.0	1	16:45:19	16:45:55	00:00:36	0.4	0.42	35.4	2300	0.79	0.52	1.51	1.27
26	2.0	1	16:47:54	16:50:24	00:02:30	1.9	0.47	44.6	2279	0.88	0.62	1.43	1.31
27	2.0	1	16:51:11	16:52:08	00:00:57	0.7	0.29	45.7	2274	0.82	0.63	1.31	1.09
28	2.0	2	16:55:37	16:56:35	00:00:58	0.7	0.43	42.9	2287	0.84	0.60	1.41	1.24
29	2.0	2	16:58:34	17:02:01	00:03:27	2.1	0.53	36.5	2300	0.82	0.53	1.54	1.38
30	2.0	2	17:02:55	17:06:58	00:04:03	2.3	0.73	33.6	2300	0.83	0.51	1.64	1.65

Run No	Veh Eng Size	Driver	Time			Length (km)	Accel. Noise (m/s^2)	Mean Speed (km/h)	Calculated Traffic Volume (PCSE/hr)	Fuel Consumption Data			
			Start	End	Run (hh:mm:ss)					Actual Used (mL/s)	Computed at Mean Speed (mL/s)	DFUEL Calculated	DFUEL Simulated
31	2.0	2	17:08:35	17:10:12	00:01:37	1.0	0.64	38.1	2300	0.87	0.55	1.59	1.49
32	2.0	2	17:17:37	17:18:36	00:00:59	0.7	0.45	42.3	2289	0.83	0.59	1.41	1.31
33	2.0	2	17:18:58	17:19:51	00:00:53	0.5	0.51	34.6	2300	0.78	0.52	1.51	1.43
34	2.0	2	17:21:19	17:22:49	00:01:30	1.1	0.71	44.1	2281	0.99	0.61	1.62	1.55
35	2.0	2	17:25:53	17:27:31	00:01:38	1.1	0.90	40.9	2296	1.01	0.58	1.76	1.81
36	2.0	2	17:32:47	17:34:07	00:01:20	0.5	0.52	21.8	2300	0.65	0.43	1.51	1.47
37	2.0	2	17:36:04	17:38:42	00:02:38	1.5	0.45	34.4	2300	0.71	0.51	1.38	1.37
38	2.0	2	17:40:18	17:41:42	00:01:24	1.0	0.45	42.3	2290	0.85	0.59	1.44	1.31
39	2.0	2	17:42:03	17:42:50	00:00:47	0.3	0.74	22.8	2300	0.78	0.44	1.79	1.69
40	2.0	2	17:46:42	17:47:47	00:01:05	0.3	0.58	14.1	2300	0.60	0.40	1.48	1.53
41	2.0	2	17:48:21	17:49:18	00:00:57	0.7	0.32	47.0	2268	0.89	0.64	1.38	1.13
42	2.0	2	17:56:26	17:57:49	00:01:23	1.0	0.39	42.8	2287	0.94	0.60	1.58	1.20
43	2.0	2	18:18:04	18:20:28	00:02:24	1.6	0.47	40.1	2300	0.93	0.57	1.64	1.31
44	2.0	2	18:23:18	18:23:47	00:00:29	0.4	0.41	53.1	2240	1.18	0.72	1.63	1.18
45	1.6	1	17:03:37	17:08:16	00:04:39	3.1	0.36	40.0	2300	0.52	0.47	1.10	1.17
46	1.6	1	17:12:15	17:12:57	00:00:42	0.5	0.31	44.0	2282	0.56	0.51	1.10	1.15
47	1.6	1	17:13:53	17:14:40	00:00:47	0.5	0.35	41.1	2295	0.51	0.48	1.05	1.17
48	1.6	1	17:15:31	17:16:35	00:01:04	0.7	0.34	41.8	2292	0.52	0.49	1.06	1.15
49	1.6	1	17:17:15	17:17:53	00:00:38	0.4	0.33	35.1	2300	0.53	0.44	1.22	1.16
50	1.6	1	17:21:43	17:22:16	00:00:33	0.4	0.27	40.5	2298	0.51	0.48	1.07	1.10
51	1.6	1	17:23:41	17:24:23	00:00:42	0.6	0.28	47.6	2265	0.54	0.55	1.00	1.08
52	1.6	1	17:26:00	17:26:57	00:00:57	0.7	0.27	42.2	2290	0.53	0.49	1.07	1.10
53	1.6	1	17:27:58	17:28:36	00:00:38	0.4	0.30	42.1	2290	0.55	0.49	1.12	1.15
54	1.6	1	17:31:32	17:32:13	00:00:41	0.4	0.33	33.4	2300	0.44	0.42	1.04	1.18
55	1.6	1	17:38:22	17:39:24	00:01:02	0.7	0.30	38.2	2300	0.48	0.46	1.04	1.16
56	1.6	1	17:41:34	17:42:09	00:00:35	0.3	0.34	27.4	2300	0.47	0.38	1.22	1.20
57	1.6	1	17:51:10	17:52:51	00:01:41	0.9	0.25	33.5	2300	0.45	0.42	1.06	1.11
58	1.6	1	18:00:14	18:02:21	00:02:07	1.1	0.43	31.4	2300	0.54	0.41	1.32	1.29
59	1.6	1	18:02:24	18:03:47	00:01:23	0.8	0.22	36.8	2300	0.50	0.45	1.12	1.08
60	1.6	1	18:08:31	18:09:57	00:01:26	1.0	0.29	40.8	2296	0.51	0.48	1.06	1.10
61	1.6	1	18:17:20	18:18:28	00:01:08	0.6	0.17	33.9	2300	0.44	0.43	1.03	1.03
62	1.6	1	18:25:09	18:26:30	00:01:21	0.9	0.32	40.0	2300	0.49	0.47	1.03	1.15

Table 11.10: 4 Lane Divided, Site 24 - 3 Sukhimvit Rd (Samut Prakan)

Run No	Veh Eng Size	Driver	Time			Length (km)	Accel. Noise (m/s^2)	Mean Speed (km/h)	Calculated Traffic Volume (PCSE/hr)	Fuel Consumption Data			
			Start	End	Run (hh:mm:ss)					Actual Used (mL/s)	Computed at Mean Speed (mL/s)	DFUEL Calculated	DFUEL Simulated
1	1.6	1	18:16:25	18:19:09	00:02:44	3.3	0.25	72.2	2153	0.93	0.86	1.08	1.08
2	1.6	1	18:20:05	18:22:57	00:02:52	2.3	0.40	48.6	2261	0.69	0.56	1.24	1.20
3	1.6	1	18:23:26	18:24:34	00:01:08	1.1	0.28	59.2	2212	0.73	0.68	1.07	1.11
4	1.6	1	18:33:35	18:36:31	00:02:56	2.8	0.20	57.4	2221	0.67	0.66	1.02	1.04
5	1.6	1	18:38:17	18:41:36	00:03:19	3.5	0.27	63.4	2193	0.78	0.74	1.06	1.09
6	1.6	1	18:43:27	18:47:24	00:03:57	3.2	0.21	48.8	2260	0.53	0.56	1.00	1.06
7	1.6	1	18:48:44	18:51:01	00:02:17	2.3	0.29	59.7	2210	0.75	0.69	1.09	1.11
8	1.6	1	18:55:14	18:58:44	00:03:30	3.0	0.17	52.1	2245	0.57	0.59	1.00	1.05
9	1.6	2	16:29:34	16:31:26	00:01:52	2.0	0.43	64.9	2186	0.88	0.76	1.16	1.12
10	1.6	2	16:31:30	16:32:43	00:01:13	1.1	0.53	54.6	2233	0.76	0.62	1.22	1.31
11	1.6	2	16:34:27	16:35:24	00:00:57	1.3	0.45	79.0	1880	1.07	0.98	1.10	1.17
12	1.6	2	16:35:53	16:37:09	00:01:16	1.3	0.26	63.3	2193	0.69	0.73	1.00	1.09
13	1.6	2	16:41:27	16:43:48	00:02:21	2.0	0.47	50.8	2251	0.71	0.58	1.22	1.25
14	1.6	2	16:44:08	16:44:53	00:00:45	0.8	0.28	64.4	2188	0.84	0.75	1.12	1.09
15	1.6	2	16:48:40	16:51:50	00:03:10	3.8	0.32	72.5	2151	0.94	0.87	1.08	1.11
16	1.6	2	16:53:40	16:54:28	00:00:48	0.9	0.28	70.2	2162	0.89	0.83	1.07	1.08
17	1.6	2	16:55:08	16:57:53	00:02:45	2.3	0.46	50.1	2254	0.69	0.57	1.21	1.25
18	1.6	2	16:59:16	17:01:18	00:02:02	2.5	0.53	72.4	2152	1.05	0.87	1.21	1.23
19	1.6	2	17:03:47	17:07:18	00:03:31	3.1	0.68	52.4	2243	0.78	0.60	1.30	1.45
20	1.6	2	17:11:01	17:14:09	00:03:08	3.5	0.41	67.5	2175	0.87	0.79	1.10	1.15
21	1.6	2	17:16:11	17:21:34	00:05:23	3.7	0.47	41.5	2293	0.58	0.49	1.19	1.32
22	1.6	2	17:26:07	17:29:03	00:02:56	3.3	0.33	66.7	2178	0.81	0.78	1.04	1.09
23	1.6	2	17:36:16	17:39:10	00:02:54	1.2	0.66	24.8	2300	0.51	0.37	1.38	1.68
24	1.6	2	17:41:39	17:44:11	00:02:32	3.3	0.49	78.1	1937	1.05	0.96	1.09	1.17
25	1.6	2	17:44:43	17:49:38	00:04:55	3.4	0.55	41.8	2292	0.65	0.49	1.33	1.42
26	1.6	2	17:59:51	18:02:57	00:03:06	3.4	0.49	65.7	2183	0.96	0.77	1.25	1.19
27	2.0	1	16:42:10	16:44:01	00:01:51	2.1	0.23	67.2	2176	0.92	0.95	1.00	1.08
28	2.0	1	16:48:35	16:51:45	00:03:10	3.8	0.32	72.8	2150	1.02	1.06	1.00	1.11
29	2.0	1	16:59:04	17:00:52	00:01:48	2.2	0.31	72.3	2153	0.99	1.05	1.00	1.11

Run No	Veh Eng Size	Driver	Time			Length (km)	Accel. Noise (m/s^2)	Mean Speed (km/h)	Calculated Traffic Volume (PCSE/hr)	Fuel Consumption Data			
			Start	End	Run (hh:mm:ss)					Actual Used (mL/s)	Computed at Mean Speed (mL/s)	DFUEL Calculated	DFUEL Simulated
30	2.0	1	17:03:19	17:06:12	00:02:53	2.9	0.42	61.0	2204	0.88	0.84	1.04	1.19
31	2.0	1	17:10:36	17:14:12	00:03:36	4.1	0.33	68.5	2170	0.96	0.98	1.00	1.11
32	2.0	1	17:18:44	17:21:24	00:02:40	1.9	0.43	43.9	2282	0.70	0.61	1.15	1.24
33	2.0	1	17:25:18	17:28:11	00:02:53	3.0	0.33	61.7	2201	0.86	0.86	1.01	1.12
34	2.0	1	17:31:01	17:33:13	00:02:12	2.2	0.39	59.4	2211	0.87	0.82	1.06	1.15
35	2.0	1	17:35:04	17:36:29	00:01:25	0.4	0.57	18.0	2300	0.52	0.42	1.25	1.55
36	2.0	1	17:38:48	17:41:34	00:02:46	3.3	0.24	72.5	2151	1.03	1.05	1.00	1.07
37	2.0	1	17:43:22	17:46:11	00:02:49	2.7	0.37	57.0	2222	0.86	0.78	1.10	1.15
38	2.0	1	17:46:45	17:50:14	00:03:29	2.0	0.64	34.6	2300	0.70	0.52	1.36	1.54
39	2.0	2	18:10:28	18:13:59	00:03:31	2.5	0.45	43.1	2286	0.79	0.60	1.32	1.31
40	2.0	2	18:15:47	18:18:56	00:03:09	4.0	0.34	75.6	2098	1.20	1.12	1.08	1.10
41	2.0	2	18:21:41	18:23:21	00:01:40	1.6	0.49	57.4	2221	0.96	0.79	1.22	1.25
42	2.0	2	18:28:11	18:29:56	00:01:45	2.2	0.41	75.1	2133	1.17	1.11	1.06	1.15
43	2.0	2	18:33:37	18:36:47	00:03:10	3.4	0.43	64.6	2188	1.10	0.91	1.22	1.19
44	2.0	2	18:39:12	18:42:28	00:03:16	4.1	0.41	74.8	2141	1.15	1.10	1.05	1.17
45	2.0	2	18:45:01	18:48:50	00:03:49	4.0	0.40	63.4	2193	1.06	0.88	1.20	1.19
46	2.0	2	18:50:40	18:53:23	00:02:43	3.4	0.37	74.8	2141	1.25	1.10	1.14	1.13
47	2.0	2	18:59:49	19:01:13	00:01:24	1.7	0.46	73.3	2148	1.30	1.07	1.22	1.20

Table 11.11: 6 Lane Divided, Site 9 - 304

Run No	Veh Eng Size	Driver	Time			Length (km)	Accel. Noise (m/s^2)	Mean Speed (km/h)	Calculated Traffic Volume (PCSE/hr)	Fuel Consumption Data			
			Start	End	Run (hh:mm:ss)					Actual Used (mL/s)	Computed at Mean Speed (mL/s)	DFUEL Calculated	DFUEL Simulated
1	2.0	1	16:54:45	16:56:17	00:01:32	1.8	0.34	71.3	2157	0.97	1.03	1.00	1.11
2	2.0	1	16:57:11	16:58:17	00:01:06	1.4	0.40	78.1	1935	1.14	1.17	1.00	1.15
3	2.0	1	16:59:31	17:01:29	00:01:58	2.4	0.51	74.2	2144	1.19	1.09	1.09	1.24
4	2.0	1	17:02:24	17:03:23	00:00:59	1.2	0.44	74.6	2142	1.13	1.09	1.03	1.17
5	2.0	1	17:08:12	17:09:42	00:01:30	1.6	0.57	63.4	2193	1.06	0.88	1.20	1.32
6	2.0	1	17:10:20	17:11:59	00:01:39	1.4	0.68	51.4	2248	0.97	0.70	1.38	1.45
7	2.0	1	17:12:59	17:13:43	00:00:44	0.7	0.51	60.1	2208	1.09	0.83	1.31	1.29
8	2.0	1	17:15:37	17:17:26	00:01:49	1.6	0.71	53.9	2236	0.99	0.74	1.35	1.50
9	2.0	1	17:18:37	17:20:54	00:02:17	2.2	0.68	56.8	2223	1.00	0.78	1.29	1.41
10	2.0	1	17:22:03	17:25:00	00:02:57	0.3	0.61	5.7	2300	0.42	0.40	1.06	1.60
11	2.0	1	17:25:22	17:27:24	00:02:02	2.3	0.49	69.3	2166	1.05	0.99	1.06	1.27
12	2.0	1	17:27:56	17:29:38	00:01:42	2.0	0.49	69.4	2165	1.09	0.99	1.10	1.27
13	2.0	1	17:30:23	17:33:53	00:03:30	0.1	0.38	2.3	2300	0.34	0.40	1.00	1.31
14	2.0	1	17:36:38	17:38:28	00:01:50	2.2	0.29	72.4	2152	1.04	1.05	1.00	1.07
15	2.0	1	17:38:59	17:40:47	00:01:48	1.9	0.47	64.2	2189	1.01	0.90	1.12	1.24

Table 11.12: 6 Lane Divided, Site 22 - Pattanakarn

Run No	Veh Eng Size	Driver	Time			Length (km)	Accel. Noise (m/s^2)	Mean Speed (km/h)	Calculated Traffic Volume (PCSE/hr)	Fuel Consumption Data			
			Start	End	Run (hh:mm:ss)					Actual Used (mL/s)	Computed at Mean Speed (mL/s)	DFUEL Calculated	DFUEL Simulated
1	1.6	1	17:11:18	17:11:53	00:00:35	0.7	0.13	69.7	2164	0.89	0.83	1.08	1.07
2	1.6	1	17:12:44	17:13:47	00:01:03	1.1	0.38	63.3	2193	0.82	0.73	1.12	1.13
3	1.6	1	17:14:57	17:15:45	00:00:48	0.9	0.23	68.5	2170	0.88	0.81	1.09	1.09
4	1.6	1	17:16:52	17:17:46	00:00:54	1.0	0.41	66.4	2179	0.93	0.78	1.20	1.15
5	1.6	1	17:18:45	17:19:36	00:00:51	0.9	0.23	66.4	2179	0.83	0.78	1.07	1.09
6	1.6	1	17:20:28	17:21:20	00:00:52	1.0	0.25	67.1	2176	0.89	0.79	1.13	1.10
7	1.6	1	17:22:45	17:23:39	00:00:54	1.0	0.28	68.9	2168	0.91	0.81	1.12	1.10
8	1.6	1	17:24:32	17:25:21	00:00:49	0.9	0.23	68.2	2171	0.87	0.80	1.08	1.09
9	1.6	1	17:27:56	17:29:08	00:01:12	1.2	0.46	59.6	2211	0.82	0.68	1.20	1.21
10	1.6	1	17:29:57	17:30:57	00:01:00	1.1	0.43	64.1	2190	0.87	0.74	1.17	1.12
11	1.6	1	17:33:32	17:34:16	00:00:44	0.8	0.19	66.0	2181	0.81	0.77	1.05	1.07
12	1.6	1	17:36:07	17:36:48	00:00:41	0.7	0.30	64.8	2187	0.87	0.75	1.15	1.12
13	1.6	1	17:42:52	17:43:50	00:00:58	1.0	0.39	59.9	2209	0.75	0.69	1.09	1.14
14	1.6	1	18:09:01	18:09:54	00:00:53	1.0	0.31	65.2	2185	0.87	0.76	1.14	1.09
15	1.6	1	18:10:49	18:11:56	00:01:07	1.0	0.26	52.3	2244	0.69	0.60	1.16	1.09
16	1.6	1	18:17:04	18:18:35	00:01:31	1.2	0.22	48.3	2262	0.57	0.55	1.03	1.06
17	1.6	1	18:20:00	18:21:20	00:01:20	1.2	0.33	52.2	2244	0.67	0.60	1.13	1.13
18	1.6	1	18:23:24	18:24:32	00:01:08	1.0	0.20	54.0	2236	0.69	0.62	1.12	1.06
19	1.6	1	18:25:24	18:26:24	00:01:00	1.0	0.19	56.7	2224	0.71	0.65	1.10	1.07
20	2.0	1	15:28:53	15:29:43	00:00:50	1.0	0.22	70.2	2162	1.01	1.01	1.00	1.07
21	2.0	1	15:30:45	15:31:27	00:00:42	0.9	0.32	75.5	2110	1.04	1.11	1.00	1.10
22	2.0	1	15:32:51	15:33:35	00:00:44	0.9	0.29	74.4	2143	1.02	1.09	1.00	1.07
23	2.0	1	16:35:13	16:36:21	00:01:08	1.1	0.39	60.0	2209	0.87	0.83	1.05	1.14
24	2.0	1	16:37:44	16:38:57	00:01:13	1.1	0.54	56.0	2227	0.89	0.77	1.16	1.29
25	2.0	1	16:40:22	16:41:10	00:00:48	0.9	0.30	67.4	2175	0.96	0.96	1.00	1.11
26	2.0	1	16:45:41	16:46:35	00:00:54	1.0	0.28	70.0	2163	1.00	1.00	1.00	1.07
27	2.0	2	17:01:38	17:02:42	00:01:04	1.2	0.49	68.4	2170	1.15	0.97	1.18	1.27
28	2.0	2	17:03:27	17:04:37	00:01:10	1.2	0.53	64.0	2190	1.09	0.89	1.22	1.29
29	2.0	2	17:05:44	17:06:30	00:00:46	0.9	0.48	70.4	2161	1.03	1.01	1.02	1.20

Run No	Veh Eng Size	Driver	Time			Length (km)	Accel. Noise (m/s²)	Mean Speed (km/h)	Calculated Traffic Volume (PCSE/hr)	Fuel Consumption Data			
			Start	End	Run (hh:mm:ss)					Actual Used (mL/s)	Computed at Mean Speed (mL/s)	DFUEL Calculated	DFUEL Simulated
30	2.0	2	17:07:39	17:08:02	00:00:23	0.4	0.52	64.0	2190	1.12	0.89	1.25	1.29
31	2.0	2	17:09:30	17:10:28	00:00:58	1.0	0.61	65.1	2185	1.03	0.91	1.13	1.34
32	2.0	2	17:11:16	17:11:57	00:00:41	0.9	0.91	82.3	1663	1.75	1.26	1.39	1.49
33	2.0	2	17:15:10	17:16:03	00:00:53	1.1	0.40	71.8	2155	1.20	1.04	1.16	1.17
34	2.0	2	17:18:26	17:18:42	00:00:16	0.2	0.63	54.6	2233	1.02	0.75	1.37	1.42
35	2.0	2	17:21:23	17:21:43	00:00:20	0.4	0.40	69.1	2167	1.11	0.99	1.12	1.15
36	2.0	2	17:24:09	17:25:01	00:00:52	1.0	0.45	66.5	2179	1.10	0.94	1.17	1.27
37	2.0	2	17:26:54	17:27:31	00:00:37	0.7	0.43	68.3	2171	1.10	0.97	1.13	1.15
38	2.0	2	17:52:27	17:52:53	00:00:26	0.4	0.81	57.1	2222	1.20	0.78	1.53	1.62
39	2.0	2	17:54:32	17:55:38	00:01:06	1.2	0.49	65.2	2185	1.27	0.92	1.39	1.27
40	2.0	2	17:57:28	17:58:35	00:01:07	1.2	0.50	63.7	2192	1.08	0.89	1.21	1.29
41	2.0	2	18:01:27	18:02:20	00:00:53	1.0	0.44	64.8	2187	1.10	0.91	1.21	1.19
42	2.0	2	18:05:09	18:05:53	00:00:44	0.9	0.32	74.4	2143	1.28	1.09	1.17	1.11
43	2.0	2	18:07:43	18:09:06	00:01:23	1.3	0.68	55.1	2231	1.09	0.75	1.45	1.41
44	2.0	2	18:12:42	18:13:34	00:00:52	0.9	0.35	61.6	2201	1.00	0.85	1.17	1.14
45	2.0	2	18:21:13	18:21:39	00:00:26	0.5	0.15	75.6	2099	1.22	1.12	1.09	1.08
46	2.0	2	18:23:09	18:24:11	00:01:02	1.2	0.31	66.9	2177	1.01	0.95	1.07	1.11
47	2.0	2	18:27:37	18:28:25	00:00:48	0.9	0.34	64.7	2187	1.06	0.91	1.17	1.12

Table 11.13: 6 Lane Motorway, Site 19 – 31 (Don Maung)

Run No	Veh Eng Size	Driver	Time			Length (km)	Accel. Noise (m/s^2)	Mean Speed (km/h)	Calculated Traffic Volume (PCSE/hr)	Fuel Consumption Data			
			Start	End	Run (hh:mm:ss)					Actual Used (mL/s)	Computed at Mean Speed (mL/s)	DFUEL Calculated	DFUEL Simulated
1	1.6	2	14:34:34	14:37:46	00:03:12	4.1	0.45	76.7	2026	1.08	0.94	1.15	1.17
2	1.6	2	14:43:23	14:44:01	00:00:38	1.2	0.18	111.9	0	1.82	1.66	1.10	1.13
3	1.6	2	14:44:09	14:46:24	00:02:15	3.2	0.49	84.4	1526	1.20	1.07	1.12	1.14
4	1.6	2	14:47:06	14:49:28	00:02:22	2.9	0.59	73.3	2148	1.06	0.88	1.20	1.25
5	1.6	2	14:50:40	14:52:00	00:01:20	1.9	0.38	85.4	1461	1.17	1.09	1.07	1.13
6	1.6	2	14:56:29	14:57:10	00:00:41	1.0	0.58	85.6	1447	1.29	1.09	1.18	1.21
7	1.6	2	14:57:21	14:59:07	00:01:46	2.1	0.51	70.6	2160	0.97	0.84	1.16	1.23
8	1.6	2	14:59:58	15:00:07	00:00:09	0.2	0.46	75.6	2098	1.77	0.92	1.93	1.17
9	1.6	2	15:10:29	15:12:54	00:02:25	3.4	0.53	83.5	1580	1.25	1.06	1.18	1.20
10	1.6	2	15:15:47	15:16:29	00:00:42	0.9	0.60	77.8	1953	1.18	0.96	1.23	1.31
11	1.6	2	15:23:56	15:26:08	00:02:12	3.1	0.67	85.0	1484	1.44	1.08	1.33	1.29
12	1.6	2	15:27:21	15:28:19	00:00:58	1.1	0.49	66.5	2179	0.96	0.78	1.23	1.19
13	1.6	2	15:30:38	15:31:36	00:00:58	1.6	0.48	100.9	0	1.48	1.40	1.05	1.15
14	1.6	2	15:31:48	15:32:25	00:00:37	0.5	0.87	43.9	2282	0.83	0.51	1.63	1.76
15	1.6	2	15:35:42	15:36:02	00:00:20	0.5	0.36	90.9	1096	1.37	1.20	1.15	1.12
16	1.6	2	15:36:44	15:38:41	00:01:57	1.8	0.71	54.8	2233	0.90	0.63	1.44	1.51
17	1.6	2	15:41:14	15:41:46	00:00:32	0.7	0.53	77.6	1966	1.02	0.95	1.07	1.22
18	1.6	2	15:52:49	15:53:26	00:00:37	1.1	0.35	105.6	0	1.60	1.51	1.06	1.13
19	1.6	2	15:57:49	15:58:46	00:00:57	0.5	0.81	32.6	2300	0.62	0.42	1.49	1.80
20	1.6	2	16:05:13	16:06:44	00:01:31	2.2	0.49	85.5	1450	1.27	1.09	1.16	1.14
21	1.6	2	16:12:02	16:15:10	00:03:08	4.0	0.47	76.7	2026	1.12	0.94	1.20	1.17
22	1.6	2	16:22:28	16:23:20	00:00:52	1.9	0.35	130.2	0	2.58	2.14	1.20	1.13
23	1.6	2	16:24:51	16:25:17	00:00:26	0.6	0.57	87.2	1338	1.36	1.12	1.21	1.21
24	1.6	2	16:26:00	16:27:02	00:01:02	0.8	0.68	44.1	2281	0.70	0.51	1.37	1.54
25	1.6	2	16:27:15	16:28:09	00:00:54	1.3	0.66	86.2	1405	1.35	1.11	1.22	1.29
26	1.6	2	16:28:44	16:29:54	00:01:10	1.2	0.56	59.6	2210	0.85	0.68	1.24	1.34
27	1.6	2	16:30:30	16:30:52	00:00:22	0.6	0.41	97.3	679	1.45	1.33	1.09	1.15
28	2.0	1	16:15:49	16:16:13	00:00:24	0.5	0.27	68.2	2171	0.89	0.97	1.00	1.08
29	2.0	1	16:16:17	16:17:21	00:01:04	1.0	0.58	57.0	2222	0.92	0.78	1.18	1.33

Run No	Veh Eng Size	Driver	Time			Length (km)	Accel. Noise (m/s^2)	Mean Speed (km/h)	Calculated Traffic Volume (PCSE/hr)	Fuel Consumption Data			
			Start	End	Run (hh:mm:ss)					Actual Used (mL/s)	Computed at Mean Speed (mL/s)	DFUEL Calculated	DFUEL Simulated
30	2.0	1	16:18:32	16:21:22	00:02:50	0.4	0.62	7.8	2300	0.39	0.40	1.00	1.60
31	2.0	1	16:23:29	16:24:07	00:00:38	0.6	0.35	54.9	2232	0.80	0.75	1.07	1.16
32	2.0	1	16:25:41	16:26:55	00:01:14	0.8	0.49	38.2	2300	0.61	0.55	1.11	1.33
33	2.0	1	16:27:11	16:27:47	00:00:36	0.7	0.26	74.8	2141	1.02	1.10	1.00	1.07
34	2.0	1	16:28:26	16:28:53	00:00:27	0.2	0.53	32.9	2300	0.63	0.50	1.26	1.43
35	2.0	1	16:30:23	16:34:28	00:04:05	0.9	0.63	13.0	2300	0.49	0.40	1.22	1.60
36	2.0	1	16:35:57	16:39:24	00:03:27	3.1	0.52	53.5	2238	0.83	0.73	1.14	1.30
37	2.0	1	16:40:31	16:41:06	00:00:35	0.9	0.30	89.6	1181	1.34	1.44	1.00	1.11
38	2.0	1	16:46:21	16:47:42	00:01:21	1.6	0.28	71.5	2156	0.96	1.03	1.00	1.07
39	2.0	1	16:50:12	16:52:53	00:02:41	3.0	0.49	66.6	2178	1.00	0.94	1.06	1.27
40	2.0	1	16:57:15	17:00:24	00:03:09	2.9	0.55	55.1	2231	0.86	0.75	1.14	1.33
41	2.0	1	17:03:02	17:04:23	00:01:21	1.5	0.26	68.4	2170	0.92	0.97	1.00	1.08
42	2.0	1	17:06:18	17:08:10	00:01:52	2.2	0.43	70.6	2160	1.01	1.02	1.00	1.17
43	2.0	1	17:10:54	17:13:16	00:02:22	2.4	0.43	61.1	2204	0.85	0.85	1.00	1.19
44	2.0	1	17:15:42	17:16:17	00:00:35	0.7	0.33	75.3	2122	0.97	1.11	1.00	1.10
45	2.0	1	17:16:54	17:17:25	00:00:31	0.6	0.38	64.8	2187	0.89	0.91	1.00	1.14

12 REFERENCES

AIMSUN. AIMSUN user manual and reference material. www.aimsun.com

An, F., Barth M., Norbeck J. and Ross M. (1997). *Development of Comprehensive Emissions Model, Operating Under Hot-Stabilized Conditions*. Transportation Research Record 1587 pp52-62, Washington DC.

Austroads (1989). *Guide to the Geometric Design of Rural Roads.* AUSTROADS, Sydney.

Bennett, C.R (1993). *Revision of Project Evaluation Manual Speed Change Cycle Costs.* Report for Transit New Zealand, Wellington.

Bennett, C.R. (1994). *A Speed Prediction Model for Rural Two-Lane Highways*. School of Engineering Report 541 and PhD Dissertation, Department of Civil Engineering, University of Auckland.

Bennett, C.R. (1999). *Calibration of HDM Speed Model to Thailand*. Report DES/99/1. Highway and Traffic Consultants Ltd. New Zealand.

Bennett, C.R. and Greenwood, I.D. (2001). *Modelling Road User and Environmental Effects in HDM-4,. Volume 4, The Highway Development and Management Series.* Asian Development Bank.

Bester, C.J. (1981). *Fuel Consumption of Highway Traffic*. Ph.D. Dissertation, University of Pretoria.

Biggs, D.C (1987). *Estimating Fuel Consumption of Light to Heavy Vehicles*. ARRB Internal Report AIR 454-1, Australian Road Research Board, Nunawading.

Biggs, D.C (1988). *ARFCOM - Models For Estimating Light to Heavy Vehicle Fuel Consumption*. Research Report ARR 152, Australian Road Research Board, Nunawading.

Biggs, D.C (1995). Correspondence with HDM-4 Technical Relationships Study (HTRS) Team in Malaysia.

Bowyer, D.P., Akcelik, R. and Biggs, D.C. (1986). *Guide to Fuel Consumption Analyses for Urban Traffic Management.* Special Report 32, Australian Road Research Board, Nunawading.

Brodin, A. and Carlsson, A. (1986). *The VTI Traffic Simulation Model*. VTI Report 321A, Linkoping.

BTCE (1996). *Working Paper 24, Costs of Reducing Greenhouse Gas Emissions From Australian Cars: An application of the BTCE CARMOD Model*. Bureau of Transport and Communications Economics, Canberra, Australia.

Burke, C.E., Nagler, L.G, Lundstrom, L.C and Associates (1975). *Where Does All the Power Go?* SAE Transactions, Vol. 65.

Cenek, P.D. (1994). *Rolling Resistance Characteristics of New Zealand Roads*. Transit New Zealand Research Report PR3-001, Wellington.

Cenek, P.D. (1995). Correspondence with HDM-4 Technical Relationships Study (HTRS) Team in Malaysia.

Chesher, A.D. and Harrison, R. (1987). *Vehicle Operating Costs: Evidence from Developing Countries.* World Bank Publications, Johns Hopkins Press.

Clean Cat (2000). *Clean Cat Diesel Engine Catalytic Converters.* http://clean-cat.com.

CRRI (1985). *Traffic Simulation Modelling Study: Part 1 - Development of Simulation Models.* Central Road Research Institute, New Delhi.

de Weille, J. (1966). Quantification of Road User Savings. World Bank Occasional Papers No. 2, World Bank, Washington D.C.

Discount Converters Ltd. (2000). *Diesel Catalytic Converters*. http://www.discountconverter. com.

du Plessis, H.W., Visser, A.T. and Curtayne, P.C. (1990). *Fuel Consumption of Vehicles as Affected by Road-surface Characteristics*. Surface Characteristics of Roadways : International Research and Technologies, ASTM STP 1301, W.E. Meyer and J. Reichert, Eds., American Society for Testing and Materials, Philadelphia: 480-496.

EFRU (1997). *Vehicle Exhaust Gas Emissions – SMF Project 5034 Final Report*. Energy and Fuels Research Unit, Auckland UniServices Report 6386.23.

EPA (1997). *Annual Emissions and Fuel Consumption for an Average Vehicle.* Downloaded from web site http://www.epa.gov/omswww/annem95.htm on 26 November 1997.

EPA (2003). *MOBILE5 Vehicle Emissions Modeling Software.* Downloaded from web site http://www.epa.gov/otaq/m5.htm on 4 March 2003.

ETSU (1997) *Emissions Modelling Framework for HDM-4.* Working Paper for Discussion with University of Birmingham and ODA. ETSU REF:RYCA 18825001/wp2/Issue 1. 4 November 1997

Francher, P.S. and Winkler, C.B. (1984). *Retarders for Heavy Vehicles: Phase III Experimentation and Analysis; Performance, Brake Savings and Vehicle Stability*. US Department of Transportation, Report no. DOT HS 806672.

Greenwood, I.D. (1999). *Calibration of the HDM-4 Congestion Model*. Thailand Department of Highways, Thailand Motorway Project in conjunction with Dessau-Soprin Consultants.

Greenwood, I.D. and Bennett, C.R. (1995a). *HDM-4 Fuel Consumption Modelling.* Preliminary Draft Report to the International Study of Highway Development and Management Tools, University of Birmingham.

Greenwood, I.D. and Bennett, C.R. (1995b). *The Effects of Traffic Congestion on Fuel Consumption.* Preliminary Draft Report to the International Study of Highway Development and Management Tools, University of Birmingham.

Greenwood, I.D. and Bennett, C.R. (1996). *Effects of Congestion on Fuel Consumption*. ARRB Road and Transport Research Journal, Vol 5, No 2 June 1996 pp 18 – 32.

Greenwood, I.D., Dunn, R.C.M. and Raine, R.R. (1998). *Predicting Non-Steady Speed Driving*. 19th ARRB Conference Proceedings, Sydney, Australia. pp 136 to 151.

Hammarstrom, U. (1999). Vehicle Emission Deterioration Factors. Personal communication via email Hammarstrom to Greenwood, 19 October 1999.

Haworth, N. and Symmons, M. (2001). *The Relationship Between Fuel Economy And Safety Outcomes*. Report No. 188, Accident Research Centre.

Hess, S.L. *Introduction to Theoretical Meteorology (1959)*. Florida State University, Holt, Rinehart and Winston, New York.

Heywood, J.B. (1988). *Internal Combustion Engine Fundamentals*. McGraw-Hill International Press.

Heywood, J.B. (1997). *Motor Vehicle Emissions. Control: Past Achievements, Future Prospects.* 1997 George Stephenson Lecture Material, Auckland New Zealand. Institute of Mechanical Engineers, London.

Hine, J. and Pangihutan, H. (1998). *Speed Profiles and Fuel Consumption: A Study of a Congested Road in Java*. Project Report PR/OSC/132/98, Transport Research Laboratory, Crowthorne.

Hoban, C., Reilly, W., and Archondo-Callao, R. (1994). *Economic Analysis of Road Projects with Congested Traffic*. World Bank Publications. Washington D.C.

Ingram, K.C., (1978). *The Wind-averaged Drag Coefficient Applied to Heavy Goods Vehicles*. TRRL Supplementary Report 392, Crowthorne, Berkshire.

IRC (1993). *Manual on Economic Evaluation of Highway Projects in India*. Indian Roads Congress, Delhi.

Knoroz, V.I and Shelukhin, A.S. (1964). *Test Data on the Rolling Resistance of Vehicle Tires on Roads with a Hard Surface*. Moscow Automotive Prom., Vehicle Research Institute, No 2, pp. 16-21.

LTSA (2000). New/used car registrations up for the year. Media Release 11 January 2000. Land Transport Safety Authority, New Zealand.

Mannering, F.L. and Kilareski, W.P. (1990). *Principles of Highway Engineering and Traffic Analyses*. John Wiley and Sons, Brisbane.

Milkins, E. and Watson, H. (1983) *Comparison of Urban Driving Patterns.* SAE Technical Paper No. 830939.

Moore, D.F. (1975). *The Friction of Pneumatic Tyres*. University College, Dublin, Ireland, Elsevier Scientific Publishing Company.

NDLI (1988). *PMIS Technical Manual: Appendix 1 - Vehicle Operating Costs.* Report to Saskatchewan Highways and Transportation, N.D. Lea International, Vancouver.

NDLI (1995). *Modelling Road User Effects in HDM-4.* Final Report Asian Development Bank RETA 5549. N.D. Lea International, Vancouver.

NRC (1992). *Automotive Fuel Economy. How Far Should We Go?* National Research Council, National Academy Press, Washington D.C.

Odoki, J.B. and Kerali, H.R.G. (1999). *HDM-4 Technical Reference Manual.* Volume 4 of HDM-4 Documentation. PIARC.

Opus (2003). List of those who downloaded the HDM Tools software from the web site www.opus.co.nz/hdmtools as at 1st February 2003. Provided by Opus International Consultants Ltd, Wellington New Zealand.

Pan, Y. (1994). *Development of a Highway Investment Benefit Analysis System (HIBA) for China*. M.Phil. Thesis, University of Birmingham.

PARAMICS. Paramics user manuals and reference material. http://www.paramics-online.com/index2.htm

Patel, T. (1996). *Power station failure adds to Delhi's woes*. New Scientist, 12 October 1996.

Paterson, D.J. and Henein, N.A. (1972). *Emissions from Combustion Engines and Their Control.* Ann Arbor Science Publishers Inc, Michigan.

PEM (1997 - 2002). *Transfund New Zealand Project Evaluation Manual, including relevant updates and amendments.*

Rajasekaran, S. (1992). *Numerical Methods in Science and Engineering*, *A Practical Approach*. Wheeler Publishing. Allahabad.

St John, A.D. and Kobett, D.R. (1978). *Grade Effects on Traffic Flow Stability and Capacity*. NHCRP Report 185, Transportation Research Board, Washington, D.C.

Sheaffer, B., Blair, G. and Lassansk, G. (1998). *Two-Stroke Engines Technology and Emissions PT-69.* Society of Automotive Engineers.

Smith, M.J. and Hawley M.D. (1993). *Start Again! Engine and vehicle designers set free by a quiet revolution in transmissions*. pp 113-123 Automobile Emissions and Combustion. Autotech '93, Mechanical Engineering Publications Limited, London.

SNRA (1995). *ISOHDM Supplementary Technical Relationship Study, Draft Final Report*. Swedish National Road Administration, November 1995.

Sovran (1984). *The effect of ambient wind on a vehicle's aerodynamic work requirement and fuel consumption*. Society Automotive Engineers (U.S). SAE Technical Paper No. 840298.

Suzuki T. (1997). *The Romance of Engines*. Society of Automotive Engineers Inc, USA.

TRB (2000). *Highway Capacity Manual*. Transportation Research Board, Washington, D.C.

Visser, A.T., and Curtayne, P.C. (1985). *A Pilot Study on the Effect of Road Surface Properties on the Fuel Consumption of a Passenger Car*. NITRR Contract Report C/PAD/46.5, Pretoria.

Walter, J.D. and Conant, F.S. (1974). *Energy Losses in Tires*. Tire Science and Technology, TSTCA, Volume 2, No 4, pp. 235-260.

Wasielewski, P. (1981). *The Effect of Car Size on Headways in Freely Flowing Freeway Traffic.* Transportation Science, pp 364-378, Volume 15, No. 4, November 1981.

Watanatada T., Harral C.G., Paterson W.D.O., Dhareshwar A.M., Bhandari A., and Tsunokawa K., (1987a), *The Highway Design and Maintenance Standards Model, Volume 1 - Description*, The World Bank, John Hopkins University Press.

Watanatada, T., Dhareshwar, A., and Rezende-Lima, P.R.S. (1987b). *Vehicle Speeds and Operating Costs: Models for Road Planning and Management.* Johns Hopkins Press, Baltimore.

Watson, H.C. (1995). *Effects of a Wide Range of Drive Cycles on the Emissions from Vehicles of Three Levels of Technology.* International Congress and Exposition Detroit, Michigan.

Wong, J.Y. (1993). *Theory of Ground Vehicles - 2nd Edition*. Wiley.

13 GLOSSARY

The following terminology is used throughout this report.

Term	Description	Units
θ	angle of incline	radians
χ	direction of the wind relative to the direction of travel	degrees
ξ	fuel-to-power efficiency factor	mL/kW/s
α	idle fuel consumption	mL/s
π	is pi constant	
ρ	mass density of air	kg/m^3
γ	rate of temperature change (0.0065 K/m)	K/m
Φ	slip angle	degrees
ψ	yaw angle	degrees
σa	total acceleration noise	m/s^2
σaal	noise due to the road alignment	m/s^2
σadr	noise due to natural variations in the driver's speed	m/s^2
$\sigma airi$	noise due to roughness	m/s^2
$\sigma amax$	maximum total acceleration noise	m/s^2
σan	natural noise ascribed to the driver and road	m/s^2
$\sigma anmt$	noise due to non-motorised transport	m/s^2
σasf	noise due to roadside friction	m/s^2
σat	noise due to traffic interactions	m/s^2
$\sigma atmax$	maximum traffic noise	m/s^2
$\sigma atrat$	traffic noise ratio	
ξb	base engine efficiency	mL/kW/s
ψc	yaw angle at which CDmult is a maximum	degrees
$\sigma spdlim$	noise due to speed limits	m/s^2
a	acceleration	m/s^2
a0 to a6	are coefficients	
AADT	total traffic entering the intersection or using the section	veh/day
AF	projected frontal area of the vehicle	m^2
ALT	altitude above sea level	m
atan	arc tan	radians
b11 to b13	are rolling resistance parameters	
beng	speed dependent engine drag parameter	
CD	aerodynamic drag coefficient	
CD(ψ)	wind averaged CD	
CDmult	CD multiplier	
ceng	speed independent engine drag parameter	
Cm	exponent in rolling resistance model	
CO	carbon monoxide	
Co	static coefficient of rolling resistance	
CO_2	carbon dioxide	
CPF	catalytic pass fraction	
CR	coefficient of rolling resistance	
CR1	is a rolling resistance tyre factor	
CR2	is a rolling resistance surface factor	
Cs	tyre stiffness coefficient	kN/rad
Cv	dynamic coefficient of rolling resistance	$1/(m/s)^{Cm}$
D	engine displacement	L

Term	Description	Units
deltavel	maximum deviation from the initial velocity	m/s
DensFuel	is the density of fuel	g/mL
DFUEL	percentage increase in fuel consumption due to congestion	per cent
Dw	diameter of the wheels	m
e	superelevation	m/m
EALC	accessory load constant	kW
ECFLC	cooling fan constant	
edt	efficiency of the drive train	
ehp	proportionate decrease in efficiency at high output power	
EMRAT	effective mass ratio	
EOE	engine out emissions	
f	side friction factor	
Fa	aerodynamic drag resistance	N
FALL	fall of the road	m/km
FC	fuel consumption	L/1000 km
FCLIM	is a climatic factor related to the percentage of driving done snow and rain	
Fcr	curvature force	N
Ff	side friction force	N
Fg	gradient resistance	N
Fi	Inertial resistance	N
Fr	rolling resistance	N
Ftr	tractive force applied to the wheels	N
FUELcong	congested fuel consumption	
FUELsteady	steady state fuel consumption	
g	acceleration due to gravity	m/s^2
GR	gradient	%
h	proportionate increase CD at angle ψc	
H	total gear reduction	
HC	hydro carbons	
HDM-4	Highway Design and Maintenance version 4	
Hmax	maximum overall height of vehicle	m
Htop	total gear reduction top gear	
Ie	moment of inertia of the engine $kg\text{-}m^2$	
IFC	fuel consumption	mL/s
IRI	roughness in International Roughness Index	m/km
Iw	moment of inertia of the wheels	$kg\text{-}m^2$
k	traffic density	veh/km
kjam	jam density	veh/km
M	vehicle mass	kg
M’	effective mass	kg
Me	inertial mass of the engine and drivetrain	kg
MinIFC	minimum fuel consumption under negative power loading (default = 0)	ML/s
Mw	inertial mass of the wheels	kg
NMT	non-motorised traffic	
NOx	oxides of nitrogen	
Nw	number of wheels	
P	air pressure	kPa
Pacc	power required to power engine accessories	kW
Pb	lead	
PCSE	are passenger car space equivalents	

Term	Description	Units
PCTDS	percentage of driving done on snow covered roads	
PCTDW	percentage of driving done on wet roads	
Peng	power required to overcome internal engine drag	kW
Pengacc	total engine and accessories power	kW
PM	particulate matter	
Pmax	maximum rated engine power	kW
Po	standard air pressure at sea level (101.325 kPa)	kPa
Prat	rated engine power	kW
PRPPeng	proportion of Pengacc ascribable to engine drag	
Ptot	total power requirements	kW
Ptr	power required to overcome tractive forces	kW
Ptre	tractive power as observed by the engine	kW
Pulse	fuel pulse width at injectors	msec
Qnom	the nominal capacity of the road	PCSE/h
Qo	flow level below which traffic interactions are negligible	PCSE/h
Qult	the ultimate capacity of the road	PCSE/h
R	radius of the curve	m
R	Reynolds gas constant (286.934 $m^2/s^2/K$)	$m^2/s^2/K$
r	rolling radius of the tyres	m
RELDEN	relative density	
rg	radius of gyration of the tyre	m
RISE	rise of the road	m/km
RPM	engine speed	
RPM100	engine speed when vehicle is at 100 km	rev/min
RPMidle	engine speed at idle	rev/min
S	vehicle speed	km/h
S1 to S3	free flow speeds of different vehicle types	km/h
Snom	the speed at the nominal capacity	km/h
SO_2	sulphur dioxide	
Sult	the speed at the ultimate capacity	km/h
T	air temperature	K
TAIR	temperature of the air	^oC
Tdsp	texture depth	mm
TMW	total mass of the wheels	kg
To	standard air temperature at sea level (288.16K)	K
TPE	tail pipe emissions	
TRPM	load governed maximum engine speed	rev/min
v	vehicle velocity	m/s
VCR	volume to capacity ratio	
vr	speed of the vehicle relative to the wind	m/s
Vw	wind velocity	m/s
Wmax	maximum overall width of vehicle	m